



Provided by the author(s) and University of Galway in accordance with publisher policies. Please cite the published version when available.

Title	Split luciferase reporters of apoptosome formation: a bio-tool to identify new drug-like molecules
Author(s)	Tashakor, Amin
Publication Date	2019-12-03
Publisher	NUI Galway
Item record	http://hdl.handle.net/10379/15608

Downloaded 2024-03-13T07:09:43Z

Some rights reserved. For more information, please see the item record link above.



Split luciferase reporters of apoptosome formation: a bio-tool to identify new drug-like molecules

A thesis submitted to the National University of Ireland in fulfilment of the
requirement for the degree of

Doctor of Philosophy

In the discipline of Pharmacology and Therapeutics

By

Amin Tashakor

Apoptosis Research Centre

National University of Ireland Galway

Thesis supervisor: Dr. Howard Fearnhead

August 2019

Acknowledgement

First of all, I would like to express all my appreciation to my supervisor Dr. Howard Fearnhead in simple words: thanks for everything. Thanks for your endless energy, enthusiasm and patience. Thanks for all your training, discussions and support over the last four years. Thanks for encouraging me to always think critically. It was very helpful in science but it put me in big trouble when Mahshid cooked food and I wanted to be very critical! It is not just about science, because you changed my life a day you introduced Smithwick's to me. I did my best to make you FAMOUS and RICH, I failed, but I tried to make your day by showing you new findings the first thing in the morning. I never forget all the moments and memories I have in your lab.

Special thanks to my friend, my college, labmate, my wife, Mahshid, for all her support. I shared every single moment of my PhD with you both in the lab and at home, which was very enjoyable. You never accepted me as your senior, but you knew that I am the boss at work!!!! Just at work! Wish you the best of luck in your life with me.

Thanks to all members of the lab. Thanks to Ricky for his patience over my every-five-minutes questions during the first months of my PhD. Thanks to Aoife who I never met but was always reliable. There were some people that were always ready to help me like Alex and Michael. Big thanks to both for all their help and discussions. Thanks to Hojjat for all his sense of humour and tea breaks! And thanks to all my friends Eion, Greg, Sangeetha (there is a long list of names) and all those visitors joined our lab who made it a happy place to work.

At the end, I thank my parents, Molouk and Mahmoud, for all their support and love. I know how hard it is to be far away at the time that you needed your only son. It was harder for me to see you only once during four years. I also thank my sister who was always proud of her brother. Thanks to Mahdi, Sepehr and my new niece baby Bahar for all the happiness they brought to my life.

Abstract

Formation of apoptosome, a key multiprotein complex in mitochondrial-mediated apoptosis, is an essential step during normal development and deregulation of this event is associated with pathological conditions. The apoptosome contains seven Apoptotic Protease-Activating Factor-1 (Apaf-1) molecules and induces cell death by activating caspase-9. Apoptosome is a protein target for therapeutic approaches. However, the lack of suitable screening assay to directly identify new modulators of apoptosome has limited the field.

Here, I define a new split luciferase reporters of apoptosome for *in vitro* studying the apoptosome. In this assay, upon apoptosome formation Apaf-1 fused to an N-terminal fragment of luciferase binds to Apaf-1 fused to a C-terminal fragment of luciferase and reconstitutes luciferase activity. The assay was validated by showing the cytochrome c/dATP-dependent luciferase activity, inhibition of the luciferase activity by apoptosome inhibitor (NS3694) and contribution of the fusion proteins in the complex with the expected molecular weight.

This assay was then used to screen a panel of compounds to identify the inhibitors of apoptosome. Screening a persistent organic pollutant library indicated that pentachlorophenol (PCP) inhibits apoptosome formation, and further investigation revealed that PCP binds to cytochrome c. Screening a library of natural products also identified a new chemical with strong inhibitory effect, although at high concentrations.

This reporter was also used to study the mechanism of inhibition by NS3694 and M50054. NS3694 is an inhibitor of apoptosome. I showed that the main target of NS3694 is cytochrome c rather than apoptosome. M50054 was also known to inhibit caspase activation. However, the mechanism and the direct target was unknown. I showed that, unlike NS3694, M50054 mainly targets apoptosome complex.

The data demonstrate the utility of the new assay in identifying apoptosome inhibitors, and I suggest that the assay may be useful in screening a large chemical collection. Luciferase-based reporters provide a quick, easy, and cost-effective *in vitro* assay.

Contents

1	Chapter 1 (Introduction).....	1
1.1	Cell death and diseases.....	2
1.2	Modes of cell death	3
1.3	Mitochondrial-mediated apoptosis is evolutionarily conserved.....	5
1.3.1	Apoptosis in <i>Caenorhabditis elegans</i>	6
1.3.2	Apoptosis in <i>Drosophila melanogaster</i>	8
1.3.3	Apoptosis in mammals.....	9
1.4	Mechanism of apoptosis.....	11
1.4.1	Extrinsic pathway of apoptosis	11
1.4.2	Intrinsic (mitochondrial- mediated) pathway of apoptosis	13
1.5	Apoptosome formation.....	22
1.6	Apoptosome-dependent caspase activation.....	30
1.7	Models describing events downstream of caspase-9 activation.....	33
1.8	Apoptosis physiological modulators	34
1.9	Apaf-1 mediated apoptosis in development and disease.....	38
1.10	Synthetic Apoptotic modulators.....	40
1.11	Reporters of monitoring protein interactions	44
2	Chapter 2 (Material & Methods)	51
2.1	Making luciferase-based reporters	52
2.2	Expression of luciferase tagged Apaf-1	57
2.3	Cell-free system.....	61
2.4	Validation of the luciferase-based reporters.....	65
2.5	Screening	66
2.5.1	Toxicant library.....	66
2.5.2	Natural product library	67
2.6	Production of the recombinant proteins	69
2.7	Biochemical assays	77
2.8	Microscopy	78
2.9	Modelling studies	78
2.10	Software and programs.....	80
3	Chapter 3 (Assay development and validation)	81
3.1	Amplification of the fragments	82
3.2	In-fusion cloning	83
3.3	Transformation of the in-fusion cloning reactions	85

3.4	Expression of the recombinant fusion proteins in the HEK293 cells	86
3.5	Detecting split luciferase activity in cells	87
3.6	Cell death in transfected cultures	89
3.7	Detection of competent apoptotic machinery in cell free system	91
3.7.1	Caspase-3 and -9 activity and processing	91
3.7.2	Apaf-1 oligomerization	94
3.8	<i>in vitro</i> validation of the assay	95
3.8.1	Split luciferase reconstitution assay	95
3.8.2	Caspase and split luciferase activity in diluted extracts expressing Nluc-Apaf-1 and Cluc-Apaf-1	96
3.8.3	Titration of cytochrome c	101
3.8.4	Titration of NS3694, an inhibitor of apoptosome formation	102
3.8.5	Apaf-1 mutant unable to form apoptosome blocks split luciferase activity	102
3.8.6	Gel filtration of apoptosome produced by fusion proteins	104
3.9	Discussion	107
4	Chapter 4 (Screening)	111
4.1	Screening the toxicant library	112
4.1.1	Titration of hits in luciferase assay	115
4.1.2	Titration of hits in caspase assay	115
4.1.3	PCP is the most potent hit that inhibits apoptosome	122
4.2	Screening the marine natural products	124
4.2.1	Fractionation and purification of the RMY-243	126
4.3	Discussion	134
5	Chapter 5 (Identifying the direct protein target of PCP)	137
5.1	Baculovirus Expression System	138
5.2	Cloning, isolation and validation of recombinant bacmids	140
5.3	Transfection and expression of Sf21 cells with recombinant bacmid	143
5.4	Expression and affinity purification of recombinant Apaf-1	145
5.5	Gel filtration to test if the recombinant protein was monomeric or oligomeric	146
5.6	Gel filtration of PCP-treated rApaf-1	148
5.7	Thermo-stability shift assay of the PCP-treated apoptosome	150
5.8	Binding of PCP-treated cytochrome c to rApaf-1	152
5.9	Modelling the binding of PCP to cytochrome c	155
5.10	Discussion	160

6	Chapter 6 (NS3696 and M50054 prevent apoptosis by different mechanisms))	161
6.1	NS3694, an apoptosome inhibitor.....	162
6.1.1	NS3694 prevents the formation of a functional apoptosome.....	162
6.1.2	NS3694 induced the formation of an inactive high molecular weight Apaf-1 complex	164
6.1.3	NS3694 prevents Apaf-1 from binding to cytochrome c.....	164
6.1.4	NS3694 mainly targets cytochrome c	167
6.1.5	NS3694 interferes with the recruitment of caspase-3 to the apoptosome..	169
6.1.6	NS3694 kills the cells	172
6.1.7	Treatment with NS3694 reveals the shrinkage and condensation of the nuclei	175
6.1.8	NS3694 kills the cells by rapidly inducing necrosis.....	177
6.1.9	Modelling the binding site of NS3694 on cytochrome c	179
6.2	M50054, a caspase-3 inhibitor	181
6.2.1	M50054 inhibits caspase-3 like activity in a concentration dependent manner	181
6.2.2	M50054 inhibits the events upstream of caspase-3	182
6.2.3	Modelling the binding of M50054 to cytochrome c	186
6.3	Discussion	188
7	Chapter 7 (Conclusion)	192
8	References.....	195
9	Publication.....	216
	Appendices.....	227
9.1	Appendix A: DNA/PROTEIN sequences of luciferase tagged Apaf-1 reporters	228
9.2	Appendix B: List of persistent pollutant toxicants.....	233
9.3	Appendix C: Natural product library	237

List of Figures

Chapter 1

Figure 1.1 Different types of cell death.	4
Figure 1.2. Conserved apoptotic machinery.	7
Figure 1.3. Apoptosis signalling pathways.	12
Figure 1.5. Binding of cytochrome c to WD repeats of Apaf-1.	18
Figure 1.6. Interactions between Apaf-1 and Cytochrome c.	20
Figure 1.7. Putative Van der Waals interactions between Apaf-1 and cytochrome c.	22
Figure 1.8. Apaf-1 CARD disk.	24
Figure 1.9. Holoapoptosome CARD-CARD disk.	25
Figure 1.10. Caspase-9 and Apaf-1 interactions at CARD disk.	27
Figure 1.11. Apoptosome complex.	29
Figure 1.12. Schematic presentation of the caspase processing.	31
Figure 1.13. Apaf-1 interacting proteins.	36
Figure 1.14. Chemical structure of Apaf-1 activators.	41
Figure 1.15. Chemical structure of Apaf-1 inhibitors.	42
Figure 1.16. The mechanism of bioluminescent reaction catalysed by firefly luciferase.	45
Figure 1.17. Different strategies used for making luciferase reporters.	47

Chapter 3

Figure 3.1. Schematic presentation of the recombinant constructs.	82
Figure 3.2. PCR-amplified fragments for in-fusion cloning.	83
Figure 3.3. in-fusion cloning fragments.	84
Figure 3.4. in-fusion cloning strategy.	84
Figure 3.5. Digestion of plasmids.	85
Figure 3.6. Expression of the recombinant fusion proteins.	86
Figure 3.7. Immunoblotting and the activity of the overexpressed proteins.	88
Figure 3.8. Cell death assay when cells transfected with the recombinant plasmids.	90
Figure 3.9. Caspase-9 processing.	92
Figure 3.10. Caspase-3 processing.	93
Figure 3.11. Size exclusion chromatography of S-100 HEK 293 extract.	94
Figure 3.12. <i>in vitro</i> split luciferase assay.	95
Figure 3.13. Split luciferase activity is Cc/dATP dependent.	97
Figure 3.14. Temperature-dependent luciferase assay.	99

Figure 3.15. Optimization of assay condition.	100
Figure 3.16. Titration of apoptosome activator (cytochrome c) and inhibitor (NS3694) using split luciferase assay.	103
Figure 3.17. Gel filtration of luciferase-tagged Apaf-1.	105
Figure 3.18. Protein complexes were formed before or during extract preparation.	106
Chapter 4	
Figure 4.1. Screening and analysis of the toxicant library.	113
Figure 4.2. Re-testing the hit compounds.	114
Figure 4.3. Titration of compounds using caspase, split luciferase and luciferase assay.	116
Figure 4.4. Caspase processing and activity before activation of cell extract.	119
Figure 4.5. Caspase processing and activity after activation of cell extract.	121
Figure 4.6. Split luciferase activity of the PCP-treated extract before and after activation of the crude extract.	123
Figure 4.7. A collection of natural product extracts was screened to identify inhibitors of caspase-3 activity.	125
Figure 4.8. Fractionation of the hit compound.	126
Figure 4.9. Fractionation of RMY-243-1-B.	127
Figure 4.10. Structural identification of a new compound.	128
Figure 4.11. Chemical structure of the zoanthid major metabolite.	129
Figure 4.12. Titration of the pure identified compound using split luciferase and caspase-3 like activity.	130
Figure 4.13. A methanol RMY-243-2 extract fractionated and eluted with water and increasing concentrations of methanol.	131
Figure 4.14. Fractionation of RMY-243-2-B.	132
Figure 4.15. 25% MeOH (RMY-243-2-B) fraction further fractionated and the fractions were tested in luciferase assay.	133
Chapter 5	
Figure 5.1. Overview of the Baculovirus expression protocol.	139
Figure 5.2. Agarose gel electrophoresis of extracted bacmids.	140
Figure 5.3. Transposition region in recombinant bacmids.	141
Figure 5.4. Screening of the picked colonies for insertion of Apaf-1 in the bacmid.	142
Figure 5.5. PCR-amplification of the control bacmids.	143

Figure 5.6. SDS-PAGE and immunoblotting of the transfected Sf21 cells with different bacmids.	144
Figure 5.7. Immunoblotting of the Sf21 cells infected with P0 viral stock.	145
Figure 5.8. The procedures used for making recombinant protein.	146
Figure 5.9. Production of rApaf1 using Sf21 cells.	147
Figure 5.10. Gel filtration of the PCP-treated rApaf-1.	149
Figure 5.11. thermo-stability shift assay.	151
Figure 5.12. Optimization of co-precipitation assay condition.	153
Figure 5.13. Co-precipitation of PCP-bound cytochrome c to rApaf-1	154
Figure 5.14. Docking of PCP into cytochrome c.	155
Figure 5.15. PCP docking to cytochrome c.	156
Figure 5.16. ATP docking to cytochrome c.	157
Figure 5.17. Docking of the PCP derivatives into cytochrome c.	159
Chapter 6	
Figure 6.1. NS3694 inhibits split luciferase and caspase-3 activity.	163
Figure 6.2. NS3694 forms a high molecular weight complex. Gel filtration of the NS3694-treated HEK293 extract.	165
Figure 6.3. Co-immunoprecipitation of NS3694-treated cytochrome c with rApaf-1. ...	166
Figure 6.4. Thermo-stability shift assay.	168
Figure 6.5. NS3694 reduces the rate of caspase-3 activation when added early after apoptosome formation.	171
Figure 6.6. Cell death in NS3694-treated cells.	172
Figure 6.7. NS3694 does not rescue etoposide-induced death.	173
Figure 6.8. TMRE staining of the NS3694-treated HT1080 cells.	174
Figure 6.9. Nuclei morphology of the NS3694-treated cells.	176
Figure 6.10. Live cells imaging of the NS3694-treated HeLa cells.	178
Figure 6.11. NS3694 docking to cytochrome c.	179
Figure 6.12. NS3694 docking to “open” Apaf-1.	180
Figure 6.13. M50054-driven inhibition of caspase-3 like activity.	182
Figure 6.14. Effect of M50054 on apoptotic machinery components.	183
Figure 6.15. M50054 does not bind to cytochrome c.	184
Figure 6.16. M50054 bind to apoptosome complex.	185
Figure 6.17. Preparation of “open” Apaf-1 PDB file.	186
Figure 6.18. M50054 docking to “open” Apaf-1.	187

List of Abbreviations

ADP	Adenosine Diphosphate
AIF	Apoptosis Inducing Factor
ANT	Adenine Nucleotide Translocator
APAF1	Apoptotic Protease Activating Factor 1
APS	Ammonium persulphate
ATP	Adenosine Triphosphate
Bcl-2	B-cell Lymphoma 2
Bcl-XL	B-cell Lymphoma-extra Large
BH Domain	Bcl-2 Homology Domain
Bp	Base Pairs
BSA	Bovine Serum Albumin
CARD	Caspase recruitment domain
Caspase	Cysteine aspartic-specific proteases
CypD	Cyclophilin D
Cc	Cytochrome C
kDa	Kilo-Dalton
DD	death domain
DIABLO	Direct IAP Binding Protein with Low PI
DISC	death-inducing signaling complex
DMEM	Dulbecco's Modified Eagle Medium
DMSO	Dimethylsulfoxide
DTT	Dithioreitol
EDTA	Ethylenediaminetetraacetic Acid
EGTA	Ethylene Glycol-bis(2-aminoethylether)-N-N-N-N-tetraacetic acid
ER	Endoplasmatic Reticulum
FADD	Fas-associated death domain
FAS	TNF Receptor Superfamily, Member 6
FBS	Foetal bovine serum
GFP	Green Fluorescent Protein
HEPES	4-(2-Hydroxyethyl)-1-Piperazineethanesulfonic Acid
IAP	Inhibitors of apoptosis protein
IgG	immunoglobulin G

IMS	Inter-membrane Space
IP	Immunoprecipitation
LB	Luria Broth
MOMP	Mitochondrial Outer Membrane Permeabilisation
MPT	Mitochondrial Permeability Transition
OMM	Outer Mitochondrial Membrane
PAGE	Polyacrylamide Gel Electrophoresis
PCR	Polymerase Chain Reaction
PI	Propidium Iodide
PMSF	phenylmethanesulphonyl fluoride
PVDF	Polyvinylidene Difluoride
RING	Really Interesting New Gene
RIP	Receptor Interaction Protein
ROS	Reactive Oxygen Species
RPM	revolutions per minute
SD	Standard Deviation
SDS	Sodium Dodecyl Sulfate
Smac	Second Mitochondria Derived Activator of Caspase
tBid	truncated Bid
TEMED	N, N, N', N'-Tetramethylethylenediamine
TMRE	TetraMethylRhodamine Ethyl Ester
TNF	Tumour Necrosis Factor
TRAIL	TNF-related Apoptosis Inducing Ligand
VDAC	Voltage Dependent Anion Channel
WT	Wild Type
XIAP	X-linked IAP
zVAD	Benzyloxycarbonyl-Val-Ala-Asp Fluoromethyl Ketone
$\Delta\Psi_m$	Mitochondrial Electrochemical Proton Gradient

INTRODUCTION

The goal of this thesis was to develop a new bio-tool for monitoring the apoptosome formation with the aim of studying the biology and pharmacology of this complex. This reporter enabled us to detect the protein-protein interaction of Apaf-1 proteins. In addition, this reporter was used as a screening tool to identify new drug-like molecules or testing the synthetic modulators of apoptosome.

This introduction will review the research and background information on the field in several sections. *Cell death and diseases* will describe the association of different modes of cell death with human diseases. Many of these modes of cell death are driven by large multiprotein complexes. As one of these, the apoptosome is the main focus of this thesis, apoptosis will be described in more detail. *Apaf-1 mediated apoptosis in development and disease* will summarize the evidence suggesting the important role of Apaf-1, a key component of apoptosome, in developmental events and how it is regulated *in vivo*. I will also review the synthetic compounds known to regulate Apaf-1. *Reporters of protein complexes* will describe the strategies used for studying the interactions among the proteins within a complex including split luciferase-based reporters as tools to investigate protein-protein interactions.

1.1 Cell death and diseases

Cell death is an important physiological event that regulates tissue homeostasis in multicellular organisms. Cell death is tightly controlled and there is a lot of evidence showing that dysregulation of cell death contributes to the pathogenesis of major diseases, such as cancer, myocardial infarction, stroke, atherosclerosis, infection, inflammation and neurodegenerative disorders, autoimmunity and premature ageing (Yu et al., 2013; Wiman and Zhivotovsky, 2017). Excessive cell death can cause neurological diseases while insufficient death can lead to tumorigenesis (Favaloro et al., 2012; Zamaraev et al., 2015). Therefore, a complex network of regulatory signalling pathways controls the growth and survival of the cells, genome integrity and DNA repair (Kitagishi et al., 2013; Papamichos-Chronakis and Peterson, 2013).

During the last few decades, many efforts have been made to uncover the mechanisms underlying cell death process at the molecular level. Different cell death pathways have been elucidated [reviewed by (Duprez et al., 2009)]. Key regulatory events in these pathways involve formation of large multiprotein complexes (Hu et al., 1998, 1999; Pick et al., 2006; Sun et al., 2012).

Thus, understanding the molecular pathways and regulation of these disease-related protein complexes is critical to identify potential therapeutic targets and apply effective and efficient treatments. Therefore, identification of a specific target protein is a key step. Once the target validated, different strategies can be used to design, synthesize or identify new drug-like molecules that affect the activity of the target. Screening a collection of compounds is one of the methods used for identifying new modulators. Here, I review one of the best-studied cell death modalities, apoptosis, with the focus on the protein complexes. I describe the apoptosome, a multiprotein complex in apoptosis, review its importance from the pathological points of view and discuss if it is a good target for therapeutic purposes.

1.2 Modes of cell death

Cell death modalities can be categorized in two broad groups: ‘accidental’ and ‘regulated’. Cells exposed to harsh physical, chemical stimuli or severe damage die by losing the structural integrity. This type of death referred to as ‘accidental cell death’ (ACD). Alternatively, cell death occurs through a genetically encoded machinery is called ‘regulated cell death’ (RCD). ‘Programmed cell death’ (PCD), is a subset of RCD that plays roles in developmental events or physiologic homeostasis of adult tissues (Figure 1.1). ACD is an unavoidable consequence of physical or chemical damage. In contrast, RCD can be modulated by either inhibiting the transduction of lethal signals or boosting the ability of the cells to respond to stress.

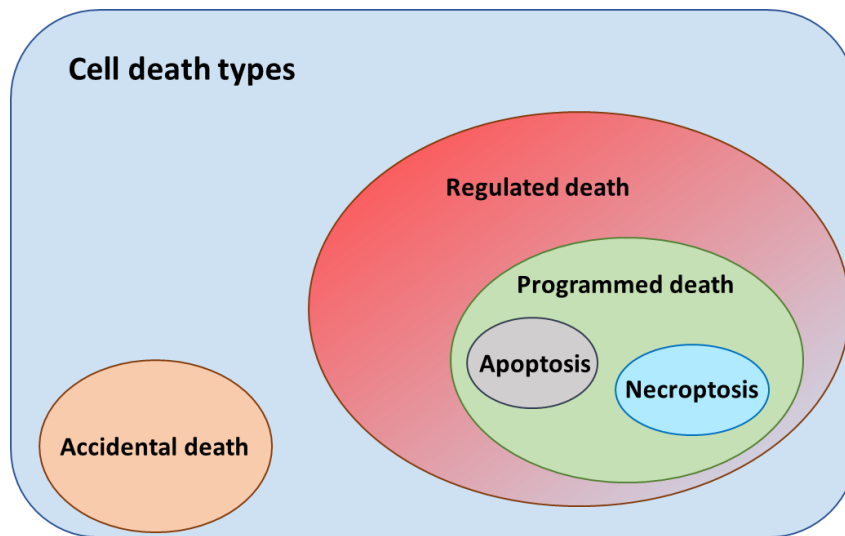


Figure 1.1 Different types of cell death. Cell death modalities are categorized in two types: accidental and regulated death. Programmed cell death is a subset of regulated cell death that contributes in development. Apoptosis and necroptosis are the examples of the most characterized programmed death.

Apoptosis is the most extensively studied type of regulated cell death. Apoptotic cells are characterized primarily by their morphology. Cell shrinkage, plasma membrane blebbing, nuclear condensation, and inter-nucleosomal DNA fragmentation occurs in apoptotic cells. The dead cells are then engulfed by adjoining cells or tissue phagocytes. This type of death is associated with minimal inflammation (Ashkenazi and Salvesen, 2014). Necroptosis, pyroptosis, ferroptosis and some other forms of regulated cell death show a morphology similar to accidental death or necrotic death such as cell and organelle swelling and loss of plasma membrane integrity. Contrary to accidental cell death, these forms of regulated necrosis are tightly controlled by regulatory signalling pathways. Here I concentrate on the apoptosis (in particular mitochondrial-mediated apoptosis) (Zmasek et al., 2007; Crawford et al., 2012).

1.3 Mitochondrial-mediated apoptosis is evolutionarily conserved

Apoptosis or programmed cell death is one of the most important physiological processes contributes to development and homeostasis in multicellular organisms. Disruption of apoptosis causes a range of diseases such as anaemia, cancer, neurodegenerative diseases and autoimmunity (Saikumar et al., 1999; Elmore, 2007; Taylor et al., 2008). For an organism, regulation of cell proliferation, cell size, and cell death is essential to provide organs and tissues with the right size.

In 1972, Kerr and colleagues coined the term “apoptosis”_ means “falling off” the leaves of a tree_ to address programmed cell death. Apoptosis term refers to morphological changes in a cell that lead to cell shrinkage, nucleus condensation, membrane fragmentation and formation of so-called apoptotic bodies, which subsequently ends to the engulfment of the cells (Kerr et al., 1972; Jiang, 2012).

Within the cells, signalling pathways convert a signal to a cell behaviour. In general, all these pathways encompass initiation and execution steps. Initiation is associated with signal transmission from a ligand to the first biochemical reaction and amplification of the signal. Execution step activates biochemical pathways and leads to an appropriate cellular response. Unlike signal transmission through phosphorylation, glycosylation and acetylation, some of signalling pathways such as apoptosis, are associated with irreversible proteolytic activities (Riedl and Salvesen, 2007). Proteases involved in apoptosis signalling are cysteine-dependent aspartate-specific protease (caspase) with a conserved cysteine residue in the active site. These proteases specifically cleave their substrate after aspartate residue (Timmer and Salvesen, 2007). Caspases not only cleave and destroy proteins, but also change the protein function through cleavage (Thornberry et al., 1992; Rodriguez and Lazebnik, 1999). Caspase cascade triggers the proteolytic activity of initiator caspases which then activates executive caspases (Cullen and Martin, 2009). Executioner caspases eventually target different intracellular substrate and induce death.

Most of our understanding of programmed cell death (PCD) is derived from *Caenorhabditis elegans*, a free-living nematode, and to some extent from *Drosophila melanogaster*, fruit fly, and from *Mus musculus* model organisms (Kumar et al., 1994; Lettre and Hengartner, 2006; Denton et al., 2013). The mechanisms involved in activation and regulation of apoptosis were revealed for the first time through genetics research on *Caenorhabditis elegans*. During development, activation of death genes kills a number of specific cells and creates a 959-cell nematode. This process is dynamic and takes place quickly, less than an hour as Sulston and Horvitz showed (Sulston and Horvitz, 1977).

1.3.1 Apoptosis in *Caenorhabditis elegans*

Extensive studies identified many *C.elegans* genes involved in cell death. These genes encode proteins that proceed different stages of death such as: EGL-1, CED-9, CED-4 and CED-3 (contribute to death), CED-1, CED-7, CED-6 and CED-10 (contribute to engulfment), NUC-1 and CPS-6 – (for degradation) (Malin and Shaham, 2015; Conradt et al., 2016). The products of CED-3 and CED-4 are essential for apoptosis. Ced-4 contains a nucleotide binding site and is mainly responsible for activation of upstream caspases (Jacobson and McCarthy, 2002). After receiving a death signal, CED-4 interacts to inactive CED-3. This interaction activates CED-3. Ced-9 is another key element that functions upstream of CED-3 and CED-4 and inhibits their lethal activities. According to the present model, in normal cells, CED-4 dimers bind to CED-9 and hence are unable to process CED-3. Under stress, EGL-1 is activated and upon binding to Ced-9, induces significant conformational changes that releases CED-4. Oligomerization of CED-4 dimers forms the apoptosome, which in turn processes CED-3 (Hengartner, 2000; Schmitz et al., 2000; Igney and Krammer, 2002) (Figure 1.2).

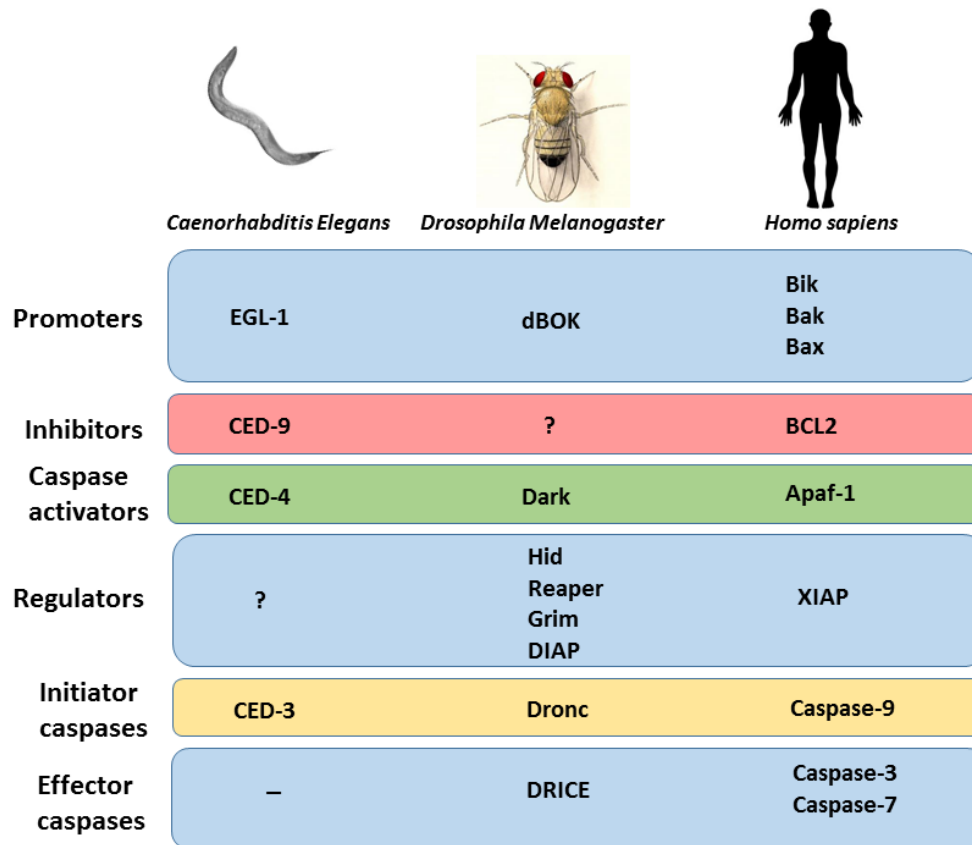


Figure 1.2. Conserved apoptotic machinery. A conserved set of proteins function to trigger caspase cascade In *Caenorhabditis elegans*, *Drosophila melanogaster* and *Homo sapiens*. In *c.elegans*, in normal condition, CED-9 (BCL2-family protein), binds to and inhibits CED-4. Apoptotic stimuli upregulate EGL-1 (BH3-only protein) which binds to CED-9 and releases CED-4. Then CED-4 activates CED-3 caspase. In *Drosophila*, different developmental signals function as apoptotic stimuli and activate IAP antagonists Reaper, Hid, and Grim. These proteins are found in mitochondria and degrade *Drosophila* inhibitor of apoptosis protein 1 (DIAP1). DIAP1 binds to and inhibits Dronc and effector caspases Drice. Therefore, caspases are released after degradation of DIAP. Dronc and its activator Ark form the apoptosome complex which further activates downstream effector caspases. In mammals, the balance between pro-apoptotic and anti-apoptotic BCL-2 family proteins regulates the release of cytochrome c and IAP antagonists such as Smac, HtrA2, and ARTS from mitochondria. These modulators remove the inhibitory function of XIAP (X-linked inhibitor of apoptosis protein), physiological caspase inhibitor, and activate the formation of the caspase-activating platform. Cytochrome c binds to the Apaf-1 and promotes the assembly of the apoptosome complex, which then recruits and activates pro-caspase-9. Proteolytic activity of processed caspase-9 further processes and activates executioner caspases-3 and -7.

From the pathological point of view, loss of function CED-3 or CED-4 or gain of function CED-9 rescue cells that are programmed to die. These animals have extra number of cells, bigger brain with less competent cells. Due to the presence of extra cells and therefore extra synapsis the nervous system is less efficient compare to the normal animals. CED-3 and CED-4 mutants grow slowly, have fewer progeny than the wild-type and show chemotaxis effect. However, these animals are viable (Metzstein et al., 1998; Aballay and Ausubel, 2001).

1.3.2 Apoptosis in *Drosophila melanogaster*

The *Drosophila melanogaster*, fruit fly, offers distinctive advantages for studying apoptosis in response to different stimuli in the context of whole organism. Transduction of different signalling pathways in *Drosophila* induces the transcriptional activation of reaper-family proteins such as reaper, hid (head involution defective) and grim. Molecular genetic studies have shown the importance of reaper, grim and hid in apoptosis in *drosophila*. Apoptosis was inhibited in mutant embryos with deletion of reaper family genes (White et al., 1994). RNA expression of grim initiated programmed cell death at all stages of embryonic development. Hid deficient embryos showed less cell death (Grether et al., 1995; Chen et al., 1996). Reaper family proteins bind to and inhibit the anti-apoptotic activity of the *Drosophila* IAP1 (DIAP1) protein, thus induce apoptosis (Hay et al., 1995). DIAP1 is an E3-ubiquitin ligase that defends cells from unwanted death by facilitating the degradation of Dronc, the initiator caspase. Apoptotic stimuli induce the auto-ubiquitination and degradation of DIAP1 which removes the inhibitory effect on caspases (Goyal et al., 2000; Steller, 2008).

There are seven caspase family in *drosophila* among which initiator caspase Dronc and the effector caspase Drice are required for developmental and stress-induced apoptosis. Loss of function mutation of caspases in *drosophila* causes severe developmental defects, often associated with lethality (Chew et al., 2004; Daish et al., 2004; Xu et al., 2005). Activation of caspases require the oligomerization of Dark, Ced-4 ortholog (Rodriguez et al., 1999).

1.3.3 Apoptosis in mammals

In mammals, apoptosis takes place through different pathways, depending on the type of stimuli. The well-studied pathway, mitochondrial dependent apoptosis, is associated with release of proteins such as cytochrome c from mitochondria. Once released, cytochrome c interacts with Apoptotic Procaspase Activating Factor 1 (Apaf-1), together with caspase-9, an initiator caspase, form the apoptosome. The apoptosome then activates executioner caspases (Green and Reed, 1998). This process is regulated at various stages. Anti-apoptotic members of BCL2 family proteins inhibit the release of cytochrome c while pro-apoptotic members promote it. Apaf-1 is found as inactive monomer in the cytosol, activation of which is dependent on cytochrome c binding. Caspases are inhibited by inhibitors of apoptosis (IAPs). The death signals activate initiator caspases, which then activates executioner caspases. The activated caspases then degrade intercellular components (Ellis and Horvitz, 1986; Jiang, 2012).

Apaf-1 is a human homolog of the CED-4 gene in *Caenorhabditis elegans* and shares the homology in the sequence of 320 amino acids and a conserved nucleotide binding site. However, *C.elegans* CED-4 lacks WDRs. Moreover, CED-4 and Apaf-1 biochemically function to activate CED-3 processing and caspase-3, respectively (Zou et al., 1997; Cecconi et al., 1998). CED-4 is blocked by Ced-9 which shows a great sequence and functional similarity with anti-apoptotic BCL-2, a human proto-oncogene protein that acts in mammals as negative regulator of apoptosis. However, mammalian Apaf-1 is blocked by itself. This shows the different function of the same family of proteins in worms and mammals.

Besides, it seems that *C.elegans* apoptosome translocates to outer nuclear membrane. This translocation has not been reported for mammalian apoptosome. Initiator and executive caspases in mammalian cells are equivalents of CED-4 and CED-3. Like CED-9 *C.elegans*, BCL-2 and BCL XL function in the regulation of apoptosis.

In mammalian cells, apoptosis is more complicated, but it follows the same principles. Mitochondria play important roles in apoptosis in most organisms, although to different extent (Oberst et al., 2008). Bax and Bak (pro-apoptotic members of BCL-2 family) knockout mice were shown to be resistant to apoptotic stimuli and the mice were developmentally defective (Lindsten et al., 2000; Wei et al., 2001). This shows the crucial role for mitochondria and its outer membrane permeabilization (MOMP) in mammals.

However, there are fundamental differences on how mitochondria and the released cytochrome c function between *C. elegans* CED-4 and *Drosophila* Dark and their homologs in other species. It seems that mitochondria do not play a key role in caspase activation and apoptosis in *C. elegans* and *D. melanogaster* during apoptosis. MOMP does not occur in *C. elegans*. In *D. melanogaster* MOMP occurs although it seems that it is a consequence rather than a cause of caspase activation (Abdelwahid et al., 2007; Ryoo and Baehrecke, 2010). Furthermore, unlike CED-4 in *C. elegans*, mammalian Apaf-1 requires cytochrome c in addition to dATP. *Drosophila* and mammalian Apaf-1 contain WD repeats that provide a binding site for regulatory proteins (Cecconi, 1999; Tittel and Steller, 2000).

Unlike *C. elegans*, the apoptotic machinery is sophisticated in vertebrates in terms of the number of the genes involved and the size of the protein families. *C. elegans* has one homolog of each CED-3, CED-4, and CED-9, while in human, 12 caspases (CED-3 homologs) and 13 Bcl-2-like proteins (CED-9 homologs) and a number BH3 motif only proteins (similar to EGL-1) exist (Shaham, 1998; Abraham and Shaham, 2004; Adrain et al., 2006; Zmasek et al., 2007). The similar protein families have been reported in birds, amphibians, and, and fish (Reed, 2000).

Considering all similarities and differences, the CED-4/Apaf-1 family is the only protein in the apoptotic machinery that was not duplicated during evolution and speciation in any of the genomes studied (Zmasek et al., 2007), suggesting the central role for CED-4/Apaf-1 in all organisms. Such one-to-one orthologs represent a high level of functional similarity (Eisen, 1998).

1.4 Mechanism of apoptosis

In mammalian cells, the extrinsic and intrinsic pathways are two of the major pathways that lead to caspase activation [reviewed by (Reed, 2000)]. The extrinsic pathway applies the death receptors on the surface of the cells. In contrast, intrinsic pathway or mitochondrial pathway, is associated with the release of cytochrome c from intermembrane space of mitochondria to cytosol. Both pathways lead to activation of caspases which break down the proteins within the cells and manifest the morphological changes such as the formation of the apoptotic bodies.

1.4.1 Extrinsic pathway of apoptosis

The extrinsic pathway is named due to the initiation point which is the extracellular receptors bind to extracellular ligands. Death receptors are members of Tumor Necrosis Factor (TNF) family, a subgroup of which shares a Death Domain (DD). When ligands bind to death receptors such as CD95, TRAIL-R1, and TRAIL-R2, the intracellular DD interacts with an adaptor protein called Fas-Associated Death Domain (FADD). FADD then forms the Death-Inducing Signalling Complex (DISC) beneath the cell membrane, which then activates procaspase-8 and procaspase-10. In the type I cells, activated caspase-8 is sufficient to induce apoptosis, however, in type II cells the activated caspase-8 is not enough and the cells amplify the death signal using mitochondrial pathway. This amplification by extrinsic pathways involves BID protein, a member of BCL2 family. Activated caspase-8 cleaves BID and the produced truncated BID (tBID) translocates into mitochondrial membrane and assists in releasing the cytochrome c and Smac (Figure 1.3) (Schmitz et al., 2000; Igney and Krammer, 2002).

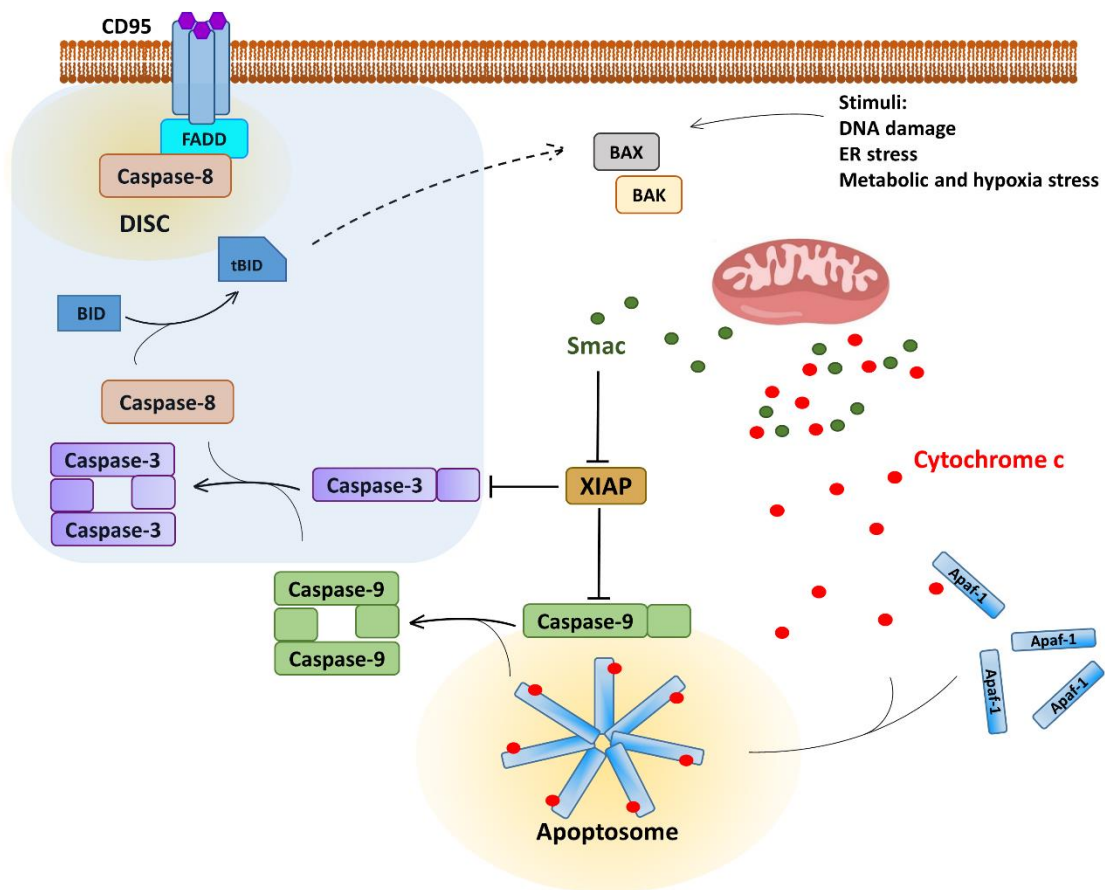


Figure 1.3. Apoptosis signalling pathways. Binding of the ligands to CD95 forms a timer that recruits adaptor proteins FADD in the intracellular space. This platform called DISC and activates caspase-8. Activated caspase-8 processes procaspase-3. Caspase-3 then cleaves the cellular compartments. In type II cells, caspase-8 cleaves BID proteins, through which extrinsic pathway cross-talks to intrinsic pathway of apoptosis. Intrinsic pathway is triggered by a range of stimuli such as DNA damage, ER stress, metabolic and hypoxia stress etc. These stimuli lead to the release of mitochondria-localized proteins like cytochrome c and Smac by activating BCL-2 family proteins. Smac inhibits the XIAP and remove the inhibitory effect of XIAP on caspase-9 and -3. Cytochrome c binds to Apaf-1 monomers and facilitates the oligomerization of Apaf-1 and apoptosome formation. Apoptosome then recruits and activates initiator caspase-9 which further processes and activates caspase-3.

1.4.2 Intrinsic (mitochondrial- mediated) pathway of apoptosis

Intrinsic or mitochondrial-dependent apoptotic pathway is associated with the release of some proteins such as cytochrome c, smac and AIF from the mitochondria into the cytosol. Cytochrome c transports electrons between complex III and IV in the respiratory chain in the inner mitochondrial membrane. When released into the cytosol, cytochrome c binds to adaptor protein Apaf-1 and assists in oligomerization of Apaf-1. Binding of cytochrome c and Apaf-1 intramolecular nucleotide exchange lead to the formation of heptameric complex called the apoptosome which then recruits and activates procaspase-9 (Lademann et al., 2003; Bao and Shi, 2007). Activated caspase-9 further activates executioner caspases-3 and 7. Therefore, apoptosis is an energy-dependent mechanism and if the ability of mitochondria to produce energy is disrupted at the early stages of apoptosis, apoptosome complex will not be formed and procaspase-9 will not be processed.

Smac and AIF (Apoptosis- Inducing Factor) are the other proteins released from the mitochondria. Smac assists in removal of the inhibitory effect of IAPs and therefore enhances caspase activation (Du et al., 2000; Emeagi et al., 2012). AIF resides in the intermembrane space of mitochondria and during apoptosis, proteolysis of AIF results in release and translocation to the nucleus. AIF, then, proceeds the chromatin condensation, and huge DNA degradation in caspase-independent fashion. Apart from its apoptotic role, AIF also contributes to cell survival, maintenance of mitochondrial morphology and energy metabolism (Candé et al., 2002, 2004; Sevrioukova, 2011).

Here, the structure of key components of mitochondrial apoptosis will be briefly overviewed. I describe how cytochrome c, a co-factor for Apaf-1 oligomerization, is released and interacts with Apaf-1. I then look at the structure of Apaf-1 and the mechanism by which it switches to its active form. Then I describe the current models for apoptosome formation and how the apoptosome activates caspases.

1.4.2.1 Cytochrome c

Cytochrome c is a heme-containing, water soluble protein (12.4 kDa) located in the inner membrane of mitochondria. When a cell receives the apoptotic signal such as DNA damage, metabolic stress or unfolded proteins, intrinsic pathway of apoptosis is triggered by release of cytochrome c into the cytosol (Ow et al., 2008). Release of cytochrome c seems to be a two-step process. First, cytochrome c dissociates from its site on inner membrane. Then it translocates to cytosol by crossing the outer membrane.

In the dissociation step, cytochrome c is detached from cardiolipin, a membrane phospholipid. It seems that the majority of cytochrome c molecules are cardiolipin-bound through 1) electrostatic bonds: in physiologic pH, the cytochrome c net charge is +8 and establishes very strong electrostatic interaction with cardiolipin, an anion in physiological pH, and 2) hydrophobic channel: cytochrome c contains a hydrophobic channel that accommodates acyl chain of cardiolipin. It is hypothesized that oxidation of cardiolipin contributes to the dissociation of cytochrome c, due to the lower affinity of oxidized cardiolipin to cytochrome c (Boussif et al., 1995; Ott et al., 2002, 2007; Kalanxhi and Wallace, 2007; O'Brien et al., 2015). Phospholipase A₂ oxidizes cardiolipin in the presence of Reactive Oxygen Species (ROS). Dissociation of cytochrome c could also be triggered by increase in the intracellular Ca²⁺ concentration, since high concentration of Ca²⁺ weakens the electrostatic bond between cytochrome c and cardiolipin. Moreover, high concentrations of ROS increases the dissociation of cytochrome c (Ow et al., 2008).

In the translocation step, dissociated cytochrome c translocates to cytosol by passing through the pores in the outer membrane of mitochondria (Ott et al., 2002; Muñoz-Pinedo et al., 2006). Several mechanisms have been proposed for permeabilization of outer membrane of mitochondria, the two of which are Bax/Bak-induced pore formation and ceramide channels.

1. Bax and Bak oligomerization form the pores

The B-cell lymphoma protein-2 (BCL-2) family of proteins are the most important regulatory factors in intrinsic pathway of apoptosis. Some members of the family promote cytochrome c release, while others prevent it. Therefore, BCL-2 family is responsible for controlling the integrity of the mitochondrial membrane and regulates the cell survival.

BCL-2 proteins like Bax and Bak are essential for permeability of the outer membrane of mitochondria (Ow et al., 2008). Under non-apoptotic conditions, Bax proteins are found as inactive monomers in cytosol. Upon induction of apoptosis, Bax proteins are activated and translocate to outer membrane of mitochondria where oligomerization occurs, and pores are formed. These pores allow cytochrome c to leave the mitochondria (Desagher and Martinou, 2000). Conformational changes in Bak proteins induces oligomerization and formation of larger pores. Bak also facilitates the movement of Bax proteins (Ow et al., 2008).

Another possible mechanism is through the Voltage Dependent Anion Channel (VDAC). Many of the studies suggest that channels formed by VDAC proteins are very small and only pass the proteins with 1.5 KDa (Shimizu et al., 1999). Another hypothesis is that close VDAC channels may cause contemporary hyperpolarization of the mitochondria leading to osmotic imbalance and disruption of outer membrane and release of proteins (Shimizu et al., 1999; Kroemer et al., 2007). The third hypothesis explains the contribution of VDAC proteins in the formation of permeability transition pore (PTP). Flow of water and low molecular weight substances in the mitochondrial matrix disrupt the membrane (Garrido et al., 2006).

2. Cytochrome c release through ceramide channel

Ceramide channel is a lipid pore made of ceramides and provides the two-way transportation of compounds. Ceramides are the precursor of some gangliosides which play roles in apoptosis. In One study, addition of GD3 ganglioside to isolated mitochondria led to the release of cytochrome c to the environment outside the mitochondria. Furthermore, addition of this ganglioside in the presence of Bax increased the rate of cytochrome c release (Ott et al., 2002; Mari et al., 2003). In the cytosol, cytochrome c binds to and activates Apaf-1. To understand how cytochrome c binds to Apaf-1, what interactions are involved and where the binding site for cytochrome c is, we need to look at the structure of Apaf-1.

1.4.2.2 Apaf-1

Apaf-1 is a multi-domain protein with three functional parts (Figure 1.4). CARD (Caspase Recruitment Domain) at the amino end, WD-40 at the carboxyl end and NOD (Nucleotide and Oligomerization Domain) between the two above mentioned domains. CARD interacts with procaspase-9 (Zhou et al., 1999). NOD is responsible for Apaf-1 oligomerization and apoptosome formation. WD-40 domain seems to be a regulatory domain and interacts with cytochrome c (Zou et al., 1997; Vaughn et al., 1999; Elmore, 2007).

Structural studies showed that NOD is subdivided into four sub-domain: NBD (Nucleotide binding domain), HD1 (Helical domain 1), WHD (Winged Helical Domain) and HD2 (Helical Domain 2) (Reubold et al., 2011). X-ray crystallography studies showed that (d)ATP binds to ATPase sub-domain of the NBD in NOD, probably when Apaf-1 is synthesized (Riedl et al., 2005; Riedl and Salvesen, 2007).

WD-40 domains are subdivided to WD1 and WD2 which consist of seven and eight blade β -propellers, respectively. A β -propeller is a symmetrical structure made of four to eight-stranded antiparallel beta sheets (also known as blades) arranged in a circle (Chen et al., 2011).

When released, cytochrome c binds to the WD-40 domains and induces conformational changes that WD-40 no longer hinders NOD and CARD (Hu et al., 1998). This is the “semi-open” form of Apaf-1 which is still unable to oligomerize and form a complex. In the semi-open state, CARD domain interacts with WHD and NBD. This interaction makes CARD domain inaccessible to caspase-9. Moreover, NBD is blocked by CARD domain which prevents oligomerization (Acehan et al., 2002a; Riedl et al., 2005). NBD is similar to the members of AAA⁺ family, characterized by forming oligomers composed of six and seven monomers. These oligomers function as a molecular machinery in biologic systems that link the ATPase activity to strong conformational changes (Riedl and Salvesen, 2007).

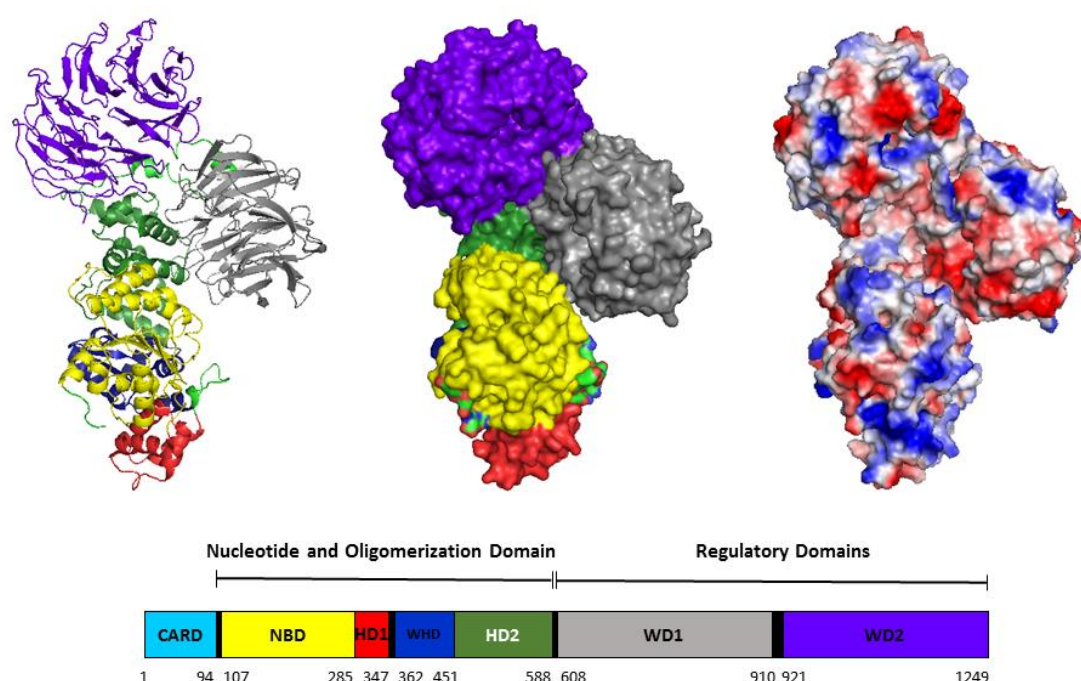


Figure 1.4. Apaf-1 structure. Apaf-1 composed of CARD, NOD and WD-repeats. NOD contains Nucleotide Binding Domain (NBD), Helical Domain 1 (HD1), Winged Helical Domain (WHD), and Helical Domain 2 (HD2). Regulatory domains contain WD1 and WD2 with seven and eight blade β -propellers, respectively (left). Surface area of the Apaf-1 (middle). Electrostatic potential surfaces of the Apaf-1. Red areas are negatively charged residues and blue areas are positively charged amino acids (right). The charge distribution on the surface of the closed Apaf-1 molecule shows that the inner face of β -propellers (WD domains) is made of negatively charged patches that is a potential site for binding of positively charged cytochrome c.

Apaf-1 is found as a monomer in cytoplasm. It is proposed that WD-40 domains hold the protein in inactive or closed form. Electron microscopy studies suggest that WD-40 domains fold back and cover the other domains and therefore keep the molecule in locked form (Acehan et al., 2002b; Yuan et al., 2010). In this position, WD-40 domains put the other domains sterically far from each other and therefore there is no chance for oligomerization (Riedl and Salvesen, 2007). Upon cytochrome c binding to an area between the two WD-40 domains, WD1 rotates $\sim 57^\circ$ upwardly and the NBD-HD1 subunit move downward 146° around an axis parallel to helix $\alpha 24$ of the WHD. The binding patch of WD1 is located at the lower half of the propeller, therefore it rotates upwardly to allow the fully binding of cytochrome c. This rotation also disconnects the only interaction between WD1 (Asp616) and NBD-HD1 (Lys192). NBD-HD1 rotation makes NOD available for oligomerization as well as relocation of CARD domain. HD1 also undergoes a minor movement to be placed at the right position (Reubold et al., 2011).

1.4.2.3 Cytochrome c binding to Apaf-1

Cytochrome c binds to a cleft between WD domains with the contribution of seven lysine residues (Lysine 25, 27, 39, 55, 72, 73 and 79). However, the interaction to WD2 (8-blade) is stronger due to the numerous van der waals interactions. A $\sim 3\text{--}5$ Å gap exists in the interface between cytochrome c and WD1 (7-blade) (Figure 1.5).

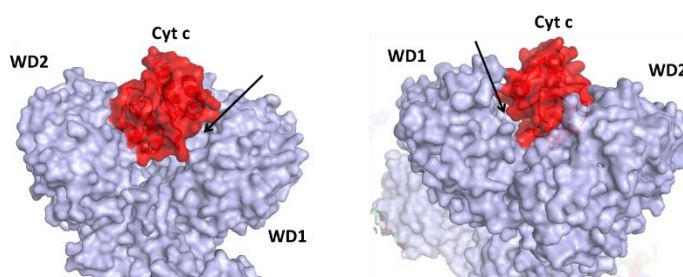


Figure 1.5. Binding of cytochrome c to WD repeats of Apaf-1. Cytochrome c interacts to both WD1 and WD2 of Apaf-1. However, the interaction with WD2 is more intensive. Front view of cytochrome c (Cyt c) bound to WDRs (left panel) and back view (right panel). The arrows display the gap between cytochrome c and WD1. The image was created using 5JUY PDB file in Pymol.

The putative interactions and the amino acids contribute to Apaf-1/cytochrome c interaction were calculated and displayed in figure 1.6, 1.7 and table 1.1. Cytochrome c binds to the area between WD1 and WD2 which is well fitted based on the shape and charge (Zhou et al., 2015). Three hypothetical H-bonds and a number of Van der Waals contacts were detected in the interface between cytochrome c and WD2 of Apaf-1. Carbonyl oxygen of Gly56 from cytochrome c makes a H-bond to the side chain of Thr1087 in WD2 domain of Apaf-1. The side chains of Lys39 from cytochrome c probably makes two H-bonds to the carbonyl oxygen of Phe1063. The interface between WD1 and cytochrome c includes the H-bond between Lys72 from cytochrome c and Asp902 from Apaf-1 and between Gln12 from cytochrome c and Glu700 from Apaf-1 (Figure 1.6).

Three boxed regions show the close-up view of interactions. Thr1087 from Apaf-1 makes a hydrogen bond to Gly56 from cytochrome c (Figure 1.6B), Phe1063 makes a H-bond to Lys39 (Figure 1.6C), Asp902 make a H-bond to Lys72 as well as a salt bridge (Figure 1.6D), and Gln12 makes a H-bond to Glu700 (Figure 1.6E).

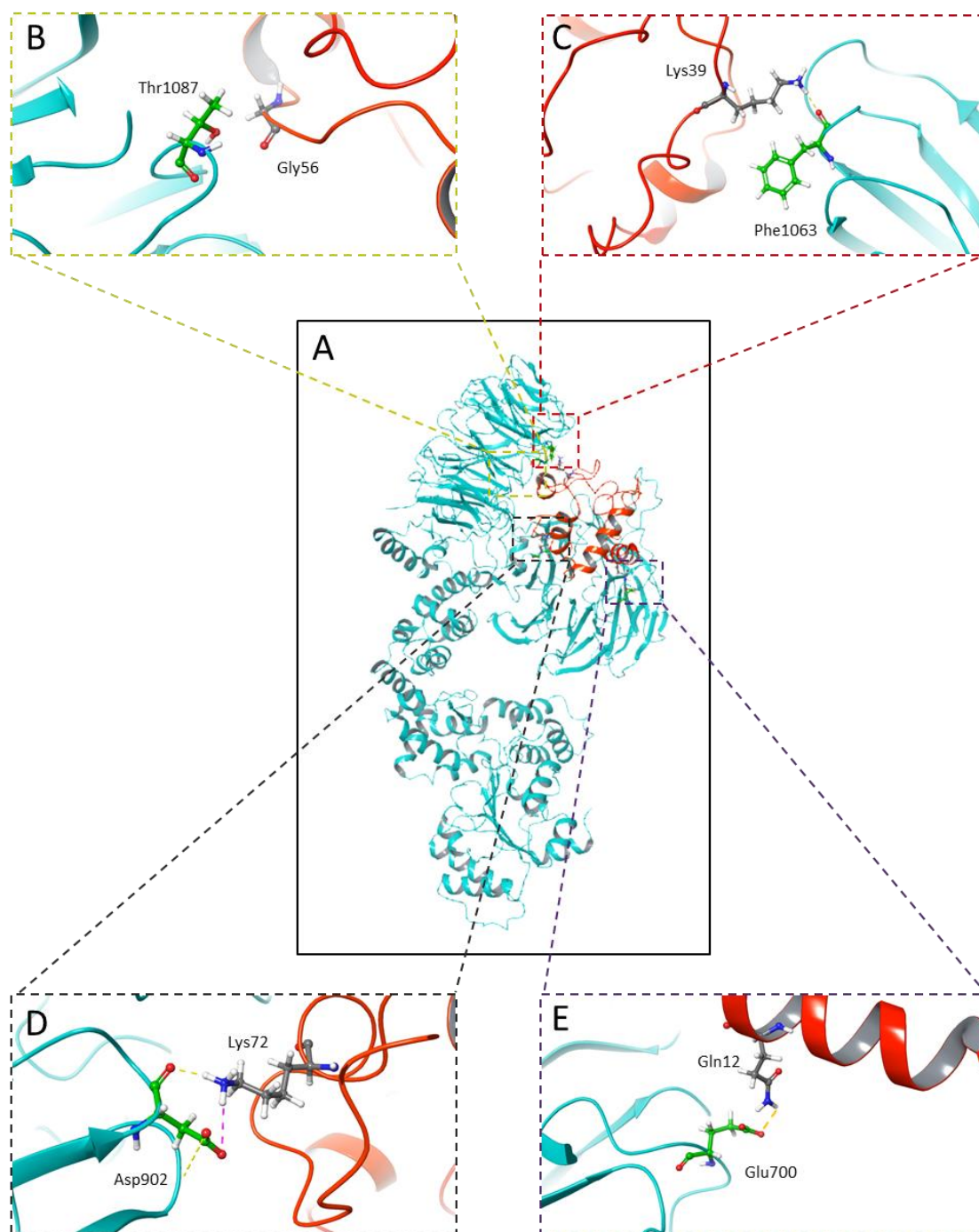


Figure 1.6. Interactions between Apaf-1 and Cytochrome c. For details see the text.

These are the most potent calculated h-bonds when the distance was less than 3Å between the residues involved in the interactions. However, considering the longer distances to 4.5Å revealed some other H-bonds as listed in Table 1.1.

Hydrogen bond		Salt Bridge	Distance (Å)
Apaf-1	Cytochrome c		
Tyr619	Ala83	-	4.5 Å
Gln700	Gln12	-	4.5 Å
Gln844	Lys79	-	4.4 Å
Asp902	Lys72	✓	2.8 Å
Phe1063	Lys39	-	3.0 Å
Gln1085	Lys39	-	4.2 Å
Thr1087	Gly56	-	2.9 Å
Asp1106	Ile57	-	4.6 Å
Arg1131	Tyr74 Glu66	-	4.1 Å 4.7 Å
Asn1219	Pro76	-	4.5 Å
Gln12	Glu700 Gln701	-	2.8 Å 4.5 Å

Table 1-1. The calculated interactions between the Apaf-1 and cytochrome c. All interactions were determined in 4.5Å distance. The residues involved in the interactions listed. The most putative interactions are those underlined in the table with distance $\leq 3\text{Å}$.

In addition to the H-bonds and salt bridges, Van der Waals contacts also contribute to the binding of cytochrome c to Apaf-1 (Figure 1.7). Pro76 and Ile81 make Van der Waals contacts to the adjacent area in WDR domains with indole ring of Trp1179 and Trp884, respectively. Gly56 also make Van der Waals contact to WD2. However, no disulfide bond and Pi stacking were identified to be important for this interaction. Lys72 plays a key role in the stable interaction of cytochrome c to Apaf-1. Although other residues at positions 7, 25, 39, 62 and 65 are also required for the proper interaction, Lys72 mutants intensely decreased the apoptotic function of cytochrome c (Abdullaev et al., 2002; Ow et al., 2008).

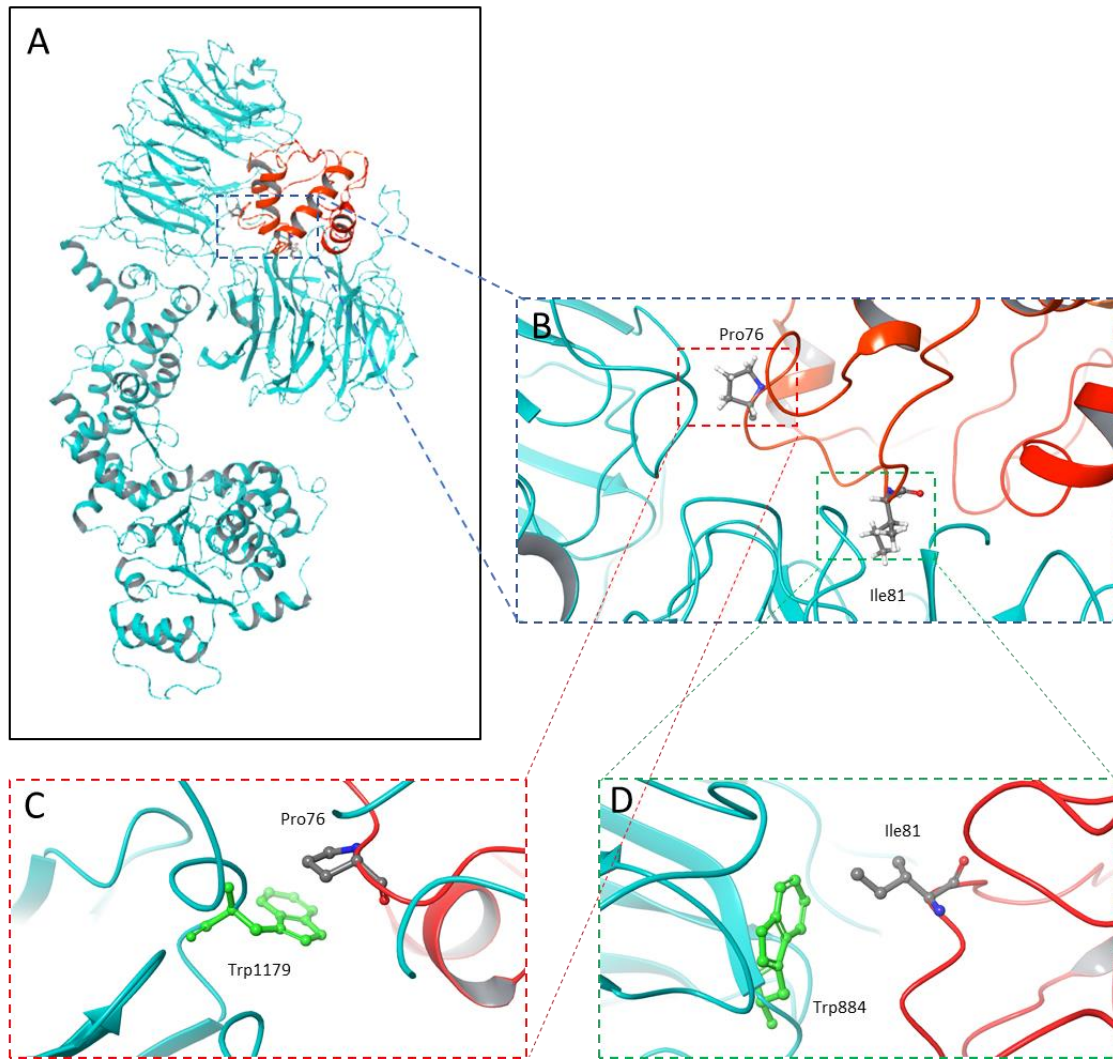


Figure 1.7. Putative Van der Waals interactions between Apaf-1 and cytochrome c.

(A) Two putative Van der Waals interactions between cytochrome c and WD domain of Apaf-1. (B) Shows the key residues in cytochrome c responsible for the interaction. (C) Pro76 from cytochrome c make an interaction with indole ring of Trp1179 in WD2 of Apaf-1. (D) Ile81 from cytochrome c make an interaction with indole ring of Trp884 in WD1 of Apaf-1.

1.5 Apoptosome formation

In the presence of strong apoptotic stimuli, the apoptosome complex is formed and activates caspase-9. Cryo-electron microscopy studies provided pictures of the complex with 12.8 Å resolution (Acehan et al., 2002a). Apaf-1 monomers form a wheel-like complex. In this

structure, WD-40 domains carrying cytochrome c are the spikes of the wheel, NBD and CARD are placed at the centre of the wheel and CARD domains are exposed for activation of caspase-9 (Riedl and Salvesen, 2007).

Two models explain how CARD and NOD are placed next to each other both based on cryo-electron microscopy. In the first model presented by Riedl, each WHD sub-domain of NOD connects the two adjunct ATPase domains leading to formation of the bigger outer ring while CARD domains are at the hub of this ring and form a smaller inner ring (Riedl and Salvesen, 2007). The second model, “classic model”, is based on simulation studies in which ATPase domains form a central ring in row and CARD domains form a bigger ring on the top of the central ring. The common issue in both models is that Apaf-1 CARDS form a ring where caspase-9 could be placed on (Diemand and Lupas, 2006).

Two recently released structures of apoptosome explain the interactions within the complex in detail, although the main ideas are very similar. A recent structure of active apoptosome determined by cryo-electron microscopy showed the formation of an acentric disk on the central hub of the apoptosome (Figure 1.8 and Figure 1.9). The central hub is a two nested ring that contains seven copies of the NBD, HD1 and WHD. HD2 spikes extend outwardly and link to 7- and 8-blade β -propellers, V-shaped sensor that accommodates cytochrome c (Cheng et al., 2016). Four pairs of Apaf-1/procaspase-9 CARDS form the CARD disk with the fourth procaspase-9 CARD at lower occupancy. Four out of the seven Apaf-1 CARDS contribute to form the disk (Figure 1.8). The remaining three Apaf-1 CARDS do not participate in the CARD disk. However, band shift assay showed that they have a partial ability to bind procaspase-9 molecules in the absence of steric restraints. Apaf-1 monomer can form a CARD-CARD-mediated complex with procaspase-9 at 1:1 ratio. However, proposed stoichiometry of 2 to 5 procaspase-9 per apoptosome limits the number of Apaf-1 CARDS that recruits procaspase-9 (Malladi et al., 2009; Yuan et al., 2011; Hu et al., 2014). Thus, Apaf-1 CARDS forming the disk and possibly one excluded CARD can recruit procaspase-9 to the apoptosome. The authors hypothesized that the parked procaspase-9 is

a backup when an odd number of zymogens are recruited to the apoptosome. Procaspase-9 make no direct interaction with central hub with their N- and C-termini pointing towards the outside. This facilitates the access of the long linker from procaspase-9 CARDs in the disk to catalytic domains bound to the apoptosome (Cheng et al., 2016).

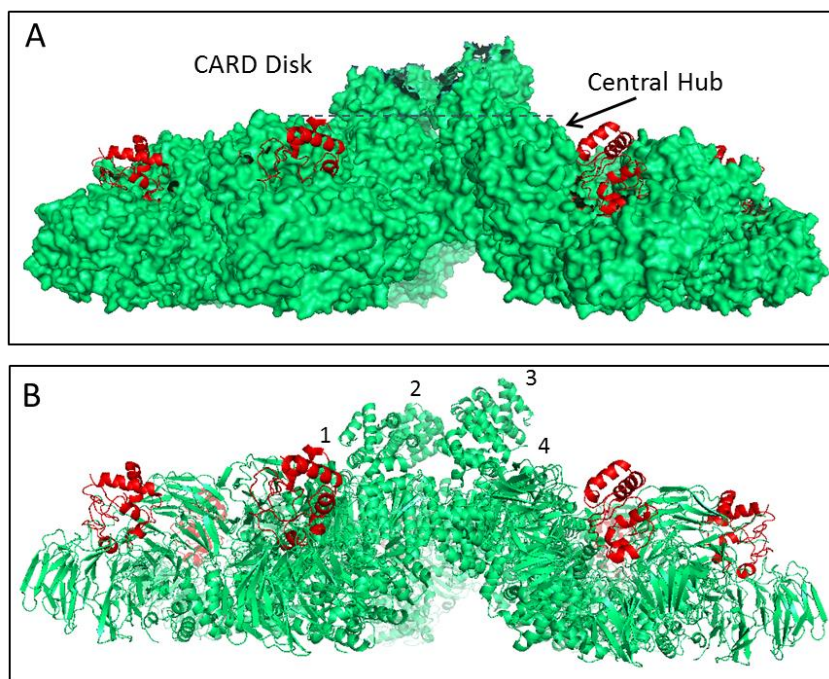


Figure 1.8. Apaf-1 CARD disk. (A) Surface presentation of the apoptosome. The central hub of apoptosome is formed by contribution of NBD, HD1 and WHD from seven Apaf-1 molecules. Apaf-1 CARDs are above the central hub. (B) Secondary structure of apoptosome. As shown, only four of the seven Apaf-1 CARDs contribute to the CARD disk. The CARD disk is acentric as orientation of Apaf-1 CARDs are different. Numbers show the Apaf-1 CARDs with the Apaf-1 number 3 placed above the other three Apaf-1 CARDs. Cytochrome c is still bound to Apaf-1 in the apoptosome (red). Images were generated using PDB file for apoptosome (5JUY) in Pymol.

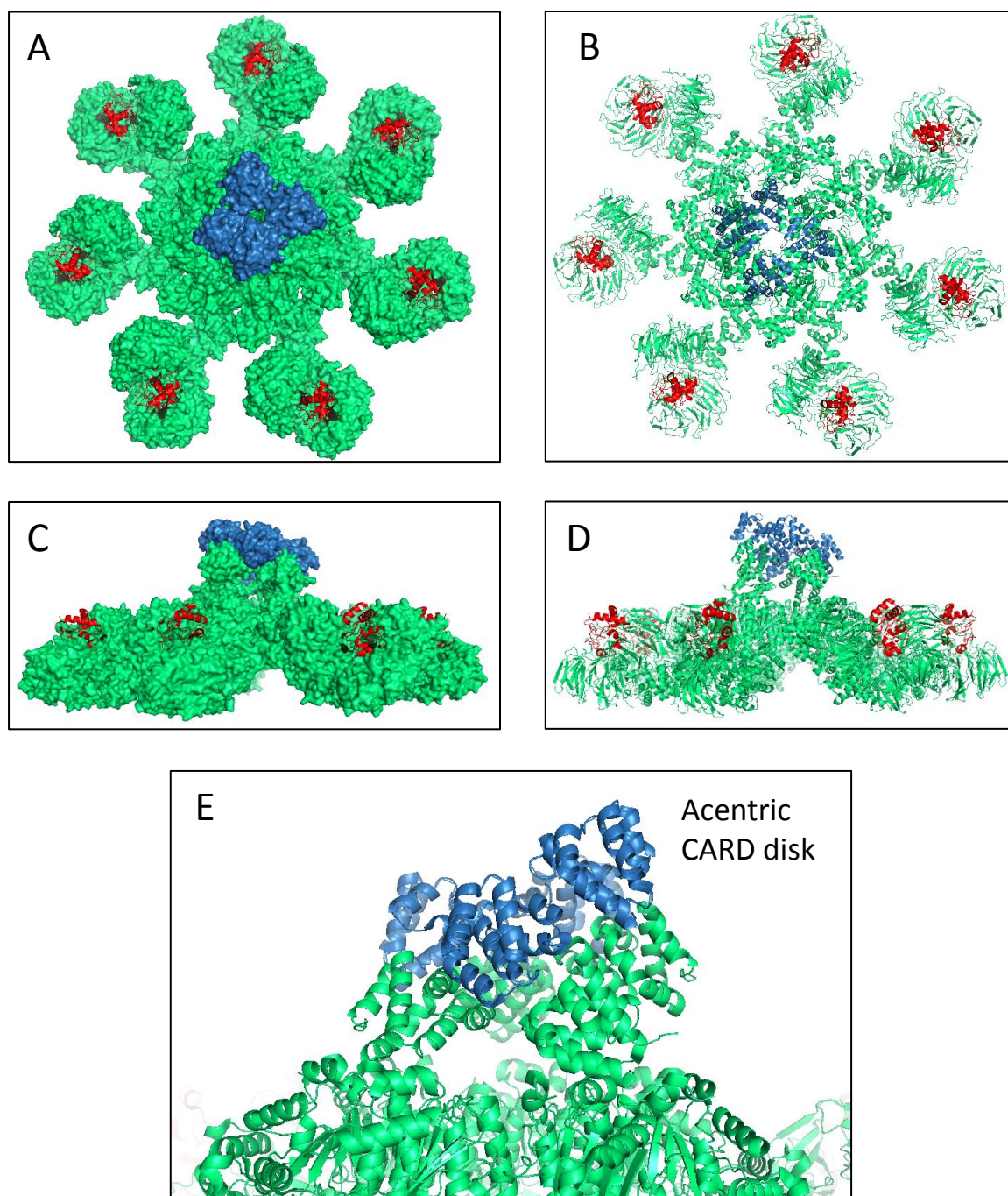


Figure 1.9. Holoapoptosome CARD-CARD disk. (A) and (B) top views of the surface area and secondary structures of the apoptosome. Four caspase-9 CARDS (blue) are placed atop the central hub. (C) and (D) side view of the complexes as in (A) and (B), respectively. (E) Eight CARDS form an acentric complex. Caspase-9 CARDS only contact Apaf-1 CARDS (Green). Even Apaf-1 CARDS are not planar. At CARD disk, every Apaf-1 CARD interacts to two caspase-9 CARD. Images were generated using PDB file for apoptosome (5JUY) in Pymol.

To get the idea of the interactions at CARD disk, the 3D structure of apoptosome complex (5JUY) downloaded from PDB (Protein Data Bank) and optimized, as described in Material and Methods. The interactions determined in 4 Å distance. In the CARD disk, every two caspase-9 proteins interact with one Apaf-1. The interactions between caspase-9 and Apaf-1 are mainly hydrogen bonds and salt bridge (Figure 1.10). Gln78, Lys81 make hydrogen bond as well as salt bridge to Arg36 and Glu33, respectively, while Asp82 make H-bond to Ser67 of one caspase-9. Asp27 makes H-bond and salt bridge to Arg52 of the other caspase-9.

Hydrogen bond		Salt Bridge	Distance (Å)
Apaf-1	Caspase-9		
Gln78	Arg36	✓	3.1
Lys81	Glu33	✓	2.6
Asp82	Ser67	-	3.1
Aap27	<i>Arg52</i>	✓	3.3

Table 1.2. Interactions between caspase-9 and Apaf-1 in the CARD disk. The *italic* residues show the interaction of the second caspase-9 with Apaf-1.

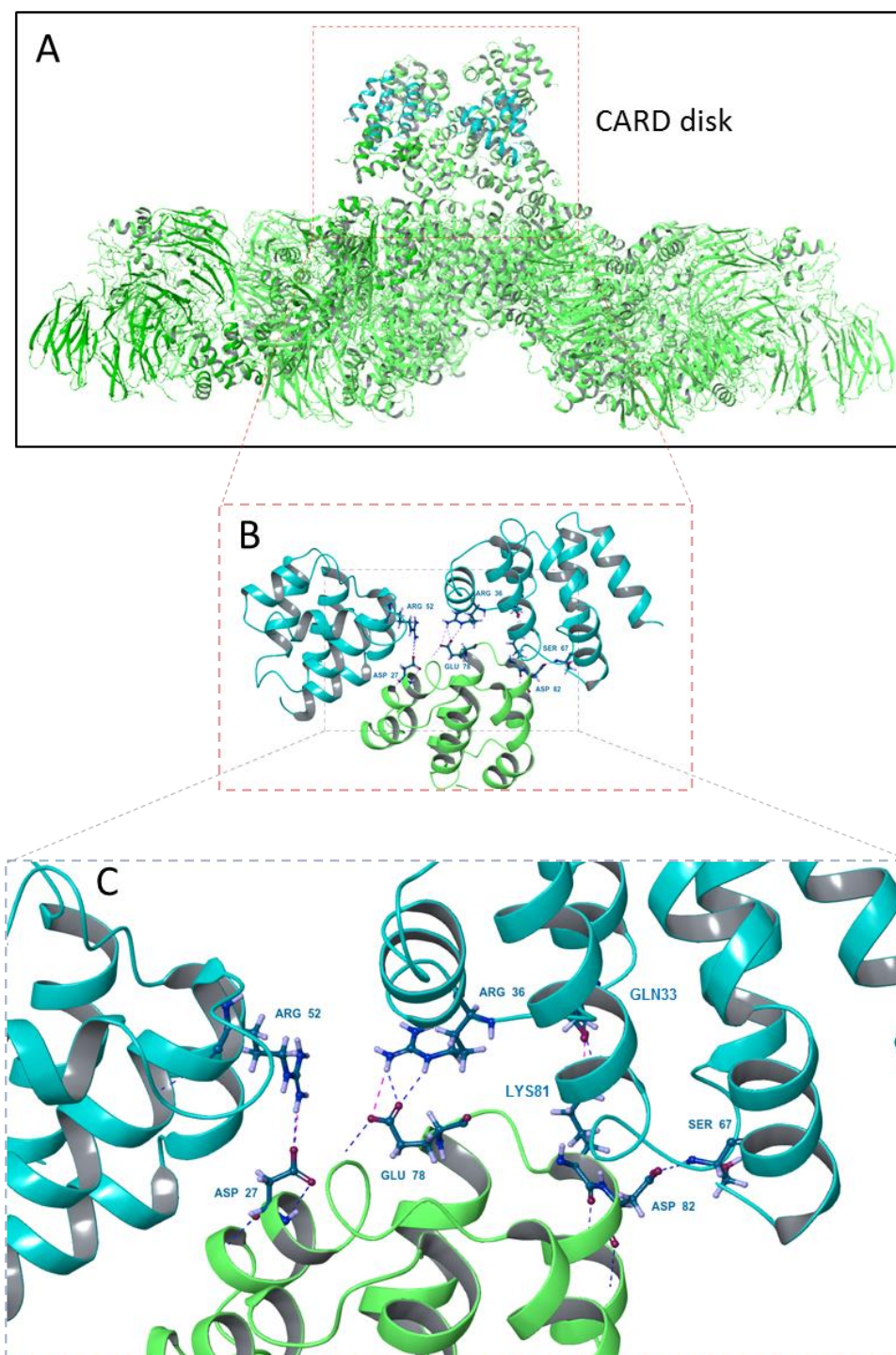


Figure 1.10. Caspase-9 and Apaf-1 interactions at CARD disk. (A) Four caspase-9 and four Apaf-1 CARDS form CARD disk above the central hub. (B) A typical interaction between two caspase-9 CARDS and Apaf-1 CARD. For clarity, the other molecules removed. Caspase-9 CARD only interacts with Apaf-1 CARD not the central hub. (C) Residues involved in making interactions. Hydrogen bonds are in blue and salt bridges are in red dashed lines. Images were generated using PDB file for apoptosome (5JUY) in Pymol.

The second model for apoptosome formation and caspase-9 activation was presented in 2017 based on cryo-EM and biochemical analysis. Accordingly, a globular density was identified above the central hub where eight CARDs form two layers of four Apaf-1 CARDs and four caspase-9 CARDs on top of the Apaf-1 CARDs (Figure 1.11). In the CARD complex, four Caspase-9 CARDs and only three of the four Apaf-1 CARDs directly interact with the apoptosome platform, due to the asymmetric interaction of Apaf-1 CARDs and apoptosome. CARD complex is made of four Apaf-1 CARDs and the other three Apaf-1 CARDs cannot be placed on top of the 4:4 CARD complex. The reason is a short 14-amino acid linker between the CARD and the NBD.

In this model a stable heterotrimeric complex is formed by two Apaf-1 CARDs and one caspase-9 CARD via type I and type II interfaces. The CARD-CARD interactions at the centre of the hub form four overlapping heterotrimeric complexes. Three of the four caspase-9 CARDs in the central CARD complex, interacts with two adjacent Apaf-1 CARDs via both type I and II interfaces and the fourth caspase-9 CARD interacts only by type II interface with Apaf-1 CARD. Stability of the type I and II interfaces makes the CARD complex thermodynamically most favourable. Besides, another sickle-shaped density was identified at the periphery of the hub including two Apaf-1 CARDs and one caspase-9 CARD (Figure 1.11) (Yuan et al., 2010, 2011; Cheng et al., 2016).

It has been shown that the interface between the CARD complex and the central hub of the apoptosome is required for activation of caspase-9. Mutation of Apaf-1 at this interface led to apoptosome formation but was unable to recruit and activate caspase-9. As Apaf-1 CARD makes stable interaction with caspase-9 CARD, the mutations that do not affect the interactions at the interface was expected to activate caspase-9. To explain this, we may hypothesize that Apaf-1 CARD is not available to caspase-9 CARD, and caspase-9 recruitment and assembly of the CARD complex take place simultaneously (Hu et al., 2014; Li, Zhou, et al., 2017).

This model considers a regulatory role for caspase-9 CARD. The CARD inhibits the proteolytic activity of caspase-9 and the following linker further increases the inhibitory effect. Therefore, one possible explanation for formation of the CARD complex is to move the CARD and the linker sequences away from the protease domain of caspase-9. Based on the biochemical analysis, the catalytic activity of the protease domain of caspase-9 is a fraction of full-length caspase-9 implying another role for apoptosome in caspase-9 activation.

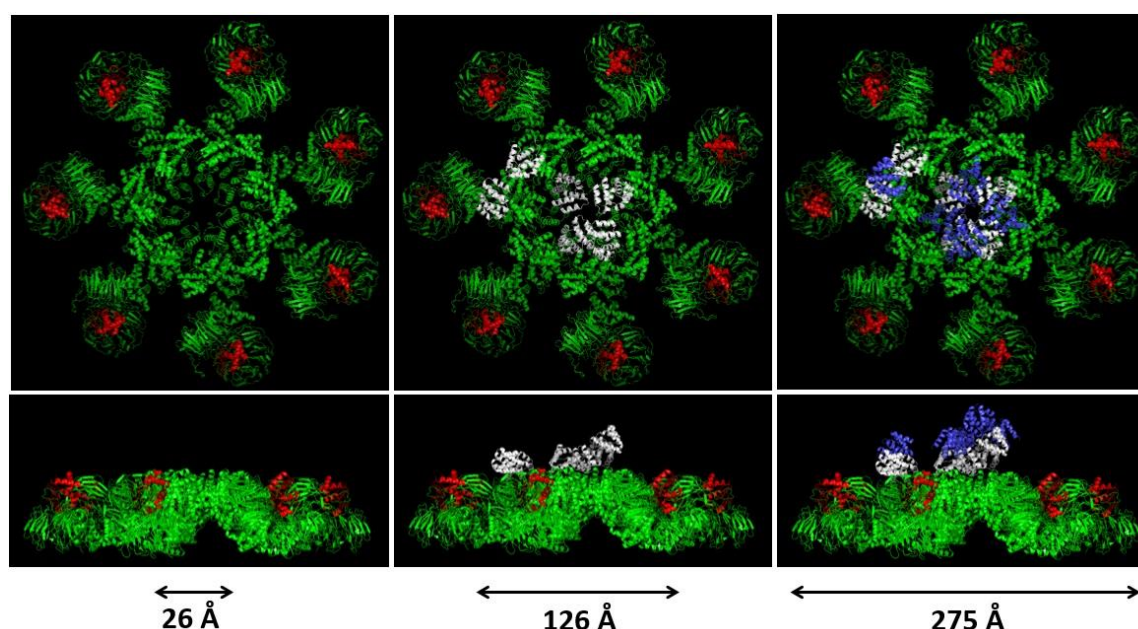


Figure 1.11. Apoptosome complex. (A) Top view of the apoptosome complex. Left: Apaf-1 CARDs have been removed to clearly show the inner ring. Cytochrome c binds to a groove between two WD-40 repeats and is coloured red. Middle: Apaf-1 CARDs are coloured white. Right: Caspase-9 CARDs are placed on the top of Apaf-1 CARDs and coloured blue. (B) Side view of the corresponding apoptosome complexes shown in (A). Four of the Apaf-1 CARDs are placed on the top of the inner ring (middle) and caspase-9 CARDs interact to Apaf-1 CARDs and placed above the Apaf-1 CARDs. The other two Apaf-1 CARDs form a heterotrimeric complex with another caspase-9 CARD. This heterotrimeric complex is placed peripherally. In this model, each caspase-9 CARD at the central hub interacts to the two neighbouring Apaf-1 CARDs. Images were generated using PDB file for apoptosome (5WVE) in Pymol.

1.6 Apoptosome-dependent caspase activation

Procaspases are categorized as initiator and executioner caspases, produced as an inactive single-chain polypeptide. These zymogens must be proteolytically cleaved to be activated and become functional. Initiator caspases, including caspase-2, -8, -9, and -10, contain moderately long prodomains by which they interact to adaptor proteins. Then caspases are activated in high molecular weight complexes by self-cleavage. Caspase-9 and -8 are activated in intrinsic and extrinsic pathways of apoptosis through apoptosome and DISC complexes, respectively. Activated initiator caspases then process and activate effector caspases, including caspase-3, -6, and -7, which possess short prodomains. Caspase-3 is the most important protease that irreversibly dismantles the cells (Wang, 2001). Caspase-8 cleaves pro-caspase-3, at Asp175 to produce active p19/p12 complexes. Subsequently, further autocatalysis at Asp28 removes the short prodomain and generates p17/p12 complexes which is the fully mature form of the caspase-3 (Figure 1.12). This complex then translocates to the nucleus and cleaves substrates.

Procaspase-9, as the initiator caspase involved in mitochondrial-dependent apoptosis, is a monomer with a long prodomain. This prodomain consists of caspase recruitment domain (CARD), catalytic domain and a linker. Procaspase-9 CARD homotypically interacts to the Apaf-1 CARD. Catalytic domain composed of a small and a large subunit. The linker connects prodomain to catalytic domain. Caspase-9 is unique enzyme in that it is fully active even without cleavage (Stennicke et al., 1999). However, dimerization is highly required for its activity and forces the autocatalysis and generation of p35/p12 fragments (Renatus et al., 2001).

Apoptosome-dependent processing of caspase-9 is associated with a cleavage at Asp 315 in PEPD motif and produces a large 35 kDa (p35) and a small 12 kDa (p12) polypeptides. Further processing takes place at Asp 330 at DQLD motif by caspase-3 and produces a smaller 10 kDa (p10) peptide. Cleavage by caspase-3 removes the 15 amino acids at the N-terminus of p12 containing XIAP BIR3-binding motif. When caspase-9 is cleaved by

apoptosome complex, ATPF motif, although it is not the only binding site, is accessible in p12 for binding of XIAP. XIAP binding then inhibits the caspase-9. Subsequently, caspase-3 cleavage at D330 removes XIAP binding site from caspase-9 and therefore, increases the specific activity of p10-bound apoptosome in comparison with p12-bound complex (Figure 1.12) (Zou et al., 2003) (Bratton et al., 2002; Scott et al., 2005).

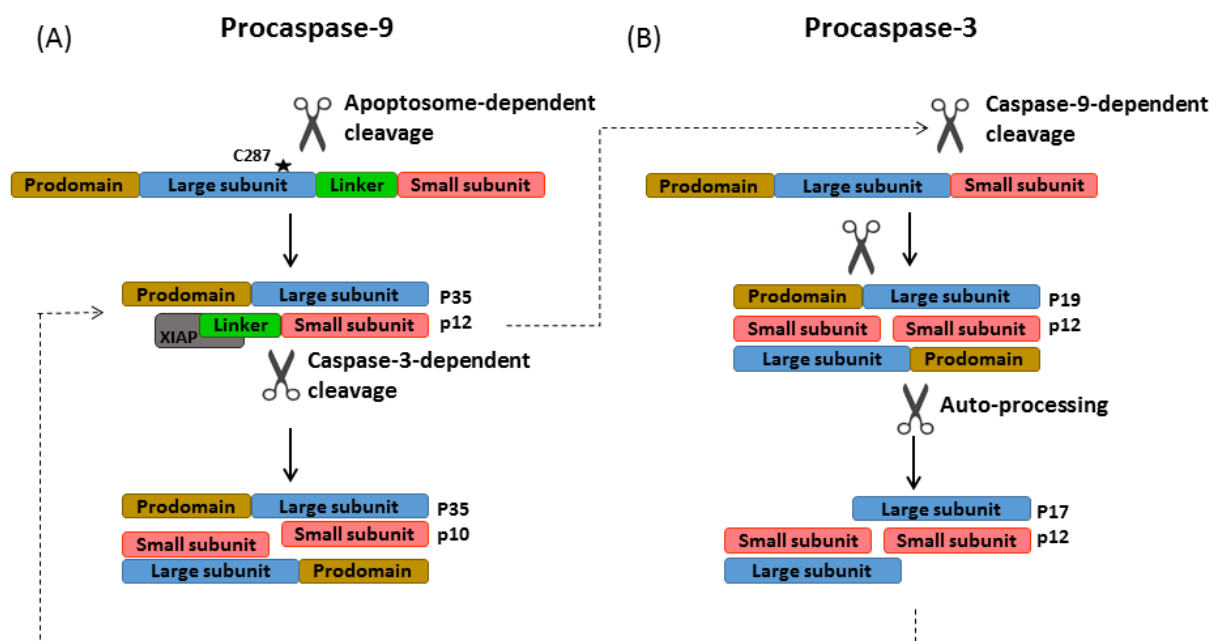


Figure 1.12. Schematic presentation of the caspase processing. (A) shows the processing of initiator procaspase-9. Procaspase-9 is a zymogen with a prodomain, large and small subunits and a linker between the subunits. Cys287 is the catalytic site in the large subunit. Prodomain encompasses a CARD and a linker. Upon binding to Apaf-1 through CARD-CARD interaction, procaspase-9 is cleaved at Asp 315 and produces p35 and p12. XIAPs are able to bind the exposed motif at the N-terminus of the p12 and inhibit the activity of caspase-9. Caspase-3 cleaves p12 at Asp 330 and removes the inhibition of XIAP and produces p35/p10, which is the fully active form of caspase-9. (B) procaspase-3 composed of a prodomain, large and small subunit. Activation of caspase-9 cleaves procaspase-3 at Asp 175 and produces p19 and p12. Then auto-processing at Asp 28 generates fully active caspase-3 which is a heterotetramer of p17/p12.

Caspase 9 is an inactive zymogen at normal physiological concentration. For procaspase-9 activation, two possible mechanisms have been suggested. One model proposed that dimerization of caspase-9 occurs upon binding to apoptosome complex. Caspase-9 dimer forms only one catalytic site, due to the asymmetric structure (Srinivasula et al., 1998; Bao and Shi, 2007). At high concentrations, caspase-9 is dimerized. The dimers possess two different active-site conformations: one similar to the functional sites of other caspases, the other is catalytically inactive due to the re-orientation of the activation loop mimics the monomeric caspase 9. Dimerization is the activation force and the interactions at the dimer interface proceeding the reorientation of the activation loop (Renatus et al., 2001). This model was challenged by studying the engineered dimeric caspase-9. Genetically modified dimeric caspase-9 with very similar structure to wild-type, showed more activity *in vitro* and induced higher cell death than the wild-type. However, the activity of dimeric caspase-9 was much lower than that of Apaf-1-activated caspase-9 and was not enhanced by Apaf-1. Therefore, it seems that dimerization is not the main mechanism of caspase-9 activation. Therefore, ‘induced conformation model’ was proposed (Chao et al., 2005).

The “induced conformational model” argues that binding of procaspase-9 to apoptosome induces an allosteric conformational change, which in turn activates caspase-9. In this model apoptosome-bound active caspase-9 more efficiently activates caspase-3. However, cytosolic cleaved caspase-9 exists as an inactive monomer (Vaughn et al., 1999; Cain et al., 2000). Although the evidence exists for both models, it is still unknown how procaspase-9 is activated in the cell. System biology-based approach supports the allosterically activation of procaspase-9 (Würtle and Rehm, 2014).

1.7 Models describing events downstream of caspase-9 activation

Two models describe the downstream events of caspase-9 activation.

1. “Molecular timer”: this model suggests that procaspase-9 has higher affinity for the apoptosome and the processed caspase-9 displaces the complex, thereby facilitating a continuous cycle of procaspase-9 recruitment/activation, processing, and release from the complex. Owing to its rapid autocatalytic cleavage, however, procaspase-9 per se contributes little to the activation of procaspase-3. Thus, the Apaf-1 apoptosome functions as a proteolytic-based ‘molecular timer’ wherein the intracellular concentration of procaspase-9 sets the overall duration of the timer, procaspase-9 auto-processing activates the timer, and the rate of the processed caspase-9 dissociation from the complex (and thus loses its capacity to activate procaspase-3) dictates how fast the timer ‘ticks’ over (Malladi et al., 2009).

2. Homo/Heterodimerization of caspase-9 with apoptosome: The very recent proposed model states that homodimerization of procaspase-9 within the apoptosome intensely increases the avidity for the apoptosome, which triggers the cleavage of procaspase-9 at Asp315. In addition, procaspase-9 is also able to form a heterodimer with NOD domain of Apaf-1 via its small subunit. This heterodimerization more efficiently activates caspase-3. Activated caspase-3 then initiates feedback activation loop and removes the intersubunit linker in processed p35/p12 form of caspase-9 by a second cleavage at Asp 330. This linker blocks the homo- and heterodimerization of caspase-9-p35/p12, removal of which restores the activity to the generated p35/p10 fragment of caspase-9. Therefore, the overall function of caspase-9 are dependent on the homo- and heterodimerization of caspase-9. Proximity-induced dimerization stably recruits procaspase-9 to the apoptosome and induces the cleavage at Asp315 whereas homo- and heterodimerization of caspase-9 intensifies the cleavage of caspase-3 (Wu et al., 2016; Wu and Bratton, 2017).

All the models proposed for apoptosome formation and caspase-9 activation are *in vitro* studies. In some cases, the output of the assay is indirect measurement of the desired target. Besides, there are some technical restrains that limit the analysis. For example, structural analysis using cryo-EM on apoptosome complex requires sample preparation, which includes rapid cooling. This method traps the protein in one specific conformation and therefore the proteins are no longer dynamic. The methods such as cryo-Em provide information about the formed apoptosome and is not informative for real time monitoring of the apoptosome formation *in cellulo*. The reporters introduced in this thesis are theoretically able to track the desired interactions during apoptosome formation. Unlike many of the current methods that target the endpoint of apoptosome formation, this reporter allows us to study the kinetics of the apoptosome formation.

1.8 Apoptosis physiological modulators

Apoptosis process is under the control of different factors. Different levels of regulations guarantee the appropriate progression or prevention of the pathway. There are several physiological substances that directly or indirectly activate or inhibit apoptosis, thus, function as either activators or inhibitors. These modulators regulate apoptosome either by direct interaction with Apaf-1 or indirect binding to the Apaf-1 interactors. Here, some of the identified modulators of apoptosis are discussed.

IAPs (inhibitor of apoptosis) are endogenous regulators of caspases include Survivin, cIAP-1, cIAP-2 and XIAP. XIAP is one of the most studied members of IAPs family. XIAP composed of three baculoviral IAP repeats (BIR), UBA and RING finger domains. XIAP inhibits caspase-9 and caspase-3/7 in a very specific manner through its BIR3 ($K_i \sim 10$ nM) and BIR2 ($K_i \sim >1$ nM) domains, respectively. The free form of caspase-3 is designed in such a way that binds to XIAP not the substrate (Ni et al., 2003). It seems that BIR-2 interacts to N-terminal of small subunit of caspase-3 and the rest of the molecules tightly

binds to the catalytic cleft of caspase-9 and therefore make the active site inaccessible to the substrate. BIR-3 on the other hand, binds to the monomeric caspase-9, but not the catalytic site, occupies the dimerization interface and forms a heterodimer with caspase-9 (Shiozaki et al., 2003). During apoptosis, Smac is released into the cytosol and binds to BIR domain leading to dissociation of BIR from caspase-9. Smac is a 239-amino acid protein with an MTS (Mitochondrial Targeting Sequence) at the N-terminal. This sequence is removed in mature Smac and as a result, AVPI motif is exposed at the N-terminus. This tetrapeptide motif then binds to conserved surface pocket of BIR domain in XIAP. Fully exposure of Ala in AVPI motif is required for this interaction (Chai et al., 2000; Srinivasula et al., 2000). Therefore, XIAP plays an important role in regulation of apoptosome-dependent apoptosis and considered as one of the constituents of this complex. Based on this model, cytochrome *c* is released from mitochondria after a stress-induced apoptosis and leads to oligomerization of Apaf-1 and formation of a wheel-like complex. Procaspase-9 binds to the hub of the complex via CARD-CARD interactions. Then caspase-9 is processed at D315 to generate a p35/p12 heterotetramer. Caspase-9 then activates procaspase-3 at IETD/S motif to form a p20/p12 heterotetramer, which then auto-processed to the mature p17/p12 heterotetramer. Then, activated caspase-3 processes caspase-9 at D330 to produce a p35/p10 heterotetramer. The presence of p10 or p12 fragments determines whether the caspase-9 can be suppressed by XIAP. As mentioned earlier, the XIAP BIR3 domain binds to ATPF at the N-terminus of the p12 subunit of caspase-9. XIAP binds to the active caspase-3 Linker-BIR2 domain, those that are going to interact with caspase-9-BIR3. Upon cleavage of the p12 to p10, XIAP is dissociated from the apoptosome and leaves the catalytically active form of caspase-9 (p35/p10) bound to the apoptosome (Bratton et al., 2002).

Acetylcholinesterase (AChE) is overexpressed in apoptotic cells, although it is not the initiator. It seems that AChE assists in cytochrome *c* and Apaf-1 interaction. siRNA knock-down of the AChE gene, inhibited caspase-9 activation, decreased the cell viability, nuclear

condensation and poly(adenosine diphosphate-ribose) polymerase cleavage (PARP) (Park et al., 2004; Zhang and Greenberg, 2012).

N-Acetyl-L-cysteine (NAC) increases caspase-3 activation in hypoxia-induced apoptosis. NAC encompasses NB and CARD domains. The CARD selectively interacts to the CARD domain of Apaf-1. Overexpression of NAC enhances the cytochrome c-dependent caspase activation and suppression of NAC inhibits it (Chu et al., 2001; Qanungo et al., 2004). Alpha-fetoprotein (AFP) recruits caspase to the apoptosome complex and enhances the apoptosis (Semenkova et al., 2003).

Aven inhibits the oligomerization of Apaf-1 (Chau et al., 2000). HSP70 binds to Apaf-1 and inhibits the recruitment of caspase-9 to the apoptosome complex and therefore block the formation of functional apoptosome (Beere et al., 2000; Chau et al., 2000). During cytotoxic stress, Nucling is upregulated by proapoptotic signals and induces apoptosis. A deficiency of Nucling-deficient cells has been shown to be resistant to apoptotic stress. UV irradiation, leads to the interaction of Nucling to Apaf-1/pro-caspase-9 complex, suggesting that Nucling assist in the formation and maintenance of apoptosome complex. Nucling also proceeds the translocation of Apaf-1 to the nucleus (Figure 1.13) (Sakai et al., 2004).

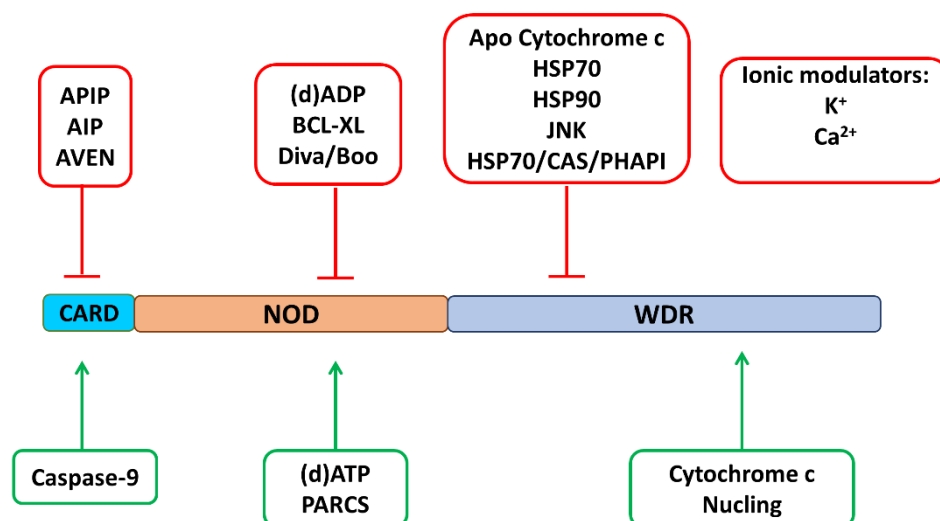


Figure 1.13. Apaf-1 interacting proteins. Different proteins interact to different domains of Apaf-1. The inhibitors are shown in red box and the activators are in green box.

PARCS (pro-apoptotic protein required for cell survival) binds to the oligomerization domain of Apaf-1. Down-regulation of PARCS in cytosolic fraction of HeLa cells decreased Apaf-1-dependent activation of caspase-9. Cell proliferation was also blocked in PARCS-deficient non-tumorigenic cells (Sanchez-Olea et al., 2008).

The ionic equilibrium within a cell is another physiological regulatory step in Apaf-1 modulation. K^+ inhibits the oligomerization of Apaf-1. Once assembled, apoptosome is resistant to ionic strength (Cain et al., 2001; Thompson et al., 2001). Furthermore, in addition to necrosis, Ca^{2+} is associated with apoptosis. *in vitro* studies have shown that pre-incubation of the Apaf-1 with Ca^{2+} disrupts the apoptosome assembly by preventing the nucleotide exchange, a key step in switching the locked Apaf-1 to open form (Bao et al., 2007).

Nitric oxide (NO) or its reaction products inhibits apoptosis. This endogenous inhibitor of apoptosis acts either at/or upstream of caspase-3-like protease activation in cGMP-dependent fashion or by directly inhibiting the activity of caspase-3-like protease by S-nitrosylation of the enzyme (Kim et al., 1997). Caspase-3 require a cysteine residue (C163) at an active site for catalytic activity (Tewari et al., 1995). The inhibition of caspase-3 activity with thiol-reactive compounds and NO and NO^+ equivalents showed that thiol modification inhibits enzyme (Kim et al., 1997).

Apoptosome-associated proteins are also regulated by post-translational modification. There are a lot of reports showing that phosphorylation is a common form of regulation for the majority of the cellular proteins including those involved in apoptosis. For example, phosphorylation of T125 decreases the activation of caspase-9 (Allan et al., 2003). Cytochrome c is also phosphorylated at Y48 and Y97 although the physiological relevance is not known (Lee et al., 2006; Yu et al., 2008). Apaf-1 is also phosphorylated at Ser268 by ribosomal S6 kinase (Rsk). This phosphorylated site is then recognized and bound by 14-3-3 ϵ and inhibits cytochrome c-dependent activation of Apaf-1 (Kim et al., 2012; Elena-

Real et al., 2018). PKA (Active protein kinase A) inhibits caspase-9 and directly phosphorylates Apaf-1 at least *in vitro* (Martin et al., 2005).

1.9 Apaf-1 mediated apoptosis in development and disease

In the last section, tightly regulation of Apaf-1 mediated apoptosis with the contribution of a range of modulators was explained. This level of regulation implies the importance of this pathway in normal life of an organism. Why apoptosis is important for the cells? Apoptosis plays critical roles in embryonic development involves sculpting the structure, elimination of redundant structures, controlling the number of cells and removal of damaged cells (Jacobson et al., 1997). Proper function of Apaf-1 is required for proper development in several tissues. Apaf-1 has been shown to play roles in different tissues such as brain, eye and ear. Apaf1^{-/-} mice with abnormal craniofacial phenotype die prenatally around stage E16.5 (Cecconi et al., 1998). These embryos have impaired brain morphology, including abnormal folding and smaller telencephalic vesicles than wild-type, brain hyperplasia (in the diencephalon and midbrain), and exencephaly because of defective skull and facial midline cleft. Apaf-1^{-/-} embryos also have thicker retina and the hyperplastic retina is accumulated in optic cup, the lens is smaller with incorrect polarization and the optic cup is eliminated by vascular endothelial cells. In other words, Apaf-1 is required for controlling the retina cell number, determining the morphology of the eye and removal of unnecessary hyaloids capillary (Cecconi and D'Amelio, 2009). Apaf-1 is also required for morphogenesis and growth of inner ear. Genetically disruption of the Apaf-1 reduces apoptosis in the inner ear epithelium and causes severe morphogenetic defects with small membranous labyrinth (Cecconi et al., 2004). These phenotypes suggest that Apaf-1 is indispensable in midline fusion of craniofacial structures and normal mammalian development.

It has been shown that caspase-9 is expressed in different mammalian tissues and deregulation of the activity of caspase-9 is associated with pathological conditions. Caspase-9 null mice die perinatally as a result of defective telencephalic development in

brain. It seems that during embryogenesis, caspase-9 deregulation is brain-specific and does not play critical role in other tissues. Moreover, embryonic stem cells and fibroblasts lacking caspase-9 are resistant to stress-induced apoptosis by UV, γ -irradiation and dexamethasone. In Huntington's disease (HD) patients and a mouse model of HD, activated caspase-9 and caspase-3 detected only at the late-stage of disease correlated to severe neuropathological grades (Kiechle et al., 2002).

The morphology of the caspase-9 null mice are reminiscent to caspase-3 null mice (Kuida et al., 1996). Both mutants displayed a serious abnormal cortical morphology, an expanded germinal zone, and hydrocephaly (Hakem et al., 1998). Caspase-3 null mice die before 3 weeks of age. These mice exhibit accumulation of the cells in cerebral cortex, the hippocampus and the striatum, the lens is compressed and the germinal layer is thick, unlike the wild-type (Kuida et al., 1996).

Apart from developmental role, defective mitochondrial-dependent apoptosis causes diseases. Deficient caspase-9, caspase-3 and Apaf-1 impair neurogenesis and lead to embryonic lethality (Kuida et al., 1996, 1998; Cecconi et al., 1998; Hakem et al., 1998; Yoshida et al., 1998). Apaf-1 null mice usually die prenatally. However, when exencephaly or cranioschisis do not take place, 5% of new-borns survive to adulthood. This suggests that the lack of Apaf-1 is probably compensated by other genes in neurons. Although no abnormalities were observed in histological studies, the survived mice showed hyperactivity. In addition, the males are infertile due to the huge deterioration of the spermatogonia in the testis which causes a dramatic reduction in the sperm (Honarpour et al., 2000). This suggests that Apaf-1 mediated apoptosis is necessary for fertilization of at least males. The similar phenotype has been reported in drosophila. Cytochrome c and caspase deficient flies showed the lack of spermatid individualization (Arama et al., 2003).

In *Drosophila*, expression of polyglutamine tract in the eye caused the degeneration of retina by reducing the size and number of rhabdomers, the structures that phototransduces in the neurons. However, the loss of function Dark mutants showed the phenotype as wild-

type in the cells expressing polyglutamine-containing proteins. The mutants suppressed progressive and late-onset neurodegeneration. Dark mutants were shown to suppress caspase and apoptosis as well as formation of polyglutamine aggregates and ubiquitination. Dark mutants suppress neurodegeneration in a range of polyglutamine-containing proteins as tested by huntingtin exon-1 and full length ataxin-1 models. Interestingly, in mice and human patients with HD (Huntington Disease), Apaf-1 co-localized with the huntingtin aggregates. All these experiments suggest a role for Apaf-1 in polyglutamine aggregate accumulation in neurodegenerative diseases (Sang et al., 2005).

Apoptosis is associated with numerous pathological conditions, however, to date no treatment has been approved based on its inhibition. Drug discovery approaches have mainly focused on targeting caspase activation and activity rather than the upstream events to identify molecules that improve the disease-associated apoptosis. Apoptosome seems to be a critical target for therapeutic purposes, although there are few reports on Apaf-1 pharmacological inhibition. Many efforts have been made to discover new drug-like molecules, some of which will be discussed here.

1.10 Synthetic Apoptotic modulators

Due to the importance of Apaf-1 dependent apoptosis in normal growth and development and association of dysregulated apoptosis with human diseases, many research programmes have been accomplished to identify small molecules that can activate apoptosis when it is blocked or inhibit apoptosis when it is activated. Oligomerization of Apaf-1 is a key step in mitochondrial-dependent apoptosis. Therefore, Apaf-1 has been paid a lot of attention as a target for therapeutic approaches.

In attempt to discover chemical modulators of Apaf-1, Nguyen and Wells initially screened a library of 3500 different compounds by *in vitro* measurement of caspase-3 activity using HeLa cell extract. 116 hit compounds further re-tested by studying the processing of caspase-3. Among the 20 candidate, compound 1 was selected for chemical optimization. Further studies presented compound 2 and 3 as more biologically active compounds that activate the Apaf-1 (Figure 1.14). The exact molecular mechanism of inhibition is not clear; however, it seems that it assists in cytochrome c-activation of Apaf-1.

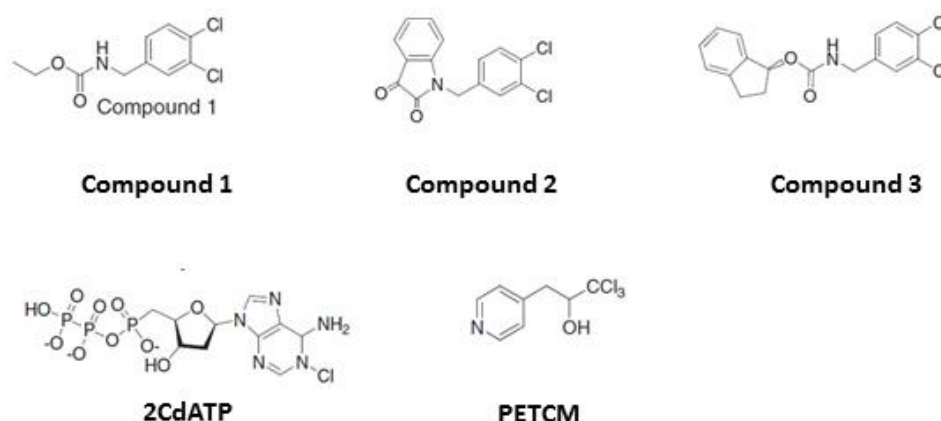


Figure 1.14. Chemical structure of Apaf-1 activators. The Reported Active Concentration (RAC) is 2-4 μ M for compound 1,2 and 3, 100-200 μ M for PETCM and 1 mM for 2CdATP.

Bioactive deoxynucleoside analogs, like cladribine (2-chlorodeoxyadenosine or 2CdA) or fludarabine (9-b-d-arabinofuranosyl-2-fluoradenine or F-Ara-A) produce some metabolites that bind to Apaf-1 (Beutler, 1992; Carrera et al., 1994).

PHAP protein, a member of tumor suppressor family, promotes caspase-9 activation after apoptosome formation. The oncoprotein prothymosin- α [ProT] negatively regulates caspase-9 activation by blocking apoptosome formation. PETCM (α -(trichloromethyl)-4-pyridineethanol), a compound identified through a high-throughput screening as an activator of caspase-3 in extracts of cancer cells, relieves ProT inhibition and allows apoptosome formation at a physiological ATP concentration (Jiang et al., 2003; Qi et al.,

2010). PETCM was also reported to induce Apaf-1 oligomerization in HeLa cell S-100 extracts independent of dATP (Figure 1.14). Elimination of ProT expression by RNA interference sensitized cells to ultraviolet irradiation-induced apoptosis and negated the requirement of PETCM for caspase activation (Jiang et al., 2003). PHAPI inhibits cell growth by inhibiting protein phosphatase 2A and histone acetylase and the oncoprotein prothymosin (Li et al., 1996).

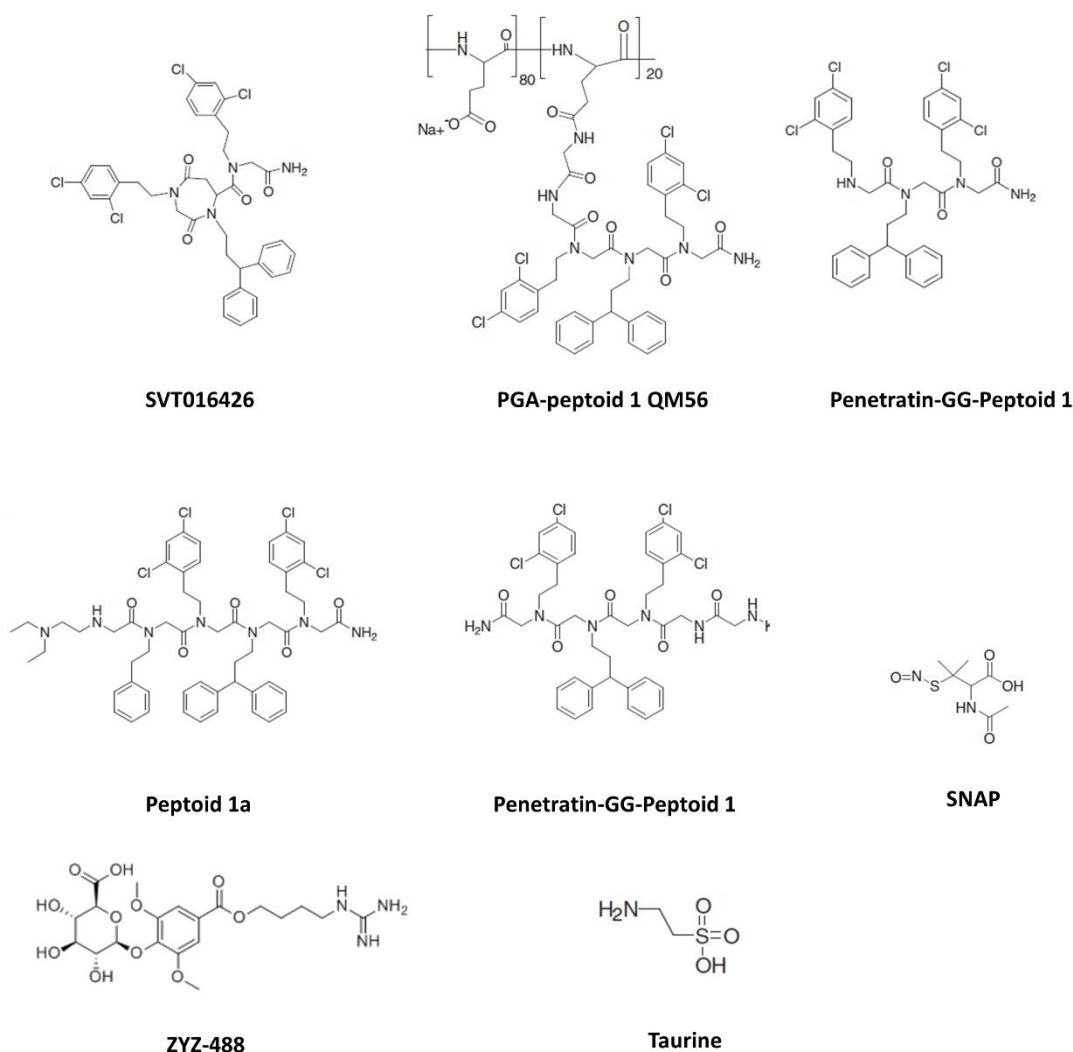


Figure 1.15. Chemical structure of Apaf-1 inhibitors. The Reported Active Concentration (RAC) is 20 mM for Taurine, 0.5 mM for SNAP, 1-5 μ M for NS3694, 5-10 μ M for Peptoid 1 and SVT016426 and 1-50 μ M for the conjugated peptoid 1.

The S-Nitroso-N-acetyl-penicillamine (SNAP), the NO donor, disrupt the right assembly of Apaf-1 and formation of active apoptosome. Thus, SNAP inhibits the CARD-CARD interactions with procaspase-9. However, SNAP promotes the formation of the inactive 1.4 MDa apoptosome (Zech et al., 2003).

Taurine is a non-essential sulfur-containing amino acid that reduces the Apaf-1-dependent caspase 9 activation (Takatani et al., 2004). Taurine inhibits ischemia-induced processing of caspase-9 and -3. Taurine suppresses the formation of the Apaf-1/caspase-9 apoptosome and the interaction of caspase-9 with Apaf-1 suggesting the preventive role of taurine in myocardial ischemia-induced apoptosis (Takatani et al., 2004). Taurine also prevents high-glucose-mediated endothelial cell apoptosis by its antioxidant activity and regulation of intracellular calcium homeostasis (Wu et al., 1999).

ZYZ-488 is a newly synthesized compound that is anti-apoptotic cardioprotective substance (Figure 1.15). ZYZ-488 increased the viability of hypoxia-induced H9C2 cardiomyocytes and decreased the release of creatine kinase and lactate dehydrogenase. It seems that Apaf-1 is required for anti-apoptotic role of ZYZ-488. However, the direct binding to Apaf-1 was not shown. The authors postulated that ZYZ-488 disrupts the interaction between Apaf-1 and procaspase-9 (Wang, Cao, et al., 2016).

The diarylurea compounds have been reported to inhibit the formation of the active 700 kDa apoptosome complex through unclear mechanism (Lademann et al., 2003). It seems that haloaryl moieties present in the chemicals make lipophilic interactions interferer with the formation of apoptosome. Peptoid 1 with two dichlorophenylethylamino moieties are similar to the activators of the Apaf-1 mediated apoptosome that possesses a dichlorobenzylamino moiety. Peptoid 1 with two additional N-alkylamine residues at the N-terminus, enhances the solubility (peptoid 1a) but lessens the cell permeability. For the ease of cellular uptake, a new series of peptoid 1 analogues were synthesized by fusing the peptoid 1 to cell penetrating peptides (e.g., penetratin, HIV-1 Tat) or to a water soluble polymeric carrier (Vicent and Pérez-Payá, 2006; Orzáez et al., 2007).

SVT016426, previously known as QM31, is an inhibitor of apoptosome identified through the screening of a chemical library (Figure 1.15) (Malet et al., 2006). SVT016426 blocks the release of cytochrome c from mitochondria and inhibits the Apaf-1-dependent intra-S-phase DNA damage checkpoint (Mondragón et al., 2009). SVT016426 has been shown to diminish the interaction of Hsp70 with Apaf-1 suggesting the indirect inhibitory role on apoptosome (Sancho et al., 2014). SVT016426, decreases both polyglutamine-induced aggregation and polyglutamine-induced apoptotic cell death in different cellular models.

1.11 Reporters of monitoring protein interactions

For years, different reporters have been designed to study the protein-protein interactions. Förster resonance energy transfer (FRET) is a suitable technique for studying protein interaction when the interacting proteins are spatially less than 10 nm far from each other (Förster, 1948; Clegg, 1995). FRET detects the fluorescent signal when two labelled proteins interact (Sekar and Periasamy, 2003). FRET allows the live cell high spatial resolution assays for protein–protein interactions when combined with multiple, coloured fluorescent proteins (Piston and Kremers, 2007). This technique does not require cofactors or exogenous substrate. This approach has several disadvantages. For example, fluorescence properties are sensitive to environmental changes such as pH, ionic concentrations, oxidation, temperature, and refractive index. Besides, signal to noise ratio is low in FRET (Nagai et al., 2004; Piston and Kremers, 2007). The slow turnover rate of fluorescent proteins causes accumulation of the reporters and make them unsuitable for monitoring fast reaction (Haugwitz et al., 2008). The non-enzymatic generation of signal reduces the assay sensitivity compared to enzyme-based reporter assays.

Luciferase based assays (bioluminescence) are the most commonly used enzymatic assays. Bioluminescence, generation of light through a chemical reaction, is found in a wide range of organisms from bacteria, fungi to fish, shrimp, and insects (Herring, 1978; Campbell, 1988; Herschman, 2003; Azad, Tashakor and Hosseinkhani, 2014). Luciferase, the enzyme catalyzing the bioluminescence reaction, uses different substrates and emits light with

different wavelengths mostly in the visible range of electromagnetic spectrum. For example, *Renilla* luciferase oxidizes coelenterazine in an oxygen-dependent reaction and generates blue light ($\lambda_{\text{max}} = 480 \text{ nm}$) while *firefly* luciferase catalyses the oxidation of D-luciferin in an ATP- and oxygen-dependent reaction and produces yellow-green ($\lambda_{\text{max}} = 550 \text{ nm}$) to red light ($\lambda_{\text{max}} = 620 \text{ nm}$) (Paulmurugan et al., n.d.; Ugarova, 1989).

Firefly luciferase from *Photinus pyralis* is a 62 kDa polypeptide and characterized as high quantum yield enzyme. This protein mainly composed of a large N-terminal domain and a small C-terminal domain connected by a flexible linker. In the presence of luciferin (a benzothiazole compound) and ATP, firefly luciferase produces luciferyl adenylate which then binds to molecular oxygen and produces carbon dioxide and excited oxyluciferin (Figure 1.16). Depending on the pH and polarity of the solvent, this excited intermediate generates green to red light when returning to the ground state (White et al., n.d.; Deluca, 1976; de Wet et al., 1986; Hosseinkhani, 2011).

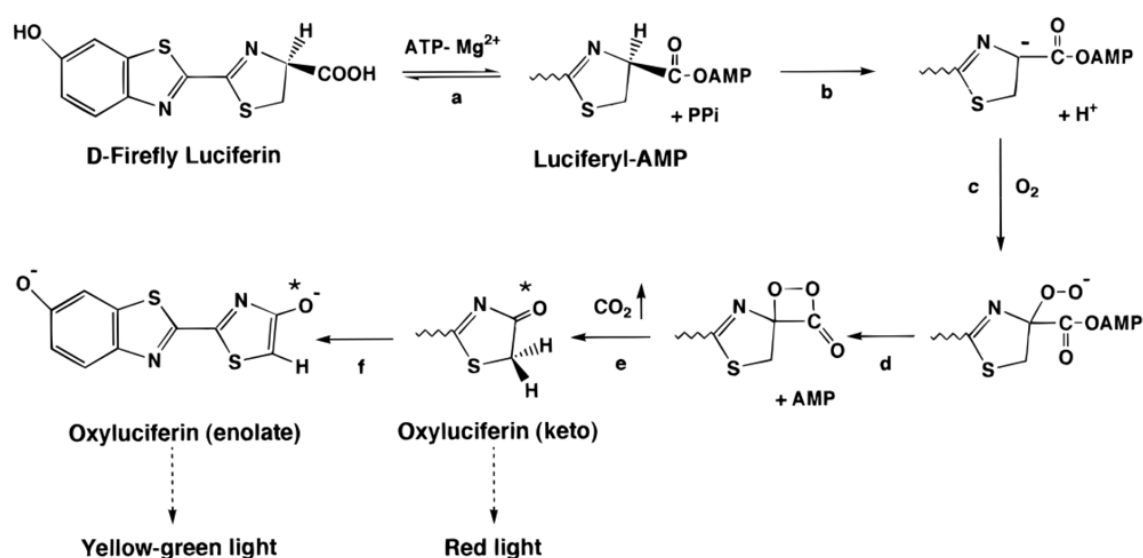


Figure 1.16. The mechanism of bioluminescent reaction catalysed by firefly luciferase.

In the first step reduced luciferin is adenylated in the presence of ATP (a). Deprotonation of luciferyl-AMP produce a carbanion intermediate (b). Molecular oxygen (c), releases AMP and forms a cyclic intermediate (d). release of carbon dioxide is associated with the formation of the excited state luciferin in either the keto (e) or enolate (f) forms (Branchini et al., 1998; Close et al., 2009).

Luciferases are widely used in bioassays because unlike fluorescence, it does not require excitation energy, and this leads to high signal to noise ratios in bioanalytical assays by reducing the background signal. Furthermore, it eliminates the possibility of the interference of the excitation light with fluorophores (Simeonov et al., 2008; Thorne et al., 2010). Although the signal is much lower than that of fluorescence, luciferase is of interest and various strategies have been applied to use it in different ways in bioanalysis. (Meighen et al., n.d.; Wilson and Hastings, 1998). The most commonly used methods are permuted luciferase, cyclic luciferase, split luciferase (Figure 1.17).

In circularly permuted luciferase, a linker with a site for specific interactor is inserted between the two domains of the enzyme. This method has been used to measure the activity of proteases by insertion of the cleavage site in the linker. Upon the cleavage, luciferase freely undergoes conformational changes and gains the ability to emit light (Wigdal et al., 2008).

Cyclic luciferase has been used for measuring the activity of caspase-3. In this strategy, N-domain and C-domain of luciferase are linked together by a target sequence of caspase-3. When expressed within the cells, cyclic luciferase is synthesized as a circular polypeptide chain with no or very low activity because of the inappropriate structure. When activated, caspase-3 cleaves the substrate and linearizes the luciferase protein which then can find its right structure and recover its activity (Kanno et al., 2007, 2009). This method accomplished for real-time tracking of the caspase-3 activity in living mice.

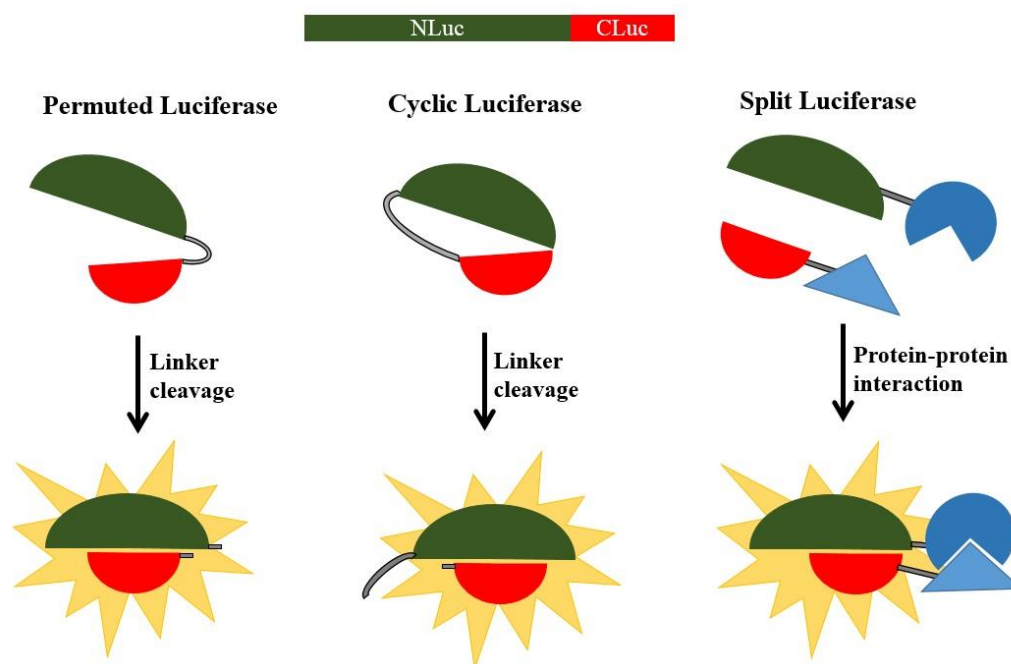


Figure 1.17. Different strategies used for making luciferase reporters. In permuted luciferase strategy, a linker with a digestive substrate sequence is inserted between the N- and C-domain of luciferase. Upon cleavage of the substrate, luciferase fold into the right conformation and in the presence of luciferase substrate emits light. In cyclic luciferase method, however, the linker connects the two end of luciferase and locks the protein. Similar to permuted luciferase, cleavage of the linker assists in the recovery of the luciferase activity. In split luciferase strategy, two domains of luciferase are individually fused to two interacting proteins. The interaction between the proteins place the two halves of luciferase in close proximity and the activity of luciferase is reconstituted.

Split luciferase strategy is used for studying the two interactors either protein-protein or protein-nucleic acid. Here, two interactors are fused individually to luciferase N-terminal and C-terminal via appropriate linkers. When expressed within the cell, the fusion interacting proteins physically interact and thus two fragments of luciferase will be placed in close proximity and reconstitute luciferase activity in the presence of the substrates (Ozawa et al., 2001).

This strategy has been largely used for studying the protein-protein interactions, mobility of the proteins to a specific organelle, measuring the concentration of the analytes, DNA damage, tracking the protease activity and oligomerization of the protein complexes (Binkowski et al., 2009; Shekhawat et al., 2009; Taneoka et al., 2009; Ishimoto et al., 2011); (Paulmurugan et al., n.d.; Ozawa and Umezawa, 2001; Ozawa et al., 2001; Ozawa, 2006; Massoud et al., 2007; Villalobos et al., 2007; Misawa et al., 2010; Stains et al., 2010; Li, Feng, et al., 2017).

Split luciferase complementary assay has also been used for sensing the glucose by inserting the galactose/glucose binding domain between the two domains of luciferase (Taneoka et al., 2009), screening the nuclear-factor-E2-related factor 2 (Nrf2) modulators (Kobayashi and Yamamoto, 2005), detecting the human epidermal growth factor receptor 2 (EGFR2) and vascular endothelial growth factor (a factor for angiogenesis and tumour growth)(Stains et al., 2010).

The length and composition of the linker and selection of the split point are the key factors contribute to successfully detection of the recovered luciferase activity. Flexible linkers, rigid linkers, and cleavable linkers are largely used to make stable and bioactive recombinant fusion proteins. Flexible linkers make the interaction possible between the domains by freely spatial movements and mainly composed of hydrophilic and small amino acid residues like Gly and/or Gly-Ser with different number of repeats.

Rigid linkers are useful for maintaining the distance between the domains and are made of helical and Pro-rich structures with different number of repeats. Cleavable linkers are used for *in vivo* cleavage by proteases and etc. (Zhang et al., 2009; Chen et al., 2013; Klement et al., 2015).

Choosing the split point of luciferase is the key element in complementation of the luciferase. For finding the best pair of fragments, in terms of recovering luciferase activity, a library of the various pairs must be made, and the split luciferase activity of all pairs should be measured. This strategy was used by Ozawa et al. in 2010 and they reported that residue 1-416 and 398-550 is the best pair for reconstitution of the firefly luciferase activity (Luker et al., 2004; Hida et al., 2009; Misawa et al., 2010). However, the 3D structure of the protein of interest may affect the structure of luciferase fragments. Depending on the size of the target protein, the luciferase activity could be fully abolished or severely attenuated due to the inappropriate spatial orientation while the interactors bind to each other.

To rectify this, the best strategy is to make a library of various pairs of luciferase fragments bound to proteins of interest and measure the split luciferase activity. Detection of split luciferase activity for measuring apoptosome formation was reported before using the luciferase fragments proposed by Ozawa (Torkzadeh-Mahani et al., 2012). Therefore, here the same split point for making the fusion Apaf-1 proteins was used. Also, flexible Gly-Ser linkers were used to allow freely movements of luciferase fragments on the CARD complex. Then, the new assay was validated to show that luciferase activity directly measures apoptosome formation. This bio-tool was then used for screening libraries to identify the apoptosome inhibitors as well as further investigating the known inhibitors of caspase activation.

Aims

The aim of this project was to design a new assay using split luciferase complementation assay that:

- specifically and directly reports Apaf-1 oligomerization
- is easy, fast and cost-effective
- is suitable for large-scale screening
- enable us to study the Apaf-1 interactions

For this, luciferase-tagged Apaf-1 was generated using flexible linkers. The assay was validated for detecting apoptosome formation. Then, the assay was used as a tool for screening approaches to identify new modulators of apoptosome and for studying the known inhibitors of apoptosis to understand their mechanism of actions.

MATERIALS

&

METHODS

2.1 Making luciferase-based reporters

PCR-Amplification of the fragments required for making fusion proteins

N- and C-terminal of *photinus pyralis* firefly luciferase were amplified using pGL-3 vector encoding the cDNA of luciferase. Apaf-1 XL was also amplified using the previously cloned pFastbac vector. The restriction site for Acc65I and Cozak sequence was inserted in forward primers and GGGGS sequences were inserted in reverse primers. (G₄S)₂ and (G₄S)₃ were used as linkers for Nluc-Apaf-1 and (G₄S)₂ as a linker for Cluc-Apaf-1 fragments. 1-415 amino acid fragment was amplified as N-domain and 394-542 as C-domain. The sequences of the primers used for amplification of the fragments are as below:

Primers	Sequence
Nluc-Forward	5'- GGTACCGCCGCCACCATGGAAGACGCCAAAAACATA -3'
Nluc-Reverse	5'-GCTACCCCCTCCGCCGCTACCCCCTCCGCCGCTACCCCCTCCGCC TCCATCCTTGTCATCAAG -3'
Cluc-Forward	5'- GGTACCGCCGCCACCATGCCTATGATTATGTCCGGT -3'
Cluc-Reverse	5'-GCTACCCCCTCCGCCGCTACCCCCTCCGCCGCTACCCCCTCCGCC GCTACCCCCTCCGCCCAATTTGGACTTTCCGCCCTT -3'
Apaf1-Forward	5'- ATGGATGCAAAAAGCTCGAAATTGTTTGC -3'
Apaf1- Reverse	5'- GGATCCTTATTCTAAAGTCTGTAAA -3'

All primers were synthesized at 0.025 μ mol scale by Sigma (Ireland).

PCR was performed in a 25- μ l reaction mixture contained following reagents:

- I. 5 μ l of 5X PrimeSTAR GXL Buffer (Mg²⁺ plus) composed of 50 mM Tris-HCl (pH 8.2), 100 mM NaCl, 0.1 mM EDTA, 1 mM DTT, 0.1% Tween 20, 0.1% Nonidet P-40, and 50% Glycerol,
- II. 2 μ l of dNTP Mixture (2.5 mM each),
- III. 1.25 μ l of each primer (10 μ M),
- IV. 50 ng of template DNA,

V. 1 μ l of PrimeSTAR GXL DNA Polymerase (1.25 U/ μ l).

The PCR program was set as below on Veriti Gradient Thermal Cycler (Applied Biosystem):

- I. Initial denaturation at 98°C for 5 min,
- II. Annealing and Elongation, 30 cycles of amplifications each cycle consisted of:
 - ✓ 30 sec at 98°C
 - ✓ 30 sec at 66°C (for Apaf-1), 60°C (for Nluc), and 63°C (for Cluc)
 - ✓ 4, 1:30 and 1 min at 68°C for Apaf-1, Nluc and Cluc respectively.
- III. Final extension at 68°C for 10 min.

DNA agarose gel electrophoresis

PCR products were then analysed by running on 1% agarose gel electrophoresis at 90 V for 1-1:30 hour. For this, 0.5 g agarose dissolved in 50 mL TAE buffer 1X containing 40 mM Tris, 20 mM acetate and 1 mM EDTA. This reaction was mixed with 5 μ L of SYBR safe DNA stain gel (10000 concentrated in DMSO). 5 μ L of each PCR products mixed with 6X loading buffer and ran on the gel.

In-fusion cloning

In-fusion cloning strategy was used for insertion and fusion of the amplified fragments into the pcDNA3.1 vector. The same PCR program was used for amplification of the in-fusion cloning fragments. The primers listed in the following table were synthesized to amplify the appropriate fragments with 15 base pair overlap at the two ends.

Primers	Sequences
Nluc-Forward	5'-ACTTAAGCTTGGTACCGGTACCGCCGCCACC -3'
Nluc-Reverse	5'-GCATCCATGCTACCCCTCCGCCG -3'
Apaf1-Nluc Forward	5'-GGGTAGCATGGATGCAAAAGCTCGAAATTGTTTG-3'
Apaf1-Nluc Reverse	5'-AGTGGATCCGGATCCTTATTCTAAAGTCTGTA-3'
Cluc-Forward	5'-ACTTAAGCTTGGTACCGGTACCGCCGCCACC-3'
Cluc-Reverse	5'-GCATCCATGCTACCCCTCCGCCGCTA-3'
Apaf1-Cluc Forward	5'-GGGTAGCATGGATGCAAAAGCTCGAAATTGTTTG-3'
Apaf1-Nluc Reverse	5'-TGGACTAGTGGATCCGGATCCTTATTCTAAAGTCTGTA-3'

PCR product reaction clean up

Qiagen spin-column clean-up PCR product kit was used to obtain purified double stranded PCR products. For this:

- I. 5 volume of PB buffer added to 1 volume of PCR product.
- II. Spin-columns placed in 2 mL Eppendorf tubes.
- III. PCR products were loaded on the columns and centrifuged for 1 min at 17900 g.
- IV. The pass-through liquid discarded.
- V. Each column washed by 750 μ L PE buffer and centrifuged as above.
- VI. The pass-through liquid removed, and the columns were centrifuged for another 1 min to remove the residual ethanol from washing buffer.
- VII. The columns were then eluted by 50 μ l Buffer EB (10 mM Tris·HCl, pH 8.5) and loaded on 1% agarose gel.

pcDNA 3.1 was used as a vector for cloning the fragments. pcDNA 3.1 vector was double digested by Acc65I and BamHI to obtain linearized plasmid. The reaction was made as below:

- ✓ Acc65I/BamHI restriction enzymes 5 µl each
- ✓ pcDNA3.1 5 µg
- ✓ 25 µl of 10X NEBuffer3.1 (1X NEBuffer™ 3.1 contains 100 mM NaCl, 50 mM Tris-HCl, 10mM MgCl₂, 100 µg/ml BSA (pH 7.9 @ 25°C))
- ✓ Make the total reaction volume up to 250 µl
- ✓ Incubated at 37°C for 15 min.

Digested vectors loaded on 1% agarose DNA gel and purified using gel extraction kit.

Briefly:

- I. DNA fragments were cut from the agarose gel and three volumes of buffer QC added.
- II. The mixture incubated at 50°C for 15 min with frequent vortexing every 2-3 min.
- III. One volume of isopropanol was added, and the mixture loaded on the column and centrifuged 1 min at 17900 g.
- IV. The flow-through removed and the column was washed with 750 µl PE buffer and centrifuged for 1 min.
- V. Finally, DNA was eluted using EB buffer.

The DNA concentration was determined using NanoDrop.

For making the cloning mixture, the following reactions were prepared:

	Nluc-Apaf1	Cluc-Apaf-1	Control***
Vector	0.82 µl (91 ng/ µl)	0.82 µl (91 ng/ µl)	1 µl
Insert 1*	0.62 µl (56 ng/ µl)	1.5 µl (17 ng/ µl)	2 µl
Insert 2**	4.00 µl (25 ng/ µl)	4.40 µl (27 ng/ µl)	-
HD-enzyme premix	2 µl	2 µl	2 µl
Deionized H₂O	2.56 µl	1.3 µl	5 µl

* Insert 1 is the luciferase fragments (either N or C domain) amplified with the 15 bp overlap with Apaf-1.

** Insert 2 is the Apaf-1 gene amplified with the 15 bp overlap with either Nluc or Cluc.

*** In the control reaction, 1 µl of pUC19 control vector and 2 µl of 2 kb control insert were used.

All the reactions incubated for 15 min at 50°C and then placed on ice. An aliquot of this reaction was used for transfection into DH5alpha *e.coli* cells.

Transformation of the in-fusion cloning reactions

Transformation carried out using Stellar™ Competent Cells (Clontech) as below:

- I. 2.5 µl of each cloning reactions mixed with 65 µl of the Stellar™ Competent Cells.
- II. The bacteria/DNA mixture placed on ice for 30 min.
- III. Then bacteria heat-shocked at 42°C for 45 sec.
- IV. incubated for 5 min on ice.
- V. 435 µl pre-warmed SOC medium added to each reaction.
- VI. Mixtures incubated at 18°C, 50 rpm shaking for two hours followed by one hour at 150 rpm.
- VII. Then, the samples spin down at 4500 rpm for 5 min.
- VIII. The pellet re-suspended in 100 µl of fresh SOC medium and plated on LB-agar plates supplemented with ampicillin.
- IX. Plates were incubated at 18°C for 3 days.

Production of recombinant plasmids

To produce the recombinant plasmids:

- I. Single clones were picked and cultured in 5 mL fresh LB medium supplemented with ampicillin.
- II. The cultures incubated at 18°C, 225 rpm shake for 3 days.
- III. Bacterial cells were harvested by spinning at 4500 rpm for 5 min.

- IV. Bacterial pellet resuspended in 250 µl buffer P1 (QIAprep Spin Miniprep Kit).
 - V. 250 µl buffer P2 added and the tubes were gently inverted 4-6 times.
 - VI. 350 µl buffer P3 added and the tubes were immediately inverted 4-6 times.
 - VII. The mixture centrifuged at 17900 g for 15 min.
 - VIII. QIAprep spin columns placed on the 2mL collection tubes and the supernatant from last step loaded on the column.
 - IX. Centrifuged for 1 min as above.
 - X. The flow-through removed and the column was washed with 750 µl buffer PE and centrifuged for 1 min.
 - XI. The flow-through discarded and centrifuged for another 1 min to remove the residual washing buffer.
 - XII. The columns were then eluted by 50 µl buffer EB (10 mM Tris-HCl, pH 8.5).
- To confirm the insertion of the genes of interest into the vector, double digestion performed using Acc65I and BamHI. The wild-type sequences of the inserted fragments were then confirmed by Primer Walking Service (Eurofinsgenomic).

2.2 Expression of luciferase tagged Apaf-1

Transfection of the recombinant plasmids in the HEK293 cells

1 mg of Polyethylenimine (PEI) diluted in 1 ml DNase and RNase free water and the pH of the solution adjusted to the acidic range. The mixture was then adjusted to pH 7 and filtered using 0.22 µm filter. The aliquots stored at -20°C.

To transiently transfect the cells:

- I. 5×10^6 HEK 293 cells seeded in the T175 flask and incubated overnight at 37°C, 5% CO₂.
- II. 50 µg of the plasmids (Nluc-Apaf1, Cluc-Apaf1, and *photinus pyralis* firefly luciferase) diluted in 150 mM NaCl in a final volume of 1000 µl.
- III. 250 µl of PEI diluted in 150 mM NaCl in a final volume of 1000 µl.

- IV. Then PEI mixture added to DNA, mixed by vortexing and incubated at room temperature for 30 min (Sang et al. 2015).
- V. The PEI/DNA complex added to the flasks and incubated at 37°C, 5% CO₂.

Production of S-100 extract

To find the optimum time of transfection and level of protein expression, cells trypsinized and harvested 24 or 48 hours after transfection.

- I. The cells were lysed by resuspending in extraction buffer containing:
 - ✓ 50 mM HEPES pH 7.4,
 - ✓ 10 mM KCl,
 - ✓ 2 mM MgCl₂,
 - ✓ 5 mM EGTA,
 - ✓ Cytochalasin B (1:1000 dilution to (10 µg/mL),
 - ✓ protease inhibitor cocktail (1:1000 dilution),
 - ✓ PMSF (100 mM final),
 - ✓ DTT (1 mM final).
- II. The cells were then undergone three cycles of freeze-thaw in liquid nitrogen.
- III. The cell lysate then spin down at 100,000 g for 60 min.
- IV. The supernatant collected and stored at -80°C.

Immunoblotting

An aliquot of the cell extract was used for immunoblotting. The protein concentration determined using Bradford reagent (Bradford 1976). For this, 2 µl of 0, 0.1, 0.2, 0.4, 0.8, and 1 mg/mL BSA were used as standard protein and 2 µl of S-100 extract mixed with 198 µl of Bradford reagent and incubated in dark for 10 min. Then the absorbance was read at 595 nm.

- I. 50 µg of proteins mixed with 6X loading buffer contains 12% SDS w/v. 30% Glycerol v/v, 0.4 mM Tris-HCl pH 6.8 and Bromophenol blue < 0.15% w/v and boiled at 95°C for 5 min.
- II. Samples were loaded on 8% polyacryl amide gel.
- III. The proteins were then electrotransferred to nitrocellulose membrane using transfer buffer containing 25mM Trizma base, 192mM Glycine, 10% Methanol for 2 hours at constant 250 mA.
- IV. The membrane was then blocked by PBS-Tween, 5 % w/v fat-free skimmed milk powder for 2 hours.
- V. The membranes washed by PBS.
- VI. The membrane exposed to primary antibody and incubated overnight at 4°C.
- VII. Then membranes washed three times in PBS, 10 min each, and exposed to a secondary antibody for 2 hours at room temperature.
- VIII. The membranes washed three times in PBS, 10 min each.
- IX. The membrane was scanned by Li-Cor machine.

in cellulo luciferase activity

- I. 5×10^5 cells seeded in 6-well plate and incubated over-night at 37°C.
- II. 2 µg DNA and 4 µl of 1 mg/mL PEI mixed with 150 mM NaCl up to 100 µl each.
- III. Then PEI solution added to DNA mixture, vortexed for 10 sec and incubated at room temperature for 30 mins.
- IV. 200 µl of DNA/PEI complex then added to each well and incubated at 37°C.
- V. As a control, pcDNA3.1 encoding *photinus pyralis* firefly luciferase was used.
- VI. After 24 hours, media removed, and cells were washed with HANKS buffer.
- VII. Cells were then trypsinized using 100 µl of trypsin-EDTA and 400 µl supplemented DMEM added to neutralize trypsin.
- VIII. Cells spin down at 1200 rpm for 5 min and re-suspended in 100 µl fresh DMEM.

- IX. 10 μ l of each sample mixed with 10 μ l of Trypan Blue and incubated for 10 min at room temperature.
- X. The number of cells was counted in all samples.
- XI. The remaining of the cell suspensions were used for luciferase activity and immunoblotting.
- XII. For luciferase assay, 90 μ l of Glo-One luciferase substrate added to each sample and the activity of luciferase was recorded as RLU/sec at 25°C for 15 mins

Cell death in transfected cultures

- I. 5×10^3 HEK293 cells seeded in ibidi μ -Plate 96 Well in a volume of 180 μ l and incubated over-night at 37°C, 5% CO₂ incubator.
- II. Cells were then transfected with 250 ng of DNA and 0.5 μ l of 1 mg/mL PEI, each made up to 10 μ l by 150 mM NaCl. PEI added to DNA and incubated at room temperature for 30 min after 10 sec vortexing.
- III. Then 20 μ l of PEI/DNA complex added to each well.
- IV. After 24 hours incubation, Hoechst 33342 and Propidium Iodide stains were added to each well at the final concentrations of 1 μ g/mL each and incubated for 10 mins. Propidium iodide is an impermeable red fluorescent dye (excitation/emission maxima = 493/636 nm) which intercalates into the DNA. Hoechst 33342 is a cell permeable blue fluorescent dye (excitation/emission maxima = 350/461 nm) and quite specific for all double strand DNA molecules.
- V. The samples were imaged by Operetta High Content Imaging System and the images were analysed using Harmony 3.

The percentage of dead cells calculated as below:

$$\% \text{ Dead Cells} = (\text{number of PI positive cells}) / (\text{number of Hoechst positive cells}) \times 100$$

2.3 Cell-free system

1. Making S-100 HEK293 extract in large scale

- I. 4×10^9 HEK 293 cells harvested from 150 T175 flasks.
- II. Cells centrifuged for 10 min at 1200 rpm at 4°C.
- III. Supernatant removed and the pellet washed with HANKS buffer and centrifuged again as mentioned.
- IV. HANKS buffer removed and the cell pellet gently and quickly re-suspended in 10 volumes of extraction buffer containing 50 mM HEPES pH 7.4, 10 mM KCl, 2 mM MgCl₂, 5 mM EGTA, Cytochalasin B (1:1000 dilution to (10 µg/mL), protease inhibitor cocktail (1:1000 dilution), PMSF (100 mM final), DTT (1 mM final).
- V. Mixture centrifuged immediately for 5 mins at 1200 rpm at 4 °C (Fearnhead et al., 1997).
- VI. Supernatant removed as much as possible, the pellet vortexed vigorously and snap-frozen in liquid nitrogen. Three cycles of snap-freezing, thawing on ice and vortexing disrupt all membranes.
- VII. Then the cell lysate transferred to Beckman-Coulter polycarbonate thick wall tubes (P60328MP, USA) and centrifuged at 100000 g for 1 hour. The cell lysate covered by Bio-Rad mineral oil (163-2129) before centrifugation.
- VIII. The mineral oil was removed and the supernatant was then collected, aliquoted, snap-froze and stored at -80°C.
- IX. Protein concentration was also determined using Bradford reagent.

2. Caspase-3 activity and processing

- I. 65 µL of S-100 HEK 293 extract in the presence and absence of cytochrome c (1.6 µM) and dATP (1mM) incubated or not at 37 °C for 15, 30, 45 and 60 min.

- II. Then 15 μ L of each reaction used for measuring caspase-3 like activity. 185 μ L of assay buffer added to the activated reactions. Caspase assay buffer composed of:

- ✓ HEPES 200mM,
- ✓ 40 μ M DEVD-AMC (ALX-260-032, Enzo)
- ✓ and 5 mM DTT

- III. Fluorescent intensity was recorded over 30 min.

Another 25 μ L of the S-100 extracts used for immunoblotting according to the protocol mentioned earlier. Briefly, 5 μ L of Laemelli Buffer added to each sample and incubated at 95°C for 5 mins. Samples were then loaded on 15% polyacryl amide gel and run at 100V for 90 min. The proteins were then electrotransferred to nitrocellulose membrane at 250 mA for 1 hour. The membrane was then incubated with either primary caspase-3 or caspase-9 monoclonal antibody over-night at 4°C. Membrane washed with TPBS 0.1% three times, 10 mins each and exposed to a secondary antibody for 1 hour at room temperature. Membrane washed with TPBS 0.1% three times, 10 mins each and the protein of interest was detected using Li-Cor.

3. Gel filtration chromatography for detecting apoptosome

- IV. 1 mL of S-100 HEK 293 extract activated or not by addition of cytochrome c (1.6 μ M) and dATP (1mM) and incubated at 37°C for 15 mins.
- V. Then the samples loaded on Sephacryl 300 HR column. The column connected to AKTAprime chromatography system.
- VI. The fractionation performed at 0.6 mL/min flow rate, 3 mL fraction size and 0.5 Pa pressure.
- VII. The column washed with ddH₂O overnight.
- VIII. Then the column equilibrated with two column volumes of the equilibration buffer containing:
- ✓ 5% (w/v) sucrose,

- ✓ 0.1 % (w/v) CHAPS,
- ✓ 20 mM HEPES/NaOH,
- ✓ 5 mM DTT
- ✓ and 50 mM NaCl. (Cain et al., 2000).

- IX. The sample injected in the column.
- X. Fractions 19 to 34 collected according to the size of thyroglobulin (669 KDa) and aldolase (158 KDa) and the number of fractions they came out of the column.
- XI. The fractions were then concentrated using 10 MW Pierce Protein Concentrator (Thermoscientific, 88517). Using these concentrators, more than 90% of the proteins are recovered after 15 min centrifugation at $4000 \times g$, 4°C.
- XII. The remaining solution on the top of the filter collected for immunoblotting.
- XIII. Then 30 μ L of each fraction loaded on 8% polyacryl amide gel. Protein transferred to nitrocellulose membrane and exposed to Apaf-1 antibody overnight at 4°C followed by Goat-anti Rat for 2 hours, as described earlier.

***in vitro* assays**

1. Plasmid extraction

- I. 250 mL LB inoculated by 250 μ L of glycerol stock bacteria previously transformed with either Nluc-Apaf1-pcDNA3.1 or Cluc-Aapf1-pcDNA3.1.
- II. The culture incubated at 18°C, 225 rpm shake for 60 hours.
- III. The bacterial culture aliquoted in 50 mL tube and centrifuged for 20 min at 4500 rpm.
- IV. The pellet in each tube then re-suspended in 4 mL Buffer P1 (QIAGEN Plasmid Midi Kit, 12143).).
- V. Cells were lysed with 4 mL Buffer P2 and incubated for 5 mins at room temperature.
- VI. Then 4 mL buffer N3 added and the mixture gently inverted for few times.

- VII. The mixture centrifuged for 30 min at 4800 rpm at 4°C.
- VIII. The Midi columns equilibrated by 4 mL of QBT buffer.
- IX. The supernatant from the last step loaded on the column. The liquid was passed through the filter by gravity flow.
- X. Then the column was washed twice using 10 mL QC buffer.
- XI. The column eluted with 5 mL QF buffer.
- XII. 3.5 mL 2-isopropanol added to precipitate DNA and centrifuged at $13000 \times g$ for 20 min at 4°C.
- XIII. Supernatant removed, and the pellet washed with 10 mL 70% ethanol and centrifuged at $13000 \times g$ for 10 min at room temperature.
- XIV. The ethanol removed, and the DNA pellet air-dried for 10 mins.
- XV. At the end, the pellets re-suspended in 1 mL TE buffer pH 8.0.
- XVI. The DNA concentration determined using NanoDrop 2000.

2. Making S-100 extract of HEK 293 cells expressing fusion proteins

- I. 1×10^{10} HEK 293 cells grew in T175 flasks.
- II. Half of the flasks used for transfection with Nluc-Apaf1-pcDNA3.1 and the other half with Cluc-Apaf1-pcDNA3.1.
- III. For each T175 flask, 50 ug plasmid DNA and 250 μ L 1 mg/mL PEI made up to 1 mL using 150 mM NaCl.
- IV. The PEI solution added to DNA and vortexed for 20 sec and incubated at room temperature for 30 mins.
- V. The PEI/DNA complex was then added to each flask and incubated for 24 hours at 37°C, 5% CO₂.
- VI. The cells harvested and S-100 HEK 293 cells prepared as mentioned earlier.
- VII. The protein concentration determined using Bradford method.

2.4 Validation of the luciferase-based reporters

1. Split luciferase reconstitution assay

- I. 5 μ L of S-100 extract expressing Nluc-Apaf-1 mixed with 5 μ L S-100 extract expressing Cluc-Apaf1.
- II. cytochrome c (1.6 μ M) and dATP (1mM) added and incubated on ice.
- III. 35 μ L of Glo-One luciferase substrate (E6110, Promega) added and the 96-well plate containing the reaction recorded for 15 min in the plate reader.

Titration of cytochrome c

- I. 5 μ L of S-100 extract expressing Nluc-Apaf-1 mixed with 5 μ L S-100 extract expressing Cluc-Apaf-1
- II. Different concentrations of cytochrome c (0.01, 0.03, 0.1, 0.3, 1.0, 2.1, 10, and 30 μ M) and dATP (1mM) were added to each reaction.
- III. Then 35 μ L of luciferase substrate added and the luminescent signal recorded over 15 mins at 25°C.

2. Titration of NS3694, an inhibitor of apoptosome formation

- I. μ L of S-100 extract expressing Nluc-Apaf-1 mixed with 4.5 μ L S-100 extract expressing Cluc-Apaf-1 and
- II. 1 μ L of NS3694 added to have final concentrations of 0.00027, 0.00083, 0.0027, 0.0083, 0.027, 0.083, 0.27, 0.83, 2.78, 5.5 mM.
- III. Then the mixture incubated on ice for 10 mins.
- IV. Cytochrome c (1.6 μ M) and dATP (1mM) added and
- IV. The activity of split luciferase recorded after addition of 35 μ L luciferase substrate.

3. Gel filtration of overexpressed extracts

- I. 1 mL of extracts expressing Nluc-Apaf-1 and Cluc-Apaf-1 or whole luciferase activated or not by adding cytochrome c (1.6 μ M) and dATP (1mM) or water, incubated at 25°C for 10 mins and loaded on Sephacryl 300 HR column as described earlier.

II. The fractions were then collected, concentrated and used for immunoblotting.

4. Cation exchange chromatography to exclude cytochrome c from S100 extract

SP-sepharose resin (Sigma) were used for removal of cytochrome c from the extract.

- I. 100 μ L of the resins were washed with extraction buffer.
- II. The resins spin down at 3000 rpm 4°C for 3 min.
- III. Supernatant replaced by 200 μ L of S100 extract.
- IV. The mixture incubated on ice for 15 min, with tapping the tube every five min.
- V. The mixture spin down and the supernatant was taken for further investigation.

2.5 Screening

2.5.1 Toxicant library

A library of known human toxicants (see appendix B), including toxicants known to interfere with spermatogenesis was tested to identify those that reduce luciferase activity in the split-luciferase assay. Toxicants were screened at 1 mM. Screening was performed using the Perkin Elmer Janus Automated Workstation in 96-well plate format. An inhibitor was defined as any toxicant that reduced mean split luciferase activity by more than Q1 minus $1.7 \times$ interquartile range (IQR).

177 toxic compounds were purchased from Sigma and 100 mM of each prepared by diluting in DMSO. Toxicants were screened at 1 mM concentration. Briefly:

- I. 10 μ L of diluted Nluc/Apaf-1 and Cluc/Apaf-1 extract added to each well.
- II. The extract was mixed with 5 μ L of 1 mM toxicant library compounds.
- III. Incubated for 10 min at 4 °C.
- IV. Then, 7 μ L of Cc/dATP (1mM and 1.6 μ M final concentration, respectively) added and mixed.
- V. Split luciferase activity was measured by adding 33 μ L of One-Glo luciferase assay system (Promega) to each well and luminescence signal recorded over 15 minutes.

2.5.2 Natural product library

The traditional method of screening, measuring the caspase-3 like activity as an indirect readout of apoptosome formation, was combined with our new split luciferase assay. In this approach, a panel of 64 crude extracts collected from marine organisms living in Irish waters were screened using DEVDase assay. Then those with inhibitory effects on caspase activity further re-tested using split luciferase assay. In this assay, 4 mM M50054, an inhibitor of caspase-3, and 1mM NS3694, an inhibitor of apoptosome, were used as the control.

Collection and extraction

All samples were collected during the scientific cruise CE16006 in the Whittard Canyon using the R/V Celtic Explorer and the ROV Holland I. Upon collection samples were photographed, catalogued and immediately frozen at -80 °C. Each sample was lyophilized and extracted in both a polar and non-polar solvent for biological screening.

*Zoanthids on *Aphrocallistes beatrix**

Once dried the zoanthids were removed from the sponge and combined resulting in a dry weight of 13.06 g. Sample locations and depths are showcased in Table 1 below. The zoanthids were placed in a Soxhlet and extracted in dichloromethane until the solvent in the extraction chamber remained colourless. The extract was filtered and the dichloromethane in the filtrate was removed under reduced pressure yielding a yellow gum (1.54 g, RMY-243-1). The extracted material was dried vented in a fumehood and subsequently extracted in methanol and sonicated for 30 minutes and left to stand for 24 hrs. The solvent was filtered and replenished and left to stand for a further 24 hrs two more times. The filtered polar extracts were combined and concentrated in vacuo, yielding a brown gum (3.2 g, RMY-243-2).

<u>Sample Id</u>	<u>Long</u>	<u>Lat</u>	<u>Depth [m]</u>
1784	-9.8840102	48.60474	1082.12
1793	-9.8831533	48.60392	1132.89
1856	-10.5308824	48.70619	1134.82
1873	-10.316680	48.63268	985.31
1878	-10.3166079	48.63283	986.08
1884	-10.3167011	48.63205	1028.79
1885	-10.3166375	48.63281	986.11

Collection sites and depths for all the zoathids growing on *Aphrocallistes beatrix* (Gray, 1858).

Crude extracts were prepared at a concentration of 30 mg.mL⁻¹ in biological grade DMSO. Fractions were prepared at 5 mg.mL⁻¹ for additional screening. Sample were sonicated into solution and loaded into a 96-well plate for screening.

Preparative HPLC was performed on a Jasco PU-2087 Plus equipped with a UV-Vis detector UV 2075 and analytical HPLC performed on Agilent 1260 analytical HPLC series equipped with a DAD detector. All standard NMR experiments were measured on a 600 MHz equipped with a cryoprobe (Varian). Chemical shifts (δ in ppm) are referenced to carbons (δ C 49.0 ppm) and residual protons (δ H 3.31 ppm) signals of MeOH-d₄. High Resolution Electrospray Ionisation Mass Spectrometry (HRESIMS) data was obtained from a qTOF Agilent 6540 in ESI (+).

64 whole extracts from marine organisms were used for screening as below:

- I. 5 μ L of each extract diluted in 45 μ L of extraction buffer.
- II. Then 5 μ L of the 1:10 diluted crude extracts mixed with 10 μ L of HEK293 S-100 extract.
- III. The reactions were incubated for 15 min at 4°C.
- IV. Then 7 μ L of cytochrome c and dATP (1.6 μ M and 1 mM, respectively) added.
- V. Incubated at 25°C for 15 mins.
- VI. Then 178 μ L 40 μ M DEVD-AMC added to each well and caspase activity was recorded for 15 min at 25°C.

In this assay, 4 mM M50054, an inhibitor of caspase-3, was used as the control. S-100 HEK293 extract treated with DMSO was also used as a control to consider the effect of DMSO on the assay. The second round of screening was performed using split luciferase assay. For doing split luciferase assay:

- I. 4.5 μ l of each S-100 HEK293 expressing Nluc-Apaf-1 and Cluc-Apaf-1 were mixed.
- II. 1 μ l DMSO or any of the hit compounds added and incubated for 15 min on ice.
- III. 30 μ L luciferase reagent added following addition of 5.5 μ l Cc/dATP.
- IV. Then the reactions were read at 25°C for 15 min.

2.6 Production of the recombinant proteins

1. Cloning of Nluc-Apaf-1 and Cluc-Apaf-1 into pFASTBAC donor plasmid

Wildtype Apaf-1 was cloned in pFASTBAC plasmid previously. PCR performed to amplify the Nluc-Apaf-1 and Cluc-Apaf-1 fragments with the sequences encoding 6 \times His affinity tag and thrombin recognition/cleavage site (LVPRGS). The PCR products also contained a 15-base pair fragment overlapped with the N-terminal of Apaf-1 and pFASTBAC plasmid.

- I. In-fusion cloning performed using 100 ng of purified vector and 100 ng of PCR-amplified fragments.
- II. The mixtures incubated at 50°C for 15 min and then placed on ice.
- III. 5 μ L of each reaction was used for transfection into 50 μ L competent DH10Bac *e.coli* cells.
- IV. The mixture of DNA and the competent cells were incubated on ice for 30 min with tapping every 5 mins.
- V. The mixture then was heat-shocked for 45 sec at 42°C and incubated on ice for 5 mins.
- VI. Then 950 μ L SOC added to each reaction and placed in shaking incubator at 37°C for 4 hours.
- VII. The cells spin down at 4500 rpm for 5 mins.

- VIII. The media removed and the pellet resuspended in 100 μ L fresh LB.
- IX. The cells streaked on LB-agar plates containing 100 μ g/mL X-gal, 50 μ g/mL kanamycin, 7 μ g/mL gentamycin, 10 μ g/mL tetracyclin and 40 μ g/mL IPTG.
- X. The plates were then incubated at 20°C until the colonies grow. Incubation at 20°C avoid the sequence rearrangements in Apaf-1 amplification (Azad, Tashakor, Ghahremani, et al., 2014).
- XI. 10 colonies of each reaction were picked and liquid culture and resuspended in LB containing kanamycin, gentamycin and tetracycline.
- XII. The cultures incubated at 20°C for 60 hours.
- XIII. The large bacmids extracted using either Midi-prep plasmid extraction kit or ZR BAC DNA mini-prep (Epigenetics Company).
- XIV. The extracted bacmids were analysed by running on the agarose gel and PCR.
- XV. 0.5 % agarose gel was made using TAE buffer and mixed with SYBR Safe DNA gel staining.
- XVI. 5 μ L of each sample was loaded and the gel was run at a constant voltage of 20 V for 16 hours. Lambda DNA HindIII Digest and 1 Kb DNA markers were used to clarify the size of the large bacmids and the plasmids.

Validation of the bacmids

To confirm the transposition and insertion of the gene of interest into the bacmid the fragment within the lacZ complementation region of the bacmid was PCR-amplified using pUC/M13 primers. To eliminate the possibility of detecting the false positive PCR products, we also used M13 forward primer and gene-specific reverse primer to amplify the insertion of Apaf-1 gene into the bacmid. 12 colonies were screened for checking the insertion of the Apaf-1. As shown in Figure 2-1, insertion of the gene of interest produces a fragment of 2300 bp plus the size of the inserted gene which is 3700 bp and produces 6000 bp fragment (Figure 2-1).

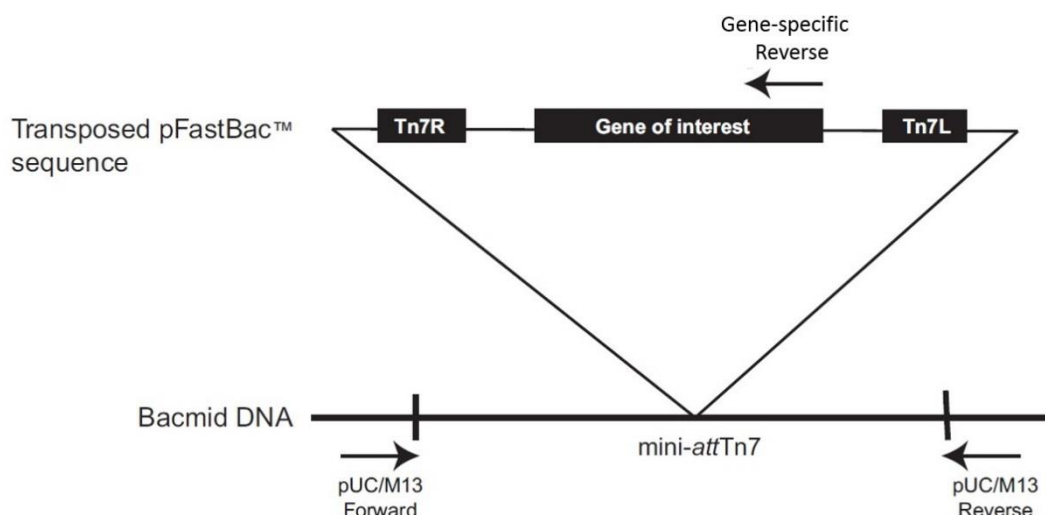


Figure 2.1. Transposition region in recombinant bacmids. The insertion site is flanked by pUC/M13 forward and reverse sequences. PCR amplification using pUC/M13 forward and reverse primers produces a 6000 bp fragment. PCR amplification using pUC/M13 forward and Apaf-1 specific reverse primers produces a 5500 bp fragment.

PCR was performed using the primers listed below:

Primer	Sequence
pUC/M13 Forward	5'-CCCAGTCACGACGTTGTAAAACG-3'
pUC/M13 Reverse	5'-AGCGGATAACAATTTCACACAGG-3'
Apaf-1 Reverse	5'-GGATCCTTATTCTAAAGTCTGTAAA-3'

2. Transfection and expression of Sf21 cells with recombinant bacmid

- I. A frozen stock of Sf21 cells thawed and cultured in 25 mL of Sf-900 II SFM supplemented with 1 X final concentration and 10 % FBS.
- II. The cells were kept growing for a week until the viability of >97% was achieved.
- III. For transfection, 7×10^5 cells were seeded in 6-well plate in 2 mL of Sf-900 II SFM supplemented with 0.5 X final concentration penicillin/streptomycin and 1.5 % FBS and incubated at 28°C for 2 hours to allow the cells adhere to the plates.

- IV. Then 3 μg of bacmid DNA (Nluc-Apaf1, Cluc-Apaf1, and wild-type Apaf-1) diluted into 100 μL of Sf-900 II SFM and mixed gently.
- V. 8 μL of CellfectinTM II Reagent was also diluted in 100 Sf-900 II SFM and mixed.
- VI. Diluted bacmid and Cellfectin mixed and incubated at room temperature for 30 mins.
- VII. Bacmid/Cellfectin mixture added to the wells dropwise and incubated at 28°C for 5 hours.
- VIII. The media removed and replaced with fresh Sf-900 II SFM supplemented with 1 X final concentration penicillin/streptomycin and 10 % FBS.
- IX. After 72 hours the supernatant collected and stored as P0 viral stock by spinning at 500g for 5 min and transferring the virus-containing supernatant to a fresh tube and storing at -80°C.
- X. The cell pellet was also harvested and lysed by extraction buffer as explained before.
- XI. The lysates were then used for SDS-PAGE to check the expression of bacmids within the insect cells.

3. Making P1 viral stock

- I. 7×10^5 cells were seeded in 6-well plate in 2 mL of Sf-900 II SFM.
- II. Then 10, 20, 30, 40 and 50 μL of the P0 viral stock was used for infecting the Sf21 cells.
- III. The cells incubated at 28°C for 5 days.
- IV. The cells were harvested, lysed and the lysate was used for immunoblotting using Anti-Apaf1 antibody.

To amplify the P1 stock in large scale:

- I. 6×10^6 cells seeded in four T175 flask and incubated at 28°C overnight.
- II. The cells were then infected by 125 μL of P0 viral stock in 25 mL culture and incubated for five days.
- III. The supernatant collected as P1 stock and stored at -80°C.

4. Adaptation of the Sf21 cells to suspension culture

For doing the large-scale infection and obtaining a high yield of recombinant proteins, we switched from adherent culture to suspension culture. We used 1 litre Corning® ProCulture® glass spinner flask (sigma) which is suitable for 200-400 mL culture.

- I. 250 mL complete medium containing 3×10^5 cells/mL was inoculated and incubated at 28°C on the shaker at 135 rpm.
- II. The cells subcultured when it reached 2×10^6 to 3×10^6 viable cells/mL. The cells should be in the mid-log-phase of the growth when subculturing.
- III. The cells were kept being subcultured until the viability reached to >95% with no cell clumping.

5. Infection and purification of the recombinant proteins

- I. 200 mL Sf21 cells with viability more than 95% and density of 1×10^6 to 2×10^6 infected with 15 mL P1 viral stock encoding wild-type Apaf-1.
- II. The culture incubated at 28°C for 36 hours.
- III. The cells were then harvested by spinning at 400g for 10 mins.
- IV. Supernatant discarded and the pellet was resuspended in five volumes of buffer A containing:
 - ✓ 20 mM HEPES pH 7.5,
 - ✓ 10 mM KCl,
 - ✓ 1.5 mM MgCl₂,
 - ✓ 1 mM EDTA,
 - ✓ 1 mM EGTA,
 - ✓ 1 mM DTT
 - ✓ and 0.1 mM PMSF.
- V. Incubated on ice for 15 mins.
- VI. Then the cells lysed using homogenizer.
- VII. The lysate then centrifuged at 100,000g for 1:30 hour to make S-100 cell extract.
- VIII. The supernatant collected for purification.

6. Column preparation and His-tag purification

- I. To prepare the resin, 1 mL Ni-NTA resin first washed with 5 mL water to remove the ethanol.
- II. Then washed with 10 mL of 1 M KCl followed by washing with 10 mL of 10 mM KCl.
- III. Then incubated the resin to settle down and the residual supernatant removed.
- IV. Cell lysate mixed with the resin in 15 mL tube and incubated at 4°C for 15 mins.
- V. Then the mixture transferred to the column.
- VI. The lysate passed through the column by gravity.
- VII. An aliquot was taken as 'unbound'.
- VIII. The column then washed with 10 volumes of a buffer containing:
 - ✓ 20 mM HEPES pH 7.5,
 - ✓ 10 mM KCl,
 - ✓ 1.5 mM MgCl₂,
 - ✓ 1 M NaCl
 - ✓ and 20 mM imidazole.
- IX. An aliquot of the last fraction was taken as 'Washed'.
- X. Finally, the column eluted using 10 mL elution buffer containing:
 - ✓ 20 mM HEPES pH 7.5,
 - ✓ 10 mM KCl,
 - ✓ 1.5 mM MgCl₂,
 - ✓ and 250 mM imidazole.
- XI. The flow through was collected in 1 mL fraction.
- XII. The fractions stored in -80 after addition of glycerol to 20% final concentration.

7. Large-scale production of the rApaf1

- I. 300 mL suspension culture of Sf21 cells were infected with baculovirus expressing wild-type Apaf1 at the density of 2.2×10^6 cells/mL and incubated at 28°C.
- II. Cells were harvested 37 hours post-infection.

- III. The cells centrifuged at 600 g and the pellet was washed with HANKS buffer.
- IV. The cells were lysed in the buffer containing 20 mM HEPES pH 8.5, 10 mM KCl, 1.5 mM MgCl₂, 1 mM DTT, 0.1 mM PMSF and 1:1000 diluted protease inhibitor cocktail.
- V. Cells incubated on ice for 15 mins and the disrupted using homogenizer.
- VI. S-100 extract prepared and used for Nickel affinity chromatography.
- VII. The resins were washed using 10 volumes of washing buffer 1 containing:
 - ✓ 20 mM HEPES pH 8.5,
 - ✓ 5 mM β -mercaptoethanol,
 - ✓ 500 mM KCl, 20 mM imidazole
 - ✓ and 10 % glycerol.
- VIII. Then washed with 2 volumes of washing buffer 2 containing:
 - ✓ 20 mM HEPES pH 8.5,
 - ✓ 5 mM β -mercaptoethanol,
 - ✓ 1 M KCl,
 - ✓ and 10 % glycerol.
- IX. Re-washed with 2 volumes of washing buffer 1.
- X. The resins eluted using a buffer containing:
 - ✓ 20 mM HEPES pH 8.5,
 - ✓ 250 mM imidazole,
 - ✓ 100 mM KCl,
 - ✓ 5 mM β -mercaptoethanol
 - ✓ and 10 % glycerol.

8. Buffer exchange

The protein concentrator (cut-off 100KDa) was used to do the buffer exchange as below:

- I. 2 mL of the collected proteins transferred to the concentrator.
- II. 4 mL of the exchange buffer containing 20 mM HEPES, 10 mM KCl, 1 mM DTT and 10 % glycerol was added

- III. The mixture spin for 20 min at 4000 rpm.
- IV. When the final volume reduced to 2 mL, another 4 mL of the buffer and added.
- V. This protocol repeated 4 times.
- VI. Then proteins aliquoted in 100 μ L fractions. The aliquots were snap-frozen and stored in -80°C .
- VII. To ensure the presence of proteins after buffer exchange and removal of degraded proteins, an aliquot was taken and used for immunoblotting

Gel filtration of PCP-treated rApaf-1

- I. 100 μ L of rApaf1 mixtures were made as shown in table below.

RXN	rApaf-1 (μ L)	Cytochrome c (1.6 μ M)	dATP (10 mM)	DMSO (μ L)
1	100	-	-	1
2	100	30	16	PCP (1 mM)
3	100	30	16	PCP (1 mM)

- II. An aliquot of each reaction was stored for caspase-9 activity assay.
- III. The fractions collected and the proteins were detected by dot blot.

Dot blot

- I. Simply 500 μ L of each fraction loaded to methanol-activated PVDF,
- II. The membrane was blocked using 8% skimmed milk in TPBS 0.1%.
- III. The membrane incubated with Anti-Apaf1 antibody overnight.
- IV. Then washed for 3 times with TPBS 0.1%.
- V. Then incubated with secondary antibody (Goat-Anti Rat) for 2 hours.
- VI. The membrane was washed with TPBS 0.1% twice and then washed with PBS.
- VII. The membrane scanned using Li-Cor system.

2.7 Biochemical assays

Thermo-stability shift assay

- I. cytochrome c (1 mg/mL) and rApaf-1 (~50 ng/μL) individually incubated with PCP 1 mM.
- II. Then incubated at 42, 46, 50, 54, 58, 62, 66, 70, 74, and 80°C for 7 mins in a PCR machine (Applied Biosystem).
- III. The mixtures were then spin for 45 mins at 4°C.
- IV. Then 10 μL of the supernatant was carefully taken for SDS-PAGE and immunoblotting, respectively for cytochrome c and rApaf-1.

Co-precipitation assay

Part A: Optimization

- I. 1 mg/mL cytochrome c dissolved in 10 mM HEPES pH 7.4, and different concentrations of NaCl (10, 20, 60, 120, 190 mM).
- II. 50 μL of each reaction added to 15 μL of pre-washed Ni beads and incubated on ice for 15 min.
- III. Spin down at 3000 rpm for 3 min.
- IV. 15 μL of supernatant was used for SDS-PAGE as well as the resins.

Part B: Assay

- I. 1 mg/mL cytochrome c incubated with DMSO or PCP (1 mM) on ice for 10 min.
- II. Then treated cytochrome c added to ~300 ng rApaf-1 in 120 mM NaCl.
- III. The mixture incubated for 10 min on ice.
- IV. The mixtures added to 20 μL of pre-washed Ni beads and incubated for 15 min at 25°C.
- V. Reactions were centrifuged at 3000 rpm for 3 min.
- VI. Supernatant collected, and the pellet washed gently four times with 4 × 1 mL of buffer containing 10 mM HEPES pH 7.4 and 120 mM NaCl.
- VII. Centrifuged as above and samples were used for immunoblotting.

2.8 Microscopy

Morphological studies of the cells and nuclei was performed by either staining the cells, by propidium iodide/7-AAD (nucleous), or TMRE (mitochondria), or by using HeLa cells expressing GFP tagged H2B in the nucleous and mCherry-tagged tubulin in the cytoplasm. The sizes and intensities of the nuclei were measured using Harmony3.1 software. The intensities of the nuclei first normalised to the nuclei area in all samples to avoid the errors causing from different numbers of nuclei in each image. The intensity to area ratio of the nuclei were calculated accordingly.

2.9 Modelling studies

Protein preparation_ The 3D structure of numerous proteins could be found on Protein Data Bank (PDB). The typical PDB structure file is not suitable for molecular modeling calculations. A typical PDB structure file consists of heavy atoms and may also covers the co-crystallized ligand, water molecules, metal ions, and other cofactors. Some proteins are multi-unit and may need to be reduced to a single unit. Proteins may have incorrect bond order assignments, charge states, or orientations of various groups. In some cases, the resolution of X-ray is not quite high and distinguishing the NH and O is difficult and the placement of these groups must be checked. Ionization and tautomeric states also need to be assigned. Besides, missing information may exist on the sequence of the proteins (missing a residue/s or atom/s like hydrogen atoms). Therefore, some modifications and corrections are required prior to modeling calculations. During protein preparation, unwanted chains and waters can be deleted, het groups would be fixed/deleted, orientations of hydrogen-bonded groups would be optimized and the structure will be minimized. Glide (Grid-based Ligand Docking with Energetics) uses an all-atom force field for evaluation of accurate energy and therefore, bond orders and ionization states should be determined. For this side chains are reoriented, and steric clashes are relieved when necessary.

Optimizing the protein hydrogen bonding network_ The hydrogen-bonding network was optimized by reorientation of hydroxyl and thiol groups, water molecules, amide groups of asparagine (Asn) and glutamine (Gln), and the imidazole ring in histidine (His); and prediction of protonation states of histidine (His), aspartic acid (Asp) and glutamic acid (Glu) and tautomeric states of histidine. These optimizations are necessary because the orientation of hydroxyl (or thiol) groups, the terminal amide groups in asparagine and glutamine, and the ring of histidine cannot be found from the X-ray structure.

Overturning the terminal amide groups and the histidine ring enhances charge-charge interactions with adjacent groups as well as hydrogen bonding. In addition, the protonation state of histidine, aspartic acid, and glutamic acid are varied to optimize hydrogen bonding and charge interactions. If waters are included, their orientations are also varied to optimize hydrogen bonding. Each of the hydrogen bond donors, His rings, and Asn and Gln terminal amides considers a separate orientable species. Optimizing the orientation of the various groups is an iterative process, which passes over all the groups whose H-bonds need to be optimized multiple times.

Minimizing the protein structure_ During protein minimization the heavy atoms are restrained, and strain can be released but not depart too much from the input geometry. Here, PDB files for solution structure of oxidized human cytochrome c (2N9J) and crystal structure of full-length murine Apaf-1 (3SFZ) and Apaf-1/caspase-9 holoenzyme (5WVE) were downloaded from protein data bank (<http://www.rcsb.org/>). The proteins were imported in Maestro 11.7 (Schrodinger) and then refined, optimized and minimized. Ramachandran plots were checked to see the changes before and after protein preparation.

Receptor grid generation_ Glide explore the favorable interactions between ligand molecules and a receptor molecule, usually a protein. The shape and properties of the receptor are defined on a grid by several different sets of fields that provide more precise scoring of the ligand poses. The hydroxyl groups of Ser, Thr, and Tyr residues can orient

differently in contact to different ligands. Therefore, I selected the hydroxyl groups as rotatable groups to generate the most favourable interactions.

2.10 Software and programs

Statistics, Analysis, Plots

- I. Graphpad prism v6.07
- II. R version 3.5.2

Molecular Biology

- I. SnapGene (SnapGene software from GSL Biotech; available at snapgene.com)
- II. Oligo 7 (Molecular Biology Insights, Inc. (DBA Oligo, Inc.))

In silico studies

- I. Maestro 11.7 (Schrodinger)
- II. Structure checker 18.5.0 (ChemAxon)
- III. MarvinView 18.5.0 (ChemAxon)
- IV. iGendock
- V. Discovery Studio Visualizer

ASSAY

DEVELOPMENT

&

VALIDATION

3.1 Amplification of the fragments

To develop new tool that would report apoptosome formation, we fused the sequence of N-terminal and C-terminal of firefly luciferase to individual Apaf-1 molecules. For this, N- and C-terminal of *photinus pyralis* firefly luciferase as well as Apaf-1 XL were PCR amplified. Apaf-1 XL is able to oligomerize and form a functional apoptosome with the ability to activate caspases. (G₄S)₂ and (G₄S)₃ were used as linkers for Nluc-Apaf-1 and (G₄S)₂ was used as a linker for Cluc-Apaf-1 fragments. The schematic presentation of the recombinant plasmids has been shown in Figure 3.1. The split point was selected based on the previous report by Ozawa (Misawa et al., 2010). Ozawa et al. made a library of 300 click beetle split luciferase fragments and measured the recovered luciferase activity when different combinations of fragments were tested. Based on their study the highest luciferase activity was recovered when 1-415 amino acid fragment considered as N-domain and 394-542 as C-domain. In this study, the corresponding residues were identified in firefly luciferase by sequence alignment to make split fragments.

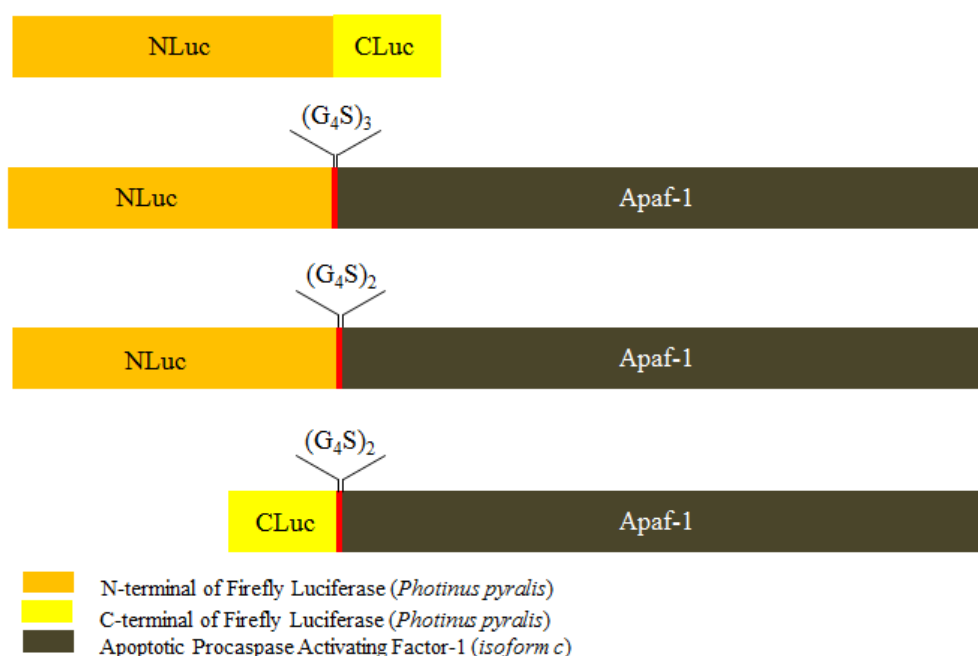


Figure 3.1. Schematic presentation of the recombinant constructs. N-domain and C-domain of luciferase fused to Apaf-1 using different repeats of flexible G4S linkers.

The corresponding fragments were PCR-amplified using High-fidelity, Hot-Start DNA polymerase. All fragments required for in-fusion cloning were synthesized with the right lengths, as detected on agarose gel electrophoresis.

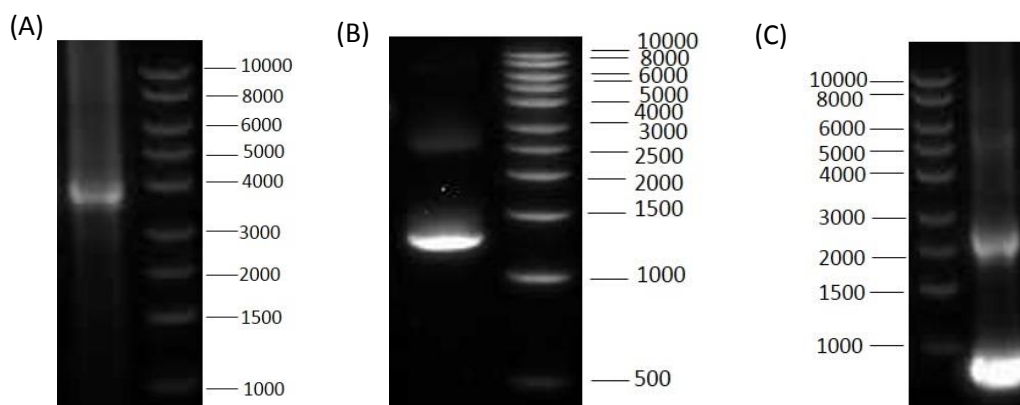


Figure 3.2. PCR-amplified fragments for in-fusion cloning. (A) Apaf-1, 3750 bp, (B) N-terminal of luciferase with inserted G₄S linker, 1330 bp and (C) C-terminal of luciferase with inserted G₄S linker, 570bp.

3.2 In-fusion cloning

In-fusion cloning system enables the cloning of one or more fragments into the vector of interest simultaneously. In this method, PCR products are amplified in such a way that shares a 15-base pair sequence with the homology to the sequences of the flanking fragments. The infusion enzyme produces the single stranded 5' overhangs which then re-annealed with the complement fragments and make the final circular vector. The overall strategy of in-fusion cloning has been shown in Figure 3.4. All the PCR products purified using Qiagen spin-column clean-up PCR product kit.

pcDNA 3.1 was used as a vector for cloning the fragments. pcDNA 3.1 is a mammalian high-level expression vector with the strong cytomegalovirus (CMV) promoter. This vector linearized using double digestion by Acc65I and BamHI. Digested vectors resolved in 1% agarose DNA gel electrophoresis and purified using gel extraction kit.

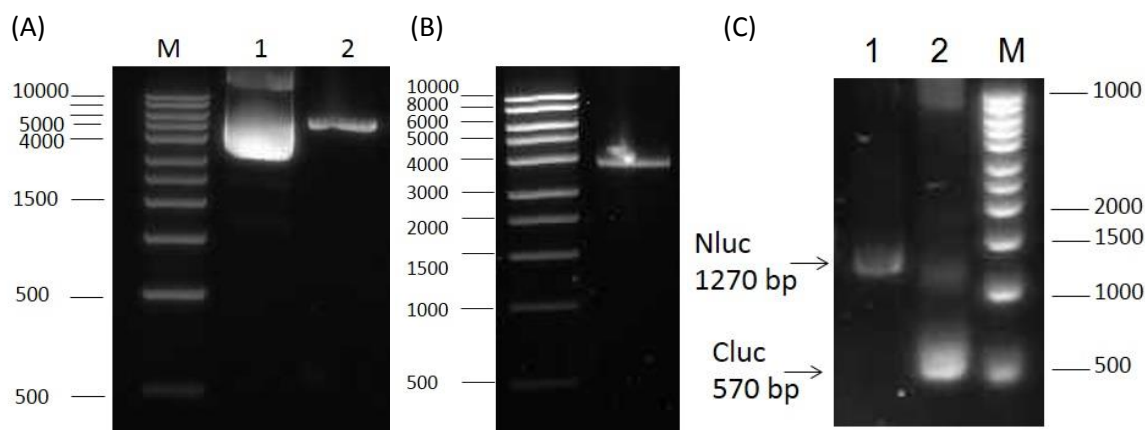


Figure 3.3. in-fusion cloning fragments. (A) pcDNA3.1 available in the lab transformed to SURE2 supercompetent cells and a single clone picked for further amplification of the plasmid. Lane 1 shows pcDNA3.1 plasmid and lane 2 is the Acc65I/BamHI double digested plasmid. (B) Apaf-1 with 15-bp overlap with G₄S linker and pcDNA3.1 at 5' and 3' respectively. (C) Split luciferase fragments. N-terminal of luciferase (lane 1) and C-terminal of luciferase (lane 2) share 15-bp overlap with pcDNA3.1 at 5' and Apaf-1 at 3'.

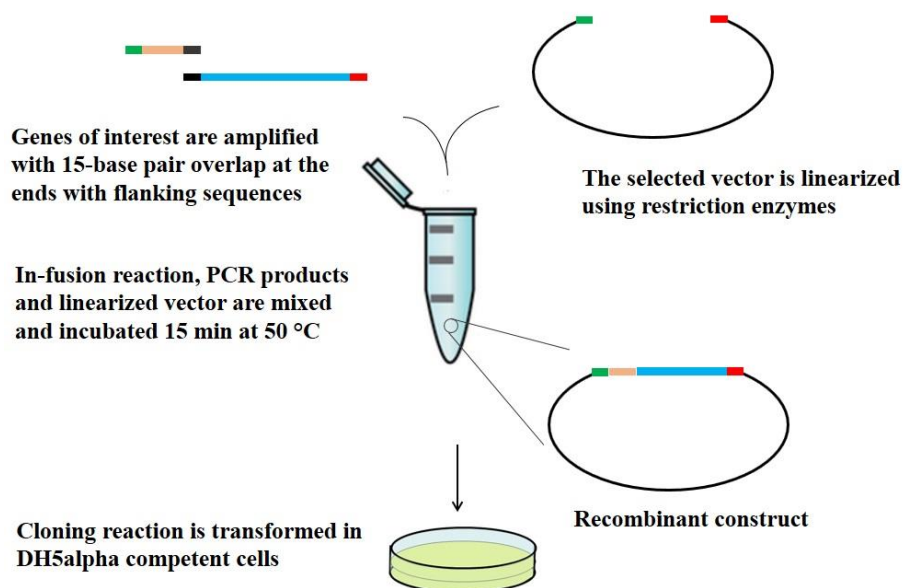


Figure 3.4. in-fusion cloning strategy. In this method, the genes of interest are amplified in such a way that share 15 base pair at each end with the flanking sequences. The vector also is linearized using single or double restriction enzyme(s). PCR products and linearized vector are mixed with in-fusion cloning reaction for 15 min at 50°C. Then cloning reaction is transformed into DH5alpha competent cells, in this case, SURE2 supercompetent cells. The transformed bacteria then plated and incubated at 18°C until the colonies grow.

3.3 Transformation of the in-fusion cloning reactions

After transformation of the in-fusion cloning reactions, single clones were picked and used for inoculation of fresh LB medium. Recombinant plasmids were extracted. To confirm the insertion of the genes of interest into the vector, double digestion performed using Acc65I and BamHI (Figure 3.5). The wild-type sequences of the inserted fragments were then confirmed by Primer Walking Service (Eurofinsgenomic).

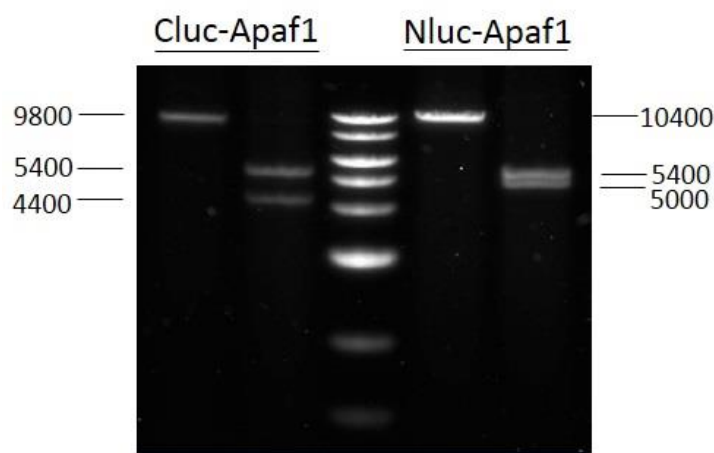


Figure 3.5. Digestion of plasmids. BamHI single digested and BamHI/Acc65I double digested recombinant plasmids. DNA loaded on 1% agarose gel. 5400 bp fragments are representatives of pcDNA3.1, 4400 bp and 5400 bp fragments are Cluc-Apaf-1 and Nluc-Apaf1, respectively.

3.4 Expression of the recombinant fusion proteins in the HEK293 cells

HEK 293 cells, derived from Human Embryonic Kidney cells, were used to analyse the expression, the level of expression and functionality of the recombinant proteins. HEK cells are fast-growing and are easy to transfect (Graham et al., 1977). Transfection of the Nluc-Apaf-1 and Cluc-Apaf-1 plasmids performed using Polyethylenimine (PEI) reagent (Polyplus). Polyethylenimine is a stable cationic polymer used largely for transient transfection of the target cells (Boussif et al., 1995; Ehrhardt et al., 2006). The cells harvested 24- and 48-hours post-transfection and used for immunoblotting. The level of overexpression did not change after 24 hours (Figure 3.6). Therefore, transfection of the plasmids for 24 hours is sufficient for obtaining the maximum overexpression of the proteins.

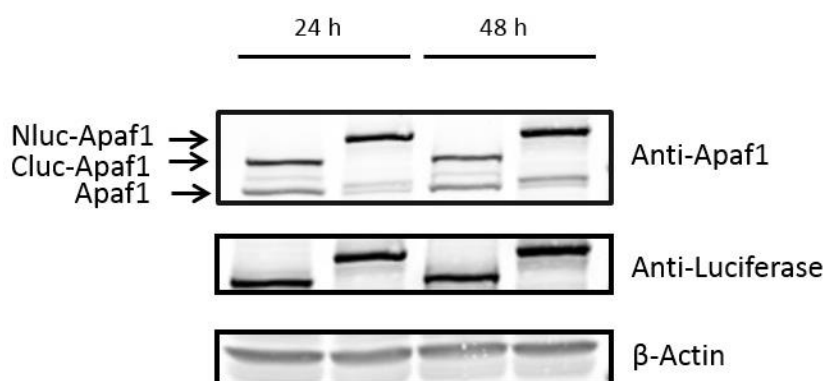


Figure 3.6. Expression of the recombinant fusion proteins. Nluc-Apaf-1 and Cluc-Apaf-1 separately transfected in HEK 293 cells. The cells harvested either 24 hours or 48 hours post transfection. Immunoblotting using anti-Apaf1 and anti-Luciferase showed the overexpression of the proteins. β -Actin was used as an internal control. The level of overexpression did not significantly change by longer incubation.

3.5 Detecting split luciferase activity in cells

To check the activity of split luciferase-fusion proteins, Nluc-Apaf-1 and Cluc-Apaf-1 transfected alone or co-transfected in HEK293 cells. The luciferase activity was only detected when Nluc-Apaf-1 with three repeats of G4S co-transfected with Cluc-Apaf-1. Therefore, for the rest of experiments Nluc-(G4S)₃-Apaf-1 (referred to as Nluc-Apaf-1) and Cluc-(G4S)₂-Apaf-1 (referred to as Cluc-Apaf-1) was used. Immunoblotting using anti-Apaf-1 and anti-luciferase confirmed the expression of the transiently transfected proteins (Figure 3.7A). The activity of luciferase was recorded as RLU/sec. All values were then normalized to the cell number and reported as RLU/sec/cell.

As shown in figure 3.7B, there is no luciferase activity when cells transfected with either Nluc-Apaf-1 or Cluc-Apaf1, very similar to the untransfected cells. However, when co-transfected, the activity of split luciferase increased by 1.45 ± 0.062 RLU/sec/cell. The control firefly luciferase activity was 3.52 ± 0.22 RLU/sec/cell. This shows that the fusion proteins are expressed, and the activity of split luciferase is detectable. However, the activity of split luciferase is not as high as luciferase. This difference could be due to the different structures of luciferase versus split luciferase, affinity to the substrate, kinetics and optimal conditions for enzyme activity.

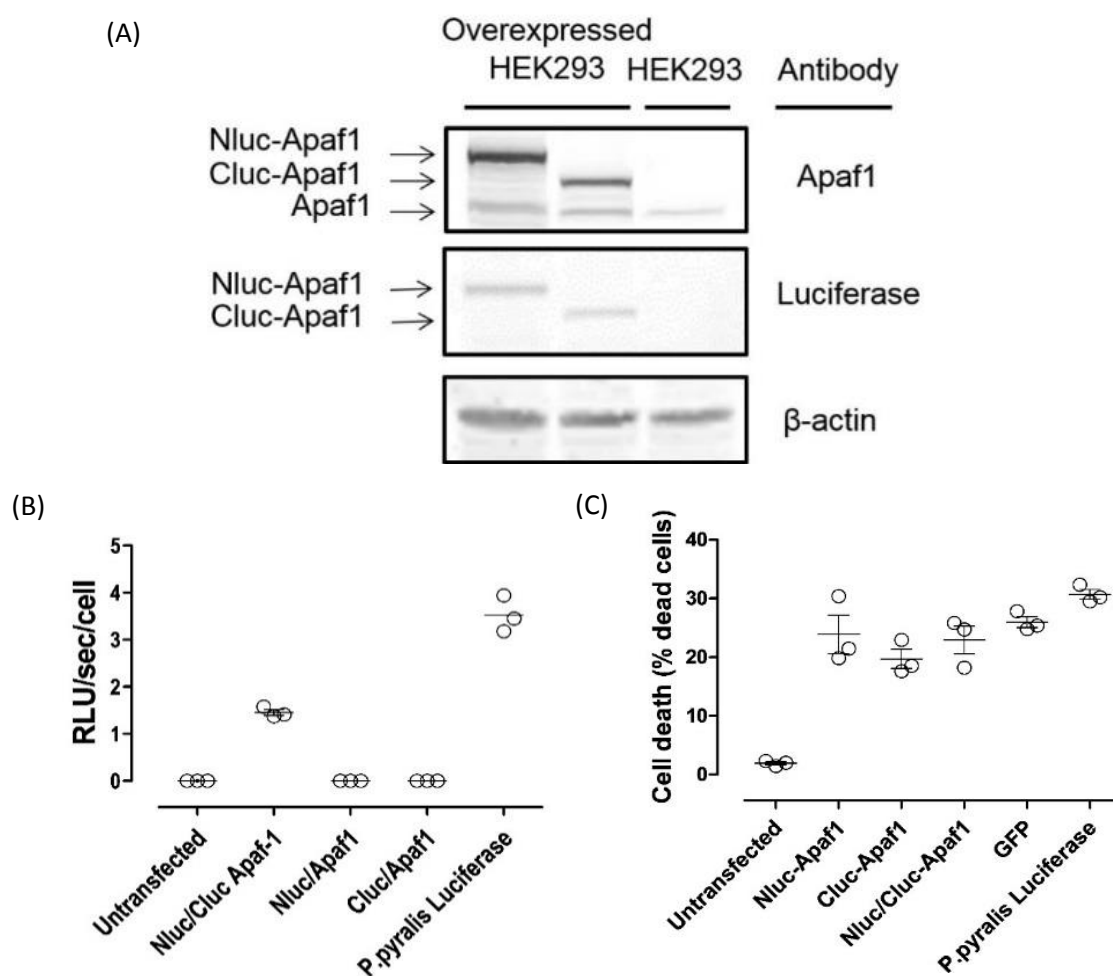


Figure 3.7. Immunoblotting and the activity of the overexpressed proteins. (A) Immunoblotting of the HEK 293 extracts expressing Nluc-Apaf-1 and Cluc-Apaf-1 using anti-Apaf-1 and anti-luciferase antibody. 60 μ g of each sample loaded on 8 % SDS-PAGE. Proteins with the expected molecular weight detected. (B) Split luciferase activity of the plasmids when transfected alone or co-transfected in HEK 293 cells. As a control, *photinus pyralis* luciferase was used. (C) Transfection-induced cell death. GFP and *photinus pyralis* luciferase were transfected as controls. HEK 293 cells were transfected or not with the plasmids. After 24 hours Hoechst 33324 and propidium iodide 1 μ g/mL added to each well and cell death measured using confocal automated microscopy.

3.6 Cell death in transfected cultures

Overexpression of Apaf-1 has been reported to induce cell death (Perkins et al., 1998). Therefore, the HEK293 cells were transfected with the Nluc-Apaf-1 and Cluc-Apaf-1 and cell death was measured. Cell death was measured using Propidium iodide and Hoechst 33342 staining.

Untransfected cells showed 1.93 ± 0.24 % death, while transfection causes 23.9 ± 3.28 %, 19.70 ± 1.65 %, 22.92 ± 2.83 %, 25.99 ± 0.92 and 30.69 ± 0.85 % death in the cells transfected with Nluc-Apaf-1, Cluc-Apaf-1, Nluc/Cluc-Apaf-1, GFP and firefly luciferase, respectively (Figure 3.7C). GFP was transfected as an irrelevant gene to cell death. Firefly luciferase was transfected to see how split luciferase activity is different to luciferase activity and to check the limit of bioluminescence detection. Similar level of cell death was observed no matter what sequences were expressed. It shows that this level of death was not sequence-dependent and was probably due to transfection method, although the ability of Apaf-1 overexpression to kill the cells has been reported before (Perkins et al., 1998).

For measuring the cell death after transfection, the culture media was not changed before addition of Hoechst 33342 and Propidium Iodide in order to avoid losing the dead cells. Therefore, due to the presence of DNA (used for transfection) in the wells, they all were stained. To calculate the accurate number of dead cells and remove the free DNA in the culture, a threshold was set based on the size of the cells in such a way that only those stained particles above that threshold were considered as desired objects (Figure 3.8).

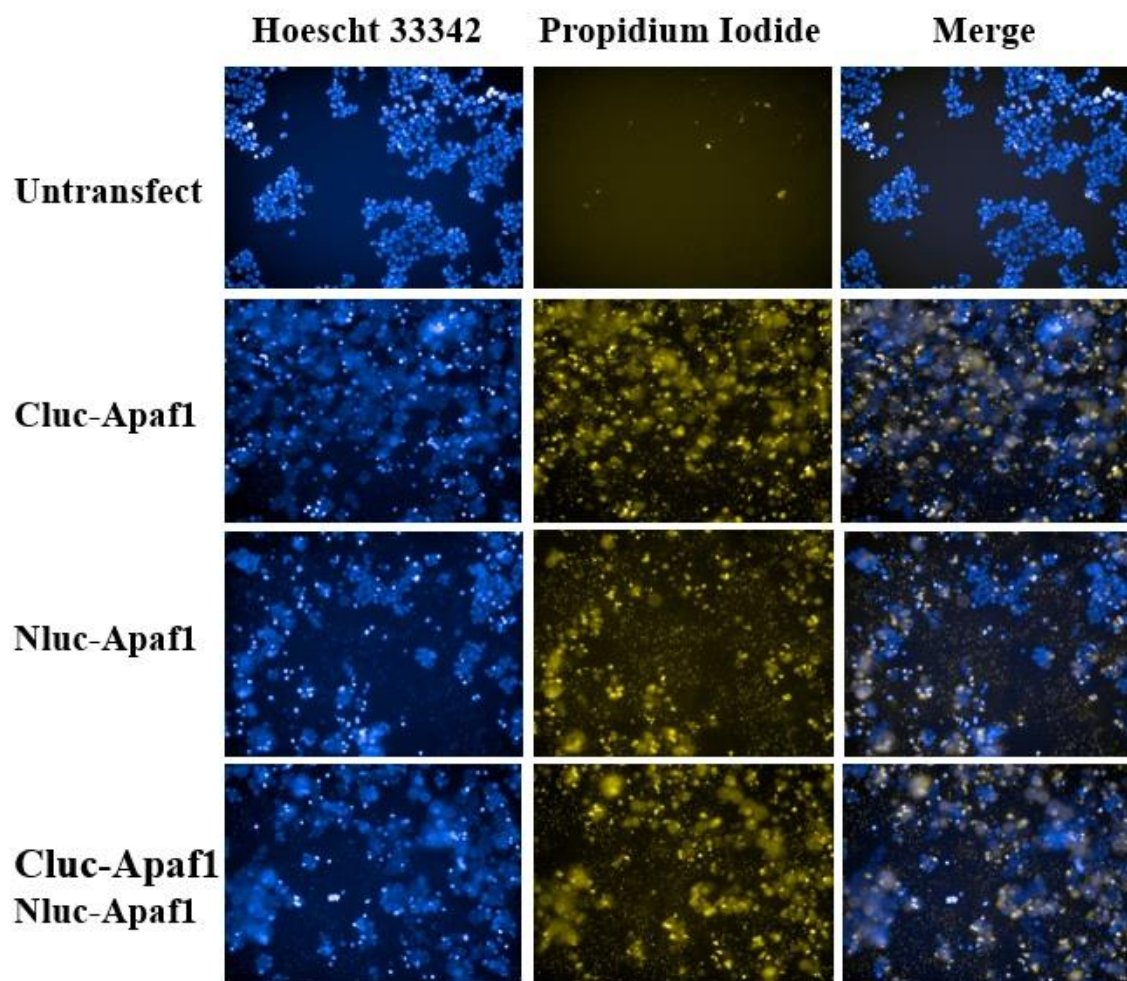


Figure 3.8. Cell death assay when cells transfected with the recombinant plasmids. HEK 293 cells were transfected or not with either Nluc-Apaf-1 or Cluc-Apaf-1 and co-transfected with Nluc-Apaf-1 and Cluc-Apaf1. After 24 hours cells were stained by adding Hoechst 33324 and propidium iodide 1 $\mu\text{g/mL}$ to each well and cell death measured using confocal automated microscopy. Quantification of the number of PI positive, Hoechst 33324 positive cells was performed by setting a threshold based on the average size of the particles to measure the cells, not the free plasmid in the culture media.

3.7 Detection of competent apoptotic machinery in cell free system

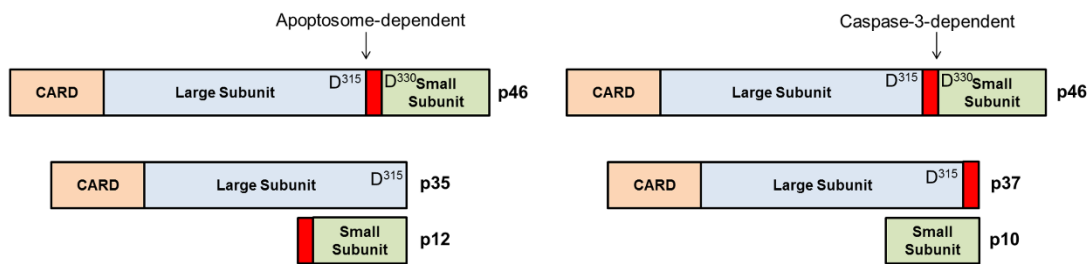
To develop the apoptotic machinery in cell free system, FPLC was used to fractionate the proteins within the extract and detect the formation of the oligomer Apaf-1, upon addition of cytochrome c and dATP. Furthermore, the activity and processing of the caspase-9 and caspase-3, the other key components of apoptotic machinery, were studied.

3.7.1 Caspase-3 and -9 activity and processing

To check the processing of caspase-9, S-100 extract was used to detect the processing of caspase-9 when incubated with or without cytochrome c and dATP. S100 extract is the cytosolic proteins that are obtained from the supernatant of the cell lysate after spinning at 100,000 g for 1 hour. The blot in figure 3.9B shows the processing of caspase-9 and generation of 37 and 35 KDa fragments in the presence of cytochrome c and dATP. Increasing the incubation time leads to more generation of 37 KDa fragment which is caspase-3 dependent.

The same experiment performed for caspase-3. There is no processing for caspase-3 when the extract is not incubated at 37°C even in the presence of cytochrome c and dATP (Figure 3.10B). However, after 15 min incubation, almost all of caspases cleaved and generated 19 and 17 KDa fragments. Longer incubations did not seem to play a further role in the processing of the caspase-3 except that p17 fragment is produced more, which is due to the auto-activation of caspase-3.

Caspase activity measured using DEVD-AMC (Cain et al., 2000). Fluorescent intensity was recorded over 30 min and normalized to the protein concentration. In each case, the rate of caspase activation calculated by measuring the slope of linear part of caspase activity plot (fluorescent intensity against time). These slopes used to plot the rate of activity over time. Figure 3.10C shows the rate of caspase activity when incubated for different periods of time. The activity of caspase-3 increases over the time with the highest rate of activity yielded after 15 mins incubation and it reaches a plateau after 30 mins.



(B)

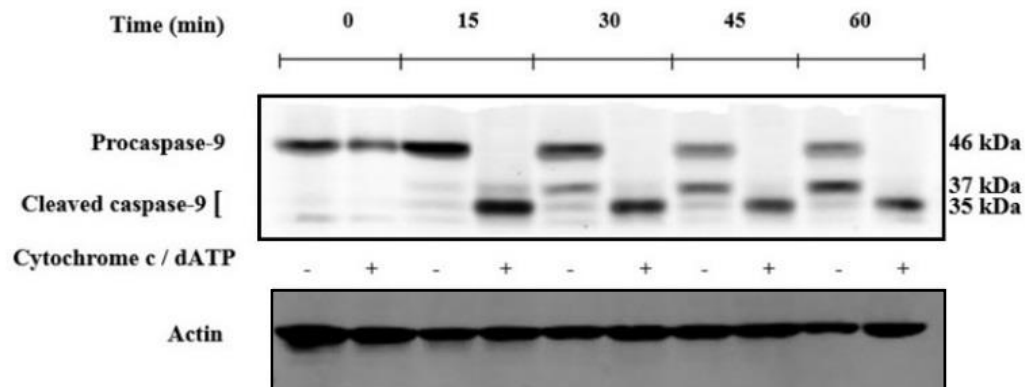


Figure 3.9. Caspase-9 processing. (A) Schematic presentation of caspase-9 processing. Cleavage at D315 is apoptosome-dependent and produces p35/p12 fragments. Second cleavage at D330 is caspase-3 dependent and generates p37/p10 fragments. (B) Processing and activity of caspase-9. HEK293 S-100 extracts incubated or not at 37°C for 15, 30, 45 and 60 min in the presence and absence of cytochrome c and dATP. Processing of caspase-9 studied by immunoblotting. The cleaved products of caspase-9 are detected after 15 min incubation. The cleaved fragments are detectable after 15 min incubation.

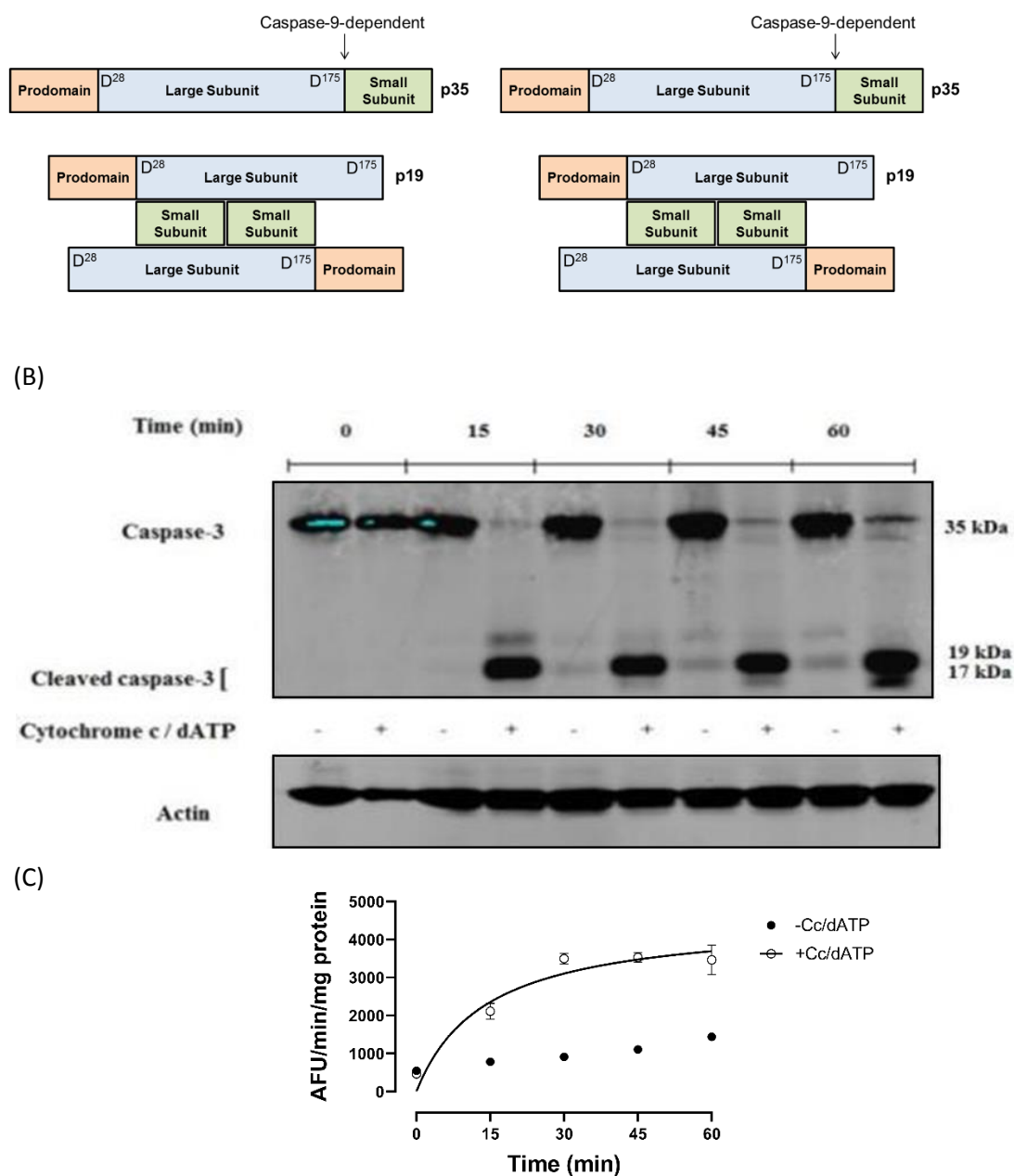


Figure 3.10. Caspase-3 processing. (A) Schematic presentation of caspase-3 processing. Cleavage after D¹⁷⁵ is caspase-9-dependent and produces p19 fragments. Second cleavage before D²⁸ is caspase-3-dependent and generates p17 fragments. (B) Processing and activity of caspase-3. HEK293 S-100 extracts incubated or not at 37°C for 15, 30, 45 and 60 min in the presence and absence of cytochrome c and dATP. Processing of caspase-3 studied by immunoblotting. The cleaved products of caspase-3 are detected after 15 min incubation. The cleaved fragments are detectable after 15 min incubation. (C) HEK293 S-100 extracts incubated as in (B) and the activity of caspase-3 measured using DEVD-AMC substrate.

3.7.2 Apaf-1 oligomerization

Oligomerization of Apaf-1 molecules is a key factor contributes to progression of mitochondrial apoptosis. To check the oligomerization of the Apaf-1, 1 mL of S-100 HEK 293 extract activated or not by addition of cytochrome c (1.6 μ M) and dATP (1 mM) and incubated at 37°C for 15 mins. Then the samples loaded on Sephacryl 300 HR column. The fractions were collected and used for Apaf-1 detection by immunoblotting.

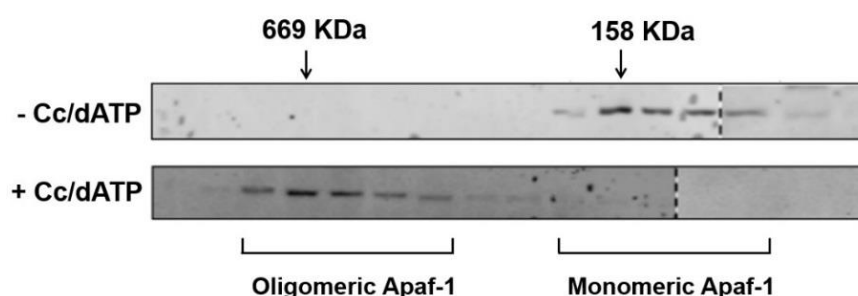


Figure 3.11. Size exclusion chromatography of S-100 HEK 293 extract. 1 mL HEK293 S-100 extract incubated for 15 min in the presence and absence of Cc/dATP and loaded on Sephacryl 300 HR column. The fractions were collected, concentrated and immunoblotted to detect Apaf-1. The arrows show the main peaks for thyroglobulin (669 KDa) and aldolase (158 KDa) which represent the oligomeric and monomeric form of Apaf-1, respectively.

All Apaf-1 molecules are detected in the fractions related to the monomeric sizes of Apaf-1 in the absence of cytochrome c and dATP (Figure 3.11). However, the addition of cytochrome c and dATP led to the detection of Apaf-1 in high molecular weight complex (~ 700 KDa). This shift from monomeric to oligomerized form in the presence of cytochrome c and dATP shows that cytochrome c, dATP, and 15 min incubation at 37°C is required for apaf-1 oligomerization.

3.8 *in vitro* validation of the assay

3.8.1 Split luciferase reconstitution assay

Having established that co-expression of split luciferase Apaf-1 could result in luciferase activity, we explored whether this activity is cytochrome c and dATP dependent.

To check the recovery of split luciferase activity *in vitro*, extracts expressing either Nluc-Apaf-1 or Cluc-Apaf-1 were mixed and split luciferase activity was measured after addition of D-luciferin substrate. Luciferase activity was measured as RLU/sec over a period of time (15 min) (Figure 3.12A). Luciferase activity was peaked 3-5 min after addition of luciferase substrate and then decreased, probably due to consumption of the D-luciferin and and/or ATP. The fold increase in luciferase activity induced by Cc/dATP varied from extract to extract and experiment to experiment from 5-35 fold (Figure 3.12B), part of which might be due to the quality of the S-100 extract originating from the purity of the plasmid, the efficiency of transfection, the level of expression and extract preparation.

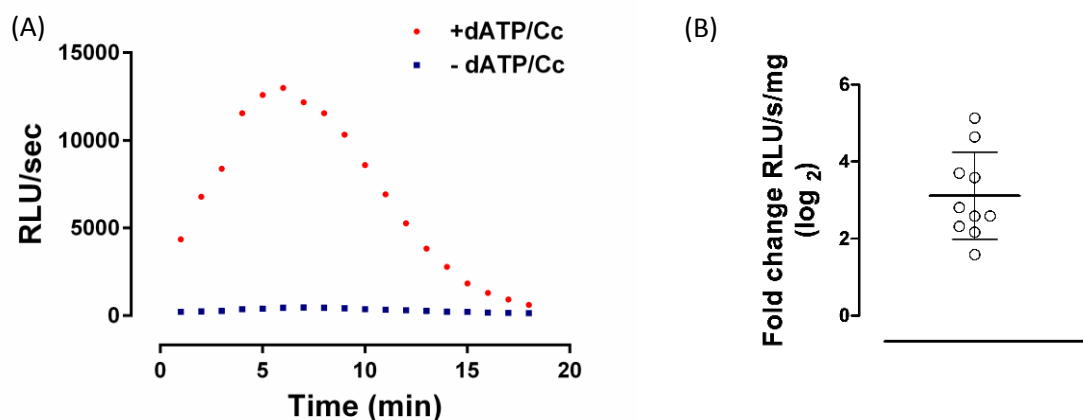


Figure 3.12. *in vitro* split luciferase assay. (A) For measuring split luciferase activity, 5 μ L of extracts expressing Nluc-Apaf-1 and Cluc-Apaf-1 mixed and the activity of luciferase recorded in the presence and absence of Cc/dATP. A randomly selected time-course of split luciferase activity. The highest luciferase activity is usually achieved 3-5 minutes after addition of substrate. (B) The fold change (log₂) of split luciferase activity was measured in separate S-100 extracts.

The split luciferase activity in unactivated S-100 extract implies an Apaf-1:Apaf-1 interaction, which could be explained by a high Apaf-1 concentration as a result of overexpression. Dilution of the extract affected split luciferase activity (Figure 3.13A). A 1:5 dilution of the extracts reduced the split luciferase activity to the background level, while the addition of Cc/dATP increased the activity by 6-fold. Even after a 1: 8 dilution of the S-100 extract addition of Cc/dATP induced a 5-fold increase in luciferase activity. In later experiments extracts were diluted to reduce the activity of unactivated extracts to background levels of luminescence and to maximize the number of experiments that could be performed with the extracts available.

3.8.2 Caspase and split luciferase activity in diluted extracts expressing Nluc-Apaf-1 and Cluc-Apaf-1.

Addition of Cc/dATP to extracts is predicted to activate caspase-3. Therefore the activity of caspase-3 was tested in diluted extracts expressing Nluc-Apaf-1 and Cluc-Apaf-1.

Caspase-3 like activity in the diluted extracts expressing Nluc-Apaf-1 and Cluc-Apaf-1 alone and the mixture of Nluc-Apaf-1 and Cluc-Apaf-1 was measured (Figure 3.13B). In the absence of dATP/Cc, low level caspase activity was detected in the extract. The addition of Cc/dATP increased caspase activity in extracts expressing either Nluc-Apaf-1 or Cluc-Apaf-1 and in the extract containing the mixture of both Nluc-Apaf-1 and Cluc-Apaf-1. This confirmed dATP/Cc-dependent caspase-3 activation in diluted extracts.

Then, the split luciferase activity was measured in the extracts (Figure 3.13C). Neither Nluc-Apaf-1 nor Cluc-Apaf-1 expressing extracts showed luciferase activity even in the presence of Cc/dATP. Luciferase activity was only detected when Nluc-Apaf-1 and Cluc-Apaf-1 extracts were mixed and Cc/dATP was added.

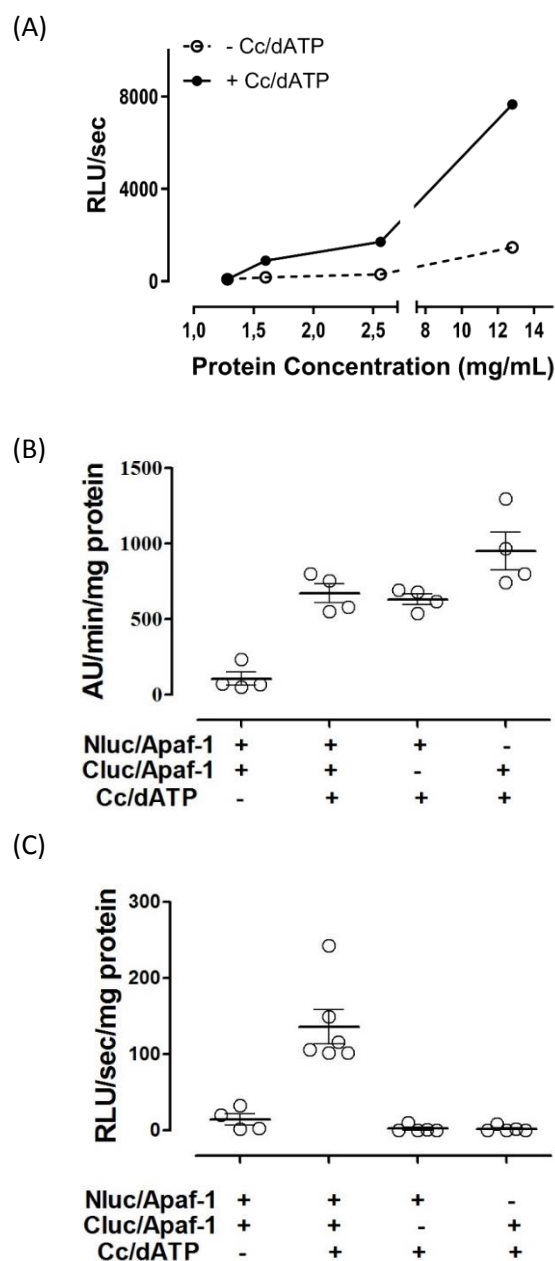


Figure 3.13. Split luciferase activity is Cc/dATP dependent. (A) The split luciferase activity of S-100 extract was measured in extracts diluted to different protein concentrations in the presence (●) and absence (○) of Cc/dATP. (B) Caspase-3 like activity of the S-100 extract was measured using DEVD-AMC in the presence and absence of Cc/dATP. (C) Diluted extracts (1.6 mg/mL) expressing Nluc-Apaf-1 or Cluc-Apaf-1 were mixed 1:1 in the presence and absence of 1.6 μ M cytochrome c and 1 mM dATP and split luciferase activity was measured.

Maximum caspase-3 like activity and fully processing of caspase-3 were achieved following 15 min incubation of the extracts at 37°C (Figure 3.10). Therefore, I hypothesized that 15 min incubation at 37°C would maximise apoptosome formation before measuring split luciferase activity and that a higher luciferase activity would be detected. Therefore, extracts containing Nluc-Apaf-1 and Cluc-Apaf-1 were mixed and incubated for 15 minutes either on ice or 37°C with or without Cc/dATP. The activity of split luciferase was then measured. As expected, extracts incubated on ice showed Cc/dATP dependent split luciferase activity (Figure 3.14A). However, rather than being increased by Cc/dATP, the luciferase activity in extracts incubated at 37°C was lower than extracts incubated without Cc/dATP. This suggests that 37°C was not compatible with the split luciferase assay. At the same time, caspase-3 like activity showed the expected Cc/dATP-dependent increase when incubated at 37°C with Cc/dATP (Figure 3.14B).

Considering the optimum temperature of purified luciferase which is 25°C (Ford and Leach, 1998), extracts were incubated for 10 minutes at 25°C and the caspases-9 and -3 activation were studied to ensure that incubation at 25°C is sufficient for fully caspase activation (Figure 3.15B). Immunoblotting showed that Cc/dATP induced partial processing of caspase-3, which is consistent with the lower level of caspase-3 activity. However, complete processing of caspase-9 was observed after 15 mins incubation at 25°C suggesting apoptosome formation was complete (Figure 3.15B). The complete processing of caspase-9 at 25°C suggested that apoptosome formation was maximal at this temperature and had occurred within 10 minutes.

Caspase activity was also measured (Figure 3.15C). Cc/dATP induced caspase-3 like activity in extracts incubated at 25°C, although the level of activity was lower than the activity in extracts incubated at 37 °C (Figure 3.15C).

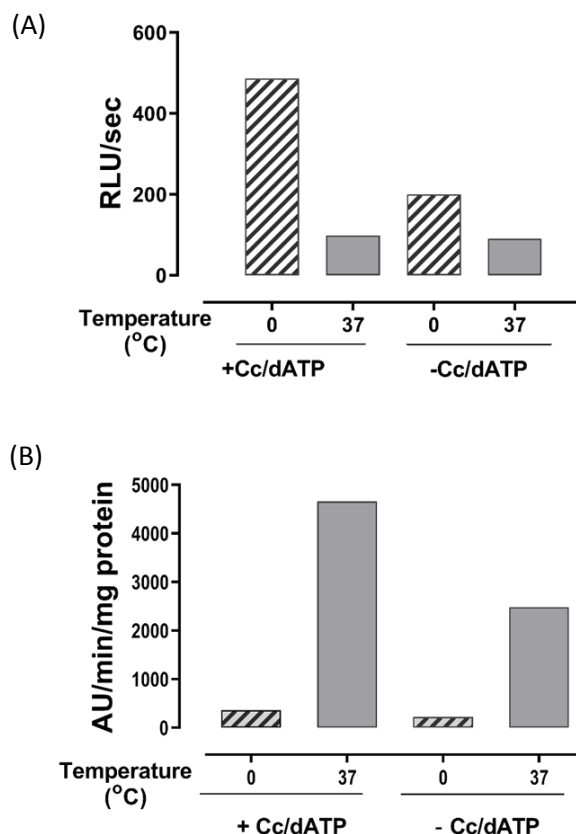


Figure 3.14. Temperature-dependent luciferase assay. (A) Extracts expressing Cluc-Apaf-1 and Nluc-Apaf-1 were mixed and split luciferase activity was measured in the presence and absence of Cc/dATP when incubated or not at 37°C for 15 min. Luciferase activity reduced to basal level when incubated for 15 min at 37°C. (B) At the same time that luciferase activity disappeared, caspase-3 like activity showed significant increase upon addition of Cc/dATP and incubation at 37°C for 15 min.

The implications of these ideas are that incubation at 25 °C for longer periods will result in a progressive loss of Cc/dATP dependent split luciferase activity and very short incubations (less than 10 minutes) at 37 °C will give measurable Cc/dATP induced split luciferase activity (Figure 3.15D).

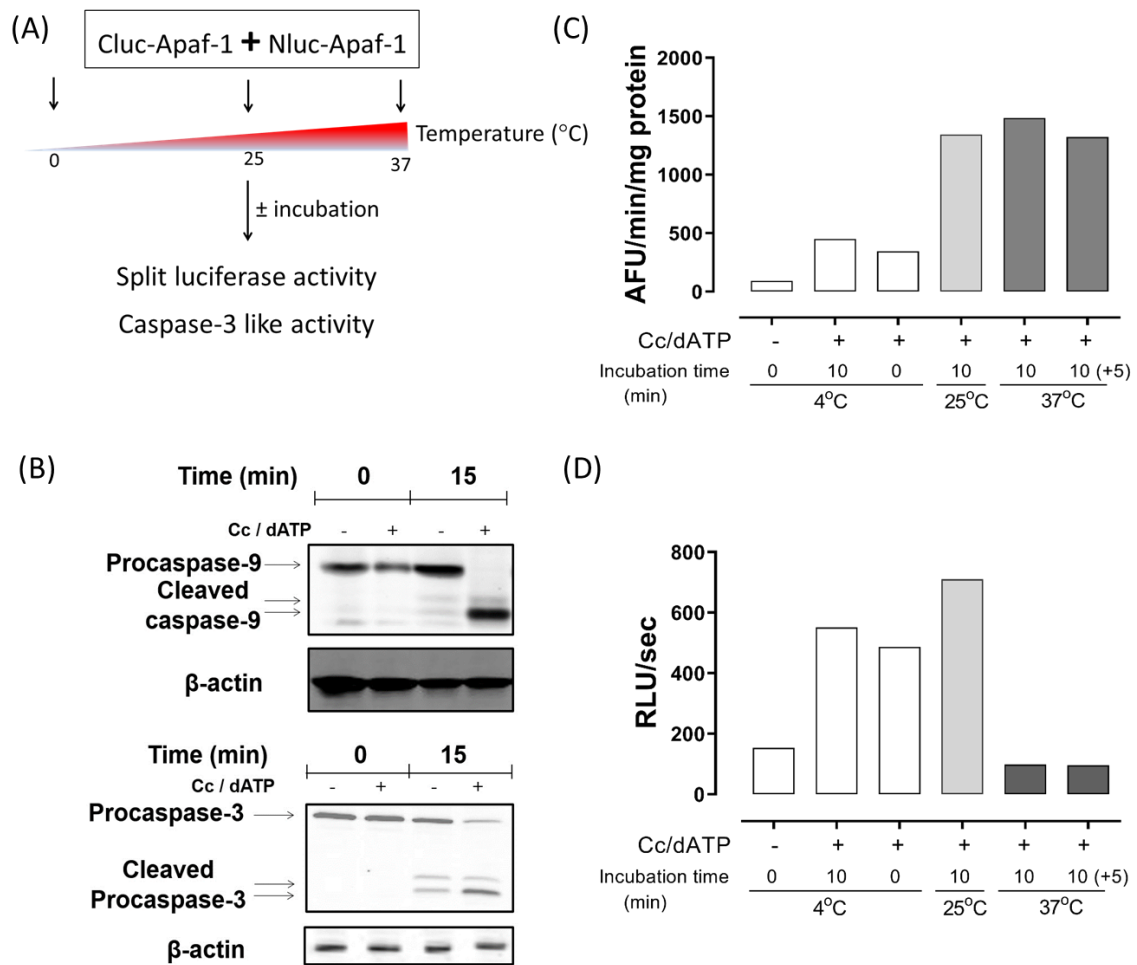


Figure 3.15. Optimization of assay condition. (A) Extracts expressing Cluc-Apaf-1 and Nluc-Apaf-1 mixed and split luciferase activity measured when incubated at 0, 25 and 37°C. (B) To check the processing of caspase-3 at 25°C, an aliquot was taken and used for immunoblotting. Incubation at 25°C and presence of Cc/dATP is sufficient for caspase activation and activity. (C) Caspase-3 like and (D) luciferase activity was measured in the HEK293 S-100 extract when incubated at 25°C and 37°C. Addition of Cc/dATP remarkably increase the activity of split luciferase and caspase-3. Incubation of the extracts at 37°C reduces luciferase activity and incubation at 25°C cannot recover luciferase activity [shown as 10(+5)].

3.8.3 Titration of cytochrome c

Previous reports show the cytochrome c concentration that is required for maximum caspase-3 like activity (Slee et al., 1999; Kluck et al., 2000; Segal and Beem, 2001) and that the affinity for Apaf-1 is $\sim 0.49 \pm 0.06 \mu\text{M}$ (association constant of $\sim 2.04 \times 10^{-6} \pm 0.25 \times 10^{-6} \mu\text{M}$) (Zhou et al., 2015). To better understand the split luciferase assay, concentrations of cytochrome c were titrated to test whether the EC_{50} was similar to the reported K_d . The highest RLU/sec values were picked for plotting the dose-response curve. All values normalized to the highest luciferase activity in each experiment. Cytochrome c concentrations lower than $0.1 \mu\text{M}$ did not change the luciferase activity, however, $0.78 \mu\text{M}$ cytochrome c was sufficient for the highest luciferase activity (Figure 3.16A). The EC_{50} of concentration of cytochrome c for inducing luciferase activity was $\sim 0.35 \mu\text{M}$, which is consistent with the previously reported K_d values.

3.8.4 Titration of NS3694, an inhibitor of apoptosome formation

To further understand the relationship between split luciferase activity and Apaf-1 oligomerization, I hypothesized that if the split luciferase activity is an indicator of apoptosome formation, an Apaf-1 inhibitor should block the split luciferase activity. Here, I tested NS3694, a diarylurea compound and inhibitor for Apaf-1 (Lademann et al., 2003), predicting that the IC_{50} for inhibition of caspase activation would be similar to the IC_{50} for split luciferase activity. The IC_{50} of NS3694 calculated as $\sim 178 \mu M$ for split luciferase activity and $\sim 170 \mu M$ for caspase-3 like activity (Figure 3.16B). The similarity between the IC_{50} for caspase-3 activity and the split luciferase activity is consistent with the idea that the split luciferase assay measures apoptosome formation. NS3694 mechanism of action is the topic of chapter 6 and will be further discussed.

3.8.5 Apaf-1 mutant unable to form apoptosome blocks split luciferase activity

To further study the assay and consider the random dimerization of luciferase fragments, Apaf-1 K160R mutant was used to measure the luciferase activity. K160R Apaf-1 mutant is unable to form a complex (Hu et al., 1999). As expected, no luciferase activity was detected when K160R Apaf-1 was overexpressed in HEK293 cells. This mutation was tested by a visitor in our lab (A. Noori, 2016).

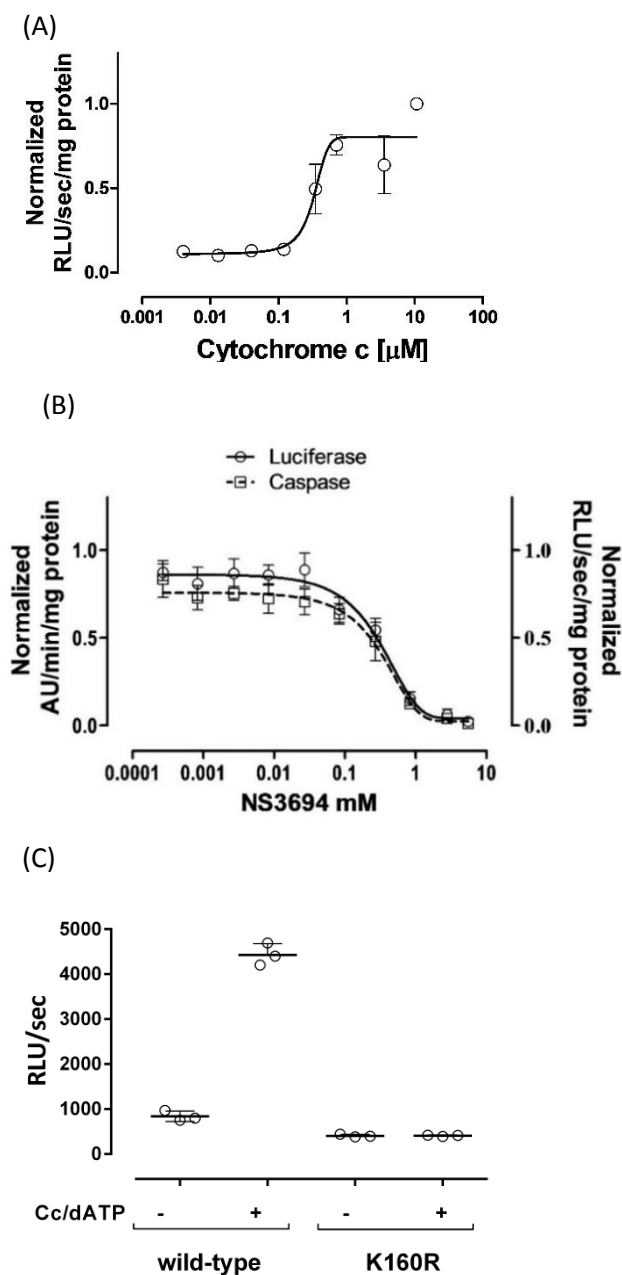


Figure 3.16. Titration of apoptosome activator (cytochrome c) and inhibitor (NS3694) using split luciferase assay. (A) The effect of cytochrome c concentration on split luciferase activity was assessed. (B) The effect of NS3694 on inhibition of split luciferase activity (\circ) and caspase-3 like activity (\square). (C) K160R Apaf-1 mutant blocks split luciferase activity (adopted from Noori, 2016). Error bars represent mean \pm SEM.

3.8.6 Gel filtration of apoptosome produced by fusion proteins

The data gathered so far suggested that the split luciferase assay reported apoptosome formation. The apoptosome has a specific molecular size and contains seven Apaf-1 molecules. Dimerization of the Apaf-1 is sufficient for detecting luciferase activity. Endogenous Apaf-1 can also form a complex and activate caspase-3 (Figure 3.13B and C). Therefore, gel filtration was performed to test whether these recombinant proteins, Nluc-Apaf-1 and Cluc-Apaf1, merely dimerized or formed complex with a size similar to the apoptosome.

In the absence of Cc/dATP, monomeric Apaf-1 and its derivatives were detected in fraction related to monomer form of Apaf-1 (aldolase, 158 KDa) and upon addition of Cc/dATP, all the monomers shifted to the fractions with larger size (Thyroglobulin, 669 KDa) (Figure 17A). This is consistent with the Nluc- and Cluc-Apaf-1 proteins being both monomeric and oligomeric in the absence of Cc/dATP and that monomeric Nluc- and Cluc Apaf-1 undergoes Cc/dATP dependent oligomerization. The size of the Nluc- and Cluc-Apaf-1 complex is consistent with the size of the apoptosome.

After showing the fusion-proteins formed a complex with the right size, split luciferase activity was also tested in the fractions. Luciferase activity was only detected in the extract incubated with Cc/dATP and only in fractions of ~669 kDa (Figure 3.17B). This is consistent with the split luciferase assay detecting apoptosome formation.

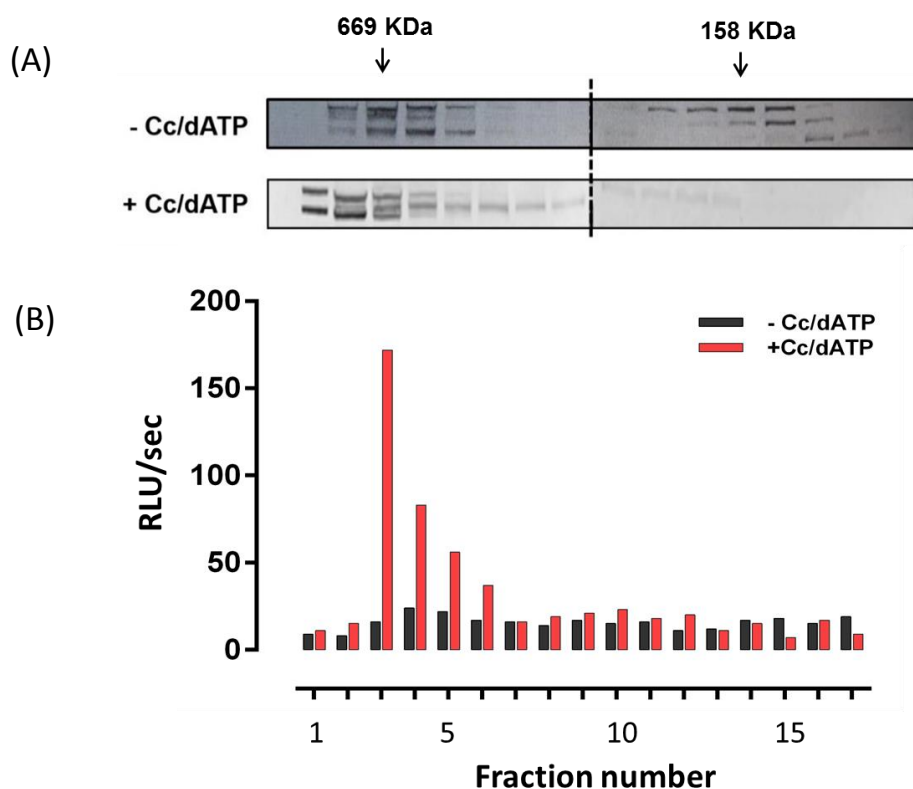
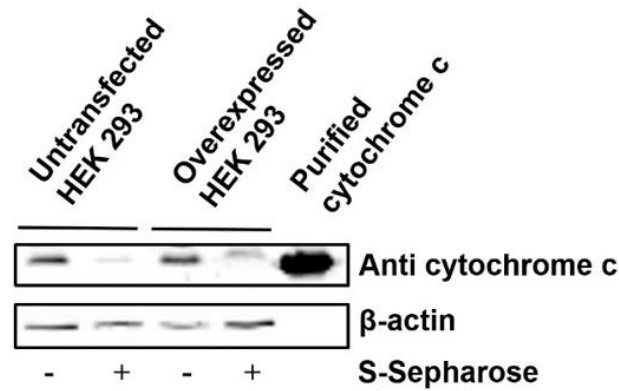


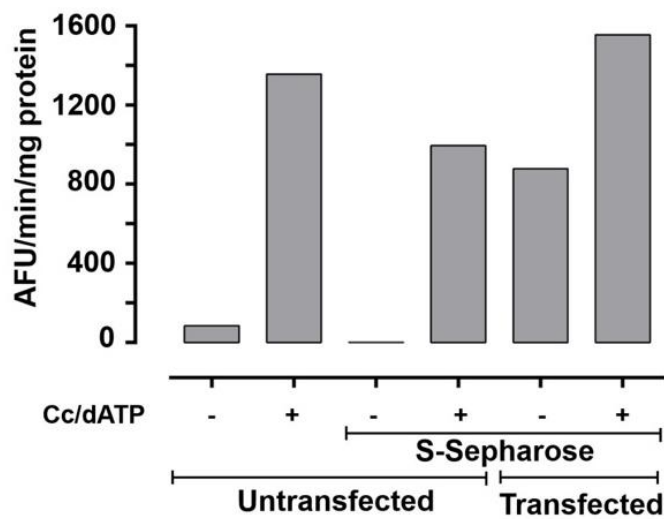
Figure 3.17. Gel filtration of luciferase-tagged Apaf-1. (A) Mixture of Nluc-Apaf-1 and Cluc-Apaf-1 extracts with or without Cc/dATP were loaded on a Sephacryl 300 HR column. The fractions were collected, concentrated and immunoblotted to detect Apaf-1. (B) Split luciferase activity in the fractions of gel filtration.

Gel filtration studies showed some high molecular weight complexes even without addition of Cc/dATP. This could be because endogenous cytochrome c triggered Apaf-1 oligomerization in the extracts or that these complexes are pre-formed in the overexpressing cells before extract preparation. To differentiate between these ideas, cytochrome c was removed from S-100 extract using cation exchange chromatography (Figure 3.18A) (Liu et al., 1996). The supernatant was then used to measure caspase-3 like activity and luciferase activity.

(A)



(B)



(C)

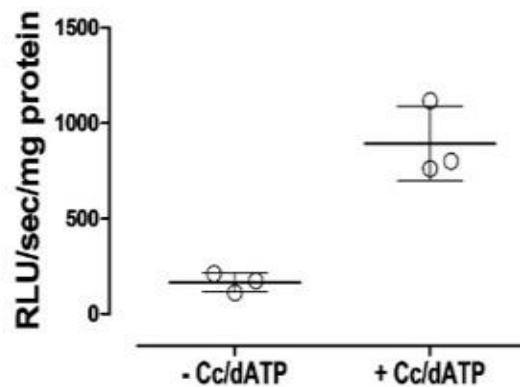


Figure 3.18. Protein complexes were formed before or during extract preparation. (A) Immunoblotting showed the removal of cytochrome c in wild-type or overexpressed S-100 HEK 293 using Sepharose beads. (B) caspase-3 activity of cytochrome c-excluded extracts. (C) Extracts expressing Nluc-Apaf-1 and Cluc-Apaf-1 used for luciferase assay after removal of cytochrome c. Luciferase activity is detectable and addition of exogenous Cc/dATP further increases the split luciferase activity.

The caspase activity of untransfected extract significantly increased (~13 times) upon addition of Cc/dATP (Figure 3.18B). In extracts depleted of cytochrome c, the basal level of caspase-3 activity was reduced and addition of Cc/dATP increased caspase activity as expected. In extracts from cells overexpressing Apaf-1, interestingly, caspase activity was still high in extracts depleted of cytochrome c and addition of Cc/dATP further increased the caspase activity. Luciferase activity was also detected and addition of Cc/dATP further increased luciferase activity (Figure 3.18C). These data suggest that the luciferase activity and complexes detected in extracts from cells overexpressing Apaf-1 were the result of complexes formed in the cells before extract preparation.

3.9 Discussion

Apaf-1 oligomerization occurs upon permeabilization of mitochondria and cytochrome c release into the cytosol. To make the reporters that detect Apaf-1 oligomerization, N-terminal and C-terminal of firefly luciferase were fused to the N-terminal of individual Apaf-1 protein. 3D structure of apoptosome complex (chapter 1), showed that N-terminal of Apaf-1 proteins form a central hub in the apoptosome. Therefore, the N-terminal of proteins are close enough to allow the luciferase fragments to be complemented.

Apaf-1 oligomerization is a cytochrome c and dATP dependent process in the cells. Apoptotic stimuli trigger the permeabilization of mitochondria in a process called Mitochondrial Outer Membrane Permeabilization (MOMP). Release of proteins such as cytochrome c, from mitochondria triggers caspase-activating pathway.

Why (d)ATP is required for apoptosome formation?

Apaf-1 is found as auto-inhibited ADP-bound monomer in the cytosol. ADP binds to the NBD either during or after the Apaf-1 synthesis. ADP interacts to the binding pocket in NBD through several hydrogen bonds and a salt bridge. Lys160 and Val127 are the key residues in these interactions (Riedl et al., 2005; Reubold et al., 2011).

It is still not clear whether ATP hydrolysis is required for apoptosome formation. Studies with WDR deleted Apaf-1 showed that procaspase-9 failed to interact to Apaf-1 CARD. Therefore, nucleotide exchange and/or hydrolysis is required for caspase-9 recruitment (Riedl et al., 2005; Yuan et al., 2011). Studies by Reubold et al with full length Apaf-1 suggests that nucleotide exchange but not the hydrolysis is required to switch Apaf-1 to the open form before apoptosome formation. (Reubold et al., 2009, 2011).

In the *in vitro* apoptosome reconstitution, to mimic the cytochrome c release and nucleotide exchange, exogenous cytochrome c and dATP was added to induce the apoptosome formation. I then showed that split luciferase activity is cytochrome c and dATP dependent. Caspase-3 like activity was also consistent with split luciferase activity. The luciferase activity was also blocked by the inhibitor of apoptosome, NS3694. The assay was further tested using mutant Apaf-1. K160R Apaf-1 mutant has been shown to be inactive and cannot form a complex (Hu et al., 1999). This mutant is locked in auto-inhibited state and therefore cannot be opened and oligomerized. I hypothesized that if split luciferase activity reflects apoptosome formation, K160R mutant should not produce luciferase activity. As expected, K160R mutant was unable to generate luciferase activity as well as caspase-3 like activity (this mutation was tested by other team members in our lab). Gel filtration studies showed that fusion proteins contribute to formation of a complex with the expected molecular weight. Luciferase activity was also measured in the fractions related to apoptosome.

This assay reports the apoptosome formation. However, it cannot report the upstream events like cytochrome c release and regulation of mitochondrial PTP by BCL-2 family proteins. Having the reporters of apoptosome formation, we are able to test different intramolecular interactions, and do the structural analysis to further study the function of each domain/subdomain in apoptosome formation. We also can use this reporter as a bio-tool to screen a panel of compound with the aim of identifying new drug-like molecules

which can inhibit or activate apoptosome formation. The former is being studied currently in our lab and the latter is the topic of the next chapters.

This assay was designed primarily for *in cellulo* studies. Split luciferase activity was detected when Nluc-Apaf-1 and Cluc-Apaf-1 were co-transfected in HEK293 cells (Figure 3.7B). However, this luciferase activity was not responsive to apoptotic stimuli such as doxorubicine and etoposide. I expected that treatment with apoptotic stimuli would increase the luciferase activity as more apoptosome are formed than untreated cells, but no significant difference was detected. I hypothesized that it could be due to the overexpression of Nluc-Apaf-1 and Cluc-Apaf-1. To rectify this, I titrated the amount of DNA for transfection. Even at low concentration of DNA, no significant difference was detected between treated and untreated cells. Therefore, this assay was switched to *in vitro* assay using cell extracts expressing fusion proteins.

Split luciferase activity was detected when Nluc-Apaf-1 and Cluc-Apaf-1 were co-transfected in HEK293 cells. Split luciferase activity was also detected *in vitro* when extracts were incubated at room temperature. However, it could not be detected when extract were incubated at 37°C.

What prevented detection of luciferase activity when extracts were incubated at 37°C was not clear. The high caspase activity implied that the apoptosome formed at 37°C. Previous reports have shown using size exclusion chromatography that the apoptosome complex is stable even after 15 min incubation at 37°C. I could also show that apoptosome is detectable 15 min after incubation at 37°C (Figure 3.11).

Furthermore, while the optimal temperature for luciferase activity is 25°C, the enzyme is still active at 37°C. One possible explanation is that the assay reports both apoptosome formation as well as post-apoptosome formation changes and that the rate these two events is different. At 25°C apoptosome formation predominates and this is detectable by the split luciferase assay. At 37°C the post-apoptosome formation reaction predominates and the

split luciferase activity is lost because either (1) its conformation changes or (2) it binds proteins that disrupt Nluc and Cluc interactions.

Another explanation could be attributed to the interaction of other proteins with luciferase-tagged Apaf-1 such as chaperones. The activity was detectable when luciferase-tagged Apaf-1 overexpressed *in cellulo*. However, these interactions might be disrupted during cell extract preparation.

In this chapter we showed that:

1. Luciferase based reporters are expressed within the cells and produce a protein with right molecular mass.
2. The assay reflects apoptosome formation because it is cytochrome c and dATP dependent.
3. The activity of reporters are inhibited pharmacologically (using inhibitor of apoptosome).
4. K160R Apaf-1 mutant blocked split luciferase and caspase activity (done by lab mates).
5. Gel filtration confirmed the involvement of fusion proteins in apoptosome complex.
6. Luciferase activity was detected in fractions with molecular weights of apoptosome.

SCREENING

Screening approaches can be used to identify the drug-like compounds, small molecules and modulators of key proteins involved in human diseases (Qian et al., 2004; Walker and Frank, 2012; Wang, Chen, et al., 2016). Different screening methods can be used like cell-based assays, *in vitro* assays and virtual screening (Hughes et al., 2011; Graepel et al., 2017). The clinical relevance and pathology of Apaf-1 was discussed earlier (chapter 1), which makes it a good target for therapeutic purposes. The lack of direct method for testing Apaf-1 oligomerization led to indirect measurements of downstream proteins such as caspases. Here, a new split luciferase-based reporter was developed and validated which directly measures the oligomerization of Apaf-1 as a target protein (chapter 3).

Having a new bio-tools for measuring apoptosome formation, I intended to test whether the assay could be used to screen a panel of chemicals/extracts for the ability to inhibit apoptosome formation. Two sets of compounds were used: 1) a library of toxic compounds (persistent organic pollutant), 2) a library of natural products obtained from marine organisms (whole extracts). In order to identify the most efficient and cost-effective method of the screening, different protocols were tested. For the toxicant library, split luciferase assay was used. For the natural product library, caspase-3 like activity was measured and the hit compounds were tested in split luciferase assay.

4.1 Screening the toxicant library

The assay was adapted to a 96-well format and used with a library of 177 persistent organic pollutants. This library was selected because some of the toxic compounds had been reported to cause infertility and Apaf-1 deficiency was also linked to abnormal spermatogenesis. The overall strategy for screening is shown in figure 4.1A. The library of known human toxicants (see appendices, list of chemicals), was tested to identify those that reduce luciferase activity in the split-luciferase assay. An inhibitor was defined as any toxicant that reduced mean split luciferase activity by more than $Q1 - 1.7 \times \text{IQR}$. As a positive control NS3694 was used (Figure 4.1B). Fourteen toxicants with inhibitory activity identified as potent inhibitors (Figure 4.1C).

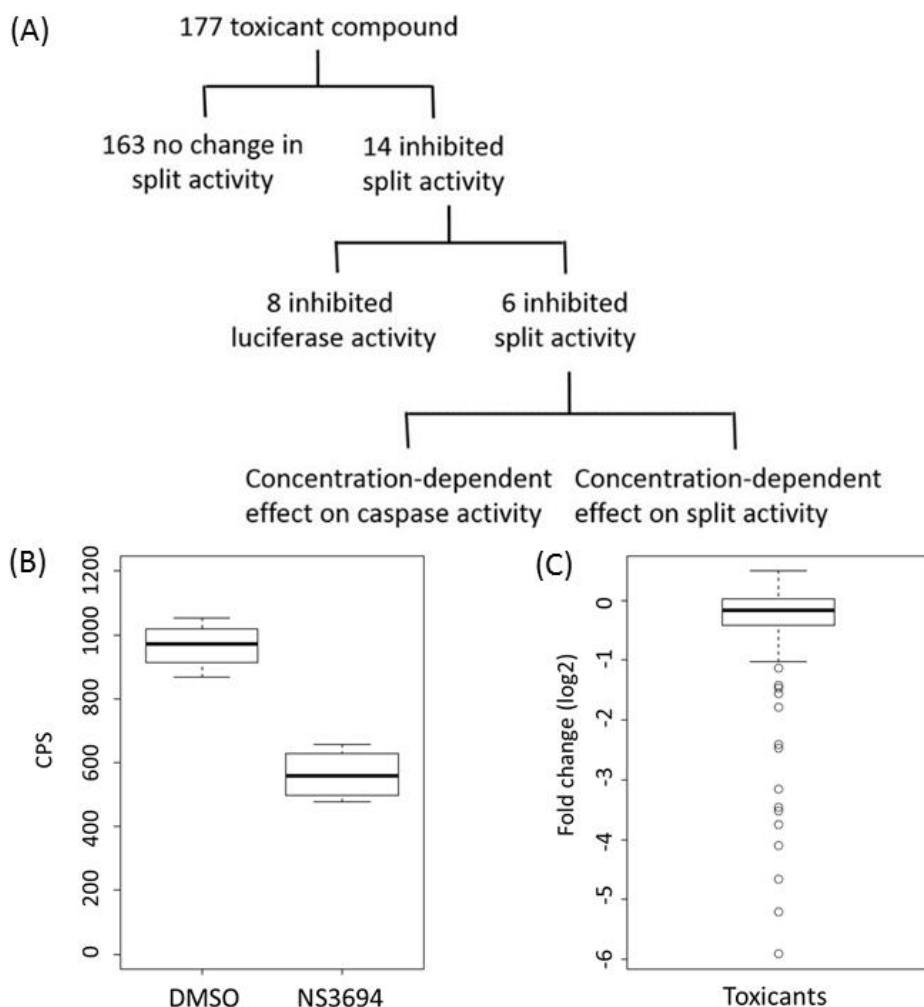
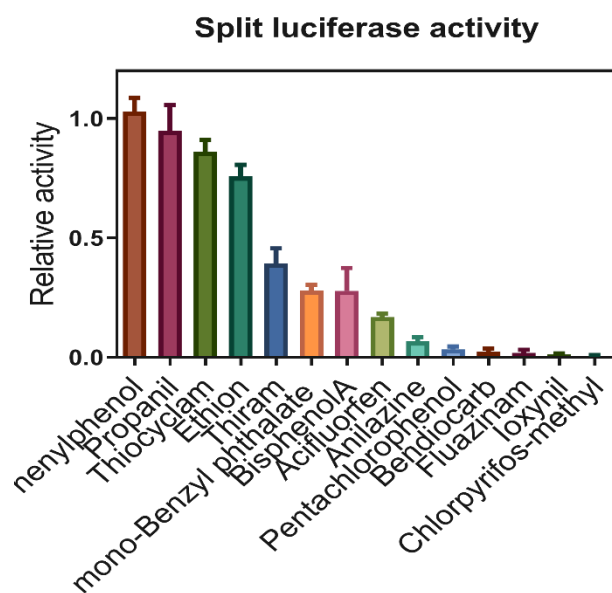


Figure 4.1. Screening and analysis of the toxicant library. (A) Schematic presentation of toxicant library screening. In the first round of screening, 14 hit compounds were identified. These compounds were then tested against luciferase activity. Only six of the hit compounds inhibited split luciferase activity rather than luciferase activity. Then these compounds titrated and IC_{50} calculated for split luciferase, luciferase and caspase-3. (B) NS3694 and DMSO were used as controls. (C) 14 compounds were defined as potential hits. (D) The effect of these toxicants was re-assessed on split luciferase activity and luciferase activity. Plotting the effect of candidate compounds on luciferase activity versus split luciferase activity identified six compounds for further investigation.

Then hit compounds were tested by an extract from cells expressing *Photinus pyralis* firefly luciferase to identify those that only affect split luciferase rather than luciferase itself (Figure 4.2).

(A)



(B)

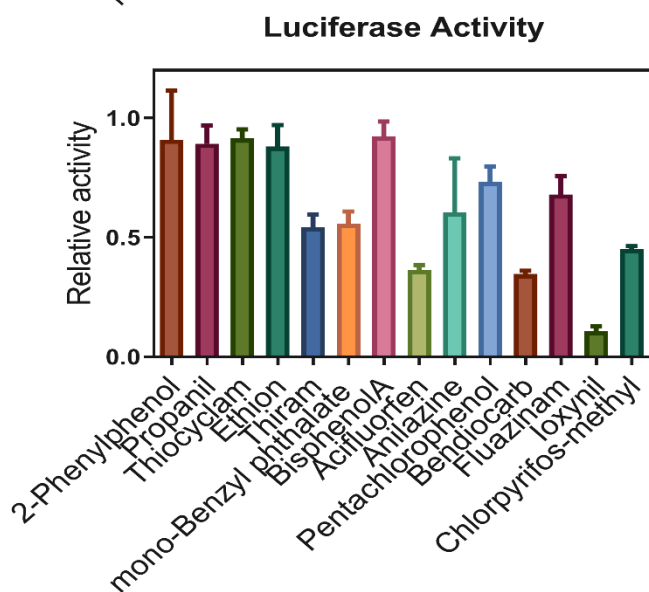


Figure 4.2. Re-testing the hit compounds. 14 hits were re-tested using (A) split luciferase and (B) luciferase assay.

Six toxicants that showed greater activity against the split luciferase (Ioxynil, Thiram, Thiocyclam, Pentachlorophenol, Chlorpyrifos-methyl and Anilazine) were then titrated to determine IC_{50} values in assays for split luciferase activity, *Photinus pyralis* firefly luciferase activity and caspase-3 like activity (Figure 4.3).

4.1.1 Titration of hits in luciferase assay

Treatment with any of these toxic compounds inhibits the split luciferase activity (Figure 4.3, and Table 4.1). Treatment with Anilazin and Chlorpyrifos-methyl did not have any significant inhibitory effect on luciferase itself. The IC_{50} for luciferase was greater than 3 mM for all hit compounds. Treatment with other hit compounds affected the luciferase activity to some extent at high concentrations. Despite the inhibition at high doses, specific concentrations could be defined where treatment largely affects the split luciferase activity rather than luciferase activity. For example, 0.3 mM pentachlorophenol reduced the activity of luciferase by 10% while inhibiting the activity of split luciferase by 80%. 1 mM Thiocyclam reduced luciferase and split luciferase activities by 30% and 80%, respectively. The inhibition of luciferase activity at high concentrations of hit toxicants might be due to degradation or oxidation of the proteins.

4.1.2 Titration of hits in caspase assay

If the split luciferase assay reported apoptosome formation, the expectation was that caspase-3 activation would also be prevented. Therefore, caspase-3 like activity was also measured at the same concentrations used for luciferase and split luciferase assay. Hit compounds were added to S-100 HEK293 extract, after 10 min incubation, cytochrome c and dATP (1.6 μ M and 1 mM) added and further incubated at 25°C and caspase-3 like activity measured. The rate of caspase activation was calculated by the slope of the linear part of caspase activity plot (Figure 4.3). In these plots, all values were reported as a fraction of caspase-3 like activity in untreated extract.

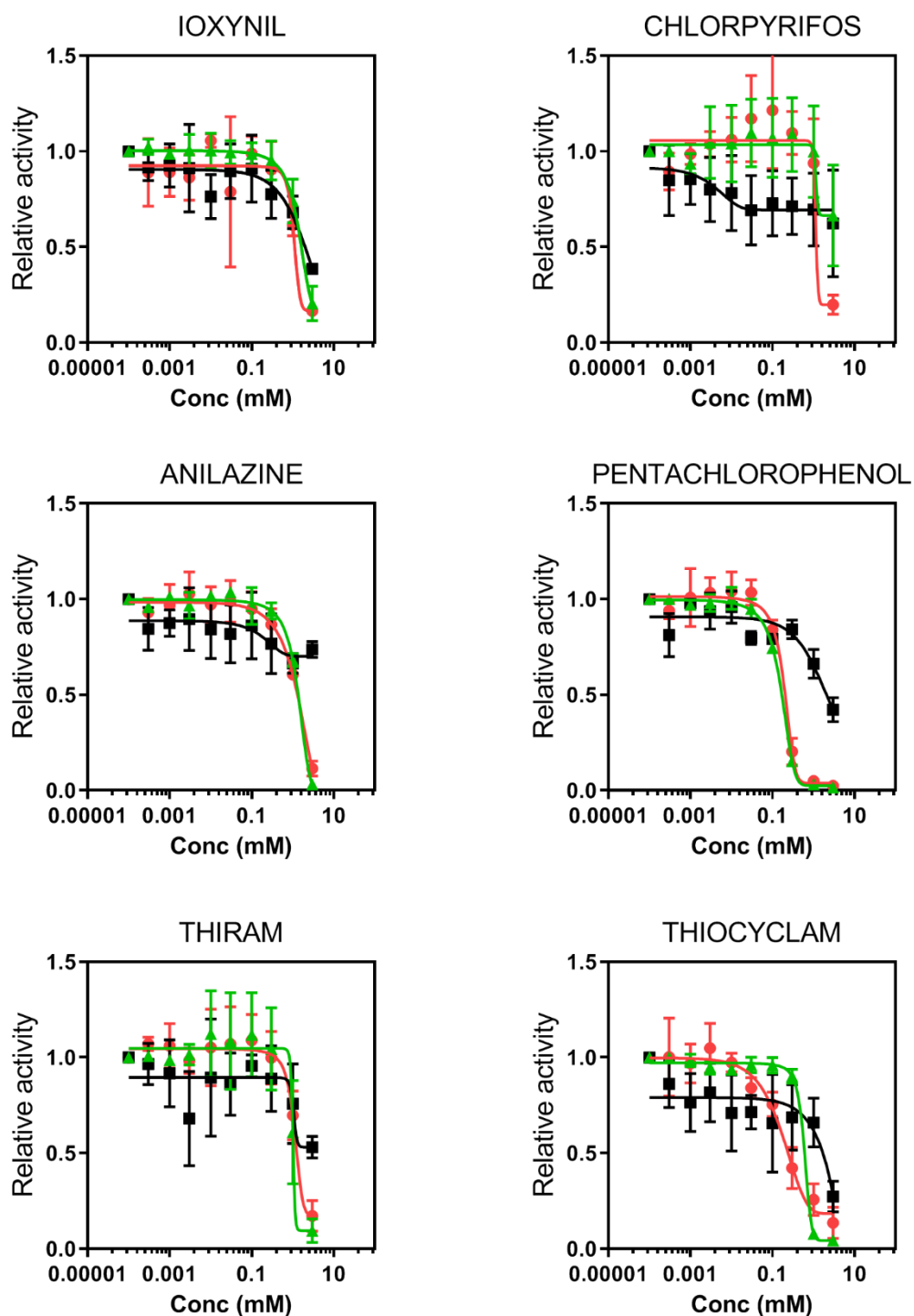


Figure 4.3. Titration of compounds using caspase, split luciferase and luciferase assay.

Ten concentrations of each compound (3, 1, 0.3, 0.1, 0.03, 0.01, 0.003, 0.001, 0.0003 mM) were used for measuring the caspase-3 like activity (\blacktriangle), split luciferase (\bullet) and luciferase (\blacksquare). S-100 HEK293 incubated for 10 min with the compounds. Then Cc/dATP added, and the caspase activity was measured. Error bars represent the mean \pm SD (n=3).

Of the hits, the IC₅₀ values of Anilazine and Pentachlorophenol for both split luciferase and caspase-3 like activities were very close (value \pm SEM for S/L; value \pm SEM for Casp3), with pentachlorophenol having the lowest IC₅₀ values. The effect of the toxicants on all three assays as well as chemical structures of hit compounds are summarized in Table 4.1.

Caspase-3 activation is accompanied by processing of caspase-3, so I investigated the effect of the chemicals on caspase-3 processing using immunoblotting. Immunoblotting showed the complete inhibition of caspase-3 processing except for Chlorpyrifos-methyl and Thiocyclam.

As caspase-9 activity is induced by the apoptosome, I also measured caspase-9 activity and processing. Except Chlorpyrifos-methyl, all the other hit compounds reduced the caspase-9 activity to the background level like unactivated extract (Figure 4.4).

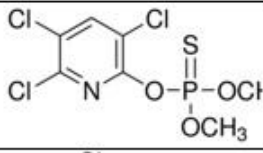
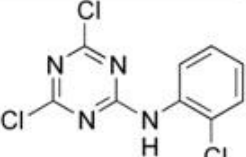
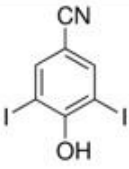
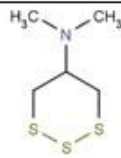
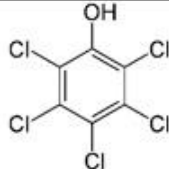
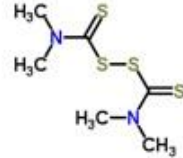
Compound	IC ₅₀ (mM)			Structure
	Luc	S. luc	Casp-3	
Chlorpyrifos-methyl	>3	>3	>3	
Anilazine	>3	2.99	2.83	
Ioxynil	>3	1.18	>3	
Thiocyclam	>3	0.20	0.51	
Pentachlorophenol	>3	0.17	0.15	
Thiram	>3	1.38	1.05	

Table 4.1. Inhibitory effect of hit compounds on luciferase (Luc) and split luciferase (S. Luc) and caspase-3 (Casp3) activity. IC₅₀ values calculated for luciferase (Luc), split luciferase (S. Luc) and caspase-3 (Casp-3) activity.

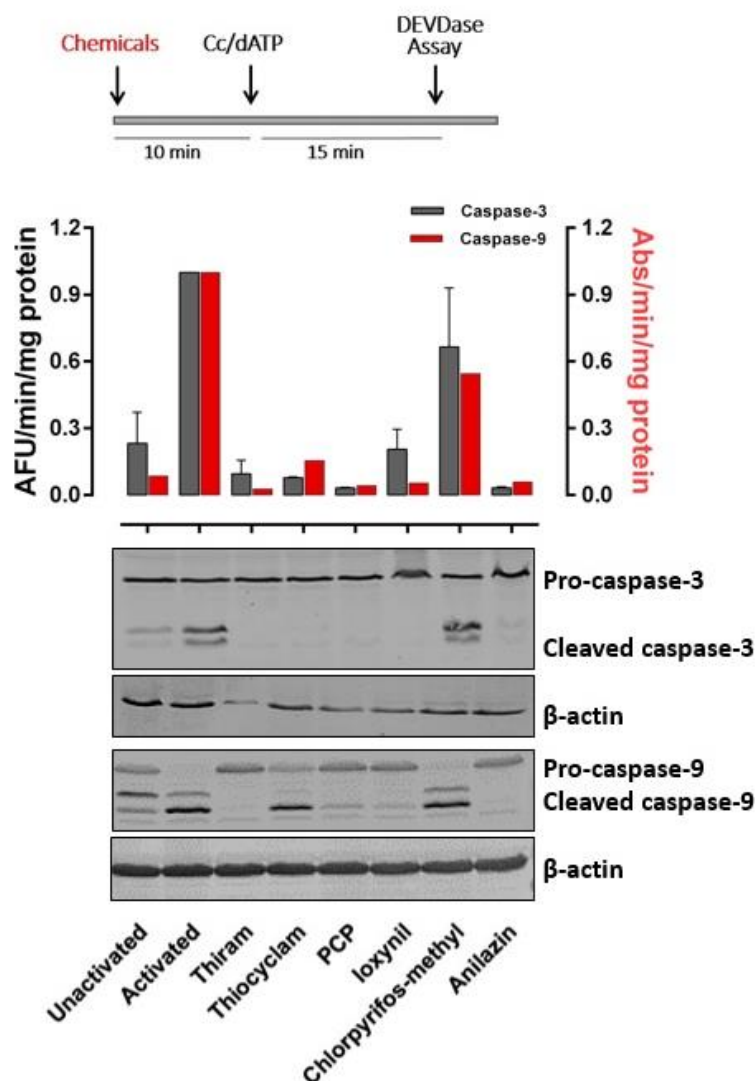


Figure 4.4. Caspase processing and activity before activation of cell extract. HEK293 S-100 extract mixed with hit compounds before addition of cytochrome c and dATP (1.6 μ M and 1 mM respectively). Then caspase-3 like and caspase-9 activity were measured, and immunoblotting showed the processing of procaspase-3 and procaspase-9. In (A) hits added to S-100 extract and incubated for 10 min. Cc/dATP added and the mixture incubated at 25°C for 15 min. Then caspase-3 like activity measured using DEVD-AMC over 30 min. The fluorescence intensity normalized to the protein concentration. Here all values have been reported as a fraction of activated extract. An aliquot of the same reaction was used for immunoblotting the processing of procaspase3. In another experiment, caspase-9 activity was measured using LEHD-pNA over two hours when hit compounds pre-incubated for 10 min with S100 extract and incubated as mentioned above. The values here are absorbance over time (min) and normalized to protein concentration. An aliquot of each reaction was used for detecting pro-caspase-9 processing. Error bars represent the mean \pm SEM. Caspase-9 activity shown here is the result of one experiment.

To exclude the possibility that the chemicals were not directly reacting with caspase-3 or caspase-9, S-100 HEK293 extract was first activated by adding cytochrome c and dATP and incubated for 15 mins at 25°C (Figure 4.5). Hit compounds were then added to activated extracts and incubated for further 10 mins. Caspase-3 like and caspase-9 activities were then measured. All the hit compounds slightly affected caspase-3 like activity except Thiram. Caspase-9 activity was either unaffected or only slightly affected. Immunoblotting of procaspase-3 and procaspase-9 also showed that chemicals had little effect on caspase processing. Based on the obtained results Ioxynil, Thiocyclam, Pentachlorophenol, Chlorpyrifos-methyl and Anilazine function upstream of caspase activation and this is compatible with the split luciferase assay. The small inhibitory effects on caspase activity, when compounds were added after activation of extracts, suggests that these compounds may also interact to processed fragments of caspase-3.

Amongst the chemicals, Chlorpyrifos-methyl showed a big variation in caspase-3 activity. To further test the inhibitory effect of this compound caspase-9 activity was measured and processing was studied. When pre-incubated, procaspase-3 was cleaved at the similar level as activated control. Caspase-9 was also processed at similar level to the control, however, the activity of caspase-9 decreased by about 40 %. When activated extract treated with Chlorpyrifos-methyl, the similar level of activity was measured for both caspase-9 and caspase-3. Although Chlorpyrifos-methyl may bind to Apaf-1, this binding is not specific because it seemed that it was also able to inhibit the activity of pro- and processed form of caspase-3 and caspase-9.

The other interesting compound was Thiram which inhibited caspase-9 and caspase-3 activity when added before Cc/dATP. It also inhibited caspase-3 activity when added after addition of Cc/dATP. However, it had only a slight effect on caspase-9 when added after Cc/dATP. These data suggest that Thiram inhibits apoptosome formation, but also directly inhibits caspase-3 activity.

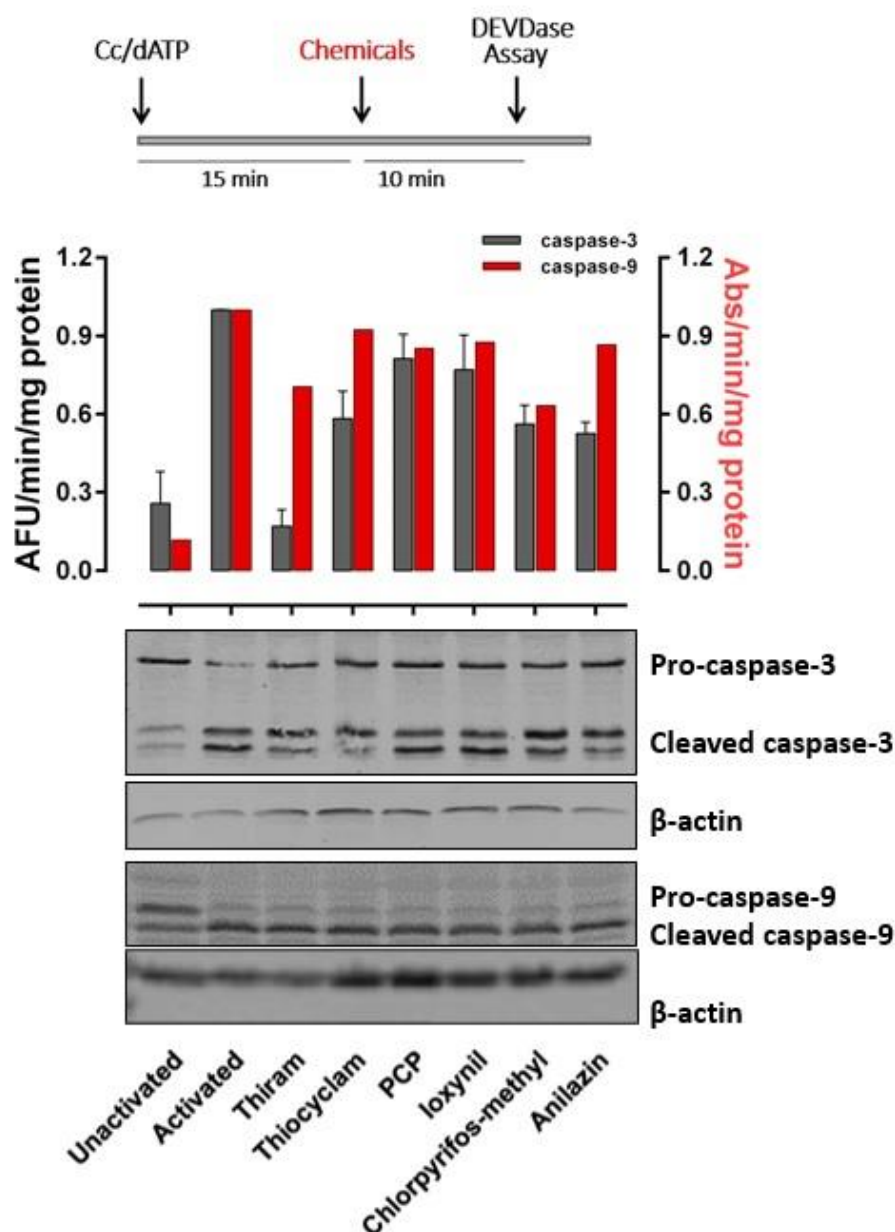


Figure 4.5. Caspase processing and activity after activation of cell extract. HEK293 S-100 extract activated by adding Cc/dATP and 15 min incubation at 25°C. hit compounds were added after extract activation and incubated for 10 min. Then caspase-3 and caspase-9 activities were recorded in the very same condition as in figure 4. An aliquot of each reaction was used for detection of caspase-3 and caspase-9 processing by immunoblotting. Caspase-3 activity was performed in three different experiment and the random aliquot was taken from one of the experiments for immunoblotting. Error bars represent the mean \pm SEM. Caspase-9 activity shown here is the result of one experiment.

Thiocyclam seemed to inhibit procaspase-3 processing and activity. The processing of caspase-9 led to generation of p35 fragment and very little p37, suggesting the inhibition of caspase-3. In other words, caspase-3 was blocked and so did the processing of caspase-9 (at Asp 330). The inhibition of fully processed caspase-9 may explain the low level of caspase-9 activity. Thiocyclam perhaps bound to Apaf-1 and induced a conformational change that was not suitable for luciferase reconstitution, but the complex was still able to recruit and process caspase-9.

Pre-incubation with PCP blocked the processing and activity of caspase-3 and caspase-9. Treatment after activation of the S-100 extract showed a small effect on caspase-3 and -9 activity compared to the control. Of all the hits, PCP showed the lowest IC_{50} for both split luciferase and caspase-3 and the values are very close to each other. The experiment in which caspase-9 and caspase-3 activity and processing were studied showed that other hit compounds are not specific to Apaf-1. PCP was also associated with infertility. On the other hand, Apaf-1 plays role in spermatogenesis and infertility. Therefore, we focused on PCP to find if there is any relationship between its toxicity and Apaf-1 inhibition.

4.1.3 PCP is the most potent hit that inhibits apoptosome

I showed that PCP inhibits luciferase activity. To test whether PCP blocks luciferase activity after apoptosome formation, split luciferase activity was measured when S100 extract incubated before or after apoptosome formation. Addition of Cc/dATP increased the luciferase activity by ~ 4-fold. However, the activity of split luciferase was totally blocked no matter when PCP was added (before or after activation of the extract) (Figure 4.6).

From previous experiments, it was known that this concentration does not have any effect on luciferase itself. In addition, PCP did not change the activity of caspase-3 and -9 when added after Apaf-1 oligomerization (Figure 4.5). At this point, all caspases have already been activated and no more apoptosome is required. PCP may dissociate the complex or it may induce some structural changes that was different to wild-type complex and hence, luciferase activity was not detected.

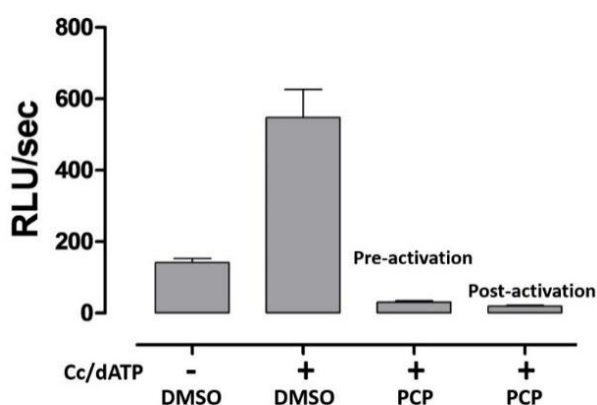


Figure 4.6. Split luciferase activity of the PCP-treated extract before and after activation of the crude extract. S-100 extract expressing either Nluc-Apaf-1 or Cluc-Apaf-1 diluted and mixed with 1:1 ratio. Treatment with PCP totally abolished the split luciferase activity no matter PCP is added before (pre-activation) or after (post-activation) activation of the extract. In controls, mixing diluted Nluc-Apaf-1 and Cluc-Apaf-1 showed low level of activity, however, this activity was increased by addition of cytochrome c and dATP.

4.2 Screening the marine natural products

Marine natural products are potential sources for new therapeutics for a range of different diseases. As part of a collaboration between NUIG and the University of South Florida, a small library of 66 extracts from marine animals collected from Irish waters was tested for chemicals that modulate apoptosome formation.

As making S-100 extracts expressing fusion proteins Nluc-Apaf-1 and Cluc-Apaf-1 was expensive in terms of time and resources, a primary screen was performed by measuring the caspase-3 like activity as an indirect readout of apoptosome formation. The “hits” emerging from this screen were then tested using the split luciferase complementation assay. To show that caspase-3 activity is dependent on cytochrome c and dATP, S-100 HEK293 extract treated with DMSO in the absence of cytochrome c and dATP and the basal caspase-3 like activity was measured. Cc/dATP increased caspase activity by ~ 20-fold (Figure 4.7A). M50054, the inhibitor of caspase activation, was used as positive control.

In the first round of testing, three extracts, RMY-255-1, RMY-258-1 and RMY-243-2, were identified with the ability to inhibit caspase-3 activity (Figure 4.7B). The second round of testing was then performed using split luciferase assay to examine whether any of these three hit compounds inhibit apoptosome formation. Of the three, RMY-243-2 showed ~80% inhibition against split luciferase compared to vehicle control (Figure 4.7C). This extract also inhibited luciferase activity by ~40%. The other extracts caused less inhibition in the luciferase assay compared to the split luciferase assay, but the inhibition of split luciferase activity by RMY255-1 and RMY-258-1 was much less than the inhibition caused by RMY-243-2, and in the case of RMY255-1, the effect was highly variable. Therefore, although RMY-243-2 showed some activity against luciferase activity, it was further investigated.

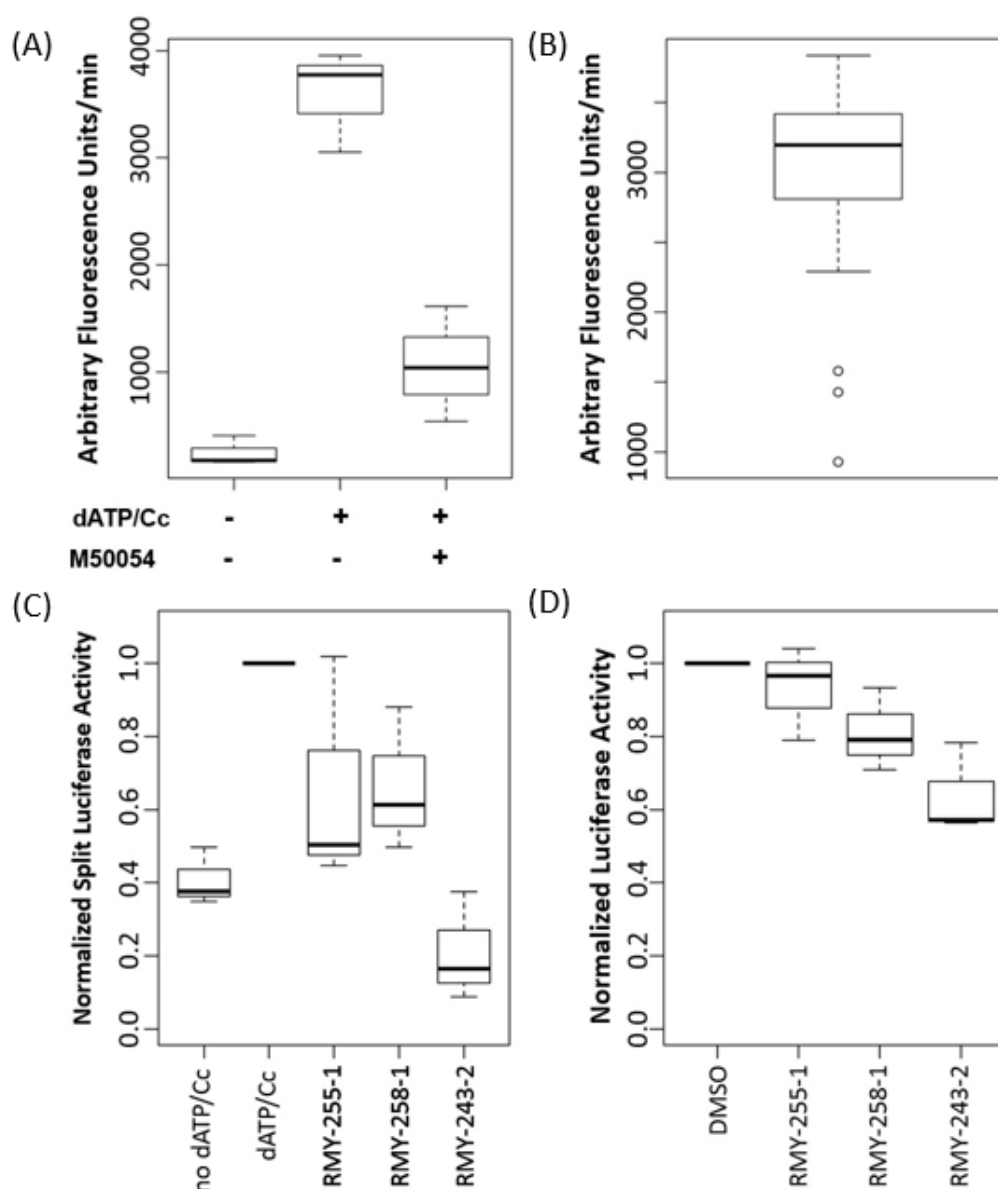


Figure 4.7. A collection of natural product extracts was screened to identify inhibitors of caspase-3 activity. (A) caspase-3 activation was induced by addition of cytochrome c (1.6 μ M) and dATP (1mM) to the S-100 HEK 293 extract in the absence and presence of caspase-3 inhibitor. (B) Extracts were tested for the ability to inhibit caspase-3 activity. Data are expressed as the change in arbitrary fluorescence units per minute. The data are shown as a box (median with upper and lower quartiles) and whisker plot (highest and lowest values, excluding outliers). Open circles are outliers and putative ‘hits’. (C) Three extracts were tested for the ability to inhibit split luciferase and (D) luciferase activity. The data are from at least three independent experiments and are shown as a box (median with upper and lower quartiles) and whisker plot (highest and lowest values).

4.2.1 Fractionation and purification of the RMY-243

RMY-243 was extracted using different procedures. Stepwise fractionation and purification of the extracts were shown in figure 4.8.

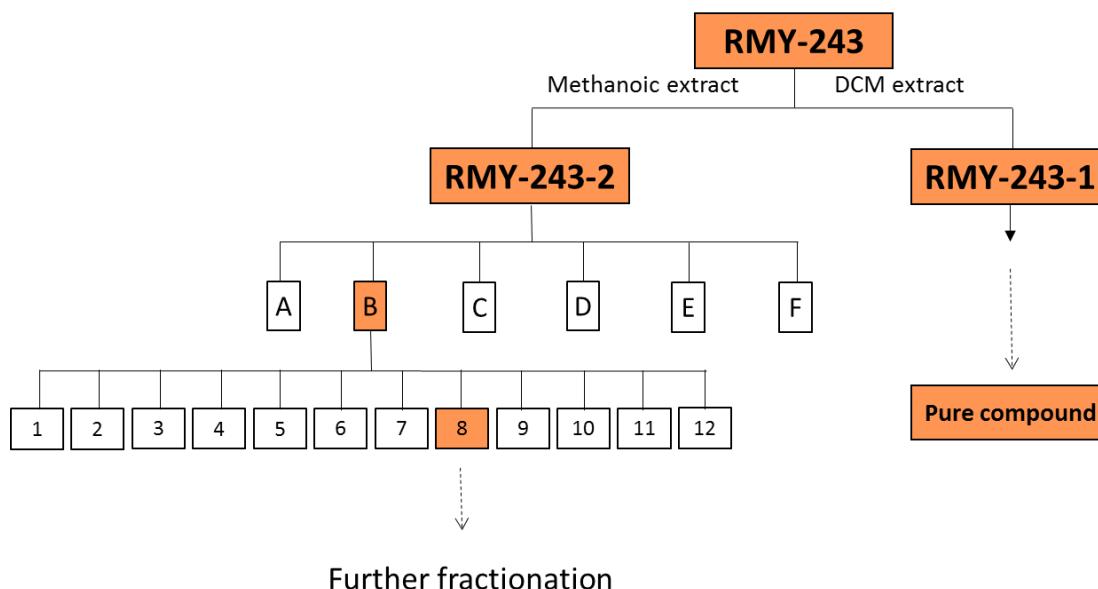


Figure 4.8. Fractionation of the hit compound. RMY-243 was extracted as methanoic or DCM extract. Orange boxes show the inhibition of split luciferase activity. RMY-243-1 was fractionated sequentially and the final pure metabolite was tested using split luciferase assay. RMY-243-2 was fractionated and the fractions were tested using split luciferase assay. The hit fraction was further fractionated and re-tested.

4.2.1.1 RMY-243-1

Initial fractionation was achieved via vacuum liquid chromatography (VLC) using C18 (4.5 g) and eluted using the following solvent mixtures using 3X column volumes of solvent: (A) 75% MeOH / 25% H₂O; (B) 100% MeOH; (C) 75% MeOH / 25% DCM; (D) 50% MeOH / 50% DCM; (E) 25% MeOH / 75% DCM; (F) 100% DCM.

Additional chemical analysis showed that fraction B contained a major metabolite and was therefore chosen for further purification. Fraction B (200 mg) was injected onto a phenyl-hexyl column (5 μ m, 19 x 250 mm) using a gradient of MeCN and water at a flow rate of

12 mL.min⁻¹. The initial mixture was at 55% MeCN for 3 minutes where it was increased to 100% MeCN over 20 minutes. This final 100% MeCN was held for a further 5 minutes (Figure 4.9). The major metabolite (RMY-243-1-B-2) was finally purified for bioactivity evaluation on a PFP column (5 μ m, 4.6x250 mm) at a flow rate of 1.2 mL.min⁻¹. The starting solvent mixture was 50% MeCN/ 50% H₂O + 0.1 % TFA this was increased to 60% MeCN + 0.1% TFA over 20 minutes, ultimately yielding the chemical pure compound (Figure 10). All fractionation, purification and structural analysis was performed by our collaborator in Zoology (Dr. Ryan Young and Professor. Louise Allcock).

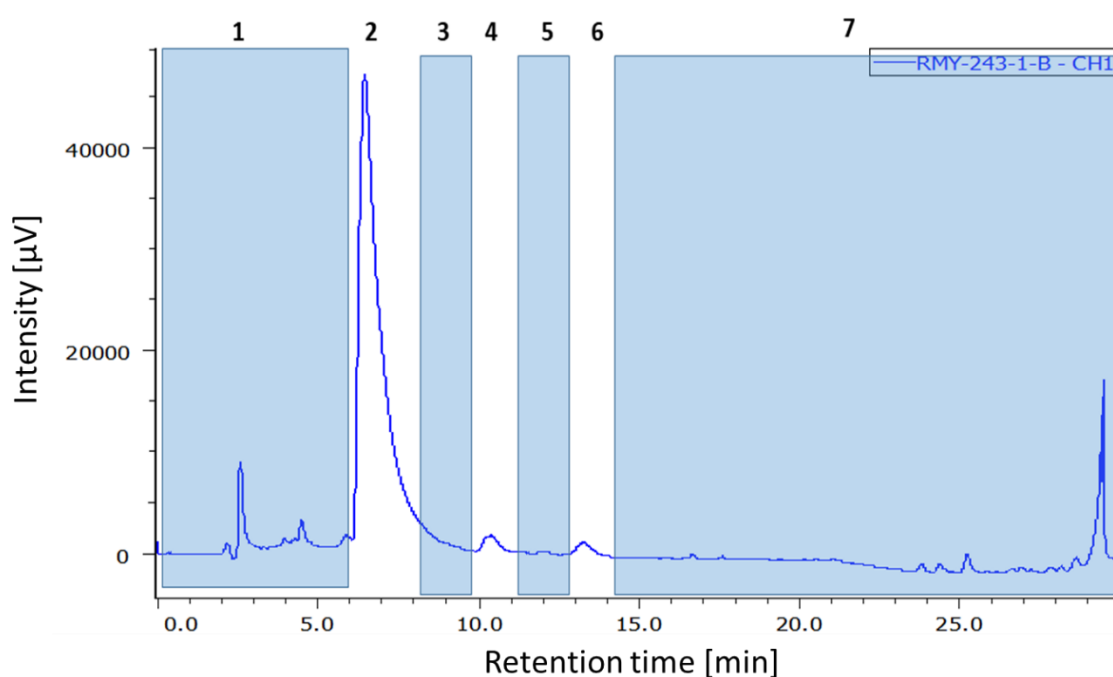


Figure 4.9. Fractionation of RMY-243-1-B. Chromatograph of RMY-243-1-B purified on a prep phenyl-hexyl column using gradient of MeCN/H₂O. UV monitored at 254 nm.

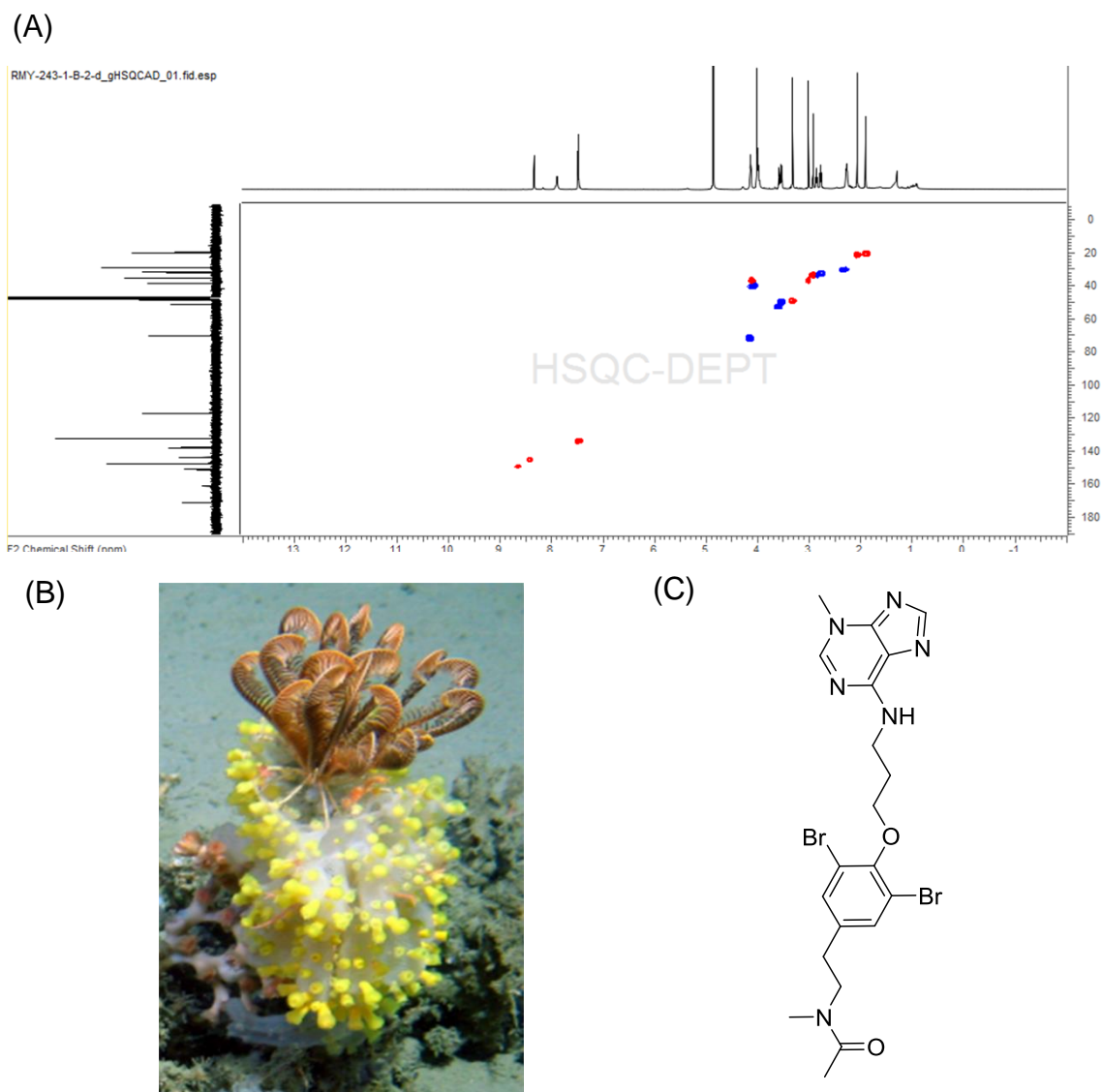


Figure 4.10. Structural identification of a new compound. (A) MS profile of the purified compound. (B) This compound was extracted from a Zoanthids on the sponge *Aphrocallistes*. (C) Chemical structure of the new compound.

4.2.1.1.1 Structural Elucidation

High resolution mass spectrometry showed the major metabolite do be dibrominated with a m/z of 539.0356 corresponding to a chemical formula of $C_{20}H_{25}Br_2N_6O_2$. The 1H NMR spectrum showed resonances which could be attributed to two N-methyl protons, an acetyl

moiety and an A2X2 spin system. Correlations observed in the HMBC from the N-methyl showed the presence of an amide in the metabolite as well as linking this amide to the brominated benzene ring through a ethyl linker (Figure 4.10C). The spectra of the right-hand side fragment showed two methine protons (δ H 8.66 (s), δ C 149.4; δ H 8.44 (s), δ C 145.5), three sp² hybridized quaternary carbons (δ C 153.4, 149.7, 112.5) and the remaining N-methyl (δ H 4.08 (3H, s), δ C 36.5), ultimately resulting in the unusual 3-methyladenine moiety. Further analysis of the HMBC and COSY data connected the adenine functionality to the dibromophenyl ring through a propyl ether linker resulting in the final structure (Figure 4.11).

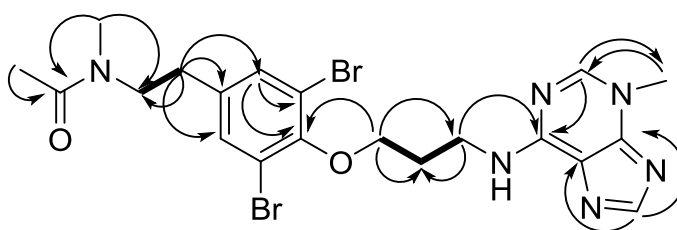


Figure 4.11. Chemical structure of the zoanthid major metabolite. Key COSY (bold lines) and HMBC (arrows) correlations of final purified structure. Bold lines signify key 1H-1H COSY correlation used to determine the final structure. Arrows denote key HMBC correlations used to elucidate the structure.

4.2.1.1.2 Titration of RMY-243-1 in split luciferase and caspase-3 assay

The pure compound was then titrated to calculate the IC₅₀ in split luciferase assay and caspase-3 assay. The IC₅₀ was ~700 μ M for caspase-3 and >1 mM for luciferase (Figure 4.12). The high IC₅₀ for RMY-243 suggests that this compound is not suitable for therapeutics approaches. However, it is interesting that this compound is produced within the organism and contains Br element, a rare compound in living organisms. Further studies are required to determine the cytotoxicity of this compound.

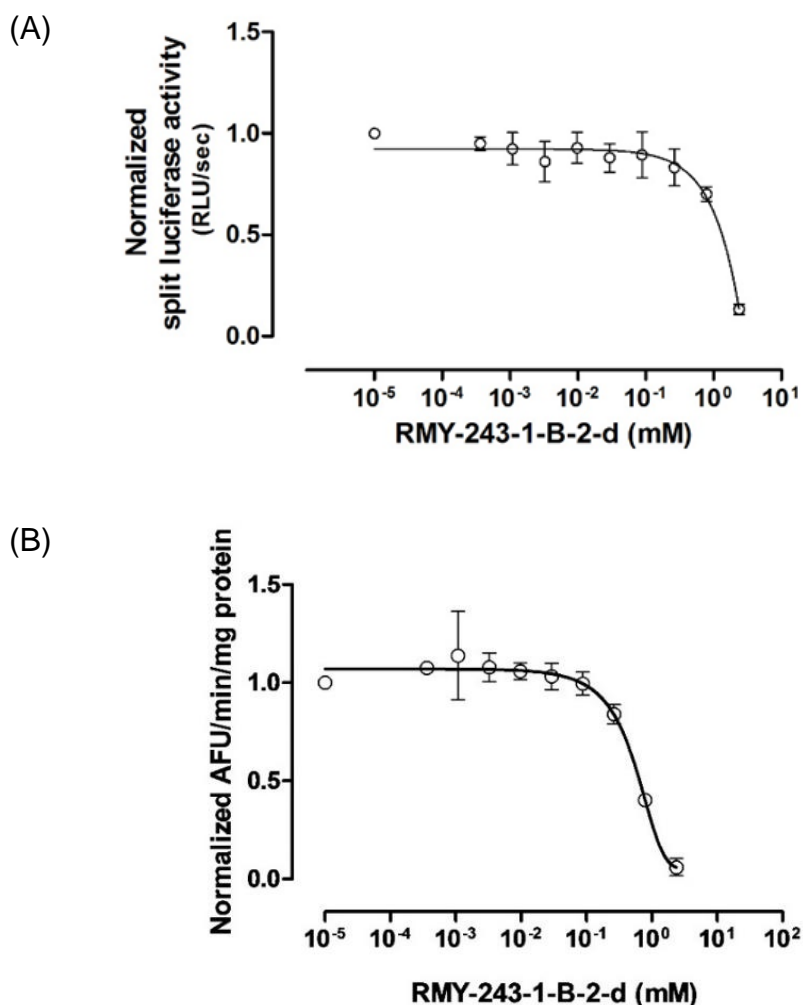


Figure 4.12. Titration of the pure identified compound using split luciferase and caspase-3 like activity. (A) titration of RMY-243 in split luciferase assay and (B) titration in caspase-3 like activity.

4.2.1.2 RMY-243-2

Initial fractionation was achieved via vacuum liquid chromatography (VLC) using C18 (4.5 g) and eluted using the following solvent mixtures using 3X column volumes of solvent: (A) 100% H₂O; (B) 25% MeOH / 75% H₂O; (C) 50% MeOH / 50% H₂O; (D) 75% MeOH / 25% H₂O; (E) 100% MeOH; (F) 75% MeOH / 25% DCM. These fractions were resubmitted to the split luciferase assay and showed the most active fraction was fraction B (Figure 4.13).

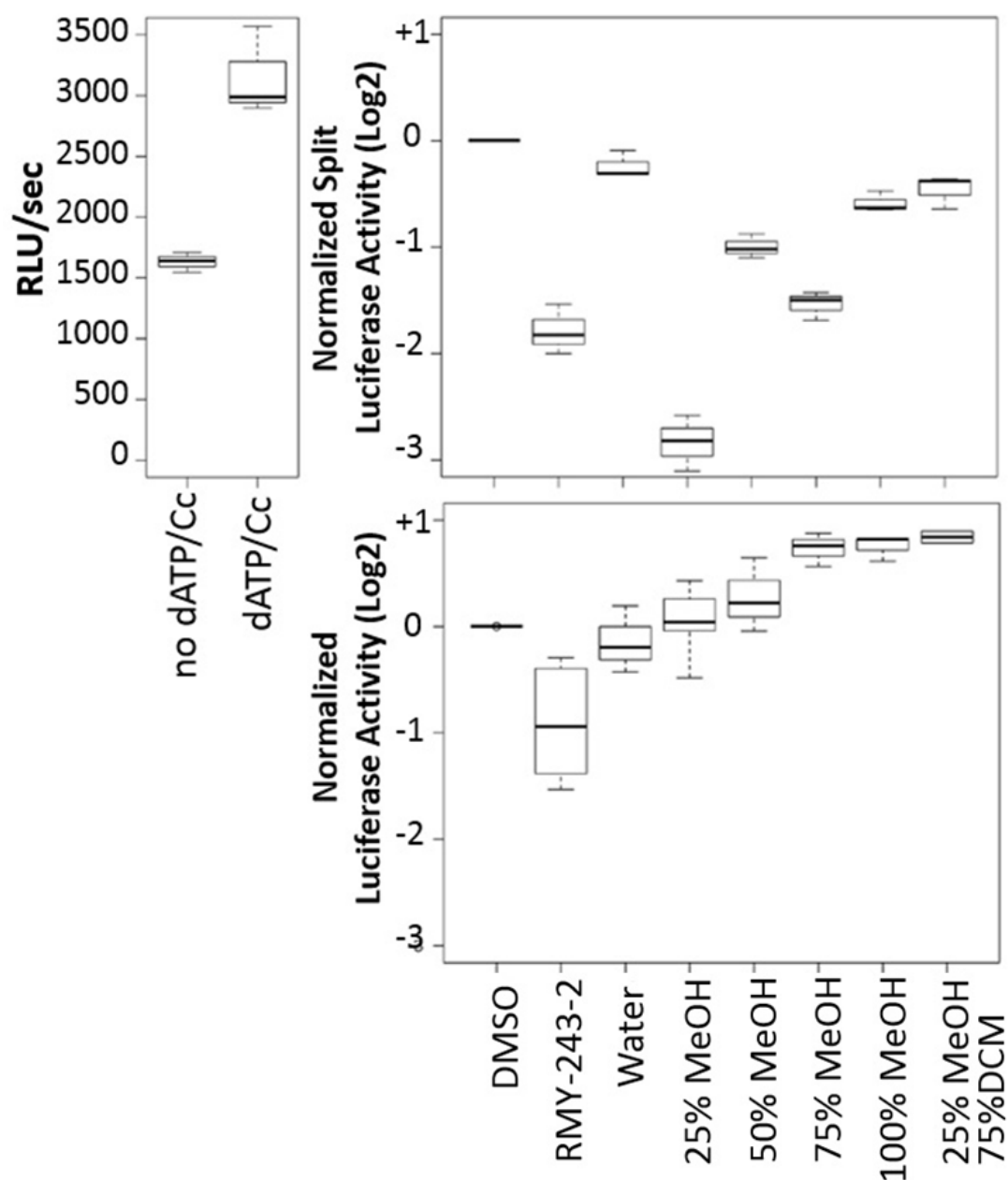


Figure 4.13. A methanol RMV-243-2 extract fractionated and eluted with water and increasing concentrations of methanol. Fractions were collected, dried and dissolved in DMSO before being tested in the split luciferase assay. (A) dATP and cytochrome c induces split luciferase activity. (B) Split luciferase (upper panel) and luciferase (lower panel) activity normalized to Cc/dATP induced activity (upper panel) or to luciferase activity (lower panel). The data are from at least three independent experiments and are shown as a box (median with upper and lower quartiles) and whisker plot (highest and lowest values).

The highest luciferase activity was picked and normalized to the split luciferase activity of DMSO-treated extract. Luciferase assay was also performed to check the possibility of the fractions affecting luciferase itself. The fraction collected using 25% methanol showed a strong inhibition against split luciferase while no detectable inhibition on luciferase activity (Figure 4.13). Compatible to the previous experiments, RMY-243-2 inhibited luciferase activity to some extent, however, fractionation of the extract seems to block the inhibitory effect on luciferase which might be due to the synergistic effect of more than one compound within the crude extract.

A phenyl-hexyl column (5 μ m, 19 x 250 mm) using a gradient of MeCN and water at a flow rate of 12 mL.min⁻¹. The initial gradient was 5% MeCN where it was increased to 70% MeCN over 25 minutes (Figure 4.14).

Then the fraction collected using 25% methanol further fractionated using HPLC, preparative hexylphenyl column (acetonitrile/water). RMY-243-2-B further fractionated using prep hexyl-phenyl column. Thirteen fractions were produced (Figure 4.14).

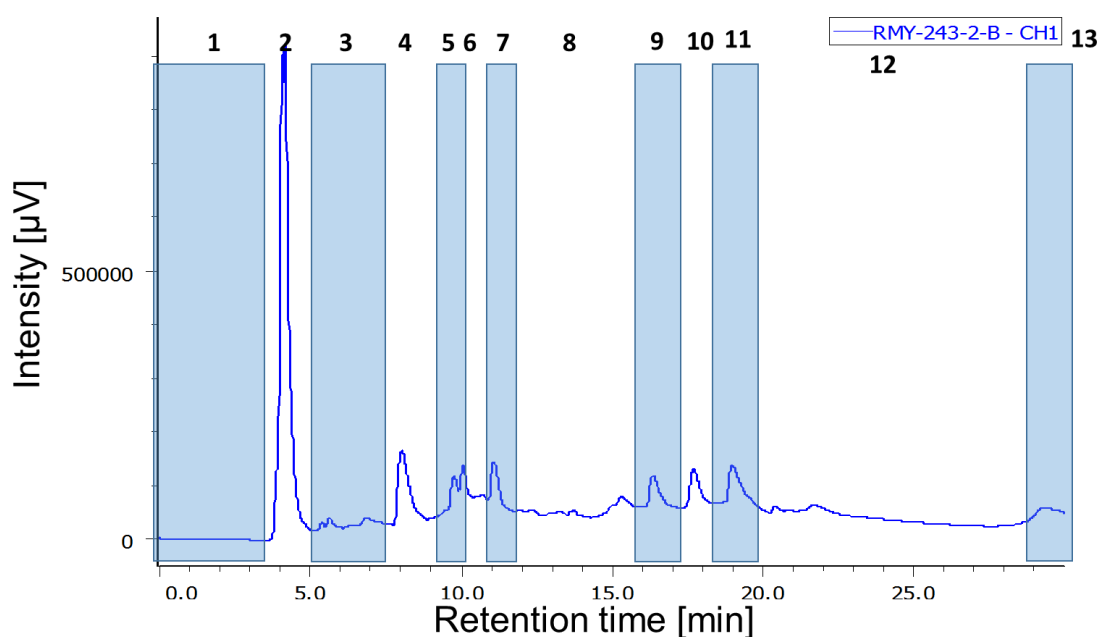


Figure 4.14. Fractionation of RMY-243-2-B. RMY-243-2-B fractionated using prep hexyl-phenyl column. Thirteen fractions were collected and used in split luciferase assay.

Split luciferase assay performed for all fractions. Fractions 2 through 12 were resubmitted to the bioassay for evaluation. Fractions 8 and 9 (Figure 4.15) showed the greatest split luciferase inhibition and were selected for further purification. Purification and structural elucidation is ongoing.

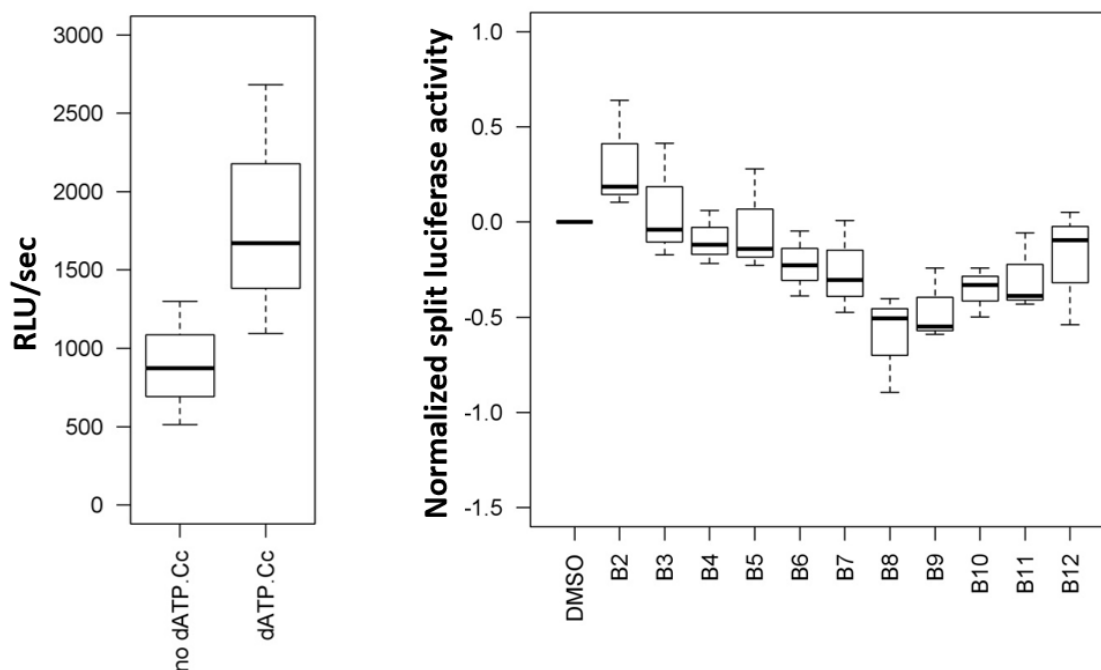


Figure 4.15. 25% MeOH (RMY-243-2-B) fraction further fractionated and the fractions were tested in luciferase assay. (A) Luciferase activity was induced by addition of cytochrome c (1.6 μ M) and dATP (1mM) to the S-100 HEK 293 extract. (B) split luciferase activity was measured when S-100 HEK 293 extract treated with each fraction. The data are from at least three independent experiments and are shown as a box (median with upper and lower quartiles) and whisker plot (highest and lowest values).

4.3 Discussion

Previous attempts to screen for Apaf-1 regulators have used indirect, caspase-based assays coupled with time consuming and very low throughput gel filtration or co-immunoprecipitation approaches. All these assays are time-consuming and in the case of gel filtration require a relatively large number of cells. As a result, only a small number of compounds can be easily tested, significantly limiting the search for Apaf-1 regulators. Here I established split luciferase-based assay for detecting Apaf-1 oligomerization and used it to screen a library of ~200 compounds.

Six compounds were identified with the ability to block split luciferase activity rather than luciferase activity, suggesting that these compounds affect apoptosome not luciferase itself. These compounds were then titrated in split luciferase assay and caspase activity assay to calculate the IC_{50} . All compounds were shown to have high IC_{50} ranging from μM to mM concentration. Thiocyclam and Pentachlorophenol (PCP) showed lower IC_{50} compared to other hit compounds. However, PCP showed close IC_{50} in luciferase and caspase assay implied that PCP target apoptosome with more specificity than Thiocyclam.

The assay has several advantages:

- The assay reports Apaf-1 oligomerization directly.
- The assay is rapid, requiring minutes as opposed to hours or days for the current alternatives.
- The assay is scalable and can be used for large numbers of chemicals.

However, there are also disadvantages to the assay. In its current format, the assay is not very cost-effective: it requires large amount of DNA, large scale cell transfections and extract preparation. To make it more economical, we diluted the extract in order to do more number of tests.

In the second screen, all the extracts collected from marine organisms were first tested for the ability to block caspase activity. The hit compounds were then tested by split luciferase

assay to identify those inhibit apoptosome. This two-step screening made the assay cheaper by removing the need to transfect large numbers of cells. The hit extracts were then tested in luciferase assay and a hit was selected for further analysis. Stepwise fractionation led to identification of a pure compound. This compound block caspase activity and luciferase activity at $IC_{50} \sim 700 \mu M$. The greatest inhibition was observed in a methanoic extract of a yet-to-be-described zoanthid growing on *Aphrocallistes* Beatrix. Bioguided fractionation identified the major metabolite as well as some minor metabolites as active against the apoptosome.

Further analysis of the HMBC and COSY data connected the adenine functionality to the dibromophenyl ring through a propyl ether linker resulting in the final structure. Preliminary docking studies have shown this zoanthid metabolite binds at the ATP-binding pocket of the apoptosome. In silico studies will be discussed in detail in chapter 7. This compound is unique in that Br is not one of the common chemicals in living organisms. Titration of this compound showed high IC_{50} for both luciferase and caspase-3.

Thus, I have shown that the assay can be used as either a primary or a secondary screen to identify compounds or natural products that affect Apaf-1 function. Further improvements in the assay could come from making stable cell lines expressing either of the plasmids (Nluc-Apaf-1 or Cluc-Apaf-1). The most efficient strategy would be an *in cellulo* assay in which luciferase activity reports apoptosome formation in live cells. In this case, not only inhibition of the apoptosome is tested, but also other pharmacologically important factors such as cell membrane permeability will be examined. This will shorten the validation process of the identified hit compounds.

This has proved difficult to accomplish for several reasons. Firstly, the current constructs use a CMV promotor that is activated by diverse cell stressors. This means induction of split luciferase activity may be caused by increased protein expression as well as complex formation. Secondly, the luciferase activity induced by apoptotic stimuli such as etoposide

and doxorubicin is relatively modest (2 fold) and variable, making the *in cellulo* assay unsuitable for high-throughput screening, at least in its current iteration.

Two-step screening can enormously reduce the cost of assay because only the wild-type extract is required for measuring caspase-3 activity in the first round of screening. However, this strategy is not suitable when tens of thousands of compounds are tested. The challenge is to make a library of hit compounds identified through the first round of screening and re-test them in the second split luciferase assay. This step adds extra costs to the whole procedure and requires more time to prepare the library.

**Identification of the
direct protein target of
PCP within the
apoptosome signalling
pathway**

The split luciferase assay that identified PCP as an inhibitor of apoptosome formation was performed using a mammalian cell extract that contains many proteins. So, while this approach can potentially allow the discovery of new processes that regulate Apaf-1 and the apoptosome, the molecular target for PCP is uncertain. To investigate how PCP inhibited apoptosome formation I moved to a defined cell-free system using purified recombinant Apaf-1 and purified cytochrome c. Using the defined system, I tested the effect of PCP on Cc/dATP dependent Apaf-1 oligomerization in the absence of any other proteins that might interfere with apoptosome formation. I also investigated whether PCP directly interacted with either Apaf-1 and/or cytochrome c.

The first step was the expression and purification of recombinant Apaf-1 from insect cells after transduction with a recombinant baculovirus and a demonstration of Apaf-1's functionality.

5.1 Baculovirus Expression System

Baculoviruses are large double-stranded DNA viruses with 134 kilo base pair genome that infect insect cells. These particles also contain strong promoters that produce large quantities of desired proteins. Autographa californica nuclear polyhedrosis virus (AcNPV) has been widely used to make recombinant proteins in eukaryotic cells when expression in other cell systems (e.g. bacterial expression systems) do not yield an active protein (Ciccarone et al., 1998).

Apaf-1 expression and purification from bacterial culture yields inactive protein. Baculovirus Expression System has been used to produce active, pure recombinant Apaf-1 (Zou et al., 1999; Kim et al., 2005). This technology is based on the production of an expression vector with the baculoviral promoter and recognition sites for the bacterial Tn7 transposase at the two ends of the gene of interest. Then, the sequence of interest is transformed into a bacmid, a large single-copy DNA, which contains the whole AcMNPV genome encoding all the required proteins for propagation in *E. coli*. The desired expression

cassette in the bacmid (recombinant bacmid) could be selected, screened, and isolated and be used for transfecting the insect cells (Mehalko and Esposito, 2016) (Figure 5.1).

pFASTBAC is the common plasmid used for generating the viral particle capable of expressing the gene of interest. The gene of interest is cloned under a control of polyhedron promoter. It also contains two attachment sites for the bacterial Tn7 transposase.

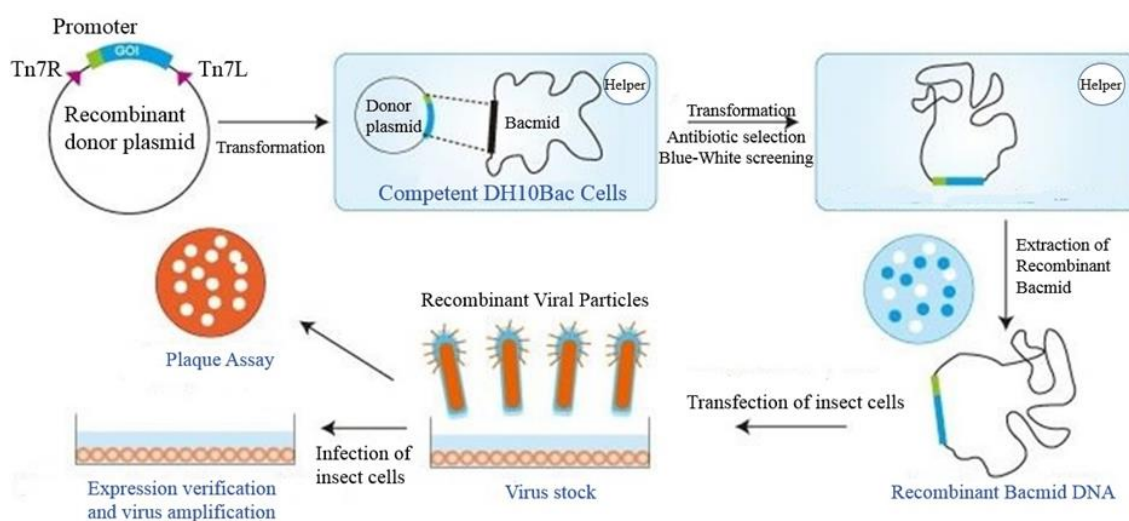


Figure 5.1. Overview of the Baculovirus expression protocol. The gene of interest is cloned into a donor vector between two Tn7R sequences. The plasmid is then transformed into the competent DH10Bac cells which already contain Bacmid and Helper plasmid. Bacmid encodes the required genes for virus assembly and Helper plasmid encodes a transposase. The desired fragment is inserted into the lacZ, and therefore, antibiotic selection and blue-white screening yield a recombinant bacmid which is then transfected into Sf21 cells. The viral particles are collected and used for titration of the virus (plaque assay) and infection of insect cells (protein production).

5.2 Cloning, isolation and validation of recombinant bacmids

Baculovirus expression system has been designed for rapid and convenient screening of the recombinant colonies. The transposase cuts the gene of interest from a donor vector and inserts it to a LacZ gene. LacZ produces blue colour in the presence of X-gal. Insertion of the gene of interest disrupts LacZ. Therefore, cells transformed with recombinant bacmid produce white colonies while cells with no insertion produce blue colonies.

As shown in figure 5.2, bacmids are indicated as a band that moves slower than 23.1 kb fragment of Lambda DNA HindIII Digest. Helper and pFASTBAC plasmids have also been shown.

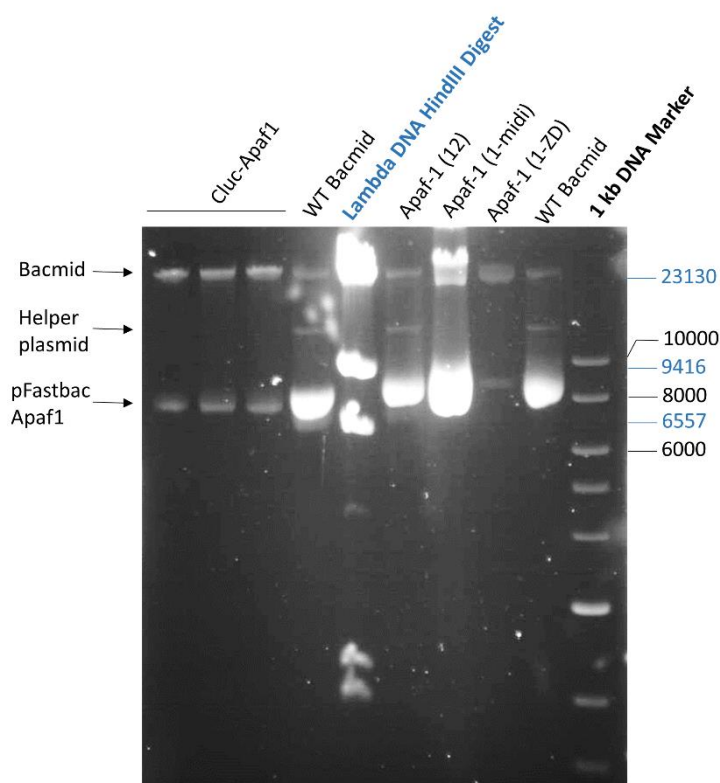


Figure 5.2. Agarose gel electrophoresis of extracted bacmids. 5 μ L of all the samples were loaded on the 0.5 % agarose gel and run at 20 V for 16 hours. Lambda DNA HindIII Digest (blue) and 1 Kb DNA (black) markers were used to specifically detect large bacmid (>134 kbp), Helper plasmid and pFASTBAC plasmid encoding Apaf-1. After screening the colonies, one colony (#12) was extracted by plasmid midi-prep (Midi) or ZR BAC DNA Mini-prep (ZD) and used for further analysis.

Since the bacmid DNA is very large, it is difficult to ensure the insertion of the gene of interest into the bacmids only by running the bacmids on the gel. Therefore, to confirm the transposition and insertion of the gene of interest into the bacmid, I PCR-amplified the fragment within the lacZ complementation region of the bacmid using pUC/M13 primers. To eliminate the possibility of detecting the false positive PCR products, I also used M13 forward primer and gene-specific reverse primer to amplify the insertion of Apaf-1 gene into the bacmid. Insertion of the gene of interest produces a fragment of 2300 bp plus the size of the inserted gene which is 3700 bp and produces 6000 bp fragment (Figure 5.3). I screened 12 colonies for checking the insertion of the Apaf-1 (Figure 5.4).

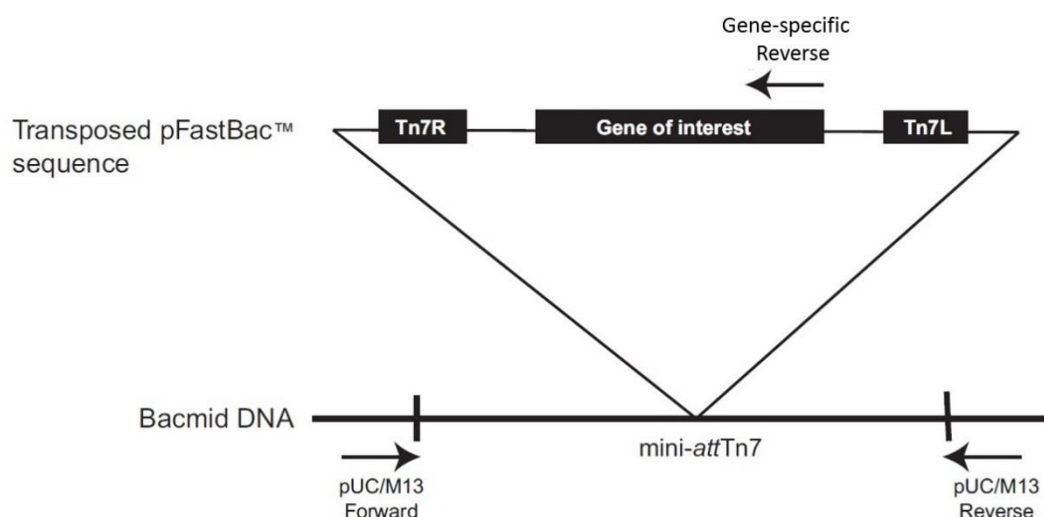


Figure 5.3. Transposition region in recombinant bacmids. The insertion site is flanked by pUC/M13 forward and reverse sequences. PCR amplification using pUC/M13 forward and reverse primers produces a 6000 bp fragment. PCR amplification using pUC/M13 forward and Apaf-1 specific reverse primers produces a 5500 bp fragment.

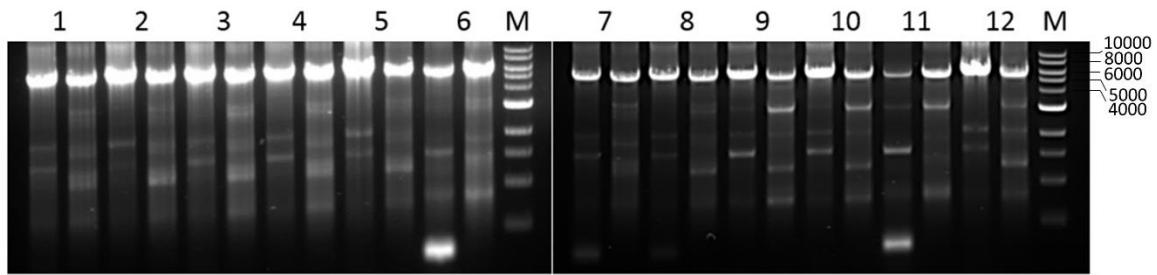


Figure 5.4. Screening of the picked colonies for insertion of Apaf-1 in the bacmid. 12 colonies identified through blue-white screening cultured and the bacmids were extracted and used for PCR-amplification of the inserted fragment using either pUC/M13 forward and reverse primers or pUC/M13 forward and Apaf-1 specific reverse primers. In each case, the left lane is the fragment amplified using pUC/M13 forward and reverse primers and the right lane is pUC/M13 forward and Apaf-1 specific reverse primers.

I also used blue colonies, indicating no insertion, to amplify the fragment without insertion. White colony shows the fragment with the right size with both pairs of primers (Figure 5.5). However, in blue colonies with no insertion, a 300 bp fragment would be amplified (not shown in the gel because it is at the very bottom of the gel). Using M13 forward and gene specific reverse primer, a 6000 bp fragment is detected. The white colonies originate from a correctly transpositioned single cell. The blue colonies also have both wild-type bacmid and the pFASTBAC donor plasmid in the plates with appropriate antibiotic selection markers. Transposition constantly happens in the cells within the blue colonies, therefore obtaining the pure wild-type bacmid in the blue colony without transposition in some cells is very unlikely. Besides, pUC/M13 primers are very short and may bind to non-specific sequences and produce the fragments. Bacmids were produced for encoding wild-type Apaf-1, Nluc-Apaf-1 and Cluc-Apaf-1. Sequencing confirmed the insertion of the fragments into the bacmids.

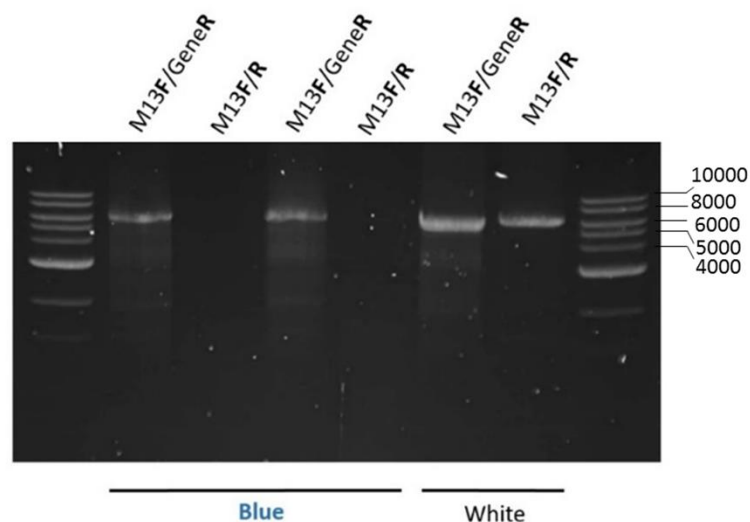


Figure 5.5. PCR-amplification of the control bacmids. Bacmids were extracted from blue colonies using either pUC/M13 forward and reverse primers or pUC/M13 forward and Apaf-1 specific reverse primers. In each case, the right lane is the fragment amplified using pUC/M13 forward and reverse primers and the left lane is pUC/M13 forward and Apaf-1 specific reverse primers.

5.3 Transfection and expression of Sf21 cells with recombinant bacmid

Sf21 is a cell line originating from the pupal ovarian tissue of the Fall Armyworm, *Spodoptera frugiperda*. The Sf21 cell line is highly prone to be infected with AcNPV baculovirus and is widely used with all baculovirus expression vectors.

Sf21 cells were transfected with the large bacmids. The cell lysates were then used for SDS-PAGE to check the expression of bacmids within the insect cells. Transfection of the Sf21 cells with Apaf1-midi showed a band with the right size related to Apaf-1, which did not exist in untransfected Sf21 cell extract (Figure 5.6). The expression of Apaf-1 was confirmed by immunoblotting. Therefore, the bacmids are able to express the desired protein. However, the bacmids encoding the Nluc- and Cluc-Apaf-1 proteins did not express the desired proteins, which limited some of my later experiments. Although the sequencing confirmed the insertion of those fragments, the bacmid was unable to express protein.

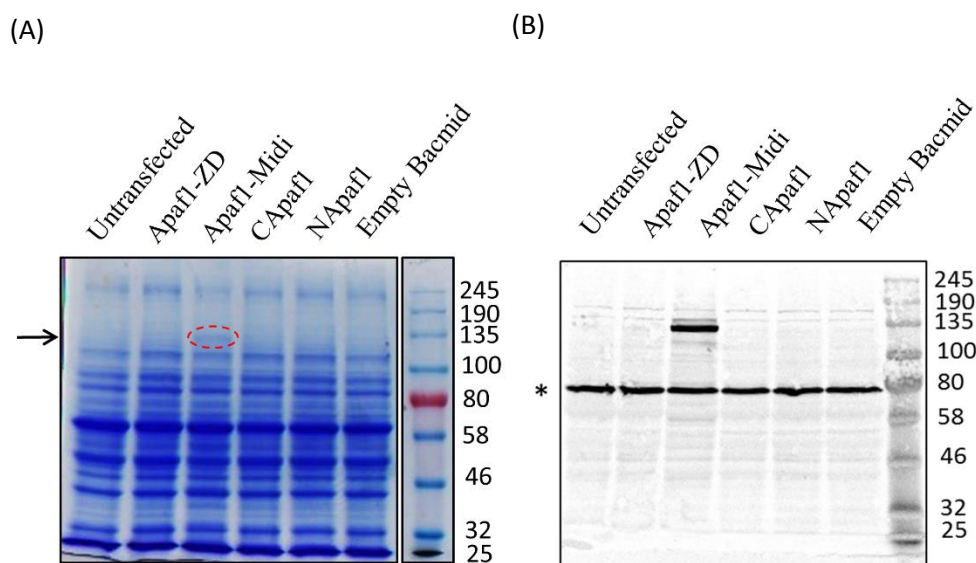


Figure 5.6. SDS-PAGE and immunoblotting of the transfected Sf21 cells with different bacmids. Cell lysates transfected or not with wild-type, Nluc-Apaf-1, Cluc-Apaf-1. (A) Apaf-1 (extracted using midi-prep and ZD BAC DNA extraction kit) loaded on 8% polyacrylamide gel. The gel was then stained using Coomassie blue and destained overnight. (B) The same samples were immunoblotted to detect Apaf-1. Arrows show the Apaf-1 protein. Asterisk shows the non-specific bands.

To check the ability of the viral particles to produce recombinant proteins, Sf21 cells were infected with 10, 20, 30, 40 and 50 μ L of the P0 viral stock. The cells harvested and lysed after 5 days incubation at 28°C. The lysate was used for immunoblotting using Anti-Apaf1 antibody. Apaf-1 protein was detected in the samples infected with the virus, but not in the un-infected samples (Figure 5.7). Infection of the Sf21 cells with a range of viral concentrations led to the same level of Apaf-1 expression. Therefore, for amplifying the viral particles the lowest amount of viral stock (10 μ L) was scaled up to make 100 mL stock. To check the production of viral particles with the ability to produce Apaf-1, the cell pellet was used for making the extract and probing the Apaf-1 proteins using Anti-Apaf1 antibody.

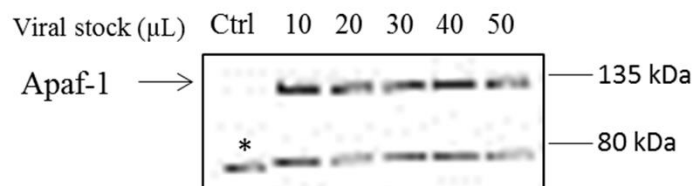


Figure 5.7. Immunoblotting of the Sf21 cells infected with P0 viral stock. Different amount of viral stock was used for infection of the cells. The supernatant was collected after 5 days and the cell pellet was used for testing the expression of the Apaf-1. The cells were lysed and loaded on 8% polyacrylamide gel. Apaf-1 protein was detected using Anti-Apaf1 antibody.

5.4 Expression and affinity purification of recombinant Apaf-1

For doing the large-scale infection and obtaining a high yield of recombinant proteins, Sf21 cells adopted to suspension culture as described in Material and Methods. Then the cells infected with P1 viral stock. 36 hours post infection, the cell harvested and S100 extract prepared. Apaf-1 gene cloned into pFASTBAC vector expresses six histidine affinity tag at the C-terminus, which makes it suitable to be purified by Ni-NTA resin.

After His-tag affinity chromatography, to check the efficiency of Apaf-1 expression and purification, SDS-PAGE was performed. No proteins were detected in the 'Wash' fraction implying the removal of the non-bound and low-binding proteins (Figure 5.8B). The Apaf-1 protein was detected mainly in the fraction 2 and to some extent in fraction 3. Immunoblotting was carried out to confirm that these purified proteins were Apaf-1 and not the other proteins with Histidine residues. Apaf-1 was detected in the same fractions as in SDS-PAGE with the right size. Lack of Apaf-1 in 'Unbound' and 'Wash' fractions confirmed the high efficiency of the purification.

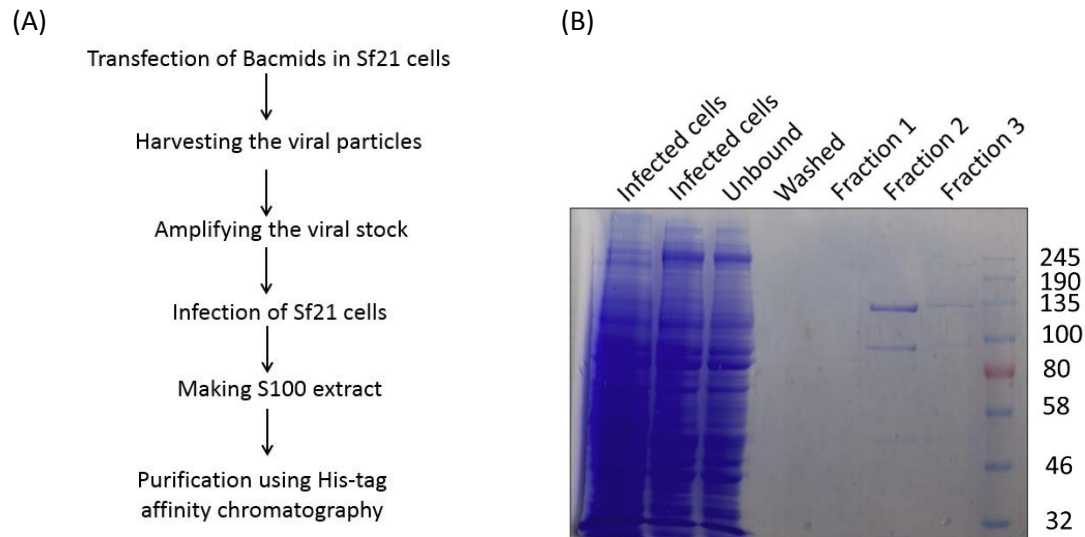


Figure 5.8. The procedures used for making recombinant protein. (A) Sf21 cells were transfected with extracted bacmids encoding wild-type Apaf1. The supernatant was collected and used for amplifying the viral particles. These particles then were used for infection of the Sf21 cells. The cell lysate was loaded on Ni-NTA. Recombinant proteins were purified using the 6 × Histidine at the C-terminus of Apaf-1. (B) SDS-PAGE (top panel) and Immunoblotting (bottom panel) of the collected fractions during protein purification. Immunoblotting confirmed that the purified proteins are Apaf-1. T: lysate of the cells transfected with bacmid encoding Apaf-1, I: lysate of the cells infected with bacmid encoding Apaf-1, U: ‘Unbound’ proteins, W: ‘Wash’ fraction, E1-E3: fractions collected after washing with 250 mM imidazole, M: protein marker.

5.5 Gel filtration to test if the recombinant protein was monomeric or oligomeric.

Overexpressed Apaf-1 can often oligomerize into inactive complexes (1.4 KDa) or form aggregates, which means apoptosome formation cannot be studied. To test if the recombinant protein was monomeric or oligomeric, gel filtration chromatography was performed. Thyroglobulin and Aldolase were used as protein markers to identify fractions that should contain the oligomeric (~700 kDa) and monomeric form (~140 kDa) of Apaf-1. The fractions were collected, the buffer exchanged and the Apaf-1 detected by dot blotting (Figure 5.9A-C). This showed that the majority of the recombinant Apaf-1 had an apparent molecular weight of ~150 kDa, which is consistent with monomeric Apaf-1 (Figure 5.9D).

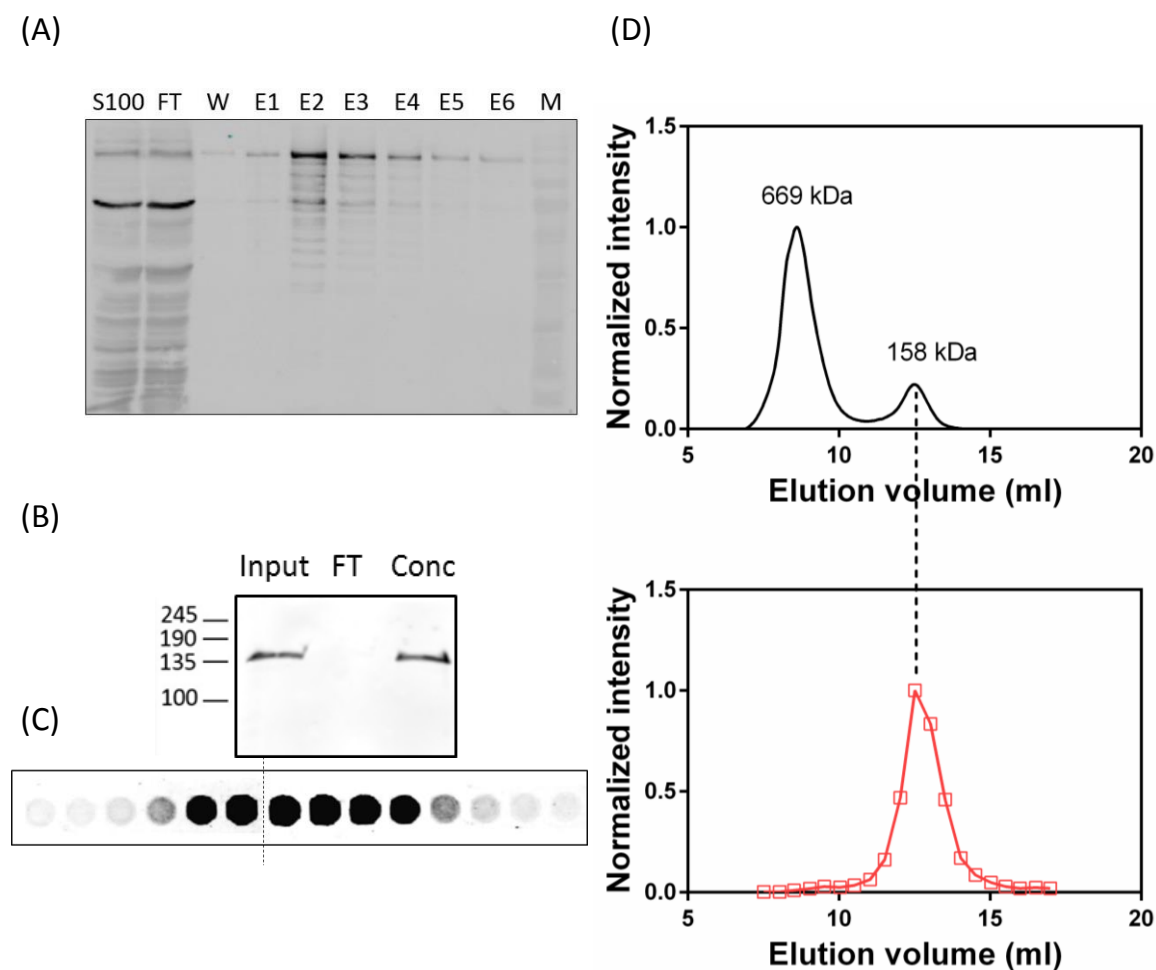


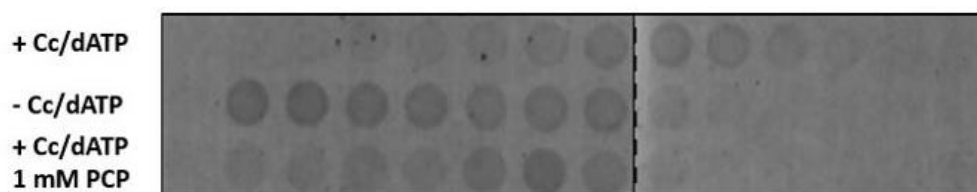
Figure 5.9. Production of rApaf1 using Sf21 cells. (A) Sf21 cells were infected with baculovirus expressing wild-type Apaf1. Cells were harvested 37 hours post-infection, lysed, S-100 extract was prepared and loaded on nickel affinity chromatography. The fractions collected and loaded on 10% polyacrylamide gel and immunoblotted using Anti-Apaf1 antibody to check the purity of the proteins. S100 : input extract, FT: Flow Through, W: Washed sample, E1-E6: Eluted fractions 1 to 7 and M: Protein marker. (B) Proteins were passed through 100 kDa cut-off filters to exchange the buffer and remove imidazole, high concentration of KCl and DTT and also to remove the degraded forms of Apaf-1 proteins. Proteins were then immunoblotted. (C) Gel filtration performed to ensure that the proteins are in their monomeric form. Thyroglobulin (669 KDa) and Aldolase (158 KDa) loaded on the column and the chromatography performed at 0.6 mL/min, fraction size: 500 μ L. The peaks showed where the oligomers and monomers could be detected. Then 100 μ L of rApaf1 loaded on the column. The fractions then loaded on PVDF membrane and analysed by dot blot. (D) Apaf-1 detected in the fractions related to monomeric form.

5.6 Gel filtration of PCP-treated rApaf-1

To test whether PCP could directly affect apoptosome formation or whether it exerted its effect through some other proteins or factors, purified recombinant Apaf-1 and cytochrome c were incubated with PCP. In the absence of Cc/dATP, Apaf-1 was detected in monomeric form. However, addition of Cc/dATP and incubation for 15 min at 25°C moved the monomeric protein into a complex of higher molecular weight (~700 kDa). These data showed that the rApaf-1 was functional. In contrast, if rApaf1 was incubated with PCP (1 mM final concentration) for 10 mins before addition of Cc/dATP and incubated for 15 min at 25°C the Apaf-1 proteins were detected between the monomer and oligomer Apaf-1 (Figure 5.10).

Interestingly, addition of PCP changed the apparent molecular weight of Apaf-1. This could be because PCP bound to the monomer rApaf-1 and to some extent unfolded the protein, causing it to elute earlier. Alternatively, PCP could have altered the oligomerization of rApaf-1 so that a smaller Apaf-1 complex was formed.

(A)



(B)

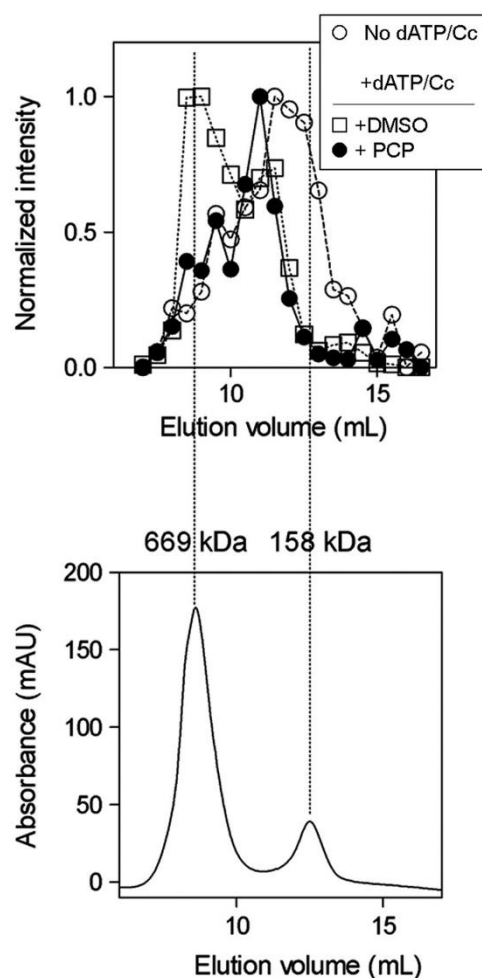


Figure 5.10. Gel filtration of the PCP-treated rApaf-1. (A) The reactions were fractionated by gel filtration and the fractions 8 to 27 were collected for dot blotting using anti-Apaf-1 antibody. (B) rApaf-1 was detected in monomeric form and after addition of cytochrome c and dATP the proteins were detected in the fractions related to the size of apoptosome. Incubation with PCP and addition of cytochrome c led to either the complexes with different size to the wild-type complex or unfolding of the monomers. (C) Thyroglobulin and Aldolase were loaded on Superdex 200 increase column as the protein markers.

5.7 Thermo-stability shift assay of the PCP-treated apoptosome

The reaction in the defined system contained only Apaf-1 and cytochrome *c*. While PCP blocked apoptosome formation, it was not clear whether PCP bound Apaf-1 or cytochrome *c*. To answer this question, thermo-stability shift assay was used. The principle of the assay is that binding of a ligand (a chemical or a protein) to protein *x* changes the conformation of *x* and so the temperature at which protein *x* is denatured.

First, the thermo-stability shift assay of pure cytochrome *c* in the presence and absence of a ligand, ATP, that is known to alter apoptosome formation, was tested (Samali et al., 2007). Cytochrome *c* was stable even at high temperatures (60-70 °C). However, in the presence of ATP, cytochrome *c* thermo-stability was altered with the protein becoming less stable and almost all the cytochrome *c* was denatured by 54 °C (Figure 5.11A,B). These data demonstrated that the assay could detect the interaction between cytochrome *c* and a ligand that alters apoptosome formation. Next, the effect of PCP on cytochrome *c* thermo-stability was assessed. Incubation with PCP also altered the thermos-stability of cytochrome *c*, de-stabilizing the protein. The IC₅₀ for apoptosome formation of PCP was ~ 0.17 mM. I therefore tested the EC₅₀ of PCP in the thermos-stability shift assay to determine the degree of similarity between the two concentrations. By titrating PCP and measuring thermos-stability of cytochrome *c* at 58°C the EC₅₀ was calculated about 600 μM, approximately 4-fold higher than the IC₅₀ for apoptosome formation (Figure 5.11D,E). This difference could be because PCP had a higher affinity for Apaf-1. I therefore tested PCP and Apaf-1 in the thermos-stability shift assay.

However, the thermos-stability shift assay using rApaf-1 showed no changes in the stability of the protein over the range of temperatures I tested (Figure 5.11C). While I cannot exclude the possibility that PCP could bind Apaf-1, the data suggest that the target is cytochrome *c*, even though there are differences between the IC₅₀ and EC₅₀ values.

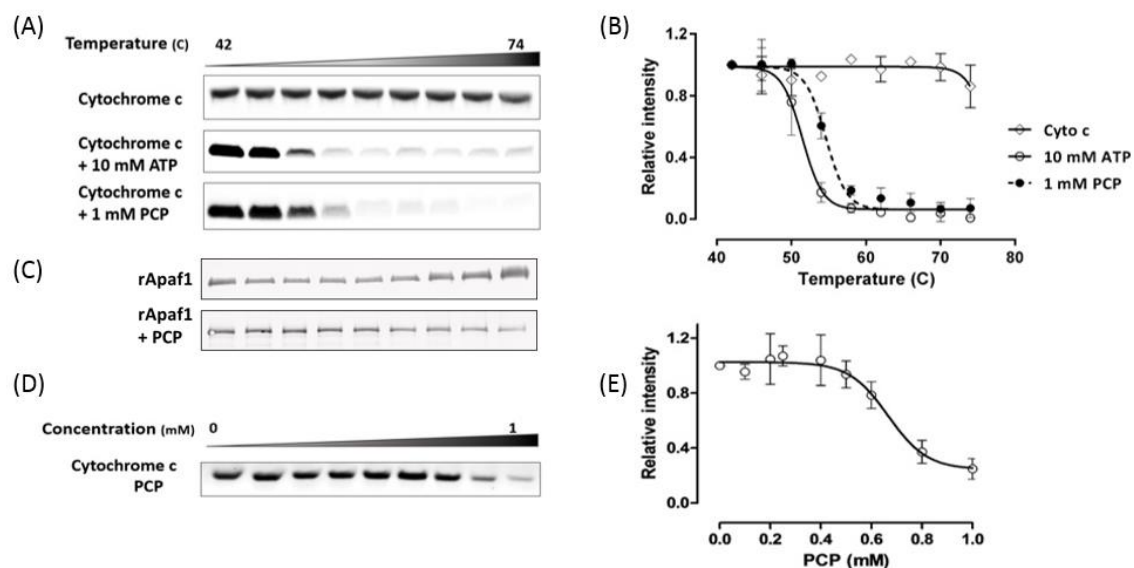


Figure 5.11. thermo-stability shift assay. (A) Cytochrome c alone and in the presence of 10 mM ATP (positive control) or 1 mM PCP incubated at different temperatures ranging from 42 to 74°C for 7 min. The samples were spin down, and the supernatant was loaded on SDS-PAGE. (B) The experiment repeated three times and the intensity of the bands quantified. Error bars are mean \pm SEM (n=3). (C) PCP-treated rApaf-1 detected by immunoblotting. (D) Titration of PCP over different concentrations ranging from 0 to 1 mM. This SDS-PAGE gel is a random selection of three separate experiments. (E) The experiment repeated three times and the intensity of the bands were quantified. Error bars are mean \pm SEM (n=3).

5.8 Binding of PCP-treated cytochrome *c* to rApaf-1

The gel filtration experiment showed that PCP affected Apaf-1 oligomerization and the thermos-stability shift assay showed that PCP bound to cytochrome *c*. I therefore examined whether PCP prevented cytochrome *c* from binding Apaf-1 using a co-precipitation assay. His-tagged Apaf-1 was used, which allowed precipitation using Ni²⁺ agarose beads.

First, the precipitation conditions were optimised to minimize non-specific binding of cytochrome *c* to the beads by titrating the salt concentration of the buffer. 120 mM NaCl prevented almost all non-specific binding to the beads (Figure 5.12A, B). To test if this salt concentration affected apoptosome formation, caspase-3 activity was measured. 120 mM NaCl did not affect Cc/dATP-mediated caspase-3 activation, although it reduced the basal level of activity (Figure 5.12C).

Then co-precipitation performed using Ni beads and the sample immunoblotted by anti-Cytochrome *c* and anti Apaf-1 antibodies. Cytochrome *c* was detected in supernatant when treated or not with PCP, although PCP-treated cytochrome *c* is lower than untreated (lane 1 and 2 in figure 5.13A). The same pattern was observed when PCP- or DMSO-treated cytochrome *c* added to rApaf-1 (lanes 4 and 5 in figure 5.13A). Cytochrome *c* still bound to Ni beads at low level, consistent with SDS-PAGE shown in figure 5.12. This level of cytochrome *c* was considered as a background. However, treatment with PCP, increased the cytochrome *c* in the pellet compared to the untreated (lanes 6 and 7). In the pellet, the level of rApaf-1 bound cytochrome *c* increased when treated with PCP (lanes 9 and 10). Therefore, the reduction of PCP-treated cytochrome *c* in the supernatant was consistent with increase in the pellet (Lanes 5 and 10). The ratio of cytochrome *c* to rApaf-1 in each reaction was calculated to see what proportion of cytochrome *c* bound to rApaf-1. Incubation with PCP increased the ratio by ~ 3-folds (Figure 5.13B). It seems that PCP did not block the interaction of cytochrome *c* and rApaf-1. However, it seems that PCP increased the affinity of cytochrome *c* to Ni beads probably by inducing some conformational changes in cytochrome *c*. PCP-bound cytochrome *c* can bind to Apaf-1,

however, structural changes may influence the appropriate function of cytochrome c in activating Apaf-1.

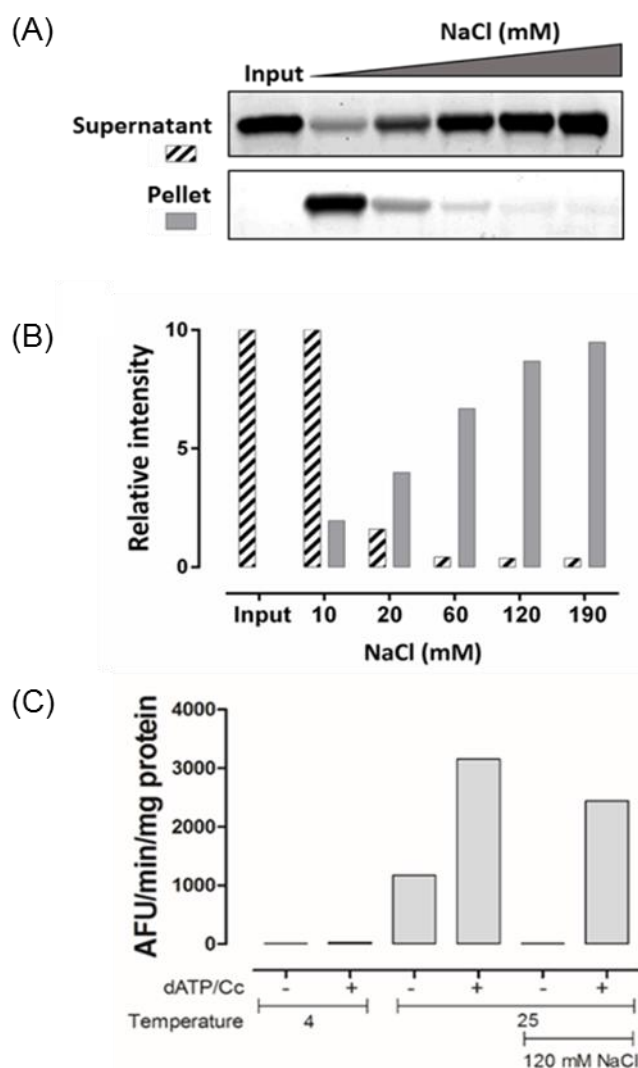


Figure 5.12. Optimization of co-precipitation assay condition. (A) 1 mg/mL cytochrome c was incubated with Ni beads at different concentrations of NaCl (10, 20, 60, 120 and 190 mM) and the ability of the cytochrome c to bind to resins was tested by SDS-PAGE. Supernatant shows the soluble cytochrome c and Pellet shows the Ni-bound cytochrome c. (B) Quantification of the SDS-PAGE band intensities. (C) Caspase activity at the high NaCl concentration (120mM) does not seem to affect the caspase activity. (D) Immunoblotting of the rApaf-1, cytochrome c when treated by PCP. For each reaction ~300 ng rApaf-1 mixed with PCP- or DMSO-treated cytochrome c and dATP at final concentration of 1.6 μ M and 1 mM, respectively.

Gel filtration studies showed that PCP caused a shift in the size of rApaf-1s which could be due to formation of the smaller complexes than the wild-type or unfolding and partially denaturation of monomer rApaf-1. TSA and co-precipitation assay showed that PCP bound to cytochrome c and PCP-bound cytochrome c can bind to Apaf-1. However, it is still not clear whether the smaller complex is formed or PCP-treated cytochrome c binds to Apaf-1 with different stoichiometry. The latter is possible since PCP induce conformational changes (increasing the affinity to Ni beads).

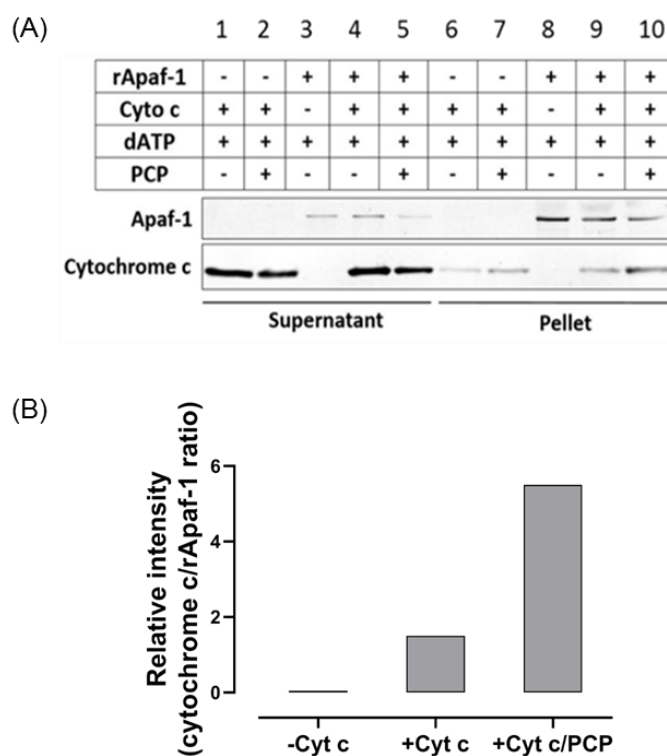


Figure 5.13. Co-precipitation of PCP-bound cytochrome c to rApaf-1. (A) Immunoblotting of the supernatant and pellet. (B) Intensities of the bands were quantified and the ratio of cytochrome c to rApaf was calculated. The ratio of cytochrome c to rApaf-1 increased by 3.7-fold.

5.9 Modelling the binding of PCP to cytochrome c

To get the idea of how PCP interacts to cytochrome c, I did the molecular docking. Four binding sites were recognized on cytochrome c (Figure 5.14).

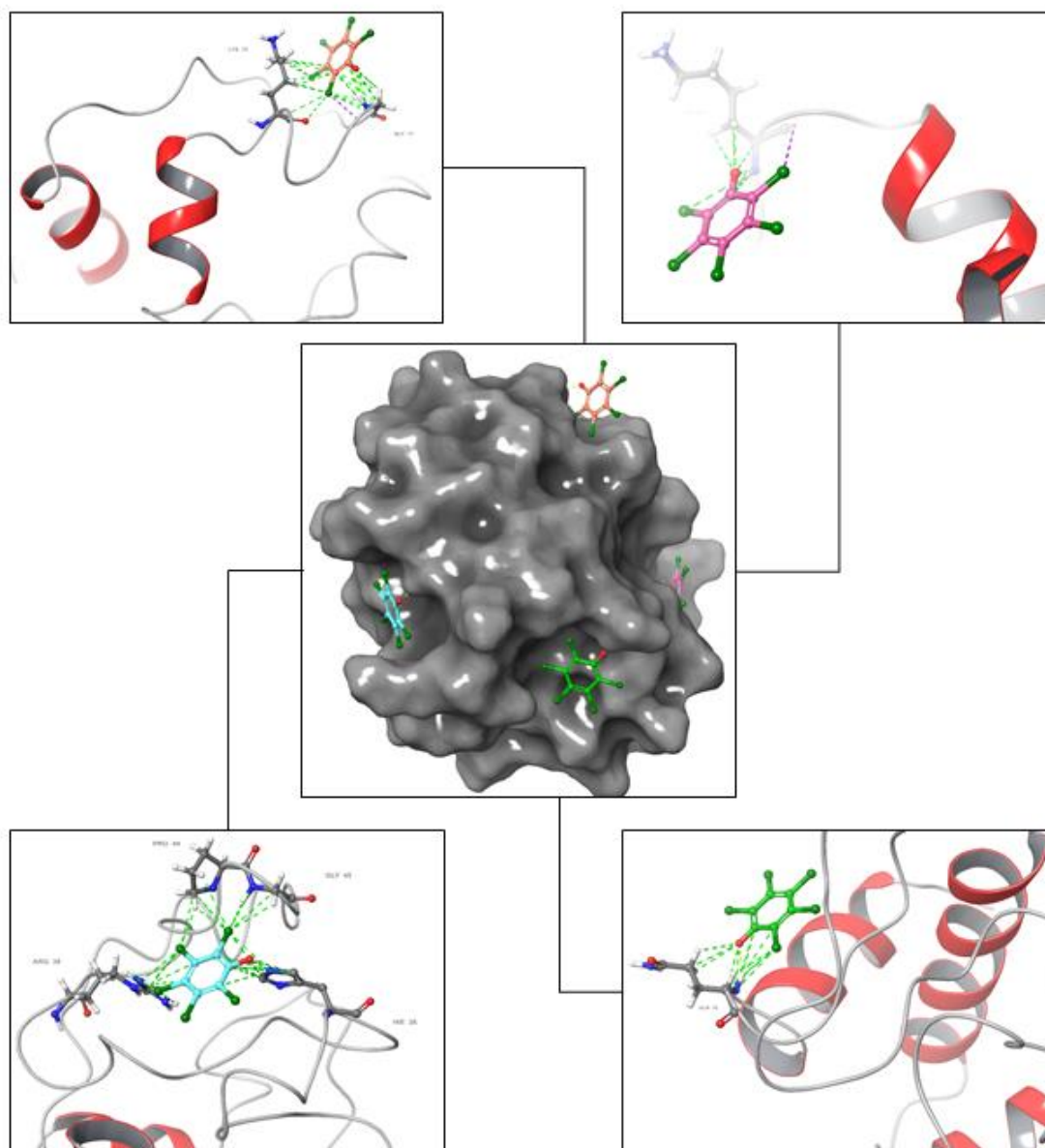


Figure 5.14. Docking of PCP into cytochrome c. The panel in the middle shows how PCP may bind to the defined pockets on the surface area. In each case, the key residues involved in the interactions have been shown in the zoomed box. Halogen bonds are in purple dashed line and hydrogen bonds are in yellow dashed line. Green lines show the good contacts/clashes.

PCP can interact to Lys 72 and Gly 77 (Figure 5.14, upper left), Lys 86 (Figure 5.14 upper right), Gln 16 (Figure 5.14, lower right), HIE 26, Gly 45, Pro 44 and Arg 38 (Figure 5.14, lower left). Based on the docking scores, it seems that interaction to Gln16 is the most favorable binding where Gln16 functions as a donor of hydrogen bond. In this model, four out of five Cl groups are exposed to solvent (Figure 5.15).

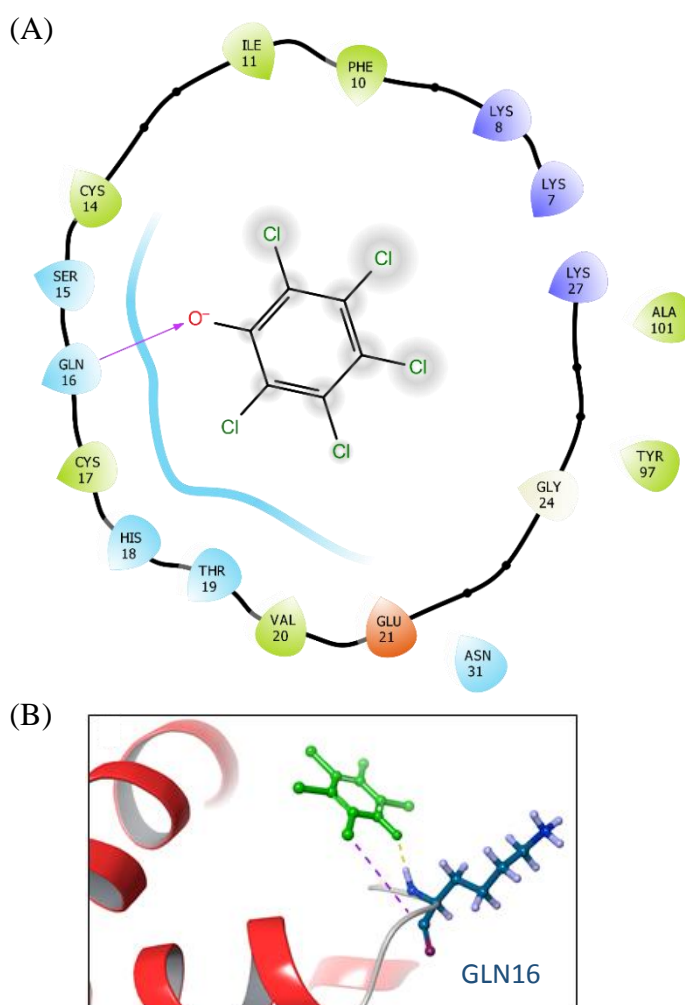
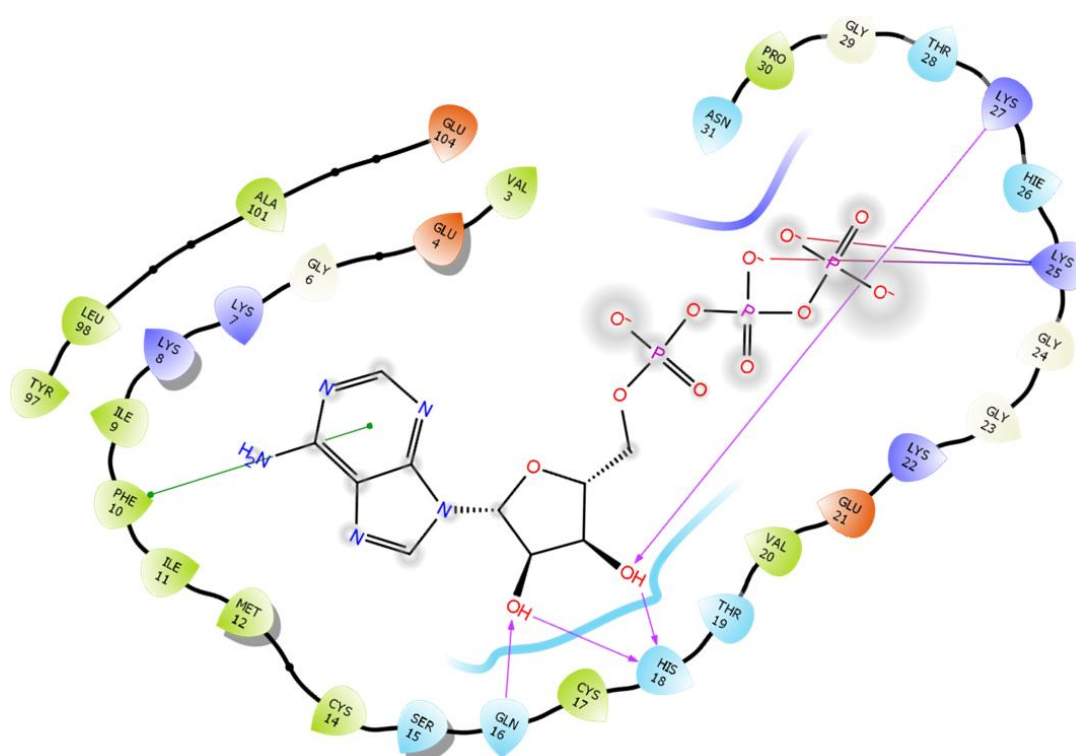


Figure 5.15. PCP docking to cytochrome c. (A) 2D representation of the PCP interactions with the cytochrome c. (B) zoom-in view of the best docked PCP with the involved amino acid residues and interactions. Yellow dashed lines represent the hydrogen bond.

ATP has been shown to block the apoptosome formation with an unknown mechanism. To gain a better insight into the mechanism by which ATP binds to cytochrome c, docking of ATP to cytochrome c was performed. The best docking score obtained when ATP interacted to Lys 25, Lys 27, His 18 and Gln 16. Lys 25 and Lys 27 make salt bridge and hydrogen bonds respectively with O in phosphate group and OH of ribose. His 18 and Gln 16 also plays role as acceptor and donor of hydrogen bond respectively. Phe 10 and the adenine group make Pi-Pi stacking force (Figure 5.16).

(A)



(B)

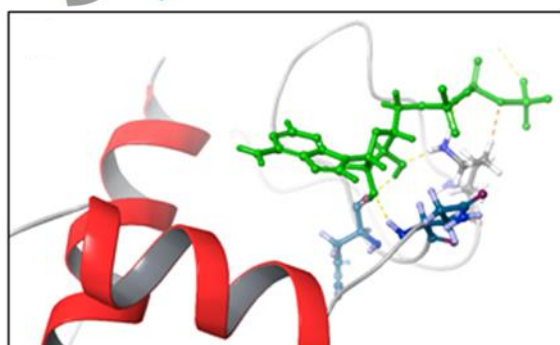


Figure 5.16. ATP docking to cytochrome c. (A) 2D representation of the ATP interactions with the cytochrome c. (B) zoom-in view of the best docked ATP with the involved amino acid residues and interactions. Yellow dashed lines represent the hydrogen bond. (C)

PCP is an organochlorine compound that is toxic. I previously confirmed experimentally that PCP inhibited apoptosis by directly targeting cytochrome c. However, PCP derivatives may have the same effect and need to be studied. Here, I studied the docking of PCP derivatives to cytochrome c. PCP derivatives are different in the number of chlorines (Figure 5.17). PCP derivatives, common names, IUPAC names and the structures are listed below:

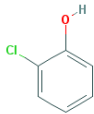
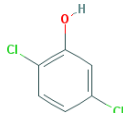
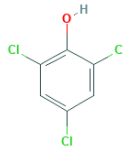
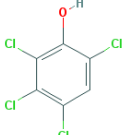
Common names	IUPAC names	structures
Monochlorophenol	2-chlorophenol	
Dichlorophenol	2,5-Dichlorophenol	
Trichlorophenol	2,4,6-Trichlorophenol	
Tetrachlorophenol	2,3,4,6-Tetrachlorophenol	

Table 5.1. Structure, common and IUPAC names of PCP derivatives.

Table 5.2 shows the docking scores when PCP and its derivatives tested against cytochrome c. It seems that none of the PCP derivatives is as efficient as PCP in binding to cytochrome c, although the docking scores for PCP and TCP are very close and probably TCP may have the similar binding affinity to cytochrome c.

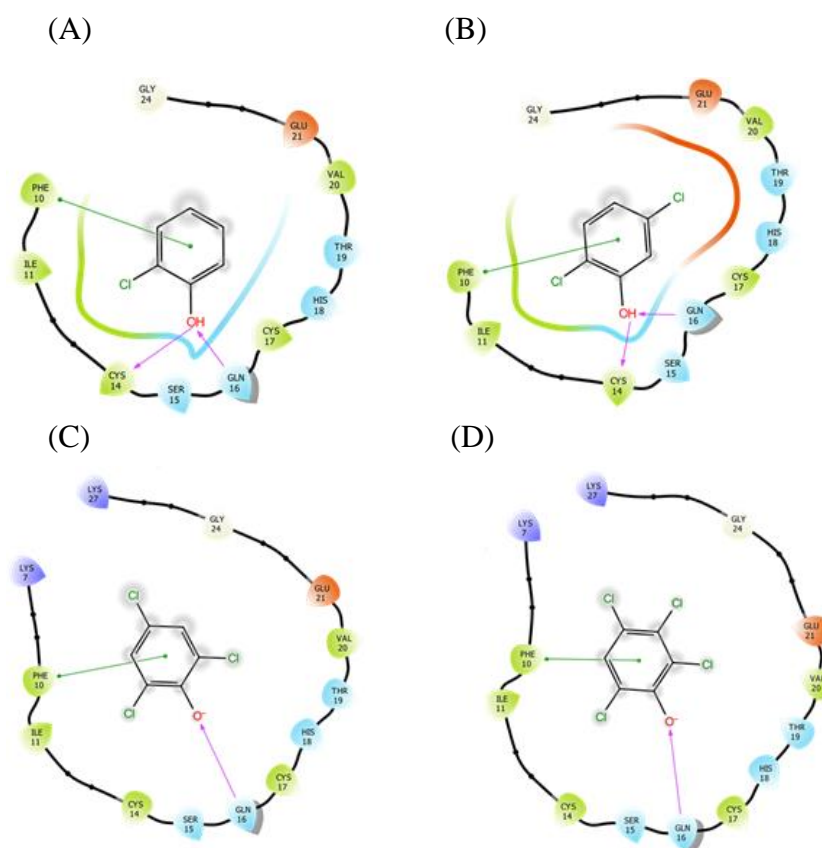


Figure 5.17. Docking of the PCP derivatives into cytochrome c. 2D interactions of (A) monochlorophenol, (B) dichlorophenol, (C) trichlorophenol, (D) and tetrachlorophenol with cytochrome c.

<i>Compounds</i>	<i>Docking scores</i>
PCP	-4.065
TCP	-4.017
TriCP	-3.904
DCP	-3.296
MCP	-3.316

Table 5.2. Docking scores for PCP and its derivatives.

5.10 Discussion

PCP was identified as an inhibitor of apoptosome. I showed that PCP primarily targets cytochrome c. It seems that PCP-bound cytochrome c can bind to Apaf-1 by a different stoichiometry. However, split luciferase showed that PCP can inhibit split luciferase activity even after induction of apoptosome formation. This is consistent with the shift observed in TSA for PCP treated sample in comparison with the vehicle control. This suggests that PCP can bind to both cytochrome c and Apaf-1.

PCP is a chemical that is mainly used in wood industry for maintenance and preservation of wood products. PCP showed the lowest IC_{50} value ($\sim 170 \mu\text{M}$) for both caspase and luciferase activity of all the toxicants tested here. Epidemiological studies report that the low-level contamination ($< 70 \text{ ppb}$) can be found in general population that is far below the levels that inhibits apoptosome formation. However, occupational exposures include plasma levels as high as 0.319 mM (Cline et al., 1989), or approximately twice PCP's IC_{50} in the apoptosome assay. In addition, animal studies show that PCP causes testicular atrophy and reduces spermatid numbers and male fertility (Beard et al., 1999). The importance of Apaf-1 in spermatogenesis, together with the data presented here, suggests that inhibition of Apaf-1 may contribute to PCP's reproductive toxicity.

However, PCP also acts to uncouple respiration. Other uncouplers such as 2,4-dinitrophenol, dinoseb, and 4,6-dinitro-o-cresol also affect sperm viability at concentrations of $\sim 10^{-5}$ – 10^{-4} M . The severity of the effect on sperm correlates with chemical's ability to uncouple respiration (Takahashi, 2003) and the IC_{50} for PCP uncoupling respiration is $\sim 5 \times 10^{-6} \text{ M}$ (Weinbach and Garbus, 1965), a concentration approximately 30-fold lower than that required to inhibit apoptosome formation. Thus, while PCP inhibits apoptosome formation, this probably makes only a minor, if any, contribution to the reproductive toxicity of PCP *in vivo*.

**NS3694 AND M50054
PREVENT APOPTOSIS
BY DIFFERENT
MECHANISMS**

6.1 NS3694, an apoptosome inhibitor

NS3694 is a diarylurea compound that inhibits apoptosome formation. NS3694 was identified by screening a nonpeptide small-molecule library using *in vitro* apoptosome activation system (Lademann et al., 2003). NS3694 does not directly inhibit caspase-3 and -9 activity, at least at the concentrations tested ranging from 25 up to 100 μ M. NS3694 inhibits the formation of ~700 KDa apoptosome complex but does not interfere with formation of the 1.4 MDa inactive apoptosome. NS3694 also blocks the association of caspase-9 to the apoptosome (Lademann et al., 2003). I used NS3694 as a tool compound to validate the split luciferase assay, however, neither the mechanism by which NS3694 acts nor its target is known. Having established that PCP prevented apoptosome formation most likely by binding to cytochrome c, I investigated whether NS3694 was acting by a similar or different mechanism.

6.1.1 NS3694 prevents the formation of a functional apoptosome

I showed in chapter 3 that NS3694 inhibits apoptosome formation (using split luciferase assay) and caspase activity with the IC_{50} of ~170 μ M. Here, I showed that split luciferase activity was completely abolished when the mixture of S100 extract expressing Nluc-Apaf-1 and Cluc-Apaf-1 pre-incubated with 1 mM NS3694 (Figure 6.1A, top panel). As expected, caspase-3 like activity was also blocked (Figure 6.1A, bottom panel). Immunoblotting for procaspase-3 and procaspase-9 showed fully inhibition of caspase-3 and -9 processing (Figure 6.1B). Then I tested whether NS3694 inhibited the split-luciferase activity directly by first inducing apoptosome formation with Cc/dATP and then adding NS3694. When extracts were incubated with Cc/dATP for 15 min at 25°C before addition of 1 mM NS3694 split luciferase and caspase-3 like activities as well as the processing of procaspase-3 and procaspase-9 were unaffected (Figure 6.1C, D). These experiments showed that NS3694 prevents split luciferase activity only if added before the formation of the apoptosome. Consistent with earlier reports, NS3694 does not directly block caspase activity.

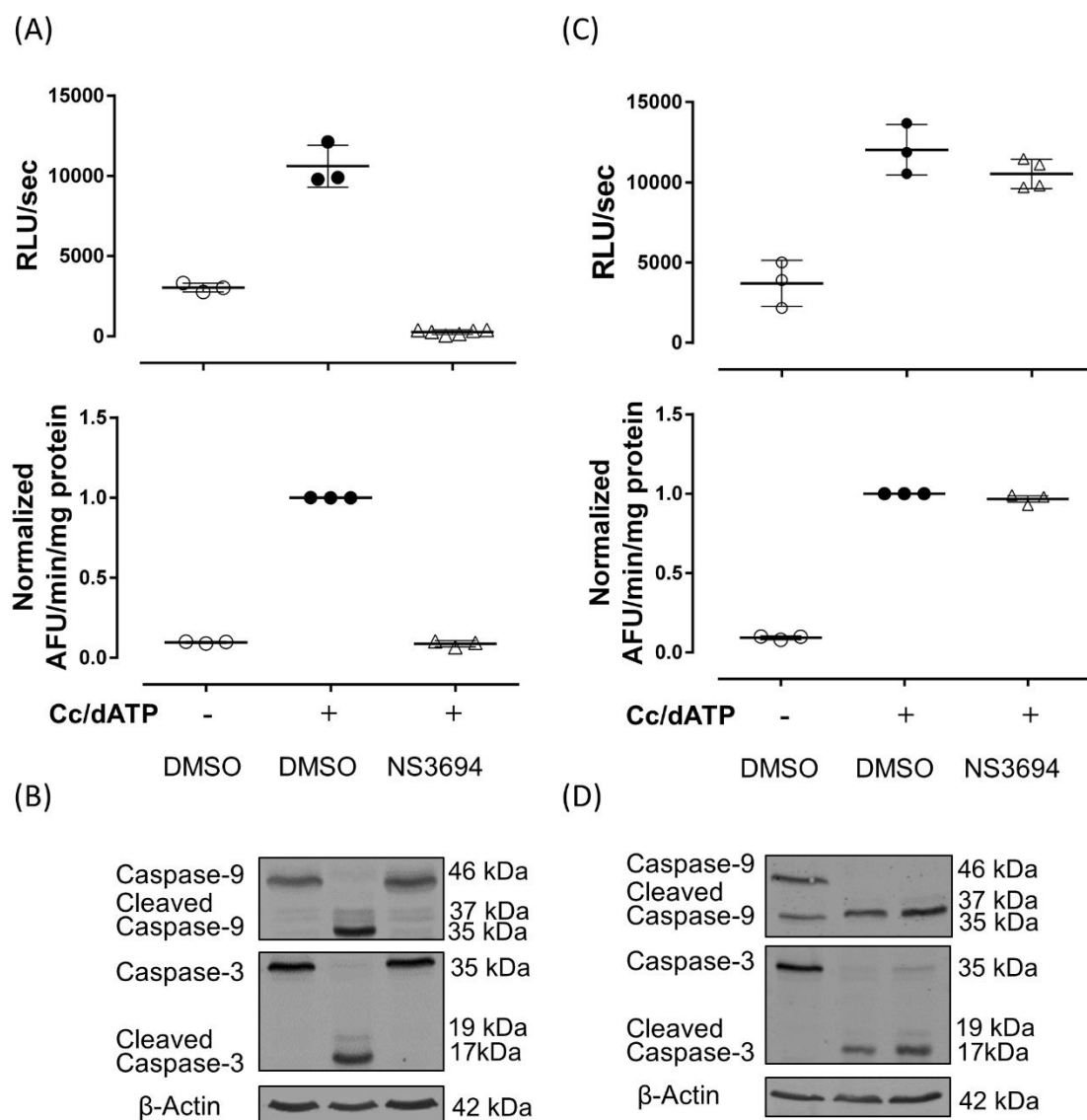


Figure 6.1. NS3694 inhibits split luciferase and caspase-3 activity. (A) Split luciferase (top panel) and caspase-3 activity (bottom panel) are completely abolished when the mixture of extracts expressing Nluc-Apaf-1 and Cluc-Apaf-1 pre-incubated with 1 mM NS3694. (B) Immunoblotting shows the inhibition of caspase-9 and -3 processing. (C) Split luciferase and caspase activity are not inhibited when 1 mM NS3694 is added 15 min after induction of apoptosome formation. (D) Immunoblotting shows the processing of caspase-9 and -3 in the same condition as in (C).

6.1.2 NS3694 induced the formation of an inactive high molecular weight Apaf-1 complex

I showed that NS3694 inhibit the split luciferase activity when incubated with the extracts expressing Nluc-Apaf-1 and Cluc-Apaf-1. However, it was not clear whether pre-treatment with 1 mM NS3694 stops the oligomerization of Apaf-1 or it induces the formation of a non-functional complex. To answer this question I performed gel filtration chromatography to determine the effect of NS3694 on Cc/dATP-induced oligomerization of Apaf-1.

In the absence of NS3694, addition of cytochrome c and dATP to the cell extract induced the formation of a ~700 kDa complex (Figure 6.2). However, pre-treatment with 1 mM NS3694 also led to the formation of a complex at ~700 kDa (Figure 6.2). It has been reported before that in THP-1 cell extract, NS3694 forms inactive 1.4 MDa complex. The complex detected here may be the 1.4 MDa complex, but due to the limited resolution of the chromatography column in the range 700 kDa – 1.4 MDa, it is not clear what size the NS3694 complex is. Nonetheless the data show that the complex cannot activate caspase-9 or caspase-3.

6.1.3 NS3694 prevents Apaf-1 from binding to cytochrome c

Apaf-1 binding to cytochrome c is required for apoptosome formation. To test whether NS3694 prevented Apaf-1 from binding to cytochrome c, co-immunoprecipitation experiment was performed. His-tagged Apaf-1 was pulled down using an anti-His-tag antibody then co-precipitation of cytochrome c was tested by immunoblotting. In the absence of NS3694, Cc/dATP induced caspase-3 activity and cytochrome c co-precipitated with Apaf-1 (Figure 6.3). However, NS3694 prevented both Cc/dATP induced caspase activity and co-precipitation of cytochrome c. These data suggest that NS3694 acts by preventing the interaction between Apaf-1 and cytochrome c, although these experiments do not reveal whether NS3694 binds Apaf-1, cytochrome c or some other protein.

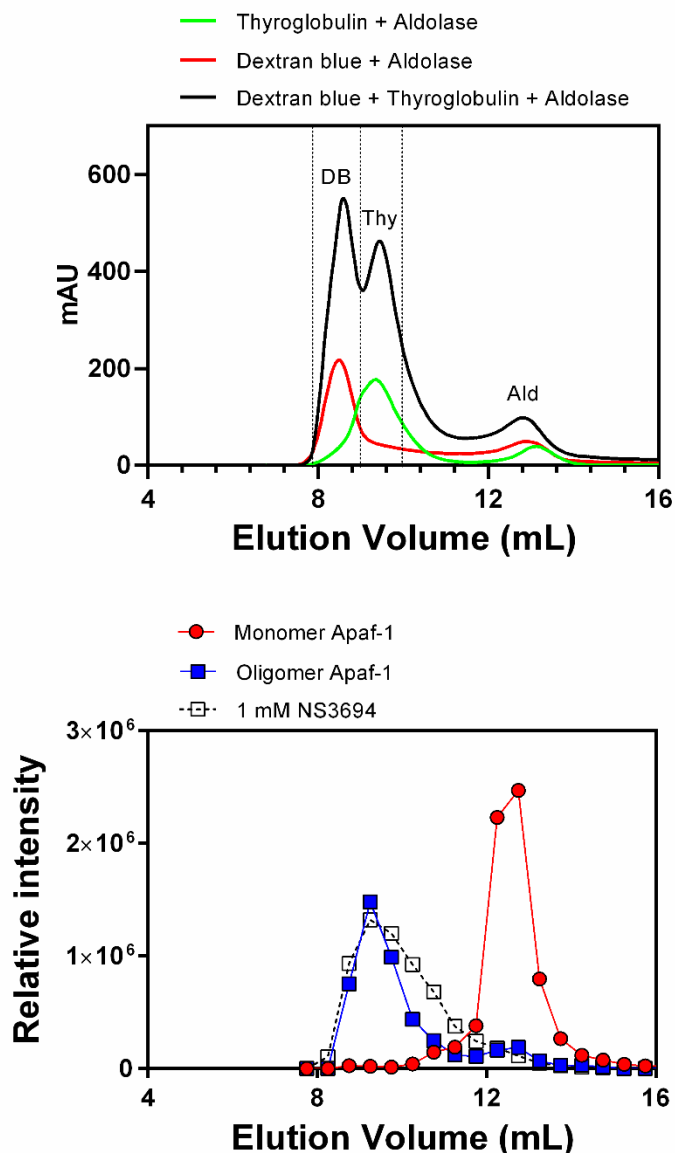


Figure 6.2. NS3694 forms a high molecular weight complex. Gel filtration of the NS3694-treated HEK293 extract. The extracts were loaded on the superdex 200 increase column, the fractions were collected and probed by anti-Apaf-1 antibody. Apaf-1 was detected in monomeric form and after addition of cytochrome c and dATP the proteins detected in the fractions related to the size of apoptosome. When incubation with 1 mM NS3694, Apaf-1 was detected in high molecular weight fractions (bottom panel). Dextran blue, Thyroglobulin and Aldolase were loaded on superdex 200 increase column as the markers (top panel).

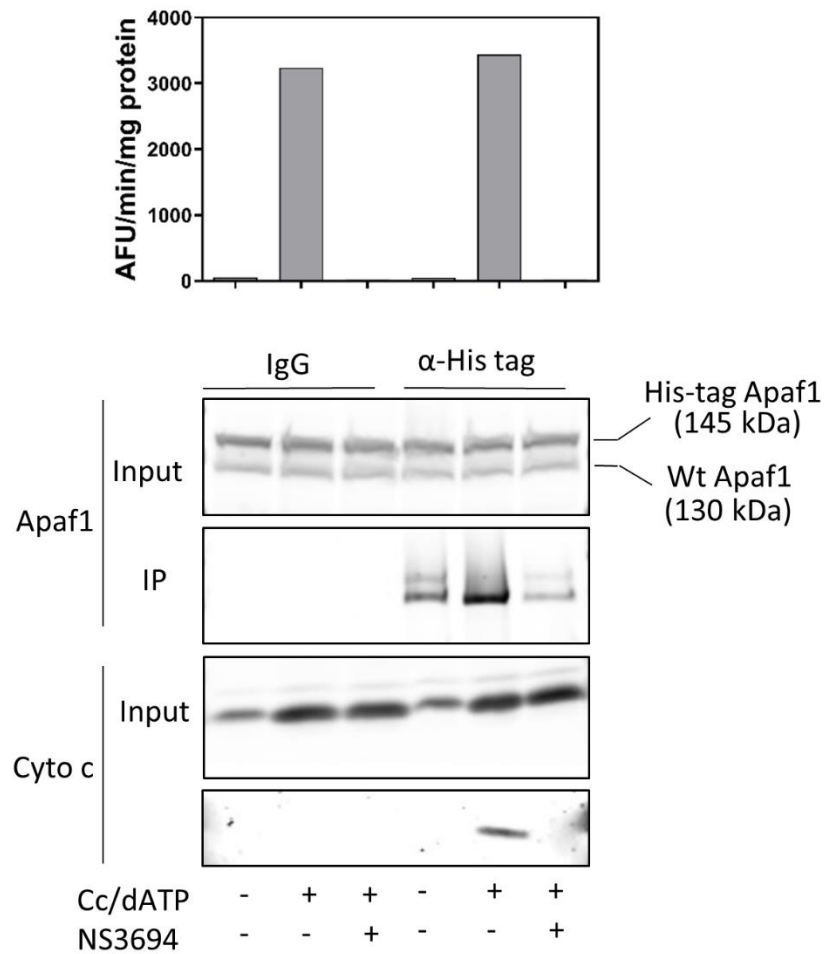


Figure 6.3. Co-immunoprecipitation of NS3694-treated cytochrome c with rApaf-1.

His-tagged Apaf-1 proteins were pulled down and association with cytochrome c was examined. Caspase activity of the input is shown (top panel). As expected, NS3694 abolished caspase-3 like activity completely. The immunoblotting of the samples using anti-Apaf1 and anti-cytochrome c (bottom panel).

6.1.4 NS3694 mainly targets cytochrome c

NS3694 blocks apoptosome formation, however, the real target is still unknown. I hypothesized that NS3694 may interact with either cytochrome c, monomeric Apaf-1, oligomeric Apaf-1, or an unknown protein or proteins in the cell extract.

The thermo-stability shift assay had proven useful when investigating the target for PCP. Therefore, I took a similar approach to investigate the target of NS3694. For this, I used purified cytochrome c and purified recombinant Apaf-1. Cytochrome c was incubated with 1 mM NS3694 at a range of temperatures and the stability of cytochrome c assessed by SDS-PAGE. 10 mM ATP was used as positive control. As I previously showed, cytochrome c was thermally stable even at 74°C. However, treatment with NS3694 clearly destabilized cytochrome c (Figure 6.4A).

I had previously established that the IC_{50} for inhibition of split luciferase activity and caspase-3 activation was ~170 mM. I therefore tested whether the EC_{50} for thermal destabilization of cytochrome c was similar to this value by titration of NS3694. This showed an EC_{50} of approximately 300 μ M, which is approximately twice that calculated for the split luciferase and caspase assay (Figure 6.4B). These data show that NS3694 can bind cytochrome c at concentrations that are relevant for inhibition of apoptosome formation, although the EC_{50} values and IC_{50} values differ.

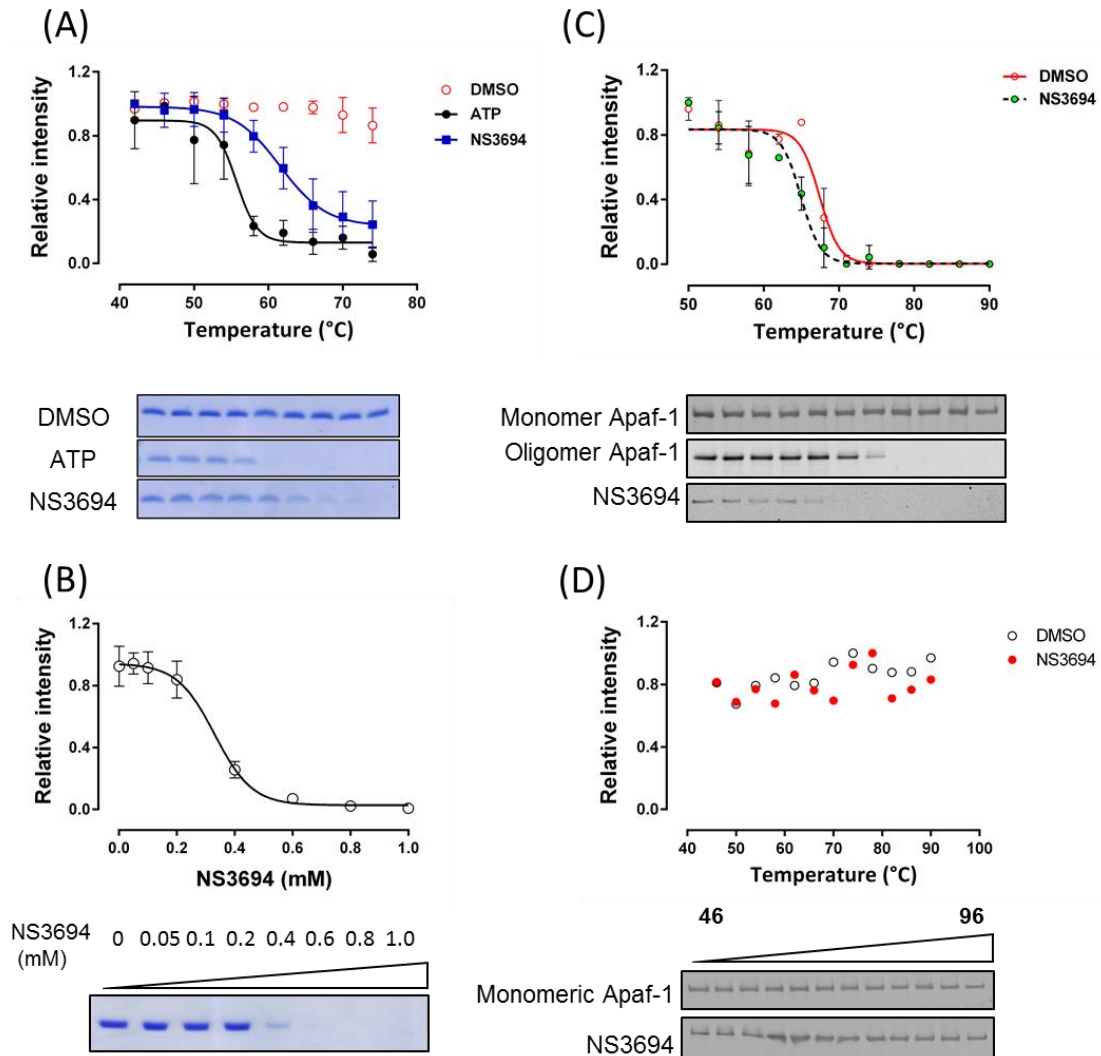


Figure 6.4. Thermo-stability shift assay. (A) Cytochrome c alone and in the presence of 10 mM ATP (positive control) or 1 mM NS3694 was incubated at different temperatures ranging from 42 to 74°C for 7 min. The samples spin down, and the supernatant was used in SDS-PAGE. The experiment repeated three times and the intensity of the bands quantified. Error bars are mean \pm SD. (B) Titration of NS3694 over different concentrations ranging from 0 to 1 mM. This SDS-PAGE gel is a random selection of three separate experiments. (C) *In vitro* reconstitution of apoptosome complex incubated with 1 mM NS3694. The experiment repeated three times and the intensity of the bands quantified. Error bars are mean \pm SD. (D) monomer rApaf-1 incubated or not with 1 mM NS3694.

I also tested the thermo-stability of Apaf-1. The thermo-stability shift assay using monomeric rApaf-1 (in the absence of dATP/Cc) did not show any changes in stability of the protein, suggested that NS3694 did not bind to monomeric Apaf-1 (Figure 6.4D). I also induced apoptosome formation *in vitro* using rApaf-1, cytochrome c and dATP, and tested the effect of 1 mM NS3694 on the thermo-stability of Apaf-1 in the apoptosome. Oligomeric Apaf-1 was less thermally stable than monomeric Apaf-1, which is consistent with wide ranging conformational changes in Apaf-1 that occur during apoptosome formation. Addition of NS3694 to the apoptosome produced a small shift in Apaf-1 thermo-stability (Figure 6.4C). To examine whether this small shift is significantly different to wild-type, I titrated NS3694 at 65°C. However, I failed to detect any changes in the thermostability of apoptosome. This assay is probably not sensitive to reveal a small change in thermostability of oligomeric Apaf-1 (data not shown).

It is hard to be sure of the significance of this small change. Based on the thermo-stability studies, here cytochrome c is a target for NS3694 at relevant concentrations of NS3694. At 1 mM NS3694 produced only a small change in Apaf-1 thermo-stability, but only in the context of the apoptosome. Thus, while NS3694 may bind Apaf-1 under some circumstances, the most relevant interaction appears to be with cytochrome c.

6.1.5 NS3694 interferes with the recruitment of caspase-3 to the apoptosome

It has been shown that low concentrations of NS3694 (up to 100 μ M) does not directly inhibit caspase-3. However, the higher concentrations, like the concentration that kills the cells or bind to cytochrome c, were not tested. Time point measurements of caspase-3 like activity showed that ~ 50% of caspase-3 activity is achieved during the first 5 min after addition of Cc/dATP, while caspase-9 is still being processed (Figure 6.5A, B).

As I showed before, 15 min incubation give rises to the maximum caspase-3 like activity and addition of 1 mM NS3694 does not show changes in the caspase activity (Figure. 6.5C). Immunoblotting also showed that caspases were active to similar level to the control. This was expected, because after 15 min incubation all caspases were processed and apoptosome is not required afterward.

We hypothesized that if NS3694 binds to apoptosome before fully activation of all caspases, then we would detect reduction in caspase activity. Therefore, NS3594 was added to the S100 extract 5 minutes after *in vitro* activation of the extract. Caspase-3 activity reduced by 70% (white bar) in NS3694-treated extract. Even 10 min further incubation did not rescue the inhibitory effect of NS3694 (hatched bar) (Figure 6.5C).

Immunoblotting the caspase-9 and -3 showed that caspase-9 is processed at the similar level as vehicle control. However, NS3694 blocked the formation of p35 of caspase-3. Considering the possibility of NS3694 binds apoptosome complex (showed by TSA), NS3694 may interact to apoptosome and reduce the recruitment of caspase-3. This suggests that some conformational changes take place in the apoptosome that is different to wildtype apoptosome, which affects the recruitment of caspase-3. This NS3694-bound apoptosome does not affect caspase-9 processing, as almost all caspase-9 molecules are processed in 5 min (lane 3, 5 and 7).

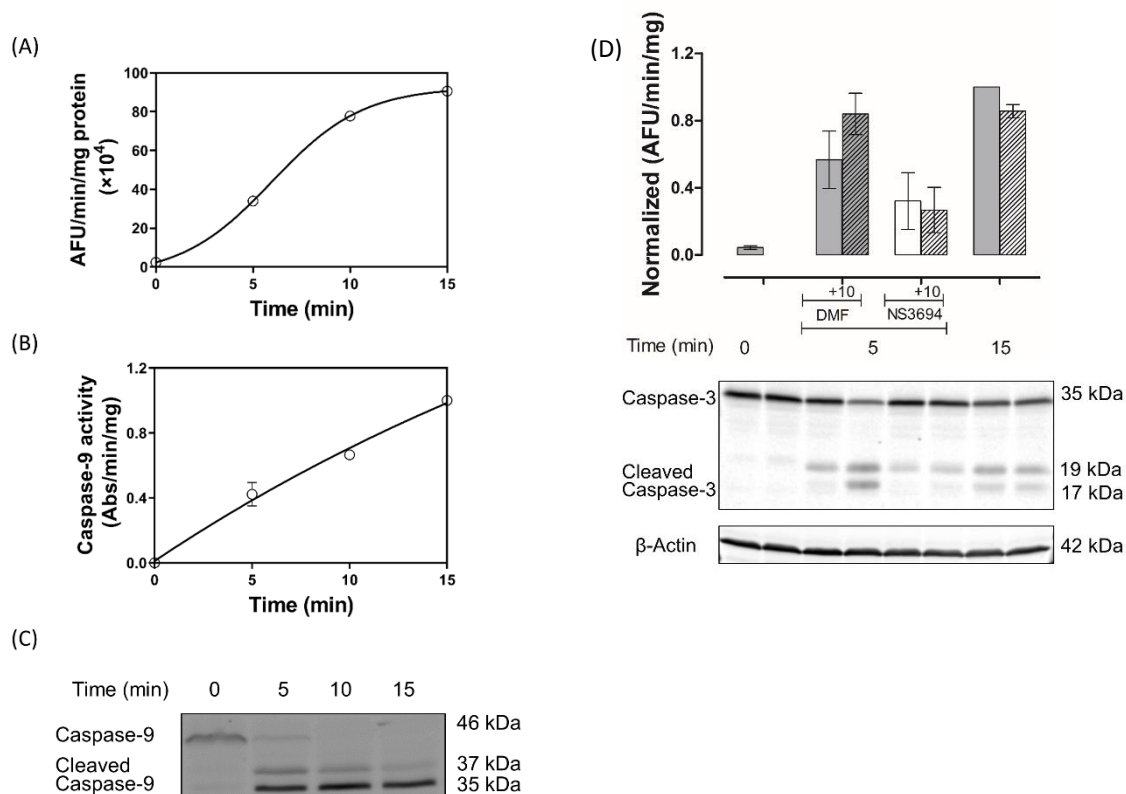


Figure 6.5. NS3694 reduces the rate of caspase-3 activation when added early after apoptosome formation. (A) Time course caspase-3 activation. The rate of caspase-3 activation was measured by incubating HEK293 S100 extract at 25°C for 0, 5, 10 and 15 min. (B) Caspase-9 activity was also measured as in (A). Caspase-9 immunoblotting shows the fully processing of procaspase-9 after 15 min. (C) caspase-3 like activity of the extracts treated with 1 mM NS3694 at different time points during caspase activation. Treatment with 1 mM NS3694 5 min after incubation with Cc/dATP slows down the rate of caspase activation. However, 15 min after incubation with 1 mM NS3694, it does not change the activity of caspase-3. Error bars are mean \pm SD.

6.1.6 NS3694 kills the cells

Others have shown that NS3694 inhibited apoptosis and suggested that NS3694 could be a lead molecule in the development of therapeutics that target Apaf-1. The molecular target was not identified, and I have shown earlier that NS3694 preferentially targeted cytochrome *c*. Apaf-1 is not essential for cell viability but cytochrome *c* is a key component of respiratory chain which contributes in energy production and the maintenance of cell viability. I was therefore interested to test if NS3694 affected cell viability.

First, HT1080 cells treated with different concentrations of NS3694 ranging from 25 μ M to 1 mM and the cell death was measured using Hoechst 33342 and 7-AAD staining (Figure 6.6). NS3694 kills the cells with IC_{50} of ~ 300 μ M. Interestingly, the IC_{50} is very close to that of cytochrome *c* binding and caspase-3 inhibition. We reasoned that the cytotoxicity of NS3694 could be due to interaction to cytochrome *c* and interference with respiratory chain.

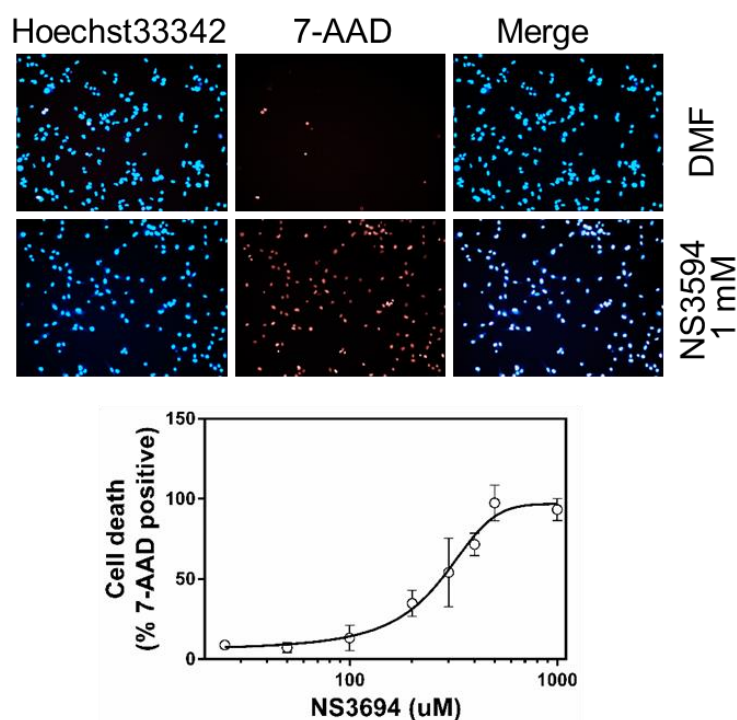


Figure 6.6. Cell death in NS3694-treated cells. HT1080 cells treated or not with a range of NS3694 concentrations from 25 μ M to 1 mM for 1 hour. The cells were stained by Hoechst 33342 and 7-AAD and the percentage of 7-AAD positive cells was calculated. Error bars are mean \pm SD.

While NS3694 is cytotoxic and kills the cells at high concentrations ($EC_{50} \sim 300 \mu\text{M}$), at low concentrations NS3694 inhibits the caspase activity and rescues cells from staurosporin-induced apoptosis (Lademann et al., 2003). I found that low concentrations of NS3694 (25 and 50 μM) did not induce cell death. To check the ability of low NS3694 concentrations to prevent cell death HeLa cells were treated with etoposide at a range of concentrations (1-250 μM) in the presence of 25 and 50 μM NS3694 before measuring cell viability (Figure 6.7). After 24 hours, NS3694 did not rescue the etoposide-treated cells.

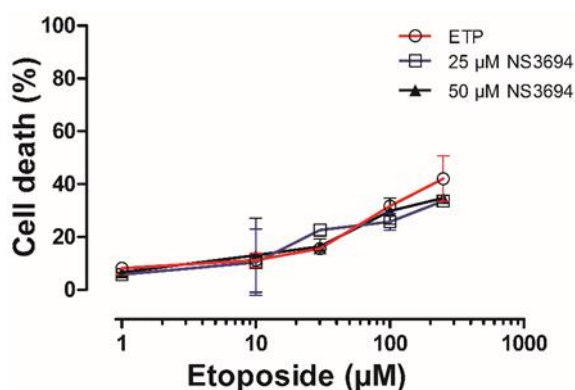


Figure 6.7. NS3694 does not rescue etoposide-induced death. The HeLa cells pre-treated with low doses of NS3694. After 1 hour, cells were treated with a range of etoposide concentrations and incubated for 24 hours. Cell death was measured using Alamar blue.

Then we sought to further investigate if mitochondrion is involved in cytotoxicity of NS3694. The cells incubated with TMRE; Tetramethylrhodamine ethyl ester is a cell-permeant fluorescent dye that is sequestered by active mitochondria. HT1080 cells incubated with different concentrations of NS3694. Then the cells stained with 200 nM TMRE for 30 min and the active mitochondria were tracked by fluorescence microscopy. NS3694 caused a large reduction in cell number, consistent with the induction of cell death. In the surviving cells the intensity of TMRE was obviously reduced by the treatment with NS3694 (Figure 6.8).

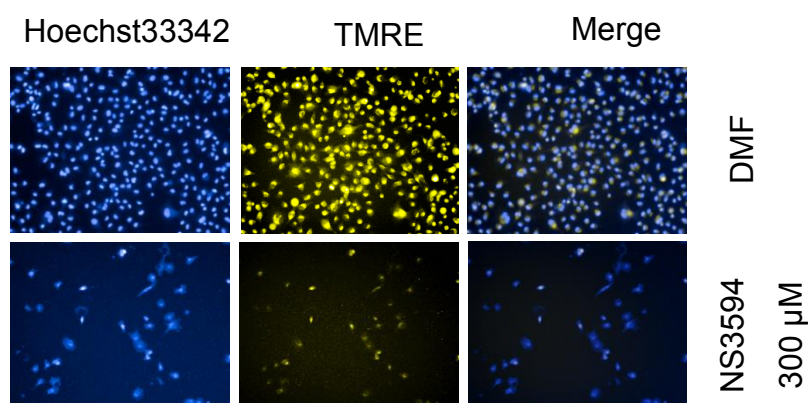


Figure 6.8. TMRE staining of the NS3694-treated HT1080 cells. The cells stained with 200 nM TMRE for 30 min before treatment with 300 μ M NS3694. The cells were washed with fresh media three times to remove the residual stain. It seems that the intensity of TMRE is lower than that of vehicle control.

6.1.7 Treatment with NS3694 reveals the shrinkage and condensation of the nuclei

To better visualize NS3694-induced cell death, I used HeLa cells expressing GFP-tagged H3B to label the nucleus and mCherry-tagged tubulin to label the cytoplasm in live cells. First, I studied the morphology of the nucleus when the cells treated by NS3694. The nuclei were monitored using fluorescence microscopy. Imaging was performed either immediately after treatment with 1 mM NS3694 (Figure 6.9A, top panel) or after 60 min (Figure 6.9A, bottom panel). The size of the nuclei was smaller, and the green fluorescence was more intense after 60 minutes treatment with 1 mM NS3694 (Figure 6.9).

Treatment with 1 mM NS3694 led to 2-fold increase in intensity/area ratio of green fluorescence, which suggests nuclear shrinkage and chromatin condensation. This finding is consistent with the nuclear 7-AAD staining mentioned earlier. Together, these data suggest a rapid (within 60 minutes) permeabilization of the plasma membrane accompanied by nuclear shrinkage and chromatin condensation.

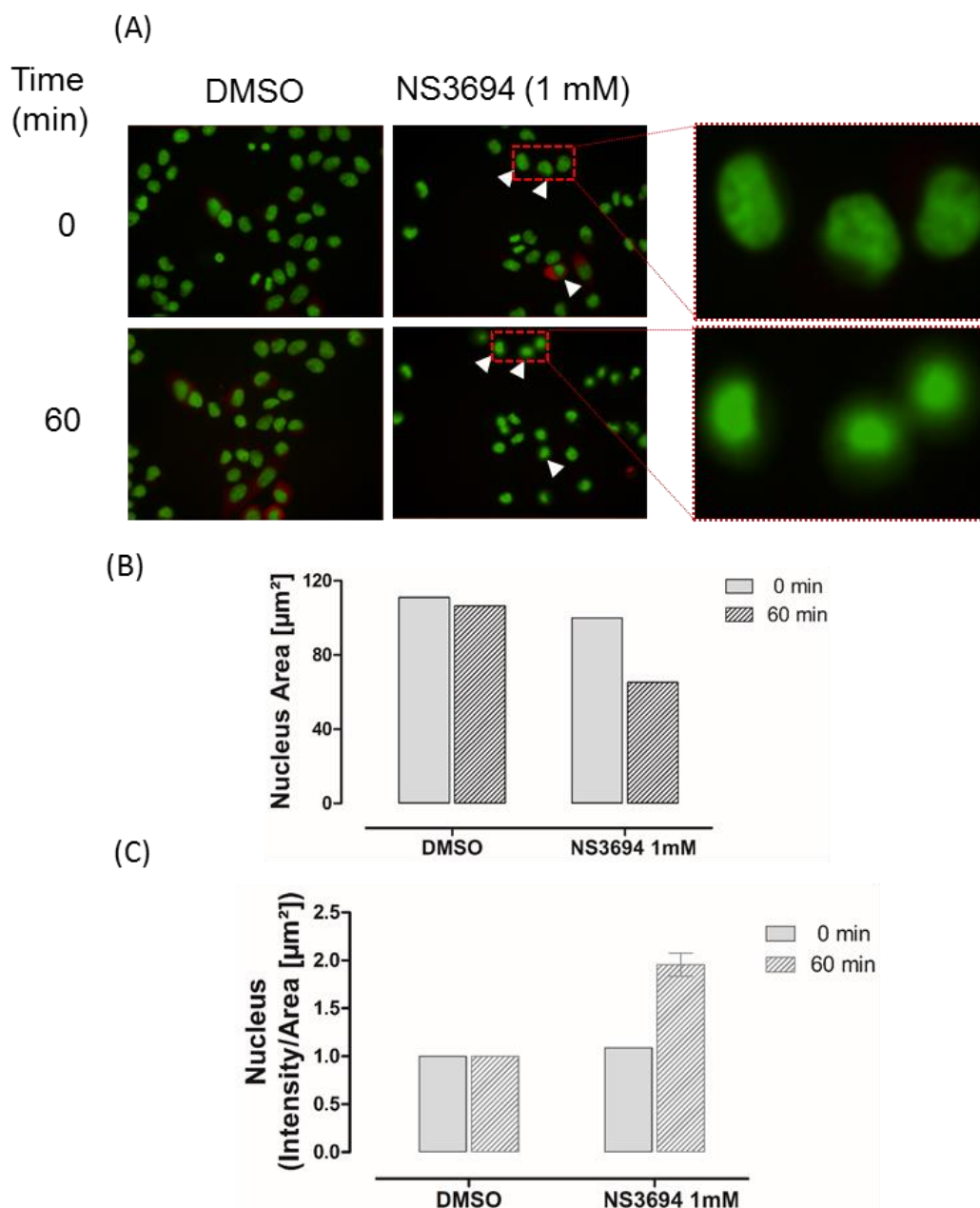


Figure 6.9. Nuclei morphology of the NS3694-treated cells. (A) HeLa cells expressing GFP-tagged H3B treated with 1 mM NS3694 and the morphology of the nuclei was studied using fluorescence microscopy. The cells were imaged either immediately after addition of the NS3694 or 60 min post-treatment. The white arrows show the same nuclei at the starting point and after 60 min. (B) The sizes of the nuclei were measured using Harmony 3.2 software. The nuclei are smaller in the NS3694-treated cells. (C) The intensity of the GFP was calculated in the nuclei and normalized to the size of the nuclei. The intensity of the NS3694-treated nuclei are 2 times more than the vehicle controls and NS3694-treated one at starting point.

6.1.8 NS3694 kills the cells by rapidly inducing necrosis

To get a better idea of the type of death that NS3694 induces, I treated the HeLa cells with 1 mM NS3694 and tracked the behaviour of the live cells. PI was added to the cell culture a few minutes before treatment with 1 mM NS3694. The cells were intact and showed a normal morphology and low PI staining at time = 0 minutes. However, within 40 minutes the nuclei of almost all NS3694-treated cells were PI-positive, with marked PI staining of the nucleoli. The ratio of red to green largely increased in the nuclei of NS3694-treated cells (Figure 6.10). Treating the cells with lower concentration of NS3694 (300 μ M) also showed the very similar result (data not shown).

In addition, tubulin filaments labelled with mCherry were degraded in NS3684-treated cells. These degradation was detected as formation of the holes in tubulin filaments (Figure 6.10). These changes are not consistent with apoptotic cell death and instead resemble necrosis. Whether NS3694 is inducing a regulated necrosis remains to be established. However, these data suggest that the earlier reports that NS3694 blocked apoptosis are probably explained by NS3694 rapidly inducing a caspase-independent cell death.

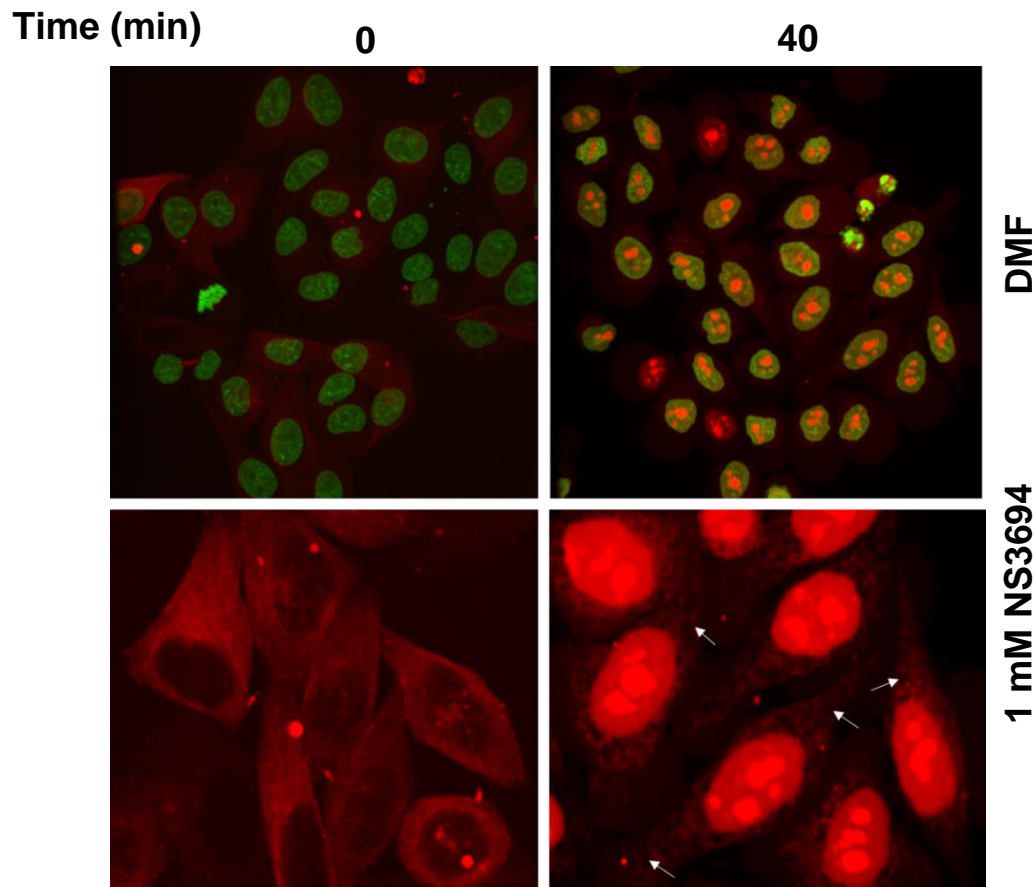


Figure 6.10. Live cells imaging of the NS3694-treated HeLa cells. Top panel shows the nuclei at the starting point and 40 min after treatment with 1 mM NS3694. Almost all the treated cells are PI positive. The bottom panel shows the degradation of the mCherry-tagged tubulins 40 min after treatment (white arrows).

6.1.9 Modelling the binding site of NS3694 on cytochrome c

NS3694 is the inhibitor of Apaf-1 (Lademann et al., 2003). I showed that NS3694 targets mainly cytochrome c and to some extent apoptosome. I did the molecular docking to see how it may interact to cytochrome c and apoptosome. NS3694 possibly makes hydrogen bonds with Gln 16, Val 20 and Glu 21. Polar and hydrophobic interactions also assist in the binding of NS3694 to cytochrome c (Figure 6.11).

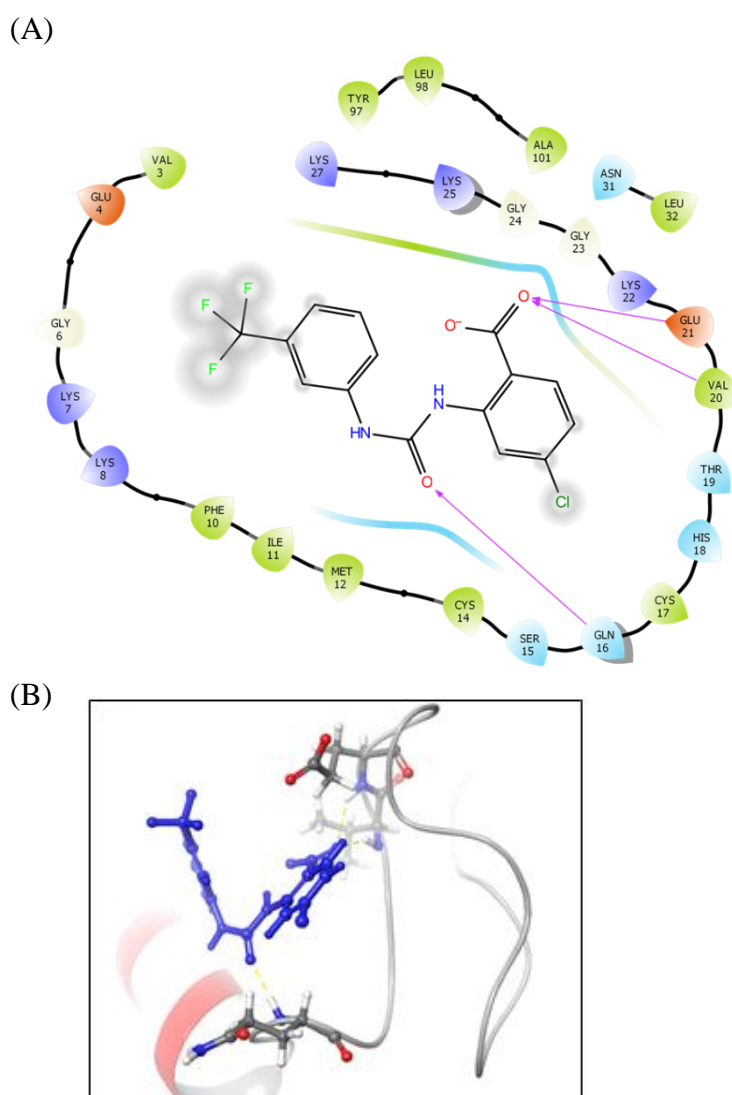


Figure 6.11. NS3694 docking to cytochrome c. (A) 2D representation of the NS3694 interactions with the cytochrome c. (B) zoom-in view of the best docked NS3694 with the involved amino acid residues and interactions. Yellow dashed lines represent the hydrogen bond.

Docking of the NS3694 to oligomeric Apaf-1 showed that it can bind to four cavities on the surface of Apaf-1. However, the maximum docking score was achieved when NS3694 binds to ADP-binding site. NS3694 makes three hydrogen bonds with Ser161, Gly159 and Gly157 and pi-pi stacking with Tyr359 (Figure 6.12).

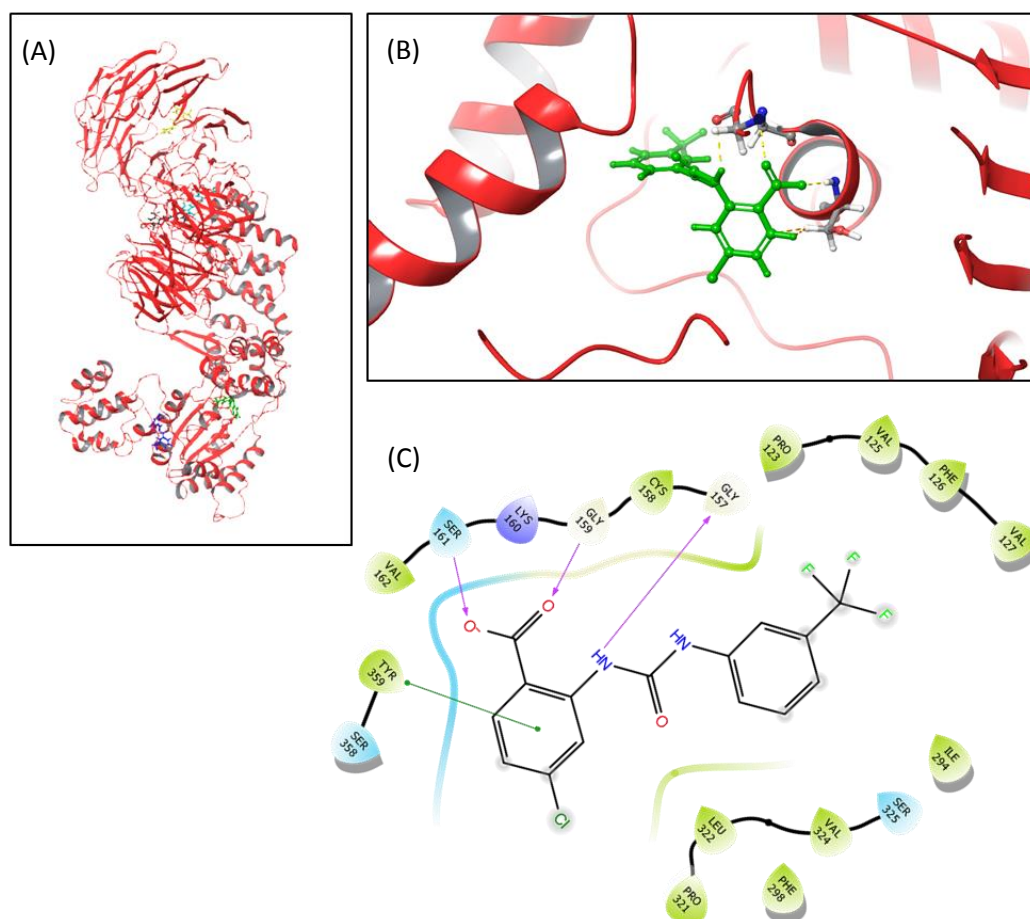


Figure 6.12. NS3694 docking to “open” Apaf-1. (A) Shows the docking of NS3694 into the four recognized binding sites on oligomeric Apaf-1. (B) zoom-in view of the best docked NS3694 with the involved amino acid residues and interactions. Yellow dashed lines represent the hydrogen bond. (C) 2D representation of the ligand interactions with the receptor.³

6.2 M50054, a caspase-3 inhibitor

2,2'-methylenebis (1,3-cyclohexanedione), also known as M50054 in the market, is an inhibitor of apoptosis which has been shown to inhibit DNA fragmentation and phosphatidylserine exposure in U937, a human monocytic leukemic cell line. The anti-apoptotic properties of this compound were attributed to inhibition of caspase-3. M50054 also inhibits the increase of the plasma alanine aminotransferase and aspartate aminotransferase after induction of apoptosis by anti-Fas antibody. Although M50054 inhibits apoptosis induced by extrinsic and mitochondrial-dependent pathways, the exact mechanism of action and the direct target are still unclear (Tsuda et al., 2001). All data show that M50054 inhibits caspase-3, however, the mechanism of action and the direct intracellular target is still unknown.

6.2.1 M50054 inhibits caspase-3 like activity in a concentration dependent manner

Caspase-3 activity was inhibited by M50054 in a concentration-dependent manner with the IC₅₀ of ~ 1 mM (Figure 6.13). 2 mM M50054 fully inhibits caspase-3 activity. I then investigated the effect of M50054 on caspase-3 processing. As reported before and has been shown in figure 11, treatment of the HEK293 extract with 2 mM M50054 reduces the caspase-3 like activity to the basal level, very similar to the unactivated extract (Figure 6.13A). This activity is compatible with caspase-3 processing detected by anti-caspase-3 antibody. Procaspace-3 remains unprocessed when either treated with M50054 in the presence of cytochrome c and dATP or incubated on ice without inducers. However, in dATP/Cc-activated extract procaspase-3 is processed (Figure 6.13B, grey bars).

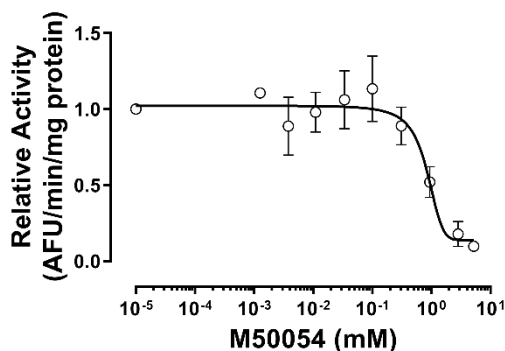


Figure 6.13. M50054-driven inhibition of caspase-3 like activity. HEK293 cell extracts incubated with a range of M50054 concentrations (up to 4 mM) and DEVDase activity was measured after addition of Cc/dATP.

6.2.2 M50054 inhibits the events upstream of caspase-3

I also investigated the activity of caspase-9 processing and activity to see if M50054 functions upstream of caspase-3 activation. Interestingly, caspase-9 activity showed the same inhibition as we detected for caspase-3. In other words, M50054 decreases caspase-9 activity to basal level, very close to the unactivated extract (Figure 6.14A, red bars). Immunoblotting using anti-caspase-9 confirmed that there is no cleavage in the activated extract treated with M50054.

Having the bio-tool to test upstream events of caspase-3 activation, I tested whether the inhibition could be upstream of caspase-9 activation which is Apaf-1 oligomerization. Then I used split luciferase assay, when S-100 HEK293 extracts expressing Nluc-Apaf-1 and Cluc-Apaf-1 were mixed 1:1 and treated or not with M50054. M50054 decreased split luciferase activity to the similar level as unactivated extract while it did not affect luciferase itself (Figure 6.14C, D).

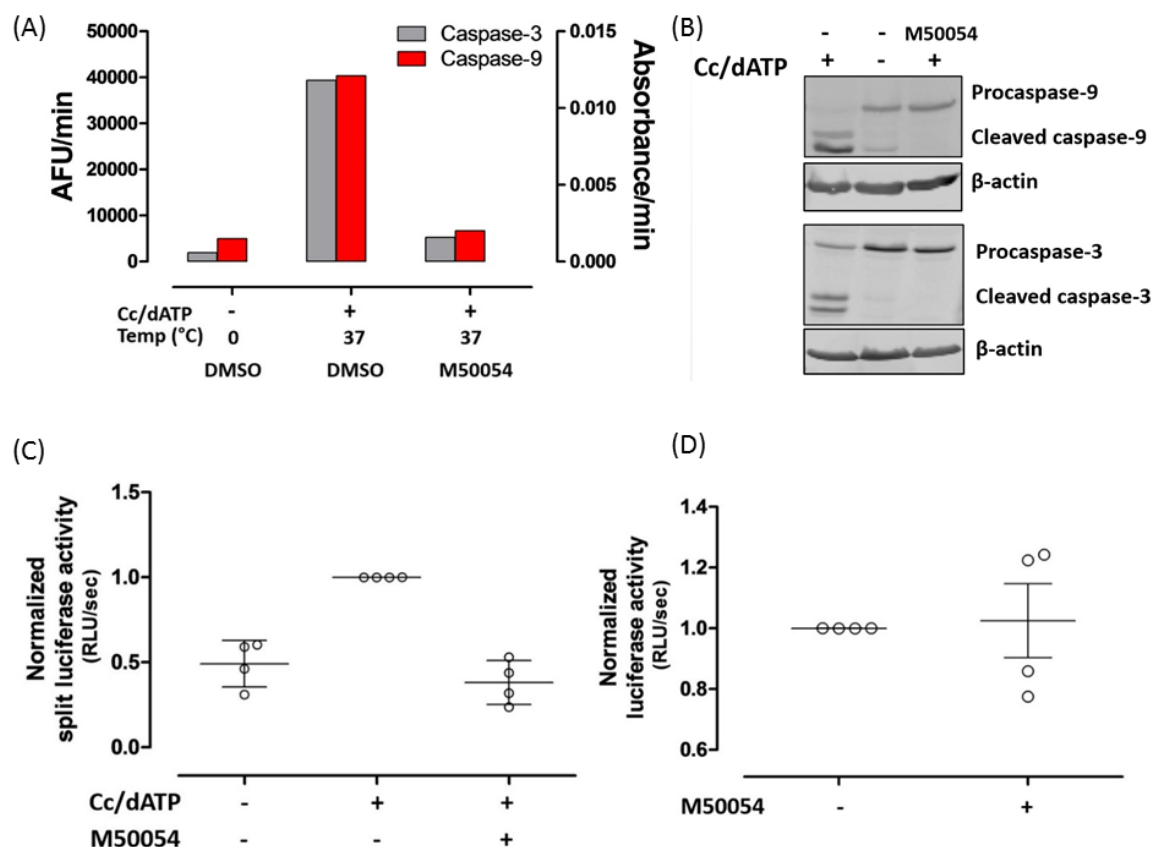


Figure 6.14. Effect of M50054 on apoptotic machinery components. (A) Caspase-3 (grey) and caspase-9 (red) activity when the S-100 HEK 293 extract treated with M50054. (B) Immunoblotting of the same samples as in (A) to show the processing of the caspase-3 and caspase-9. (C) Split luciferase assay and (D) luciferase assay.

Reduction of split luciferase activity showed that M50054 may function upstream of apoptosome complex formation. To identify the direct target, I did the thermal stability assay using recombinant cytochrome c. Even 2 mM M50054, a concentration that totally block caspase activity and split luciferase activity, does not influence the thermostability of cytochrome c (Figure 6.15). Therefore, thermostability assay performed using rApaf-1, the other protein involves in apoptosome. Immunoblotting of the samples showed that rApaf-1 is quite stable even at high temperatures (over 80°C) and incubation with 2 mM M50054 did not affect the stability of rApaf-1 (data not shown).

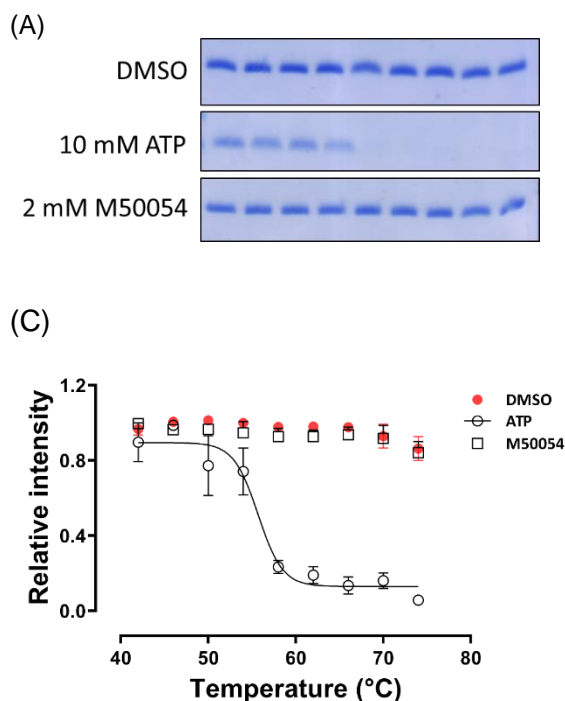


Figure 6.15. M50054 does not bind to cytochrome c. (A) Cytochrome c incubated with DMSO, 2 mM M50054 and ATP and thermal stability assay was performed at different temperatures. The amounts of soluble proteins were assessed by SDS-PAGE. The M50054-treated cytochrome c is as stable as the vehicle control. 10 mM ATP destabilized the complex. (B) The intensity of the bands was quantified and normalized to the highest intensity in that experiment. Error bars are mean \pm SD.

M50054 did not directly target cytochrome c and monomer rApaf-1. To test whether it binds to apoptosome complex, I made an *in vitro* apoptosome using recombinant proteins_ cytochrome c, rApaf-1_ and then incubated with M50054. Incubation with 2 mM M50054 significantly destabilized the complex (Figure 6.16).

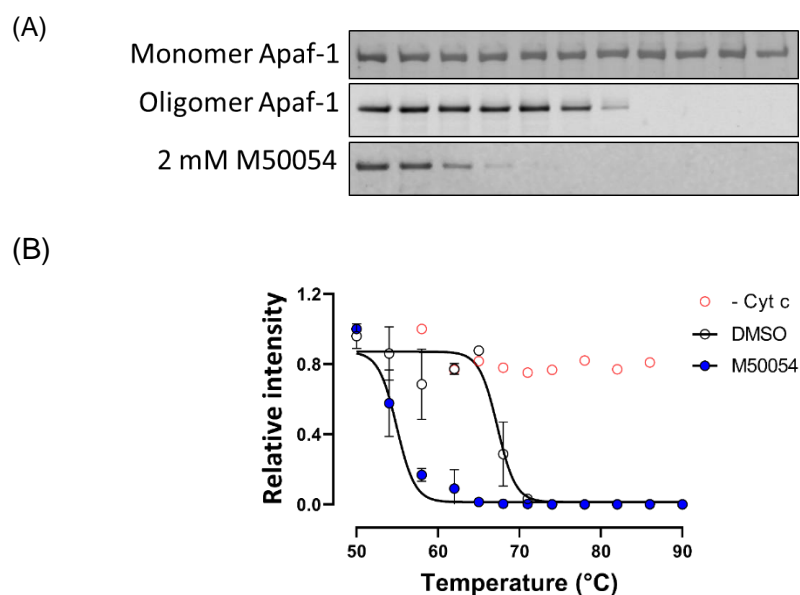


Figure 6.16. M50054 bind to apoptosome complex. (A) Apoptosome complex was reconstituted *in vitro* and incubated with 2 mM M50054. The thermal stability assay was performed at different temperatures. The amounts of soluble proteins were assessed by immunoblotting. The M50054-treated apoptosome showed a great shift in comparison with vehicle control. This blot is a representative of three independent experiments. (B) The intensity of the bands was quantified and normalized to the highest intensity in that experiment. Error bars are mean \pm SD.

6.2.3 Modelling the binding of M50054 to Apaf-1

To do the docking of M50054 to Apaf-1 with the conformation at the open form, I used the crystal structure of Apaf-1/Caspase-9 holoenzyme PDB file (5WVE). This structure obtained via electron microscopy with 4.4Å resolution. For docking, I extracted a single unit (monomer) from the heptameric complex (Figure 6.17A). I selected the Apaf-1, cytochrome c of one unit. However, I found a gap between the Apaf-1 CARD and the remaining of the protein (Figure 6.17B, C). To fill the gap, I used homology modeling and molecular dynamic. The inserted fragment has been shown in figure 6.17D, E.

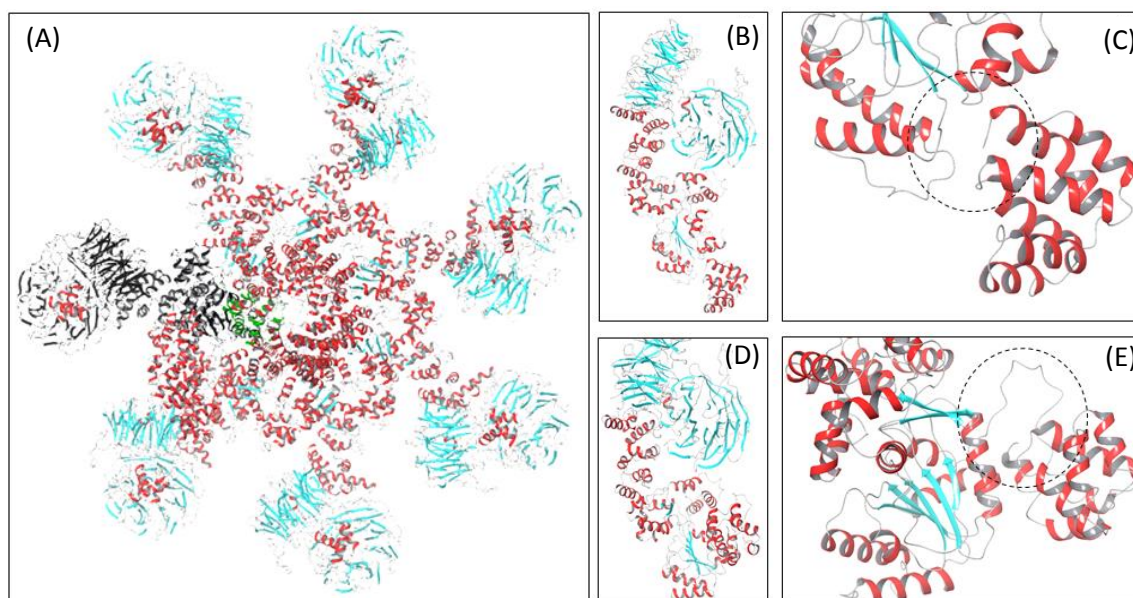


Figure 6.17. Preparation of “open” Apaf-1 PDB file. (A) One unit of the heptameric apoptosome was extracted from the PDB file (shown in black for Apaf-1 and red for cytochrome c). (B) and (C) show the gap in the structure of Apaf-1 between the CARD and The NDB domains. (D) and (E) show the inserted fragment after homology modeling and molecular dynamic. This optimized structure was used for the docking.

Thermal stability assay as well as split luciferase assay showed the binding of M50054 to apoptosome. Therefore, docking was performed using structure of M50054 as a ligand. The maximum docking score was achieved when M50054 interacted with Val127 and Arg129 (Figure 6.18).

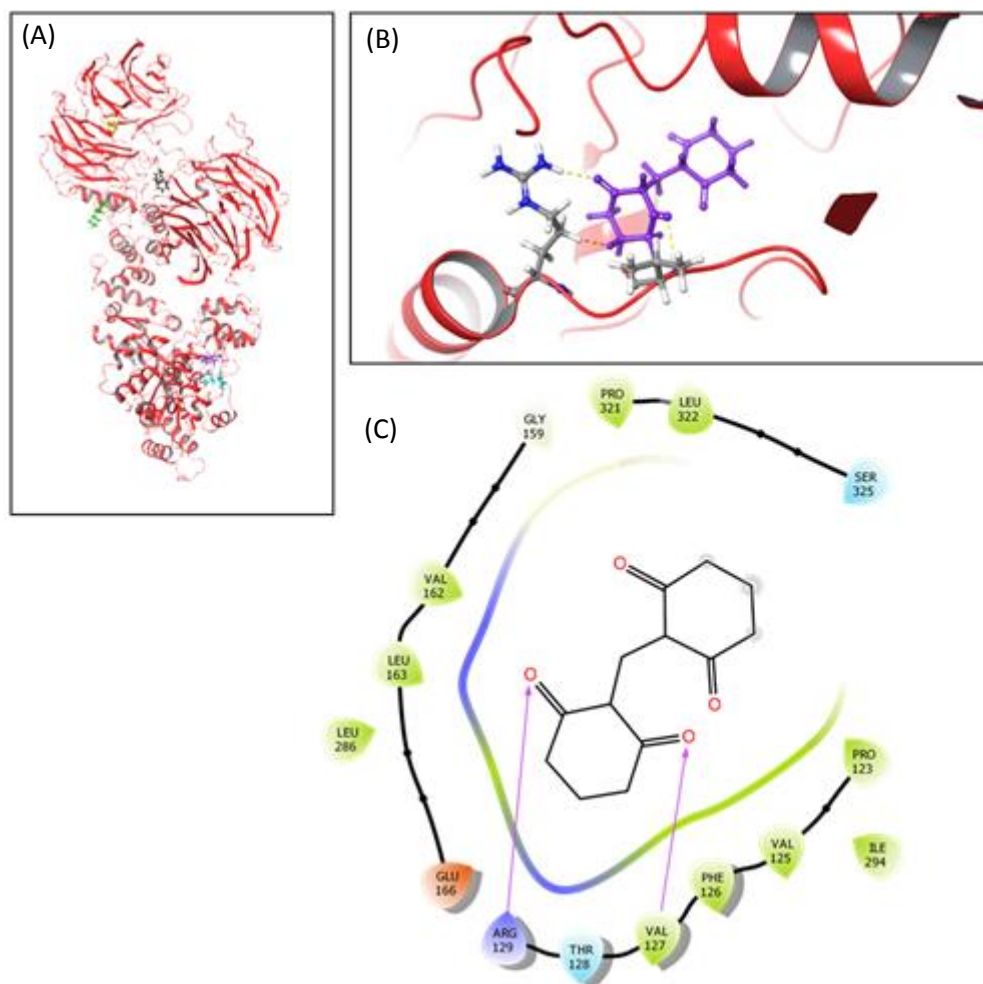


Figure 6.18. M50054 docking to “open” Apaf-1. (A) Shows the docking of M50054 into all the four grids. (B) zoom-in view of the best docked M50054 with the involved amino acid residues and interactions. Yellow dashed lines represent the hydrogen bond. (C) 2D representation of the ligand interactions with the receptor.

6.3 Discussion

NS3694 was identified as an inhibitor of apoptosome. However, the mechanism of action was not fully understood. I showed in chapter 3 that NS3694 inhibits both split luciferase and caspase activity in concentration-dependent manner. The IC_{50} was $\sim 170 \mu M$. Here, I showed that NS3694 inhibits caspase activation only if it is pre-incubated with extract before inducing apoptosome formation. In other words, once the complex is formed and all caspases are activated, NS3694 cannot inhibit caspase activation.

To identify the direct target of NS3694 in apoptosome machinery, I performed TSA using recombinant cytochrome *c*, Apaf-1. TSA showed that NS3694 binds to cytochrome *c* with EC_{50} of $\sim 300 \mu M$ while it does not bind to monomer Apaf-1. However, small shift was observed when NS3694 incubated with oligomeric Apaf-1, implying the possibility of binding to either cytochrome *c* or open form of Apaf-1 within the apoptosome complex.

I hypothesized that NS3694 may block the formation of the complex or it may form a non-functional complex. Therefore, gel filtration was performed. Incubation with NS3694 led to the formation of a large size complex similar to apoptosome. However, the complex is incompetent in caspase activation.

To test whether NS3694 can block caspase-dependent cell death I tested NS3694 against etoposide treatment. In my experiments, even low concentration (25 and 50 μM) of NS3694 did not rescue the etoposide-treated cells.

Moreover, I found that NS3694 kills the cells quickly with EC_{50} of $\sim 300 \mu M$. This concentration is very close to that of cytochrome *c* binding uncovered by the thermal stability assay. This similarity suggested that NS3694 might affect electron transport and mitochondrial function. To test whether mitochondrial were implicated, cells were stained by TMRE to determine mitochondrial polarization. NS3694 caused a decrease in TMRE staining, which is consistent with an effect on mitochondrial, but I have not determined whether this is a cause or consequence of cell death.

I found that NS3694 kills the cells quickly. To find the possible mode of death caused by NS3694, I treated HeLa cells with NS3694 and studied the morphology of the nuclei. As a result, nuclei condensation was detected. The nuclei were smaller and more intense (in terms of GFP intensity) than the untreated cells. In addition, signs of degradation of the tubulins were seen in the cytoplasmic tubulin filaments. All the data suggest that NS3694 kills the cells by necrosis.

M50054 has been reported to inhibit caspase activation and thus reduce apoptosis at the concentration of ~ 1.3 mM. Treatment of the WC8 cells with different concentrations of M50054 did not change the cell viability, suggesting that it is non-toxic. Besides, 1.3 mM M50054 rescued the U937 cells from etoposide-induced death (Tsuda et al., 2001). However, the mechanism of action and the direct target was unknown. Here, I reproduced the previous data that M50054 inhibits caspase activation with the complete inhibition at ~ 2 mM. Caspase-3 activation was also blocked. I tested the inhibition of upstream proteins. Caspase-9 processing and activity was blocked by M50054. Split luciferase assay showed that M50054 can inhibit apoptosome. Thermal stability assay confirmed the binding of M50054 to apoptosome, but not cytochrome c.

NS3694 and M50054 both prevent the formation of apoptosome. (Lademann et al., 2003; Nikolettou et al., 2013). Molecular docking studies suggested that NS3694 can bind to cytochrome c as well as apoptosome. These data are consistent with thermal stability assay and split luciferase activity. M50054 was also shown to interact with open form of Apaf-1. The most probable target for both compounds is ADP binding site.

Apaf-1 is found as auto inhibited ADP-bound monomer in the cytosol. ADP binds to the NBD either during or after the Apaf-1 synthesis. ADP interacts to the binding pocket in NBD through several hydrogen bonds and a salt bridge. ADP interacts mainly to NBD and HD1 subunits of NOD domain, although His438 and Ser422 of WHD also contribute via a H-bond to oxygen atom of β -phosphate. These interactions deeply bury ADP within the NOD and CARD blocks the narrow channel to be exposed to the solvent.

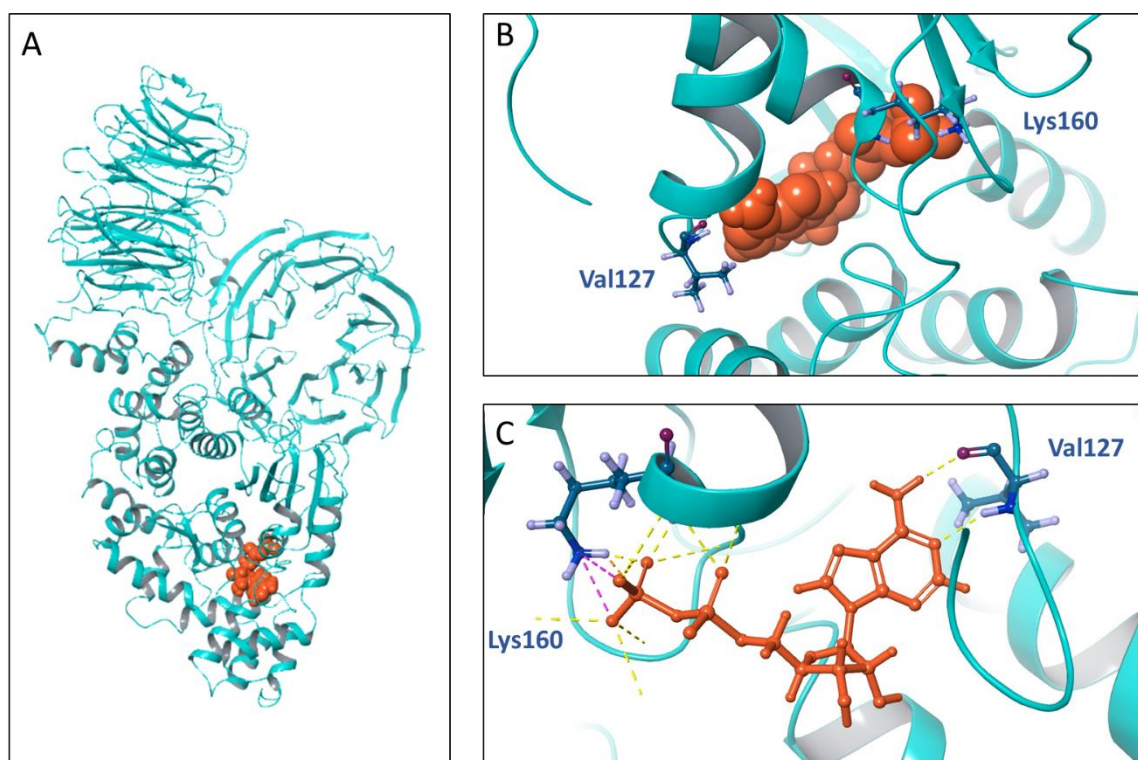


Fig. 6.19. ADP binding site. (A) ADP binds to the nucleotide binding pocket in NBD. (B) Val127 and Lys160 contribute to the interaction with ADP. (C) Interaction between ADP and key residues, Val127 and Lys160. Yellow: H-bonds, Purple: salt bridge.

Lys160 and Val127 are the key residues in these interactions (Figure 6.19). Lys160 makes two salt bridges and a hydrogen bond with oxygens of β -phosphate. The *anti* conformation of adenine relative to the deoxyribose ring makes hydrogen bonds to the backbone carbonyl and amide of Val127 (Figure 19). ADP binds to the binding pocket by nine direct H-bonds, two of which are to the adenine base of ADP and the remaining H-bonds are to the phosphate group and two salt bridges. Val127 interacts to adenine base of ATP. Gly157, Gly159, Lys160 make H-bond to β phosphate and Ser161 Val162 makes H-bonds to α phosphate of ADP through their amide groups. The imidazole group of His 438 and a water-mediated interaction make the last two H-bonds. It seems that Arg129, Gly159, Val125 and Ser422 make water-mediated H-bonds to adenine base and ribose ring (Riedl et al., 2005; Reubold et al., 2011).

NS3694 binds to Apaf-1 by interacting with Gly157, Gly 159 and Ser 161. Gly157 is a critical residue for ADP/ATP binding. M50054 also interacts with Val127 and Arg129. As mentioned earlier, Val127 is another key residue in ADP binding site. Therefore, it seems that inhibition of apoptosome occurs by occupying the ADP binding site. However, structural analysis like NMR is required to confirm the binding to predicted sites.

In this chapter we showed that split luciferase reporters can provide mechanistic insight into the interaction between chemical inhibitors and Apaf-1. NS3694 was known to inhibit apoptosome. Here I showed the measurement of apoptosome inhibition. In case of M50054, no specific target was known except that it inhibits caspase activation. I showed that M50054 functions upstream of caspase activation, indeed. Inhibition of split luciferase activity and thermal stability assay showed the binding of M50054 to Apaf-1. Although further studies should be accomplished to determine the precise mechanism of inhibition, the assay is capable of testing the compounds that specifically target Apaf-1.

CONCLUSION

In this thesis a new split luciferase-based reporter was designed and validated for detection of apoptosome formation. This *in vitro* assay is different to commonly used methods for studying apoptosome in that it directly reports Apaf-1 oligomerization.

This assay was then used for screening a panel of compounds. Screening a persistent pollutant toxicant identified pentachlorophenol as an inhibitor of apoptosome. As pentachlorophenol causes infertility and Apaf-1 is also important in spermatogenesis, further analysis was performed. Thermo-stability shift assay showed that pentachlorophenol binds to cytochrome c. It seems that pentachlorophenol increases the affinity of cytochrome c to Apaf-1, which interferes with the formation of functional apoptosome. Modelling studies showed that pentachlorophenol can bind to different sites on cytochrome c and interacts with some of the key residues required for caspase activation. Among all, interaction with Gln 16 is more likely.

Screening of the natural product library identified an extract with the ability to inhibit Apaf-1. Stepwise fractionation and bio-guided assay identified a unique compound that blocks caspase activation, although at high concentrations. Further analysis should be performed to identify the main target using a similar strategy used for pentachlorophenol. Furthermore, the cytotoxicity of this compound needs to be tested. Modelling studies can help to identify the likely binding site and then chemically modify the structure of this compound to increase the affinity to target protein, although this strategy might be difficult in practice.

Apart from screening, luciferase reporters were also used to investigate the known apoptosis inhibitors, NS3694 and M50054. NS3694 was known as an inhibitor of Apaf-1. However, I showed that NS3694 primarily targets cytochrome c, although it can bind to apoptosome. It seems that binding to apoptosome inhibits the caspase-3 recruitment to apoptosome. This is consistent with gel filtration studies that showed the formation of a large complex (inactive ~ 1.4 kDa) incompetent in caspase activation in the presence of NS3694.

NS3694 is cytotoxic, unlike previous reports and kills the cells. To better understand the type of death, morphological studies were performed. Shrinkage of the nucleus and DNA condensation was detected only one hour after treatment which is a characteristic of apoptotic and necrotic cells. Degradation of tubulin filaments and membrane disintegration were also detected one hour after treatment. This death was also shown to be mitochondrial dependent. Further analysis is required to test whether cell death induced by NS3694 is caspase-dependent or caspase-independent. NS3694 interacts to cytochrome c and may make it dysfunction its role in respiratory chain. As a result, ROS generation may be the cause of death. Therefore, cells can be treated with ROS inhibitor such as N-acetyl-L-cysteine and see if NS3694 toxicity is blocked.

M50054 is an inhibitor of caspase activation, however the direct target is unknown. Here, biochemical assays showed that M50054 binds to active Apaf-1 and blocks caspase-9 processing. Modelling studies suggested that ADP binding site in Apaf-1 is the most likely site for M50054 to interact with Apaf-1. According to docking analysis M50054 interacts with Val127 and Arg129. Val127 is a key residue in nucleotide binding in Apaf-1. However, more experiments need to be done to better understand the inhibitory effect of M50054. For example, it is not known whether binding of M50054 forms large complex. Therefore, gel filtration can reveal whether the complex is 700 kDa, inactive 1.4 MDa or it forms an aggregate. M50054 has been shown to be non-toxic for the cells. Therefore, the effect of Apaf-1 inhibition can be tested on disease-related models. For example, the formation of polyglutamin tract, a characteristic of ALS disease, is expected to be blocked by M50054, as Apaf-1 is required for formation of the aggregates.

REFERENCES

Bibliography

- ABALLAY, A., AND F.M. AUSUBEL. 2001. Programmed cell death mediated by ced-3 and ced-4 protects *Caenorhabditis elegans* from *Salmonella typhimurium*-mediated killing. *Proceedings of the National Academy of Sciences of the United States of America* 98: p.2735–2739.
- ABDELWAHID, E., T. YOKOKURA, R.J. KRIESER, ET AL. 2007. Mitochondrial disruption in *Drosophila* apoptosis. *Developmental Cell* 12: p.793–806.
- ABDULLAEV, Z.K., M.E. BODROVA, B.V. CHERNYAK, ET AL. 2002. A cytochrome c mutant with high electron transfer and antioxidant activities but devoid of apoptogenic effect. *The Biochemical Journal* 362: p.749–754.
- ABRAHAM, M.C., AND S. SHAHAM. 2004. Death without caspases, caspases without death. *Trends in Cell Biology* 14: p.184–193.
- ACEHAN, D., X. JIANG, D.G. MORGAN, ET AL. 2002a. Three-Dimensional Structure of the Apoptosome. *Molecular cell* 9: p.423–432.
- ACEHAN, D., X. JIANG, D.G. MORGAN, ET AL. 2002b. Three-dimensional structure of the apoptosome: implications for assembly, procaspase-9 binding, and activation. *Molecular Cell* 9: p.423–432.
- ADRAIN, C., G. BRUMATTI, AND S.J. MARTIN. 2006. Apoptosomes: protease activation platforms to die from. *Trends in Biochemical Sciences* 31: p.243–247.
- ALLAN, L.A., N. MORRICE, S. BRADY, ET AL. 2003. Inhibition of caspase-9 through phosphorylation at Thr 125 by ERK MAPK. *Nature Cell Biology* 5: p.647–654.
- ARAMA, E., J. AGAPITE, AND H. STELLER. 2003. Caspase activity and a specific cytochrome C are required for sperm differentiation in *Drosophila*. *Developmental Cell* 4: p.687–697.
- ASHKENAZI, A., AND G. SALVESEN. 2014. Regulated cell death: signaling and mechanisms. *Annual Review of Cell and Developmental Biology* 30: p.337–356.

- AZAD, T., A. TASHAKOR, M. GHahremani, ET AL. 2014. Apoptotic protease-activating factor 1 (Apaf-1) as a liable gene for spontaneous mutations in vitro. *Progress in Biological Sciences*.
- AZAD, T., A. TASHAKOR, AND S. HOSSEINKHANI. 2014. Split-luciferase complementary assay: applications, recent developments, and future perspectives. *Analytical and Bioanalytical Chemistry* 406: p.5541–5560.
- BAO, Q., W. LU, J.D. RABINOWITZ, ET AL. 2007. Calcium blocks formation of apoptosome by preventing nucleotide exchange in Apaf-1. *Molecular Cell* 25: p.181–192.
- BAO, Q., AND Y. SHI. 2007. Apoptosome: a platform for the activation of initiator caspases. *Cell Death and Differentiation* 14: p.56–65.
- BEARD, A.P., P.M. BARTLEWSKI, R.K. CHANDOLIA, ET AL. 1999. Reproductive and endocrine function in rams exposed to the organochlorine pesticides lindane and pentachlorophenol from conception. *Reproduction* 115: p.303–314.
- BEERE, H.M., B.B. WOLF, K. CAIN, ET AL. 2000. Heat-shock protein 70 inhibits apoptosis by preventing recruitment of procaspase-9 to the Apaf-1 apoptosome. *Nature Cell Biology* 2: p.469–475.
- BINKOWSKI, B., F. FAN, AND K. WOOD. 2009. Engineered luciferases for molecular sensing in living cells. *Current Opinion in Biotechnology* 20: p.14–18.
- BOUSSIF, O., F. LEZOUALC'H, M.A. ZANTA, ET AL. 1995. A versatile vector for gene and oligonucleotide transfer into cells in culture and in vivo: polyethylenimine. *Proceedings of the National Academy of Sciences of the United States of America* 92: p.7297–7301.
- BRANCHINI, B.R., R.A. MAGYAR, M.H. MURTIASHAW, ET AL. 1998. Site-directed mutagenesis of histidine 245 in firefly luciferase: a proposed model of the active site. *Biochemistry* 37: p.15311–15319.
- BRATTON, S.B., J. LEWIS, M. BUTTERWORTH, ET AL. 2002. XIAP inhibition of caspase-3 preserves its association with the Apaf-1 apoptosome and prevents CD95- and Bax-induced apoptosis. *Cell Death and Differentiation* 9: p.881–892.

- CAIN, K., S.B. BRATTON, C. LANGLAIS, ET AL. 2000. Apaf-1 oligomerizes into biologically active approximately 700-kDa and inactive approximately 1.4-MDa apoptosome complexes. *The Journal of Biological Chemistry* 275: p.6067–6070.
- CAIN, K., C. LANGLAIS, X.M. SUN, ET AL. 2001. Physiological concentrations of K⁺ inhibit cytochrome c-dependent formation of the apoptosome. *The Journal of Biological Chemistry* 276: p.41985–41990.
- CAMPBELL, A.K. 1988. Chemiluminescence: principles and applications in biology and medicine. VCH . E. Horwood.
- CANDÉ, C., I. COHEN, E. DAUGAS, ET AL. 2002. Apoptosis-inducing factor (AIF): a novel caspase-independent death effector released from mitochondria. *Biochimie* 84: p.215–222.
- CANDÉ, C., N. VAHSEN, C. GARRIDO, ET AL. 2004. Apoptosis-inducing factor (AIF): caspase-independent after all. *Cell Death and Differentiation* 11: p.591–595.
- CECCONI, F. 1999. Apaf1 and the apoptotic machinery. *Cell Death and Differentiation* 6: p.1087–1098.
- CECCONI, F., G. ALVAREZ-BOLADO, B.I. MEYER, ET AL. 1998. Apaf1 (CED-4 homolog) regulates programmed cell death in mammalian development. *Cell* 94: p.727–737.
- CECCONI, F., AND M. D'AMELIO. 2009. Apoptosome: An up-and-coming therapeutical tool. books.google.com.
- CECCONI, F., K.A. ROTH, O. DOLGOV, ET AL. 2004. Apaf1-dependent programmed cell death is required for inner ear morphogenesis and growth. *Development* 131: p.2125–2135.
- CHAI, J., C. DU, J.W. WU, ET AL. 2000. Structural and biochemical basis of apoptotic activation by Smac/DIABLO. *Nature* 406: p.855–862.
- CHAO, Y., E.N. SHIOZAKI, S.M. SRINIVASULA, ET AL. 2005. Engineering a dimeric caspase-9: a re-evaluation of the induced proximity model for caspase activation. *PLoS Biology* 3: p.e183.
- CHAU, B.N., E.H. CHENG, D.A. KERR, ET AL. 2000. Aven, a novel inhibitor of caspase activation, binds Bcl-xL and Apaf-1. *Molecular Cell* 6: p.31–40.

- CHEN, C.K.-M., N.-L. CHAN, AND A.H.-J. WANG. 2011. The many blades of the β -propeller proteins: conserved but versatile. *Trends in Biochemical Sciences* 36: p.553–561.
- CHEN, P., W. NORDSTROM, B. GISH, ET AL. 1996. grim, a novel cell death gene in *Drosophila*. *Genes & Development* 10: p.1773–1782.
- CHEN, X., J.L. ZARO, AND W.-C. SHEN. 2013. Fusion protein linkers: property, design and functionality. *Advanced Drug Delivery Reviews* 65: p.1357–1369.
- CHENG, T.C., C. HONG, I.V. AKEY, ET AL. 2016. A near atomic structure of the active human apoptosome. *eLife* 5: .
- CHEW, S.K., F. AKDEMIR, P. CHEN, ET AL. 2004. The apical caspase dronc governs programmed and unprogrammed cell death in *Drosophila*. *Developmental Cell* 7: p.897–907.
- CHU, Z.L., F. PIO, Z. XIE, ET AL. 2001. A novel enhancer of the Apaf1 apoptosome involved in cytochrome c-dependent caspase activation and apoptosis. *The Journal of Biological Chemistry* 276: p.9239–9245.
- CICCARONE, V.C., D.A. POLAYES, AND V.A. LUCKOW. 1998. Generation of recombinant baculovirus DNA in e.coli using a baculovirus shuttle vector. *Methods in Molecular Medicine* 13: p.213–235.
- CLEGG, R.M. 1995. Fluorescence resonance energy transfer. *Current Opinion in Biotechnology* 6: p.103–110.
- CLINE, R.E., R.H. HILL, D.L. PHILLIPS, ET AL. 1989. Pentachlorophenol measurements in body fluids of people in log homes and workplaces. *Archives of Environmental Contamination and Toxicology* 18: p.475–481.
- CLOSE, D.M., S. RIPP, AND G.S. SAYLER. 2009. Reporter proteins in whole-cell optical bioreporter detection systems, biosensor integrations, and biosensing applications. *Sensors*.
- CONRADT, B., Y.-C. WU, AND D. XUE. 2016. Programmed Cell Death During *Caenorhabditis elegans* Development. *Genetics* 203: p.1533–1562.

- CRAWFORD, E.D., J.E. SEAMAN, A.E. BARBER, ET AL. 2012. Conservation of caspase substrates across metazoans suggests hierarchical importance of signaling pathways over specific targets and cleavage site motifs in apoptosis. *Cell Death and Differentiation* 19: p.2040–2048.
- CULLEN, S.P., AND S.J. MARTIN. 2009. Caspase activation pathways: some recent progress. *Cell Death and Differentiation* 16: p.935–938.
- DAISH, T.J., K. MILLS, AND S. KUMAR. 2004. Drosophila caspase DRONC is required for specific developmental cell death pathways and stress-induced apoptosis. *Developmental Cell* 7: p.909–915.
- DE WET, J.R., K.V. WOOD, D.R. HELINSKI, ET AL. 1986. Cloning firefly luciferase. *Methods in Enzymology* 133: p.3–14.
- DELUCA, M. 1976. Firefly luciferase. *Advances in Enzymology and Related Areas of Molecular Biology* 44: p.37–68.
- DENTON, D., M.T. AUNG-HTUT, AND S. KUMAR. 2013. Developmentally programmed cell death in Drosophila. ... *Biophysica Acta (BBA)-Molecular Cell*
- DIEMAND, A.V., AND A.N. LUPAS. 2006. Modeling AAA+ ring complexes from monomeric structures. *Journal of Structural Biology* 156: p.230–243.
- DU, C., M. FANG, Y. LI, ET AL. 2000. Smac, a mitochondrial protein that promotes cytochrome c-dependent caspase activation by eliminating IAP inhibition. *Cell* 102: p.33–42.
- DUPREZ, L., E. WIRAWAN, T. VANDEN BERGHE, ET AL. 2009. Major cell death pathways at a glance. *Microbes and Infection* 11: p.1050–1062.
- EHRHARDT, C., M. SCHMOLKE, A. MATZKE, ET AL. 2006. Polyethylenimine, a cost-effective transfection reagent. *Signal transduction* 6: p.179–184.
- EISEN, J.A. 1998. Phylogenomics: improving functional predictions for uncharacterized genes by evolutionary analysis. *Genome Research* 8: p.163–167.
- ELENA-REAL, C.A., A. DÍAZ-QUINTANA, K. GONZÁLEZ-ARZOLA, ET AL. 2018. Cytochrome c speeds up caspase cascade activation by blocking 14-3-3ε-dependent Apaf-1 inhibition. *Cell death & disease* 9: p.365.

- ELLIS, H.M., AND H.R. HORVITZ. 1986. Genetic control of programmed cell death in the nematode *C. elegans*. *Cell* 44: p.817–829.
- ELMORE, S. 2007. Apoptosis: a review of programmed cell death. *Toxicologic Pathology* 35: p.495–516.
- EMEAGI, P.U., K. THIELEMANS, AND K. BRECKPOT. 2012. The role of SMAC mimetics in regulation of tumor cell death and immunity. *Oncoimmunology* 1: p.965–967.
- FAVALORO, B., N. ALLOCATI, V. GRAZIANO, ET AL. 2012. Role of apoptosis in disease. *Aging* 4: p.330–349.
- FEARNHEAD, H.O., M.E. MCCURRACH, J. O’NEILL, ET AL. 1997. Oncogene-dependent apoptosis in extracts from drug-resistant cells. *Genes & Development* 11: p.1266–1276.
- FORD, S.R., AND F.R. LEACH. 1998. Improvements in the application of firefly luciferase assays. *Methods in Molecular Biology* 102: p.3–20.
- FÖRSTER, T. 1948. Zwischenmolekulare Energiewanderung und Fluoreszenz. *Annalen der Physik* 437: p.55–75.
- GOYAL, L., K. MCCALL, J. AGAPITE, ET AL. 2000. Induction of apoptosis by *Drosophila* reaper, hid and grim through inhibition of IAP function. *The EMBO Journal* 19: p.589–597.
- GRAEPEL, R., L. LAMON, D. ASTURIOL, ET AL. 2017. The virtual cell based assay: Current status and future perspectives. *Toxicology in Vitro* 45: p.258–267.
- GRAHAM, F.L., J. SMILEY, W.C. RUSSELL, ET AL. 1977. Characteristics of a human cell line transformed by DNA from human adenovirus type 5. *The Journal of General Virology* 36: p.59–74.
- GREEN, D.R., AND J.C. REED. 1998. Mitochondria and apoptosis. *Science* 281: p.1309–1312.
- GRETHER, M.E., J.M. ABRAMS, J. AGAPITE, ET AL. 1995. The head involution defective gene of *Drosophila melanogaster* functions in programmed cell death. *Genes & Development* 9: p.1694–1708.

- HAKEM, R., A. HAKEM, G.S. DUNCAN, ET AL. 1998. Differential requirement for caspase 9 in apoptotic pathways in vivo. *Cell* 94: p.339–352.
- HAUGWITZ, M., O. NOURZAIE, T. GARACHTCHENKO, ET AL. 2008. Multiplexing bioluminescent and fluorescent reporters to monitor live cells. *Current chemical genomics* 1: p.11–19.
- HAY, B.A., D.A. WASSARMAN, AND G.M. RUBIN. 1995. Drosophila homologs of baculovirus inhibitor of apoptosis proteins function to block cell death. *Cell* 83: p.1253–1262.
- HENGARTNER, M.O. 2000. The biochemistry of apoptosis. *Nature* 407: p.770–776.
- HERRING, P.J. 1978. Bioluminescence in action.
- HERSCHMAN, H.R. 2003. Molecular imaging: looking at problems, seeing solutions. *Science* 302: p.605–608.
- HIDA, N., M. AWAIS, M. TAKEUCHI, ET AL. 2009. High-sensitivity real-time imaging of dual protein-protein interactions in living subjects using multicolor luciferases. *Plos One* 4: p.e5868.
- HONARPOUR, N., C. DU, J.A. RICHARDSON, ET AL. 2000. Adult Apaf-1-deficient mice exhibit male infertility. *Developmental Biology* 218: p.248–258.
- HOSSEINKHANI, S. 2011. Molecular enigma of multicolor bioluminescence of firefly luciferase. *Cellular and Molecular Life Sciences* 68: p.1167–1182.
- HU, Q., D. WU, W. CHEN, ET AL. 2014. Molecular determinants of caspase-9 activation by the Apaf-1 apoptosome. *Proceedings of the National Academy of Sciences of the United States of America* 111: p.16254–16261.
- HU, Y., M.A. BENEDICT, L. DING, ET AL. 1999. Role of cytochrome c and dATP/ATP hydrolysis in Apaf-1-mediated caspase-9 activation and apoptosis. *The EMBO Journal* 18: p.3586–3595.
- HU, Y., L. DING, D.M. SPENCER, ET AL. 1998. WD-40 repeat region regulates Apaf-1 self-association and procaspase-9 activation. *The Journal of Biological Chemistry* 273: p.33489–33494.

- HUGHES, J.P., S. REES, S.B. KALINDJIAN, ET AL. 2011. Principles of early drug discovery. *British Journal of Pharmacology* 162: p.1239–1249.
- IGNEY, F.H., AND P.H. KRAMMER. 2002. Death and anti-death: tumour resistance to apoptosis. *Nature Reviews. Cancer* 2: p.277–288.
- ISHIMOTO, T., T. OZAWA, AND H. MORI. 2011. Real-time monitoring of actin polymerization in living cells using split luciferase. *Bioconjugate Chemistry* 22: p.1136–1144.
- JACOBSON, M., AND N. MCCARTHY. 2002. Apoptosis:[the molecular biology of programmed cell death].
- JACOBSON, M.D., M. WEIL, AND M.C. RAFF. 1997. Programmed cell death in animal development. *Cell* 88: p.347–354.
- JIANG, L. 2012. Apoptosis: A Basic Biological Phenomenon with Wide-Ranging Implications in Tissue Kinetics"(1972), by John FR Kerr, Andrew H. Wyllie and Alastair R. Currie. *Embryo Project Encyclopedia*.
- JIANG, X., H.-E. KIM, H. SHU, ET AL. 2003. Distinctive roles of PHAP proteins and prothymosin- α in a death regulatory pathway. *Science* 299: p.223–226.
- KANNO, A., Y. UMEZAWA, AND T. OZAWA. 2009. Detection of apoptosis using cyclic luciferase in living mammals. *Methods in Molecular Biology* 574: p.105–114.
- KANNO, A., Y. YAMANAKA, H. HIRANO, ET AL. 2007. Cyclic luciferase for real-time sensing of caspase-3 activities in living mammals. *Angewandte Chemie* 46: p.7595–7599.
- KERR, J.F.R., A.H. WYLLIE, AND A.R. CURRIE. 1972. Apoptosis: a basic biological phenomenon with wideranging implications in tissue kinetics. *British journal of cancer*.
- KIECHLE, T., A. DEDEOGLU, J. KUBILUS, ET AL. 2002. Cytochrome C and caspase-9 expression in Huntington's disease. *Neuromolecular Medicine* 1: p.183–195.
- KIM, H.-E., F. DU, M. FANG, ET AL. 2005. Formation of apoptosome is initiated by cytochrome c-induced dATP hydrolysis and subsequent nucleotide exchange on

- Apaf-1. *Proceedings of the National Academy of Sciences of the United States of America* 102: p.17545–17550.
- KIM, J., A.B. PARRISH, M. KUROKAWA, ET AL. 2012. Rsk-mediated phosphorylation and 14-3-3 ϵ binding of Apaf-1 suppresses cytochrome c-induced apoptosis. *The EMBO Journal* 31: p.1279–1292.
- KIM, Y.M., R.V. TALANIAN, AND T.R. BILLIAR. 1997. Nitric oxide inhibits apoptosis by preventing increases in caspase-3-like activity via two distinct mechanisms. *The Journal of Biological Chemistry* 272: p.31138–31148.
- KITAGISHI, Y., M. KOBAYASHI, AND S. MATSUDA. 2013. Defective DNA repair systems and the development of breast and prostate cancer (review). *International Journal of Oncology* 42: p.29–34.
- KLEMENT, M., C. LIU, B.L.W. LOO, ET AL. 2015. Effect of linker flexibility and length on the functionality of a cytotoxic engineered antibody fragment. *Journal of Biotechnology* 199: p.90–97.
- KLUCK, R.M., L.M. ELLERBY, H.M. ELLERBY, ET AL. 2000. Determinants of cytochrome c pro-apoptotic activity. The role of lysine 72 trimethylation. *The Journal of Biological Chemistry* 275: p.16127–16133.
- KOBAYASHI, M., AND M. YAMAMOTO. 2005. Molecular mechanisms activating the Nrf2-Keap1 pathway of antioxidant gene regulation. *Antioxidants & Redox Signaling* 7: p.385–394.
- KUIDA, K., T.F. HAYDAR, C.Y. KUAN, ET AL. 1998. Reduced apoptosis and cytochrome c-mediated caspase activation in mice lacking caspase 9. *Cell* 94: p.325–337.
- KUIDA, K., T.S. ZHENG, S. NA, ET AL. 1996. Decreased apoptosis in the brain and premature lethality in CPP32-deficient mice. *Nature* 384: p.368–372.
- KUMAR, S., M. KINOSHITA, M. NODA, ET AL. 1994. Induction of apoptosis by the mouse Nedd2 gene, which encodes a protein similar to the product of the *Caenorhabditis elegans* cell death gene *ced-3* and the mammalian IL-1 beta-converting enzyme. *Genes & Development* 8: p.1613–1626.

- LADEMAN, U., K. CAIN, M. GYRD-HANSEN, ET AL. 2003. Diarylurea compounds inhibit caspase activation by preventing the formation of the active 700-kilodalton apoptosome complex. *Molecular and Cellular Biology* 23: p.7829–7837.
- LEE, I., A.R. SALOMON, K. YU, ET AL. 2006. New prospects for an old enzyme: mammalian cytochrome c is tyrosine-phosphorylated in vivo. *Biochemistry* 45: p.9121–9128.
- LETTRE, G., AND M.O. HENGARTNER. 2006. Developmental cell biology: Developmental apoptosis in *C. elegans*: a complex CEDnario. *Nature Reviews Molecular Cell Biology*.
- LI, L., L. FENG, M. SHI, ET AL. 2017. Split luciferase-based biosensors for characterizing EED binders. *Analytical Biochemistry* 522: p.37–45.
- LI, M., A. MAKINJE, AND Z. DAMUNI. 1996. Molecular identification of I1PP2A, a novel potent heat-stable inhibitor protein of protein phosphatase 2A. *Biochemistry* 35: p.6998–7002.
- LI, Y., M. ZHOU, Q. HU, ET AL. 2017. Mechanistic insights into caspase-9 activation by the structure of the apoptosome holoenzyme. *Proceedings of the National Academy of Sciences of the United States of America* 114: p.1542–1547.
- LINDSTEN, T., A.J. ROSS, A. KING, ET AL. 2000. The combined functions of proapoptotic Bcl-2 family members bak and bax are essential for normal development of multiple tissues. *Molecular Cell* 6: p.1389–1399.
- LIU, X., C.N. KIM, J. YANG, ET AL. 1996. Induction of apoptotic program in cell-free extracts: requirement for dATP and cytochrome c. *Cell* 86: p.147–157.
- LUKER, K.E., M.C.P. SMITH, G.D. LUKER, ET AL. 2004. Kinetics of regulated protein-protein interactions revealed with firefly luciferase complementation imaging in cells and living animals. *Proceedings of the National Academy of Sciences of the United States of America* 101: p.12288–12293.
- MALET, G., A.G. MARTIN, M. ORZAEZ, ET AL. 2006. Small molecule inhibitors of Apaf-1-related caspase-3/-9 activation that control mitochondrial-dependent apoptosis. *Cell Death and Differentiation* 13: p.1523–1532.

- MALIN, J.Z., AND S. SHAHAM. 2015. Cell Death in *C. elegans* Development. *Current Topics in Developmental Biology* 114: p.1–42.
- MALLADI, S., M. CHALLA-MALLADI, H.O. FEARNHEAD, ET AL. 2009. The Apaf-1*procaspase-9 apoptosome complex functions as a proteolytic-based molecular timer. *The EMBO Journal* 28: p.1916–1925.
- MARTIN, M.C., L.A. ALLAN, M. LICKRISH, ET AL. 2005. Protein kinase A regulates caspase-9 activation by Apaf-1 downstream of cytochrome c. *The Journal of Biological Chemistry* 280: p.15449–15455.
- MASSOUD, T.F., R. PAULMURUGAN, A. DE, ET AL. 2007. Reporter gene imaging of protein-protein interactions in living subjects. *Current Opinion in Biotechnology* 18: p.31–37.
- MEHALKO, J.L., AND D. ESPOSITO. 2016. Engineering the transposition-based baculovirus expression vector system for higher efficiency protein production from insect cells. *Journal of Biotechnology* 238: p.1–8.
- MEIGHEN, E.A., PV DUNLAP - ADVANCES IN MICROBIAL PHYSIOLOGY, AND 1993. Physiological, biochemical and genetic control of bacterial bioluminescence.
- METZSTEIN, M.M., G.M. STANFIELD, AND H.R. HORVITZ. 1998. Genetics of programmed cell death in *C. elegans*: past, present and future. *Trends in Genetics* 14: p.410–416.
- MISAWA, N., A.K.M. KAFI, M. HATTORI, ET AL. 2010. Rapid and high-sensitivity cell-based assays of protein-protein interactions using split click beetle luciferase complementation: an approach to the study of G-protein-coupled receptors. *Analytical Chemistry* 82: p.2552–2560.
- MONDRAGÓN, L., L. GALLUZZI, S. MOUHAMAD, ET AL. 2009. A chemical inhibitor of Apaf-1 exerts mitochondrioprotective functions and interferes with the intra-S-phase DNA damage checkpoint. *Apoptosis: An International Journal on Programmed Cell Death* 14: p.182–190.
- NAGAI, T., S. YAMADA, T. TOMINAGA, ET AL. 2004. Expanded dynamic range of fluorescent indicators for Ca(2+) by circularly permuted yellow fluorescent

- proteins. *Proceedings of the National Academy of Sciences of the United States of America* 101: p.10554–10559.
- NI, C.-Z., C. LI, J.C. WU, ET AL. 2003. Conformational restrictions in the active site of unliganded human caspase-3. *Journal of Molecular Recognition* 16: p.121–124.
- NIKOLETOPOULOU, V., M. MARKAKI, K. PALIKARAS, ET AL. 2013. Crosstalk between apoptosis, necrosis and autophagy. *Biochimica et Biophysica Acta* 1833: p.3448–3459.
- OBERST, A., C. BENDER, AND D.R. GREEN. 2008. Living with death: the evolution of the mitochondrial pathway of apoptosis in animals. *Cell Death and Differentiation* 15: p.1139–1146.
- ORZÁEZ, M., L. MONDRAGÓN, I. MARZO, ET AL. 2007. Conjugation of a novel Apaf-1 inhibitor to peptide-based cell-membrane transporters: effective methods to improve inhibition of mitochondria-mediated apoptosis. *Peptides* 28: p.958–968.
- OW, Y.-L.P., D.R. GREEN, Z. HAO, ET AL. 2008. Cytochrome c: functions beyond respiration. *Nature Reviews. Molecular Cell Biology* 9: p.532–542.
- OZAWA, T. 2006. Designing split reporter proteins for analytical tools. *Analytica Chimica Acta* 556: p.58–68.
- OZAWA, T., A. KAIHARA, M. SATO, ET AL. 2001. Split luciferase as an optical probe for detecting protein-protein interactions in mammalian cells based on protein splicing. *Analytical Chemistry* 73: p.2516–2521.
- OZAWA, T., AND Y. UMEZAWA. 2001. Detection of protein-protein interactions in vivo based on protein splicing. *Current Opinion in Chemical Biology* 5: p.578–583.
- PAPAMICHOS-CHRONAKIS, M., AND C.L. PETERSON. 2013. Chromatin and the genome integrity network. *Nature Reviews. Genetics* 14: p.62–75.
- PARK, S.E., N.D. KIM, AND Y.H. YOO. 2004. Acetylcholinesterase plays a pivotal role in apoptosome formation. *Cancer Research* 64: p.2652–2655.
- PAULMURUGAN, R., SS GAMBHIR - ANALYTICAL CHEMISTRY, AND 2003. Monitoring protein– protein interactions using split synthetic renilla luciferase protein-fragment-assisted complementation.

- PERKINS, C., C.N. KIM, G. FANG, ET AL. 1998. Overexpression of Apaf-1 promotes apoptosis of untreated and paclitaxel- or etoposide-treated HL-60 cells. *Cancer Research* 58: p.4561–4566.
- PICK, R., S. BADURA, S. BÖSSER, ET AL. 2006. Upon intracellular processing, the C-terminal death domain-containing fragment of the p53-inducible PIDD/LRDD protein translocates to the nucleoli and interacts with nucleolin. *Biochemical and Biophysical Research Communications* 349: p.1329–1338.
- PISTON, D.W., AND G.-J. KREMERS. 2007. Fluorescent protein FRET: the good, the bad and the ugly. *Trends in Biochemical Sciences* 32: p.407–414.
- QANUNGO, S., M. WANG, AND A.-L. NIEMINEN. 2004. N-Acetyl-L-cysteine enhances apoptosis through inhibition of nuclear factor-kappaB in hypoxic murine embryonic fibroblasts. *The Journal of Biological Chemistry* 279: p.50455–50464.
- QI, X., L. WANG, AND F. DU. 2010. Novel small molecules relieve prothymosin alpha-mediated inhibition of apoptosome formation by blocking its interaction with Apaf-1. *Biochemistry* 49: p.1923–1930.
- QIAN, J., M.J. VOORBACH, J.R. HUTH, ET AL. 2004. Discovery of novel inhibitors of Bcl-xL using multiple high-throughput screening platforms. *Analytical Biochemistry* 328: p.131–138.
- REED, J.C. 2000. Mechanisms of apoptosis. *The American Journal of Pathology* 157: p.1415–1430.
- RENATUS, M., H.R. STENNICKE, F.L. SCOTT, ET AL. 2001. Dimer formation drives the activation of the cell death protease caspase 9. *Proceedings of the National Academy of Sciences of the United States of America* 98: p.14250–14255.
- REUBOLD, T.F., S. WOHLGEMUTH, AND S. ESCHENBURG. 2009. A new model for the transition of APAF-1 from inactive monomer to caspase-activating apoptosome. *The Journal of Biological Chemistry* 284: p.32717–32724.
- REUBOLD, T.F., S. WOHLGEMUTH, AND S. ESCHENBURG. 2011. Crystal structure of full-length Apaf-1: how the death signal is relayed in the mitochondrial pathway of apoptosis. *Structure* 19: p.1074–1083.

- RIEDL, S.J., W. LI, Y. CHAO, ET AL. 2005. Structure of the apoptotic protease-activating factor 1 bound to ADP. *Nature* 434: p.926–933.
- RIEDL, S.J., AND G.S. SALVESEN. 2007. The apoptosome: signalling platform of cell death. *Nature Reviews. Molecular Cell Biology* 8: p.405–413.
- RODRIGUEZ, A., H. OLIVER, H. ZOU, ET AL. 1999. Dark is a Drosophila homologue of Apaf-1/CED-4 and functions in an evolutionarily conserved death pathway. *Nature Cell Biology* 1: p.272–279.
- RODRIGUEZ, J., AND Y. LAZEBNIK. 1999. Caspase-9 and APAF-1 form an active holoenzyme. *Genes & Development* 13: p.3179–3184.
- RYOO, H.D., AND E.H. BAEHRECKE. 2010. Distinct death mechanisms in Drosophila development. *Current Opinion in Cell Biology* 22: p.889–895.
- SAIKUMAR, P., Z. DONG, V. MIKHAILOV, ET AL. 1999. Apoptosis: definition, mechanisms, and relevance to disease. *The American Journal of Medicine* 107: p.489–506.
- SAKAI, T., L. LIU, X. TENG, ET AL. 2004. Nucling recruits Apaf-1/pro-caspase-9 complex for the induction of stress-induced apoptosis. *The Journal of Biological Chemistry* 279: p.41131–41140.
- SAMALI, A., M. O'MAHONEY, J. REEVE, ET AL. 2007. Identification of an inhibitor of caspase activation from heart extracts; ATP blocks apoptosome formation. *Apoptosis: An International Journal on Programmed Cell Death* 12: p.465–474.
- SANCHEZ-OLEA, R., S. ORTIZ, O. BARRETO, ET AL. 2008. Parcs is a dual regulator of cell proliferation and apaf-1 function. *The Journal of Biological Chemistry* 283: p.24400–24405.
- SANCHO, M., A.E. HERRERA, M. ORZÁEZ, ET AL. 2014. Inactivation of Apaf1 reduces the formation of mutant huntingtin-dependent aggregates and cell death. *Neuroscience* 262: p.83–91.
- SANG, T.-K., C. LI, W. LIU, ET AL. 2005. Inactivation of Drosophila Apaf-1 related killer suppresses formation of polyglutamine aggregates and blocks polyglutamine pathogenesis. *Human Molecular Genetics* 14: p.357–372.

- SCHMITZ, I., S. KIRCHHOFF, AND P.H. KRAMMER. 2000. Regulation of death receptor-mediated apoptosis pathways. *The International Journal of Biochemistry & Cell Biology* 32: p.1123–1136.
- SCOTT, F.L., J.-B. DENAULT, S.J. RIEDL, ET AL. 2005. XIAP inhibits caspase-3 and -7 using two binding sites: evolutionarily conserved mechanism of IAPs. *The EMBO Journal* 24: p.645–655.
- SEGAL, M.S., AND E. BEEM. 2001. Effect of pH, ionic charge, and osmolality on cytochrome c-mediated caspase-3 activity. *American Journal of Physiology. Cell Physiology* 281: p.C1196–204.
- SEKAR, R.B., AND A. PERIASAMY. 2003. Fluorescence resonance energy transfer (FRET) microscopy imaging of live cell protein localizations. *The Journal of Cell Biology* 160: p.629–633.
- SEMENKOVA, L., E. DUDICH, I. DUDICH, ET AL. 2003. Alpha-fetoprotein positively regulates cytochrome c-mediated caspase activation and apoptosome complex formation. *European Journal of Biochemistry / FEBS* 270: p.4388–4399.
- SEVRIUKOVA, I.F. 2011. Apoptosis-inducing factor: structure, function, and redox regulation. *Antioxidants & Redox Signaling* 14: p.2545–2579.
- SHAHAM, S. 1998. Identification of multiple *Caenorhabditis elegans* caspases and their potential roles in proteolytic cascades. *The Journal of Biological Chemistry* 273: p.35109–35117.
- SHEKHAWAT, S.S., J.R. PORTER, A. SRIPRASAD, ET AL. 2009. An autoinhibited coiled-coil design strategy for split-protein protease sensors. *Journal of the American Chemical Society* 131: p.15284–15290.
- SHIOZAKI, E.N., J. CHAI, D.J. RIGOTTI, ET AL. 2003. Mechanism of XIAP-mediated inhibition of caspase-9. *Molecular Cell* 11: p.519–527.
- SIMEONOV, A., A. JADHAV, C.J. THOMAS, ET AL. 2008. Fluorescence spectroscopic profiling of compound libraries. *Journal of Medicinal Chemistry* 51: p.2363–2371.

- SLEE, E.A., M.T. HARTE, R.M. KLUCK, ET AL. 1999. Ordering the cytochrome c-initiated caspase cascade: hierarchical activation of caspases-2, -3, -6, -7, -8, and -10 in a caspase-9-dependent manner. *The Journal of Cell Biology* 144: p.281–292.
- SRINIVASULA, S.M., M. AHMAD, T. FERNANDES-ALNEMRI, ET AL. 1998. Autoactivation of procaspase-9 by Apaf-1-mediated oligomerization. *Molecular Cell* 1: p.949–957.
- SRINIVASULA, S.M., P. DATTA, X.J. FAN, ET AL. 2000. Molecular determinants of the caspase-promoting activity of Smac/DIABLO and its role in the death receptor pathway. *The Journal of Biological Chemistry* 275: p.36152–36157.
- STAINS, C.I., J.L. FURMAN, J.R. PORTER, ET AL. 2010. A general approach for receptor and antibody-targeted detection of native proteins utilizing split-luciferase reassembly. *ACS Chemical Biology* 5: p.943–952.
- STELLER, H. 2008. Regulation of apoptosis in *Drosophila*. *Cell Death and Differentiation* 15: p.1132–1138.
- STENNICKE, H.R., Q.L. DEVERAUX, E.W. HUMKE, ET AL. 1999. Caspase-9 can be activated without proteolytic processing. *The Journal of Biological Chemistry* 274: p.8359–8362.
- SULSTON, J.E., AND H.R. HORVITZ. 1977. Post-embryonic cell lineages of the nematode, *Caenorhabditis elegans*. *Developmental Biology* 56: p.110–156.
- SUN, L., H. WANG, Z. WANG, ET AL. 2012. Mixed lineage kinase domain-like protein mediates necrosis signaling downstream of RIP3 kinase. *Cell* 148: p.213–227.
- TAKAHASHI, K. 2003. Effects of dinoseb, 4,6-dinitro-o-cresol, and 2,4-dinitrophenol on rat Sertoli-germ cell co-cultures. *Reproductive Toxicology* 17: p.247–252.
- TAKATANI, T., K. TAKAHASHI, Y. UOZUMI, ET AL. 2004. Taurine inhibits apoptosis by preventing formation of the Apaf-1/caspase-9 apoptosome. *American Journal of Physiology. Cell Physiology* 287: p.C949–53.
- TANEOKA, A., A. SAKAGUCHI-MIKAMI, AND T. YAMAZAKI. 2009. The construction of a glucose-sensing luciferase. *Biosensors and*
- TAYLOR, R.C., S.P. CULLEN, AND S.J. MARTIN. 2008. Apoptosis: controlled demolition at the cellular level. *Nature Reviews. Molecular Cell Biology* 9: p.231–241.

- TEWARI, M., L.T. QUAN, K. O'ROURKE, ET AL. 1995. Yama/CPP32 β , a mammalian homolog of CED-3, is a CrmA-inhibitable protease that cleaves the death substrate poly(ADP-ribose) polymerase. *Cell* 81: p.801–809.
- THOMPSON, G.J., C. LANGLAIS, K. CAIN, ET AL. 2001. Elevated extracellular [K⁺] inhibits death-receptor- and chemical-mediated apoptosis prior to caspase activation and cytochrome c release. *The Biochemical Journal* 357: p.137–145.
- THORNBERRY, N.A., H.G. BULL, J.R. CALAYCAY, ET AL. 1992. A novel heterodimeric cysteine protease is required for interleukin-1 beta processing in monocytes. *Nature* 356: p.768–774.
- THORNE, N., J. INGLESE, AND D.S. AULD. 2010. Illuminating insights into firefly luciferase and other bioluminescent reporters used in chemical biology. *Chemistry & Biology* 17: p.646–657.
- TIMMER, J.C., AND G.S. SALVESEN. 2007. Caspase substrates. *Cell Death and Differentiation* 14: p.66–72.
- TITTEL, J.N., AND H. STELLER. 2000. A comparison of programmed cell death between species. *Genome Biology* 1: p.REVIEWS0003.
- TORKZADEH-MAHANI, M., F. ATAIEI, M. NIKKHAH, ET AL. 2012. Design and development of a whole-cell luminescent biosensor for detection of early-stage of apoptosis. *Biosensors & Bioelectronics* 38: p.362–368.
- TSUDA, T., Y. OHMORI, H. MURAMATSU, ET AL. 2001. Inhibitory effect of M50054, a novel inhibitor of apoptosis, on anti-Fas-antibody-induced hepatitis and chemotherapy-induced alopecia. *European Journal of Pharmacology* 433: p.37–45.
- UGAROVA, N.N. 1989. Luciferase of *Luciola mingrelica* fireflies. Kinetics and regulation mechanism. *Journal of bioluminescence and chemiluminescence* 4: p.406–418.
- VAUGHN, D.E., J. RODRIGUEZ, Y. LAZEBNIK, ET AL. 1999. Crystal structure of Apaf-1 caspase recruitment domain: an alpha-helical Greek key fold for apoptotic signaling. *Journal of Molecular Biology* 293: p.439–447.

- VICENT, M.J., AND E. PÉREZ-PAYÁ. 2006. Poly-L-glutamic acid (PGA) aided inhibitors of apoptotic protease activating factor 1 (Apaf-1): an antiapoptotic polymeric nanomedicine. *Journal of Medicinal Chemistry* 49: p.3763–3765.
- VILLALOBOS, V., S. NAIK, AND D. PIWNICA-WORMS. 2007. Current state of imaging protein-protein interactions in vivo with genetically encoded reporters. *Annual Review of Biomedical Engineering* 9: p.321–349.
- WALKER, S.R., AND D.A. FRANK. 2012. Screening approaches to generating STAT inhibitors: Allowing the hits to identify the targets. *JAK-STAT* 1: p.292–299.
- WANG, L., L. CHEN, M. YU, ET AL. 2016. Discovering new mTOR inhibitors for cancer treatment through virtual screening methods and in vitro assays. *Scientific reports* 6: p.18987.
- WANG, X. 2001. The expanding role of mitochondria in apoptosis. *Genes & Development* 15: p.2922–2933.
- WANG, Y., Y. CAO, Q. ZHU, ET AL. 2016. The discovery of a novel inhibitor of apoptotic protease activating factor-1 (Apaf-1) for ischemic heart: synthesis, activity and target identification. *Scientific reports* 6: p.29820.
- WEI, M.C., W.X. ZONG, E.H. CHENG, ET AL. 2001. Proapoptotic BAX and BAK: a requisite gateway to mitochondrial dysfunction and death. *Science* 292: p.727–730.
- WEINBACH, E.C., AND J. GARBUS. 1965. The interaction of uncoupling phenols with mitochondria and ' ' with mitochondrial protein. *The Journal of Biological Chemistry* 240: p.1811–1819.
- WHITE, E.H., E. RAPAPORT, H.H. SELIGER, ET AL. The chemi-and bioluminescence of firefly luciferin: an efficient chemical production of electronically excited states.
- WHITE, K., M.E. GREYER, J.M. ABRAMS, ET AL. 1994. Genetic control of programmed cell death in *Drosophila*. *Science* 264: p.677–683.
- WIGDAL, S.S., J.L. ANDERSON, G.J. VIDUGIRIS, ET AL. 2008. A novel bioluminescent protease assay using engineered firefly luciferase. *Current chemical genomics* 2: p.16–28.

- WILSON, T., AND J.W. HASTINGS. 1998. Bioluminescence. *Annual Review of Cell and Developmental Biology* 14: p.197–230.
- WIMAN, K.G., AND B. ZHIVOTOVSKY. 2017. Understanding cell cycle and cell death regulation provides novel weapons against human diseases. *Journal of Internal Medicine* 281: p.483–495.
- WU, C.-C., AND S.B. BRATTON. 2017. Caspase-9 swings both ways in the apoptosome. *Molecular & Cellular Oncology* 4: p.e1281865.
- WU, C.-C., S. LEE, S. MALLADI, ET AL. 2016. The Apaf-1 apoptosome induces formation of caspase-9 homo- and heterodimers with distinct activities. *Nature Communications* 7: p.13565.
- WU, Q.D., J.H. WANG, F. FENNESSY, ET AL. 1999. Taurine prevents high-glucose-induced human vascular endothelial cell apoptosis. *The American Journal of Physiology* 277: p.C1229–38.
- WÜRSTLE, M.L., AND M. REHM. 2014. A systems biology analysis of apoptosome formation and apoptosis execution supports allosteric procaspase-9 activation. *The Journal of Biological Chemistry* 289: p.26277–26289.
- XU, D., Y. LI, M. ARCARO, ET AL. 2005. The CARD-carrying caspase Dronc is essential for most, but not all, developmental cell death in *Drosophila*. *Development* 132: p.2125–2134.
- YOSHIDA, H., Y.Y. KONG, R. YOSHIDA, ET AL. 1998. Apaf1 is required for mitochondrial pathways of apoptosis and brain development. *Cell* 94: p.739–750.
- YU, H., I. LEE, A.R. SALOMON, ET AL. 2008. Mammalian liver cytochrome c is tyrosine-48 phosphorylated in vivo, inhibiting mitochondrial respiration. *Biochimica et Biophysica Acta* 1777: p.1066–1071.
- YU, X., Q. DENG, A.M. BODE, ET AL. 2013. The role of necroptosis, an alternative form of cell death, in cancer therapy. *Expert Review of Anticancer Therapy* 13: p.883–893.
- YUAN, S., X. YU, J.M. ASARA, ET AL. 2011. The holo-apoptosome: activation of procaspase-9 and interactions with caspase-3. *Structure* 19: p.1084–1096.

- YUAN, S., X. YU, M. TOPF, ET AL. 2010. Structure of an apoptosome-procaspase-9 CARD complex. *Structure* 18: p.571–583.
- ZAMARAEV, A.V., G.S. KOPEINA, B. ZHIVOTOVSKY, ET AL. 2015. Cell death controlling complexes and their potential therapeutic role. *Cellular and Molecular Life Sciences* 72: p.505–517.
- ZECH, B., R. KÖHL, A. VON KNETHEN, ET AL. 2003. Nitric oxide donors inhibit formation of the Apaf-1/caspase-9 apoptosome and activation of caspases. *The Biochemical Journal* 371: p.1055–1064.
- ZHANG, J., J. YUN, Z. SHANG, ET AL. 2009. Design and optimization of a linker for fusion protein construction. *Progress in Natural Science* 19: p.1197–1200.
- ZHANG, X.-J., AND D.S. GREENBERG. 2012. Acetylcholinesterase involvement in apoptosis. *Frontiers in Molecular Neuroscience* 5: p.40.
- ZHOU, M., Y. LI, Q. HU, ET AL. 2015. Atomic structure of the apoptosome: mechanism of cytochrome *c*- and dATP-mediated activation of Apaf-1. *Genes & Development* 29: p.2349–2361.
- ZHOU, P., J. CHOU, R.S. OLEA, ET AL. 1999. Solution structure of Apaf-1 CARD and its interaction with caspase-9 CARD: a structural basis for specific adaptor/caspase interaction. *Proceedings of the National Academy of Sciences of the United States of America* 96: p.11265–11270.
- ZMASEK, C.M., Q. ZHANG, Y. YE, ET AL. 2007. Surprising complexity of the ancestral apoptosis network. *Genome Biology* 8: p.R226.
- ZOU, H., W.J. HENZEL, X. LIU, ET AL. 1997. Apaf-1, a human protein homologous to *C. elegans* CED-4, participates in cytochrome *c*-dependent activation of caspase-3. *Cell* 90: p.405–413.
- ZOU, H., Y. LI, X. LIU, ET AL. 1999. An APAF-1zCytochrome *c* Multimeric Complex Is a Functional Apoptosome That Activates Procaspase-9*. *The Journal of Biological Chemistry* 273: p.11549–56.
- ZOU, H., R. YANG, J. HAO, ET AL. 2003. Regulation of the Apaf-1/caspase-9 apoptosome by caspase-3 and XIAP. *The Journal of Biological Chemistry* 278: p.8091–80

PUBLICATIONS